

Resonant Inelastic X-ray Scattering on Elementary Excitations

Jeroen van den Brink



Leibniz Institute
for Solid State and
Materials Research
Dresden



TECHNISCHE
UNIVERSITÄT
DRESDEN

PSI Summer School
Zugerberg 12.08.2014

Resonant Inelastic X-ray Scattering on Elementary Excitations

Jeroen van den Brink



Leibniz Institute
for Solid State and
Materials Research
Dresden



TECHNISCHE
UNIVERSITÄT
DRESDEN

Ament, van Veenendaal, Devereaux, Hill & JvdB
Rev. Mod. Phys. 83, 705 (2011)

PSI Summer School
Zugerberg 12.08.2014

Outline

1. Introducing RIXS

2. Magnetic RIXS on low dimensional magnets

1. Introducing RIXS

Basic Scattering Process

Direct & Indirect RIXS

5 features of RIXS

*Elementary Excitations
Accessible to RIXS*

Progress in past decade

2. Magnetic RIXS on low dimensional magnets

Quasi 2D cuprates

Quasi 1D cuprates

Quasi 2D iron pnictide

Quasi 2D iridate

Doped Cu & Fe systems

Basic Scattering Process

Direct and Indirect RIXS

What is

Resonant

Inelastic

X-ray scattering

RIXS

What is

Resonant

Inelastic

X-ray scattering

RIXS

X-ray scattering: photon in → solid → photon out

inelastic: $\omega_{out} < \omega_{in}$

resonant: tune ω_{in} to an atomic absorption edge

What is

Resonant

Inelastic

X-ray scattering

RIXS

X-ray scattering: photon in → solid → photon out

inelastic: $\omega_{out} < \omega_{in}$

resonant: tune ω_{in} to an atomic absorption edge

Cu

K-edge

4 p



~9 KeV



1 s



What is

Resonant

Inelastic

X-ray scattering

RIXS

X-ray scattering: photon in → solid → photon out

inelastic: $\omega_{out} < \omega_{in}$

resonant: tune ω_{in} to an atomic absorption edge

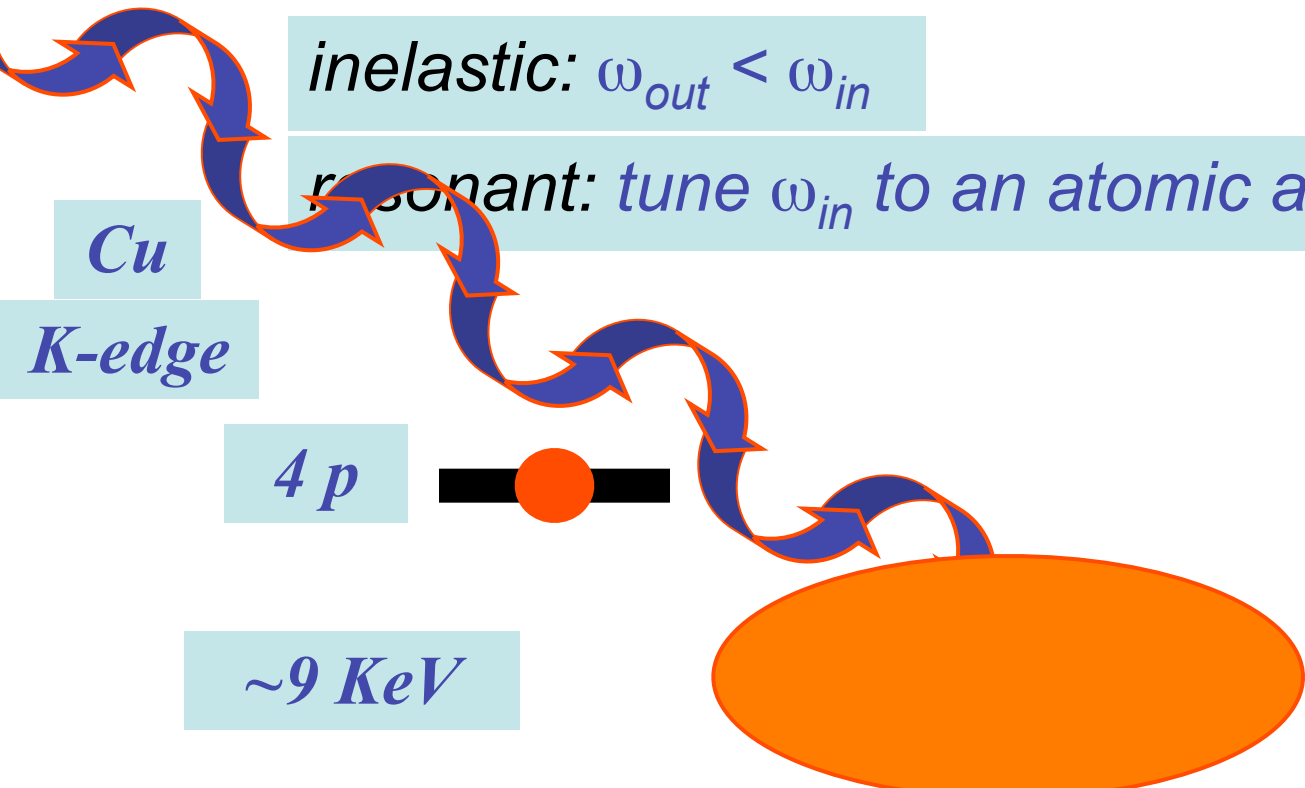
Cu

K-edge

4 p

~9 KeV

1 s



What is

Resonant

Inelastic

X-ray scattering

RIXS

X-ray scattering: photon in → solid → photon out

inelastic: $\omega_{out} < \omega_{in}$

resonant: tune ω_{in} to an atomic absorption edge

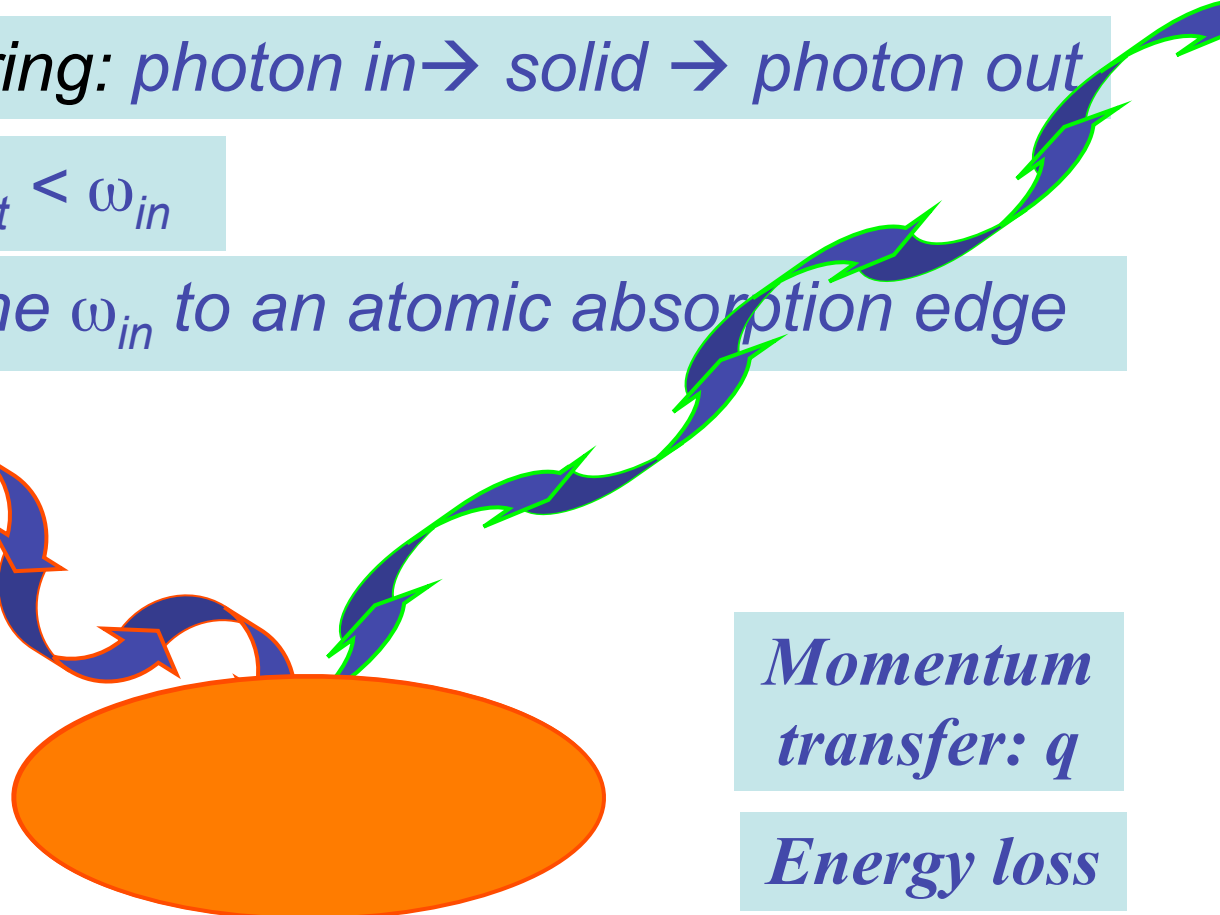
Cu

K-edge

4 p

~9 KeV

1 s



Momentum transfer: q

Energy loss

What is

Resonant

Inelastic

X-ray scattering

RIXS

X-ray scattering: photon in → solid → photon out

inelastic: $\omega_{out} < \omega_{in}$

resonant: tune ω_{in} to an atomic absorption edge

*Cu
K-edge*

4 p

~9 KeV

1 s

INDIRECT

*Momentum
transfer: q*
Energy loss

What is

Resonant

Inelastic

X-ray scattering

RIXS

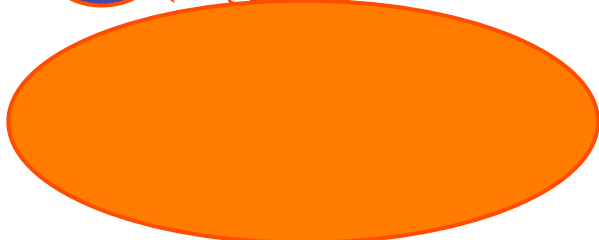
X-ray scattering: photon in → solid → photon out

inelastic: $\omega_{out} < \omega_{in}$

resonant: tune ω_{in} to an atomic absorption edge

Cu

L-edge



*Momentum
transfer: q*

Energy loss

What is

Resonant

Inelastic

X-ray scattering

RIXS

X-ray scattering: photon in → solid → photon out

inelastic: $\omega_{out} < \omega_{in}$

resonant: tune ω_{in} to an atomic absorption edge

Cu

L-edge

2 p



Momentum transfer: q

Energy loss

What is

Resonant

Inelastic

X-ray scattering

RIXS

X-ray scattering: photon in → solid → photon out

inelastic: $\omega_{out} < \omega_{in}$

resonant: tune ω_{in} to an atomic absorption edge

Cu

L-edge

~900 eV

2 p

*Momentum
transfer: q*

Energy loss

What is

Resonant

Inelastic

X-ray scattering

RIXS

X-ray scattering: photon in → solid → photon out

inelastic: $\omega_{out} < \omega_{in}$

resonant: tune ω_{in} to an atomic absorption edge

Cu

L-edge

3 d

~900 eV

2 p



Momentum transfer: q

Energy loss

What is

Resonant

Inelastic

X-ray scattering

RIXS

X-ray scattering: photon in → solid → photon out

inelastic: $\omega_{out} < \omega_{in}$

resonant: tune ω_{in} to an atomic absorption edge

Cu

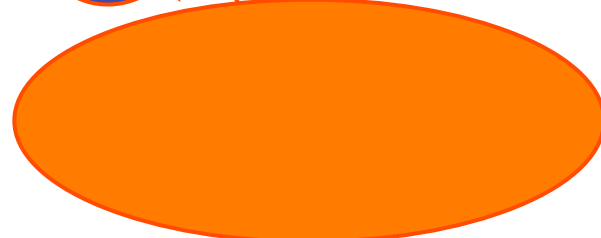
L-edge

3 d

~900 eV

2 p

DIRECT

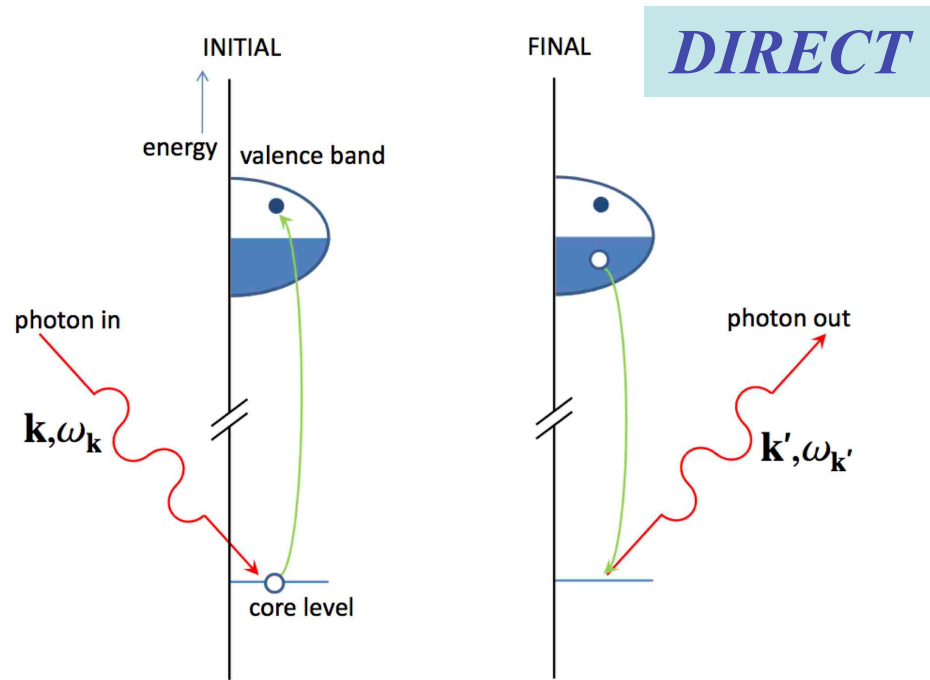


Momentum transfer: q

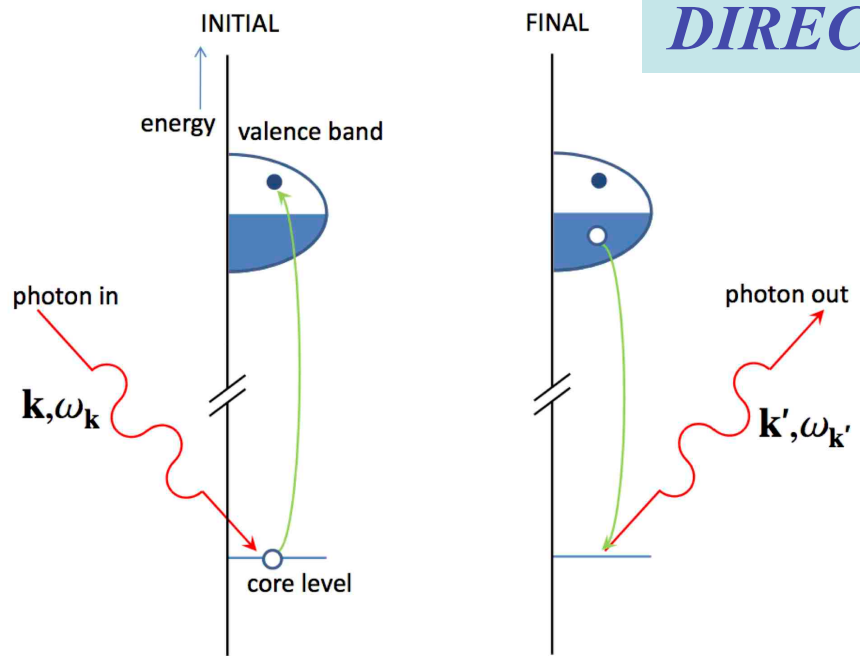
Energy loss

resolution < 100 meV

Direct and Indirect RIXS



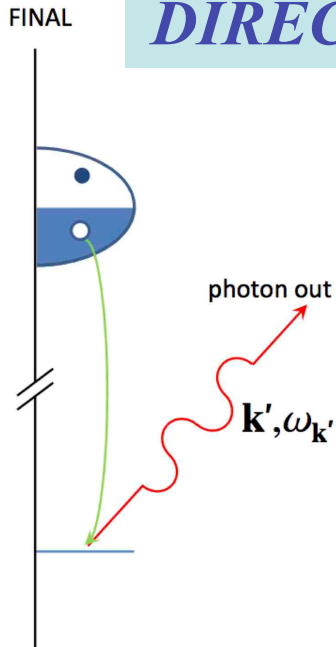
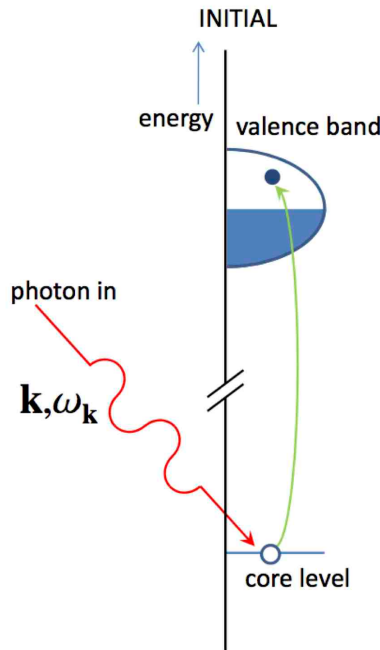
Direct and Indirect RIXS



DIRECT

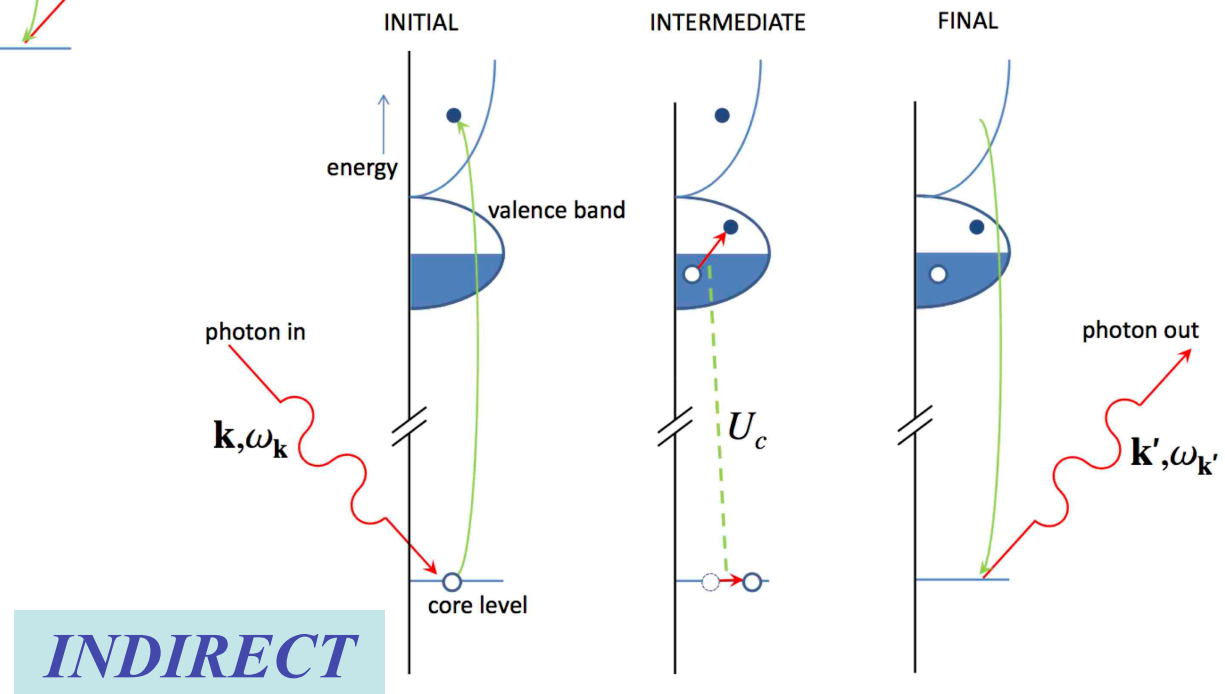
scattering via absorption-emission matrix elements

Direct and Indirect RIXS



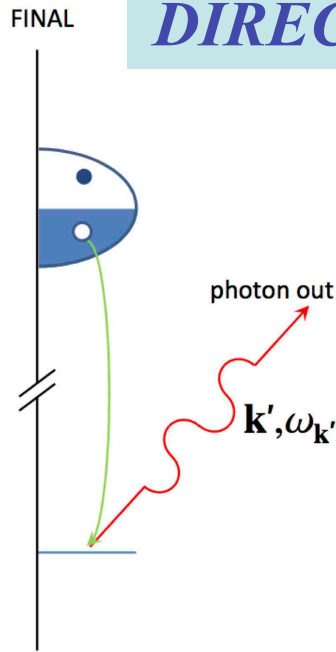
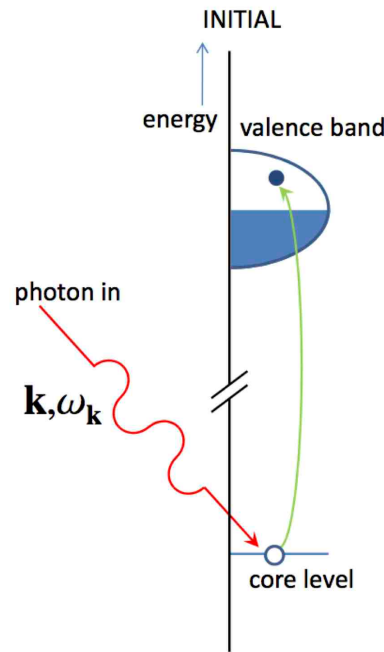
DIRECT

scattering via absorption-emission matrix elements



INDIRECT

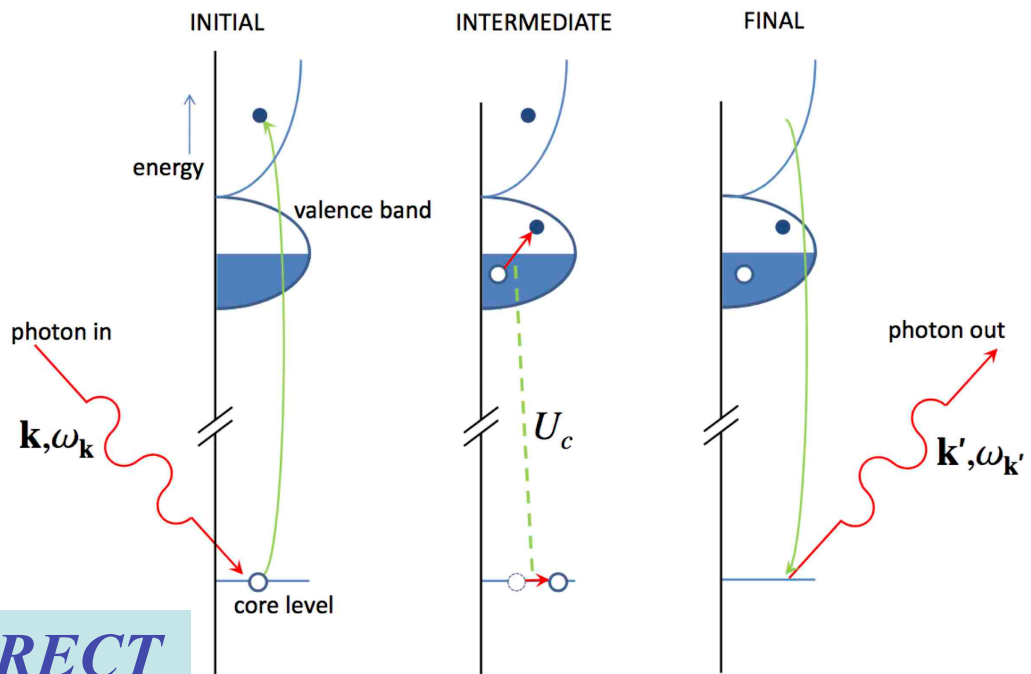
Direct and Indirect RIXS



DIRECT

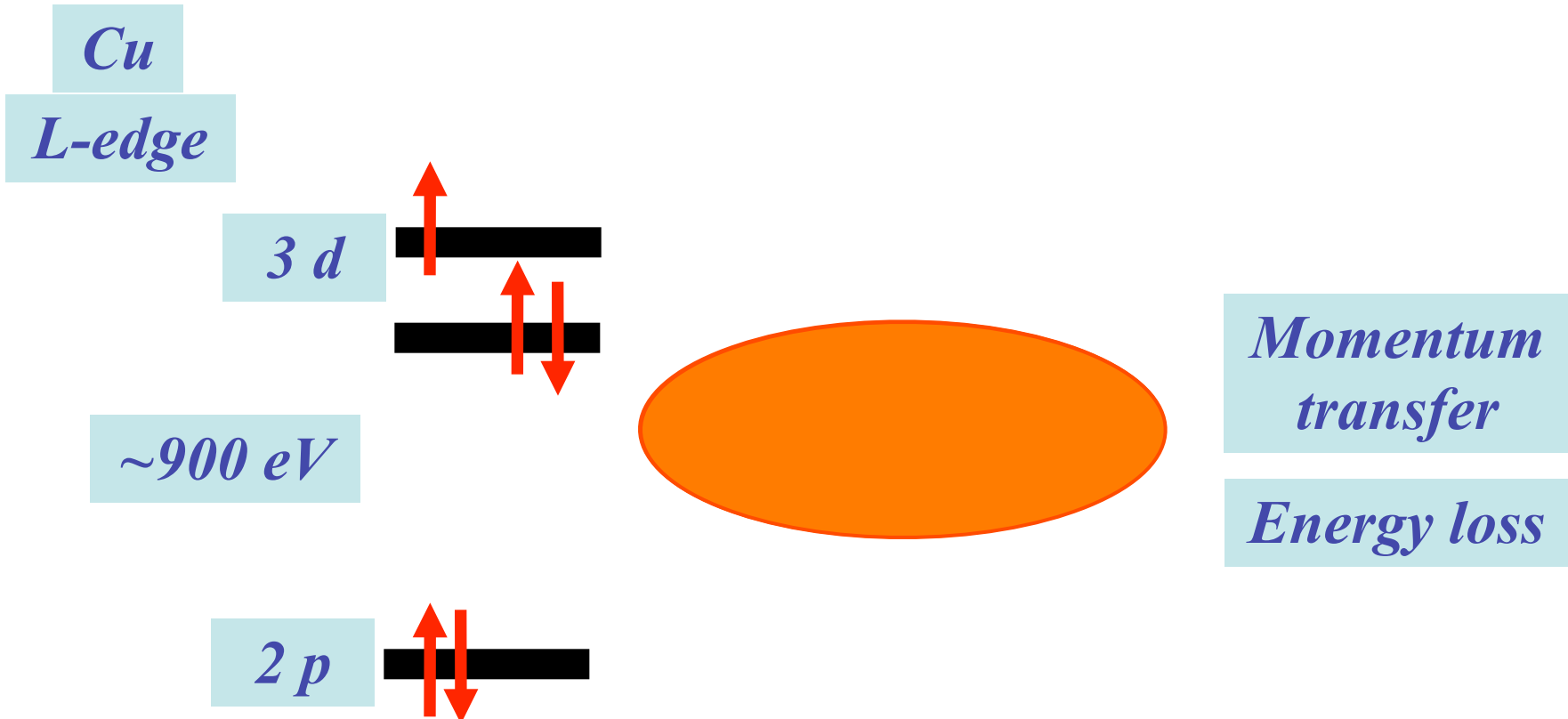
scattering via absorption-emission matrix elements

scattering via intermediate state core-hole shake-up

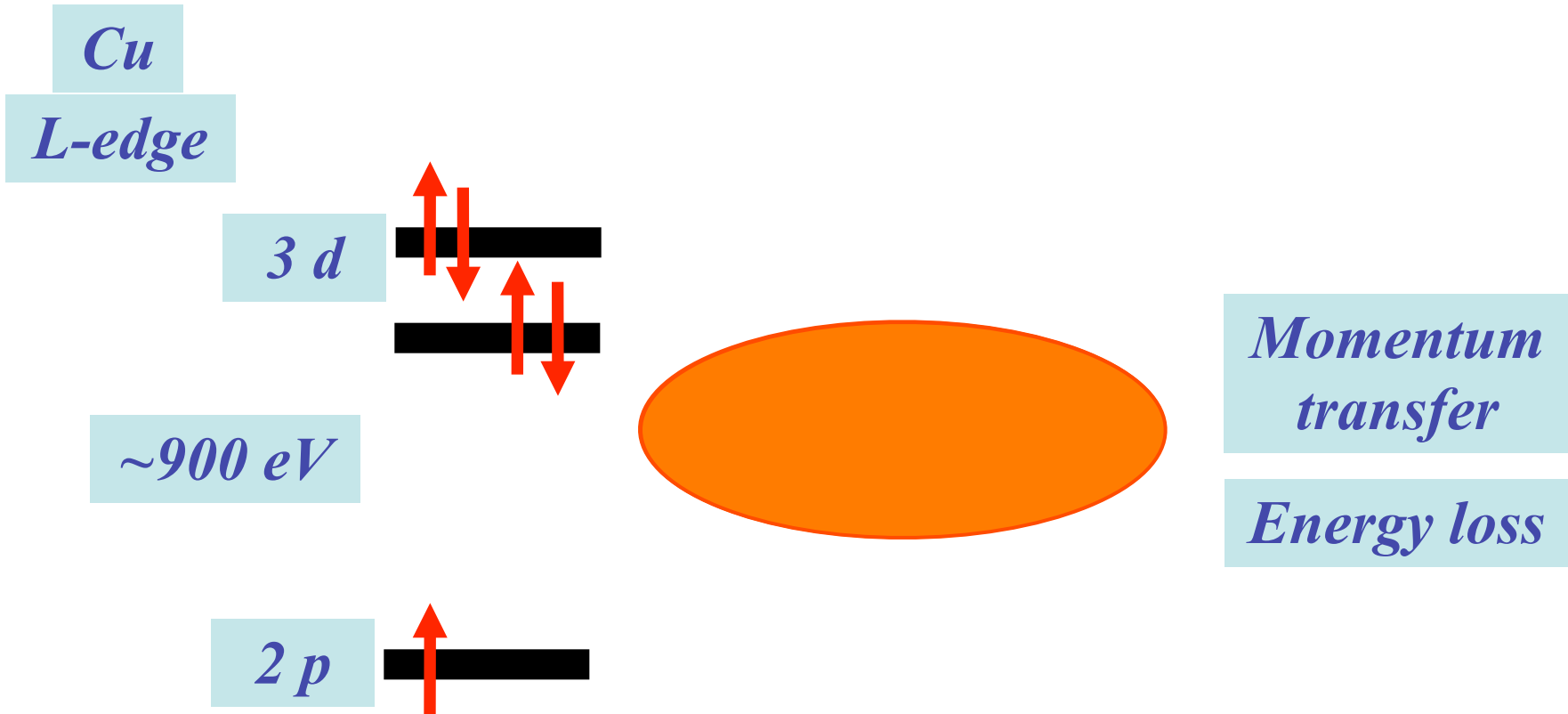


INDIRECT

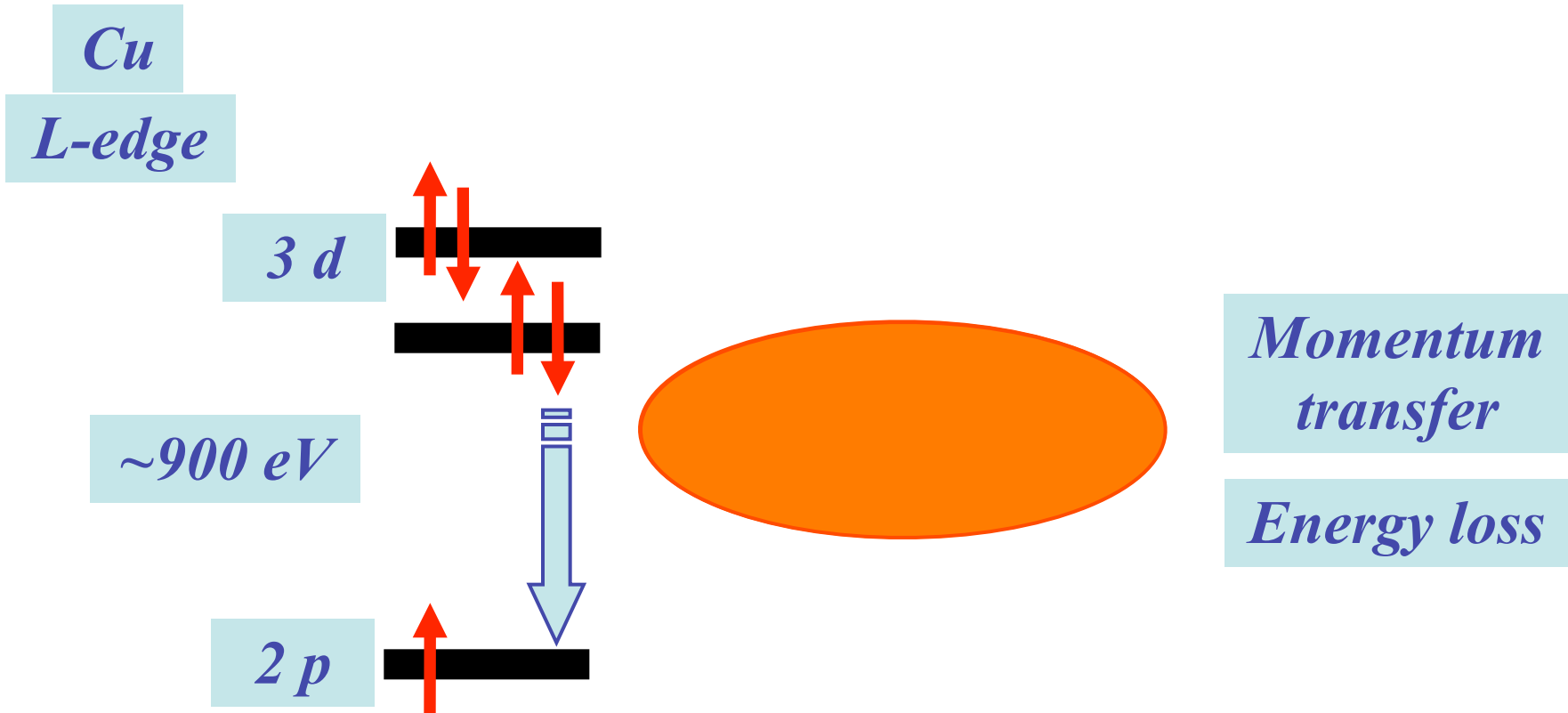
Direct RIXS @ TM L-edges



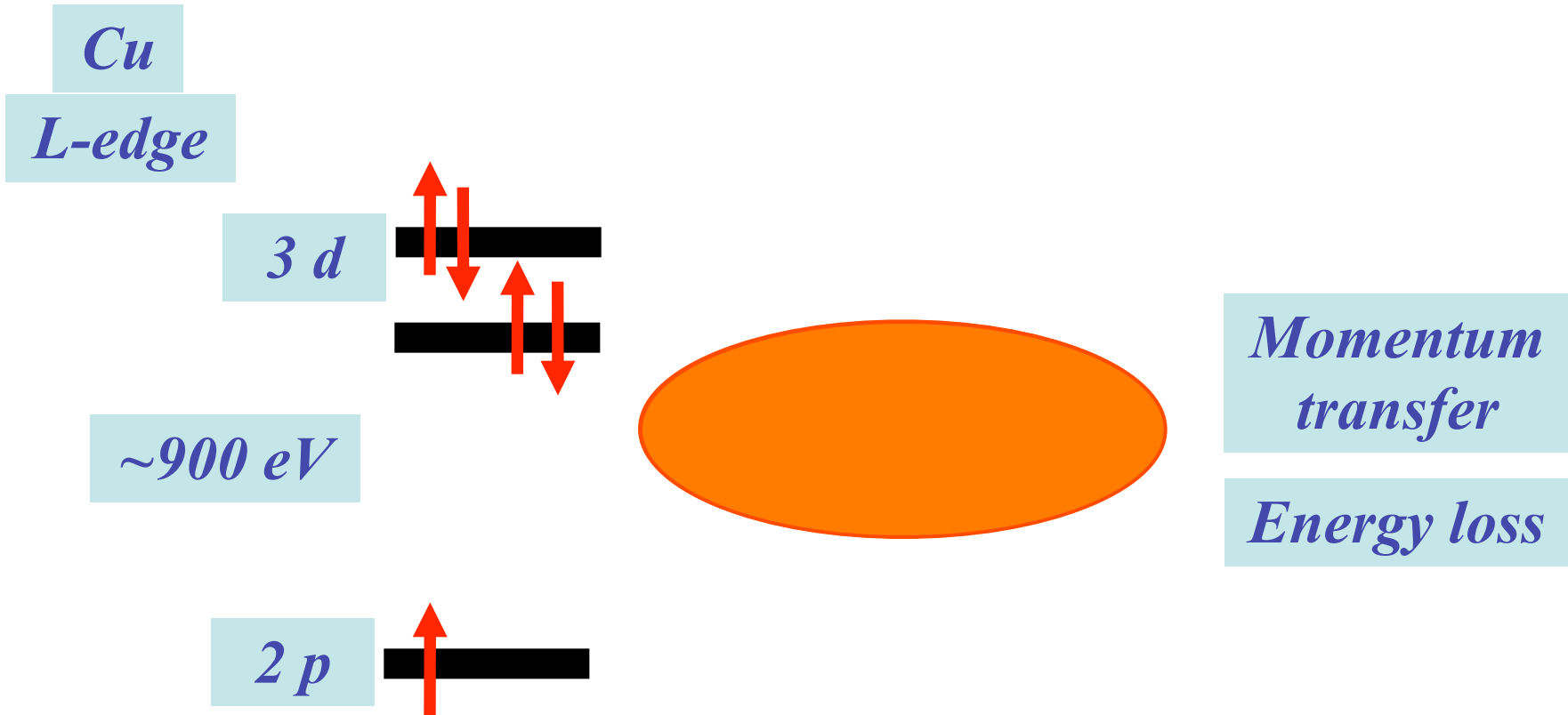
Direct RIXS @ TM L-edges



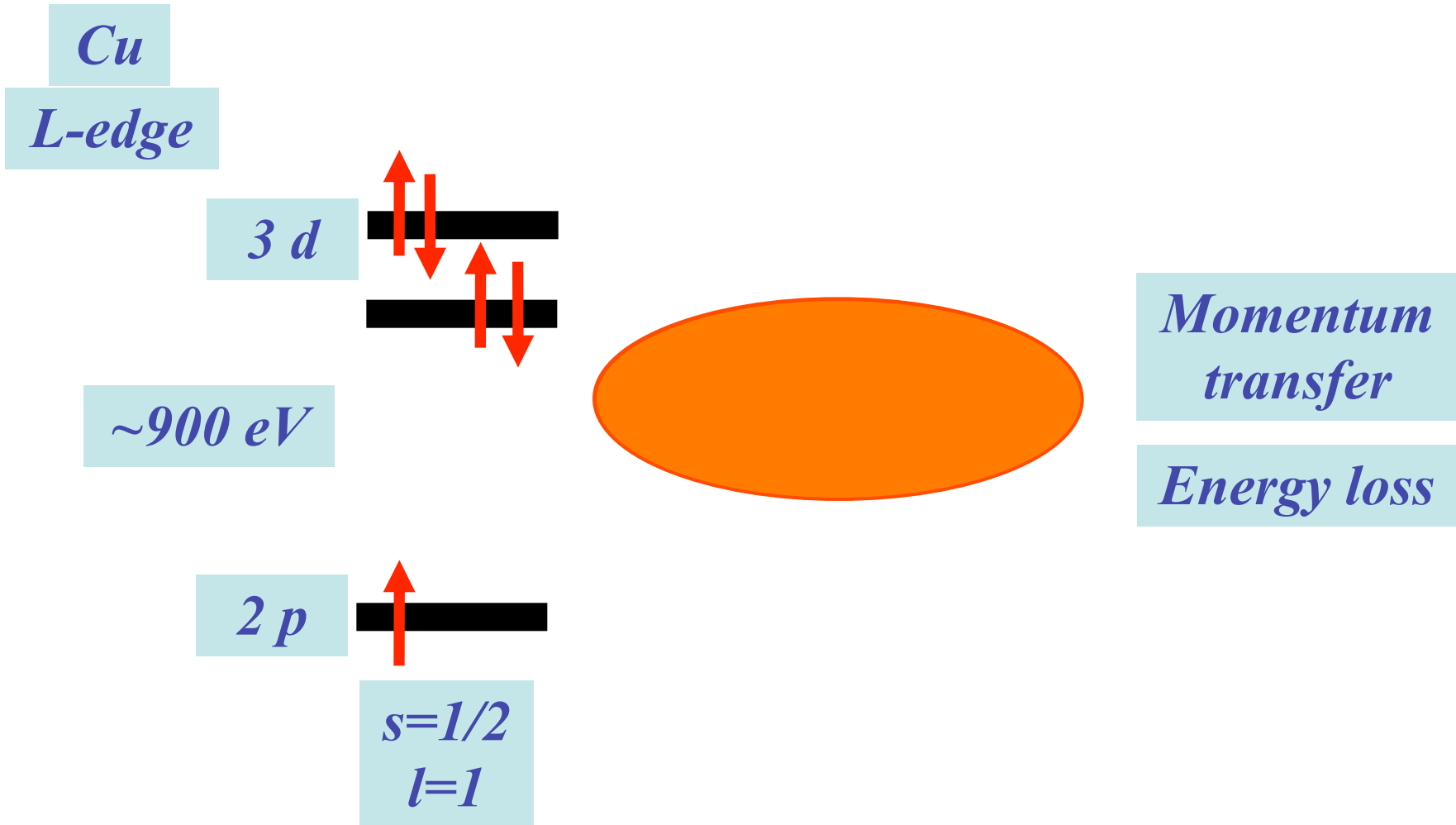
Direct RIXS @ TM L-edges



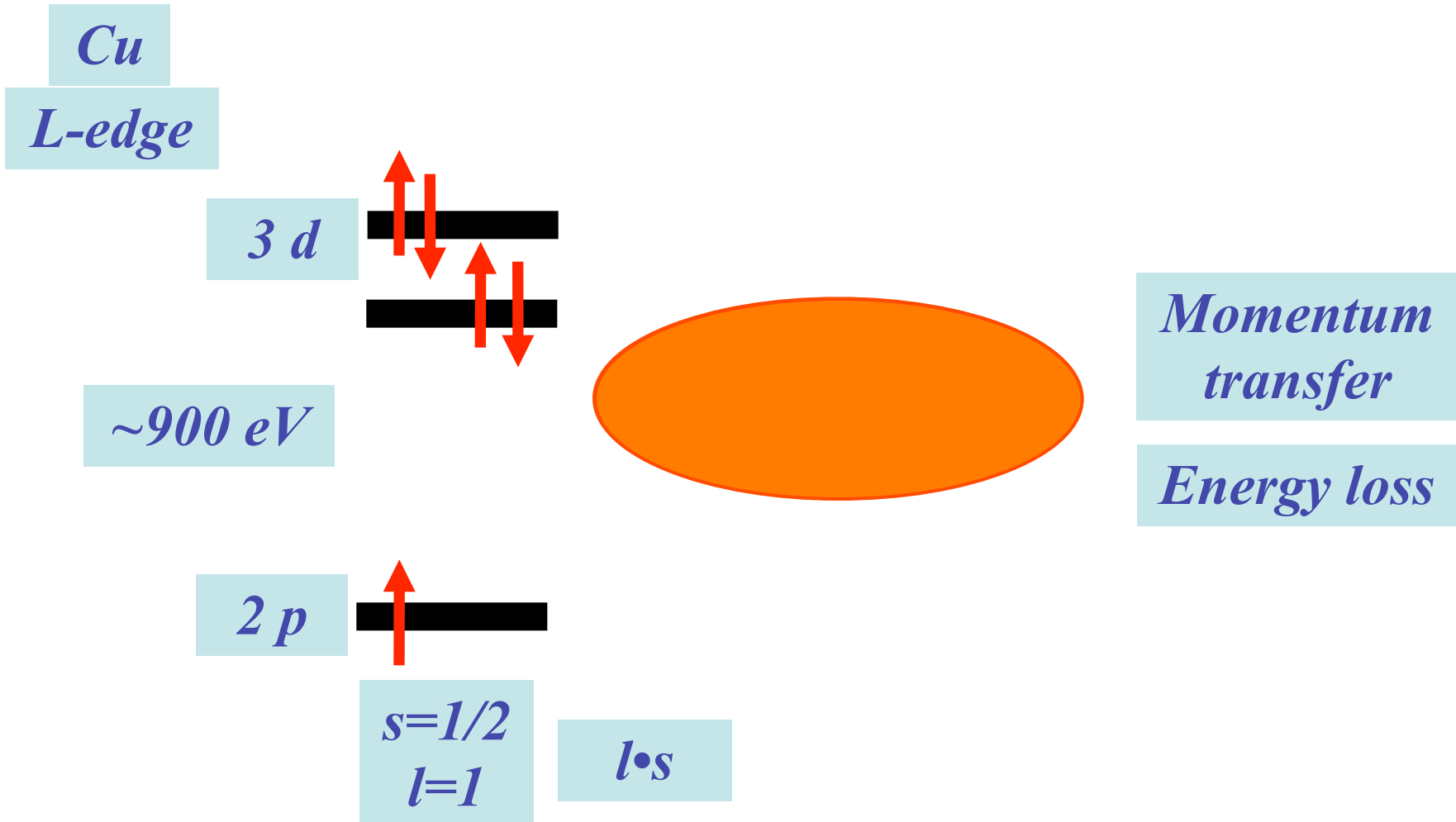
Direct RIXS @ TM L-edges



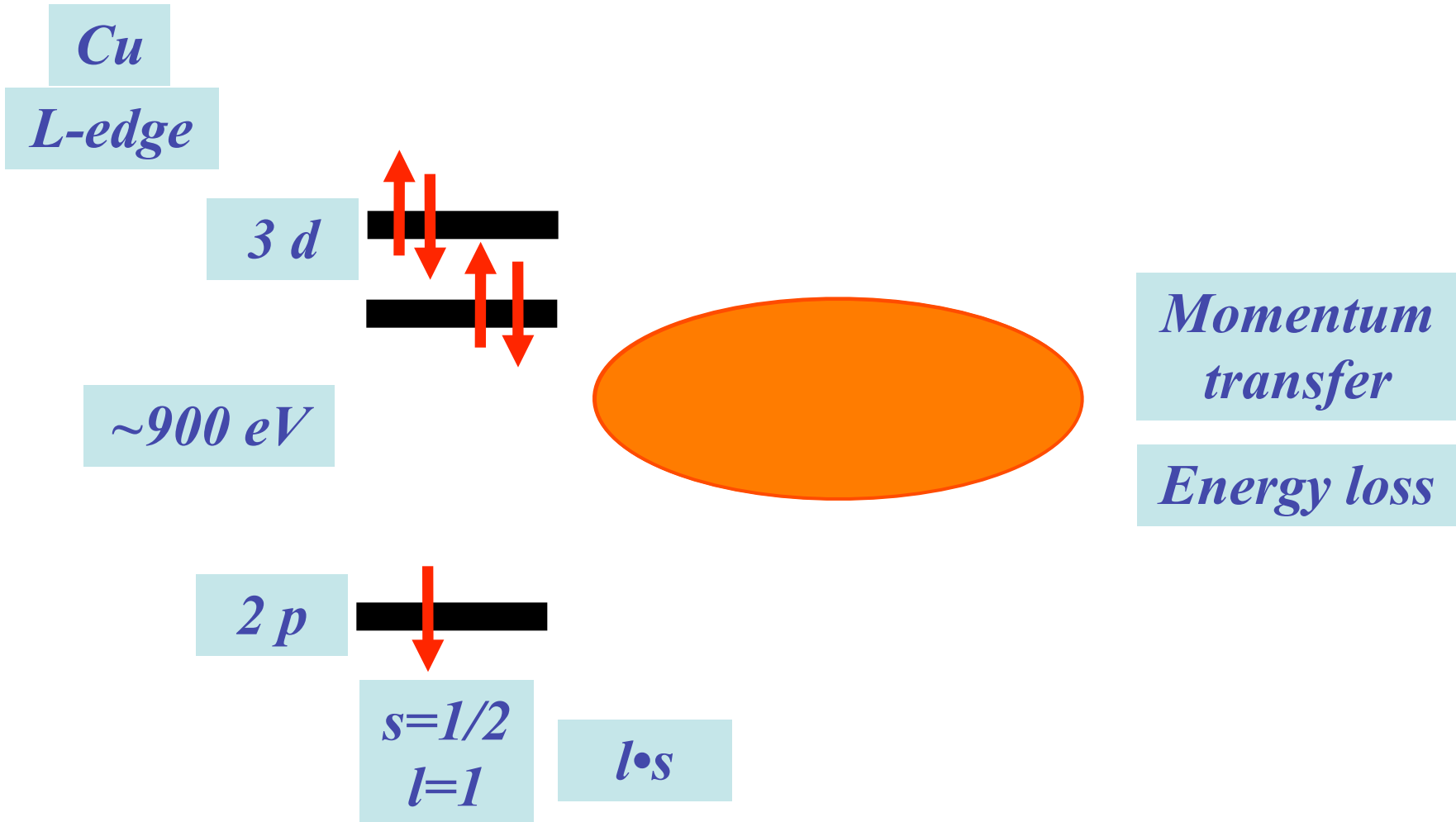
Direct RIXS @ TM L-edges



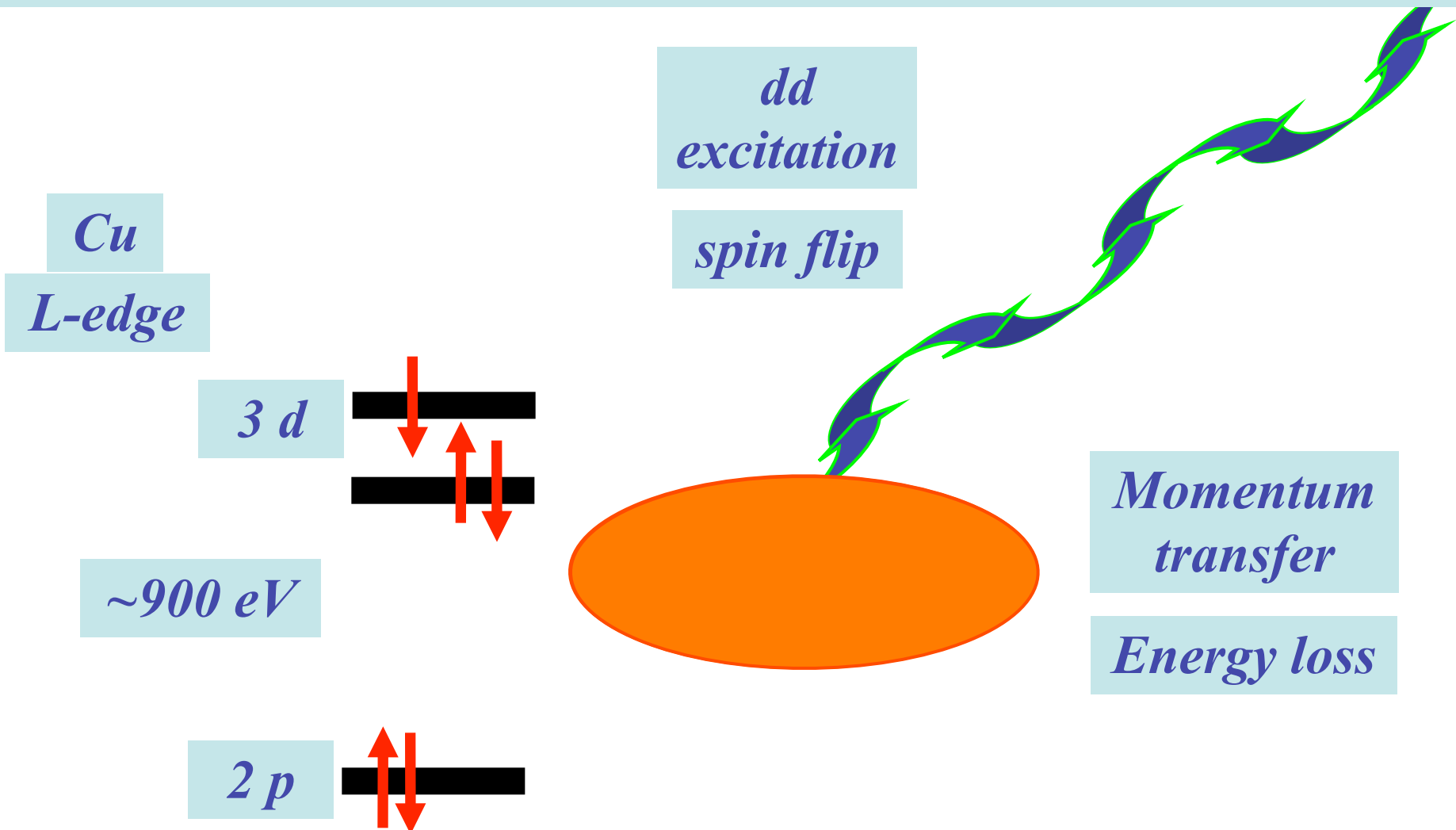
Direct RIXS @ TM L-edges



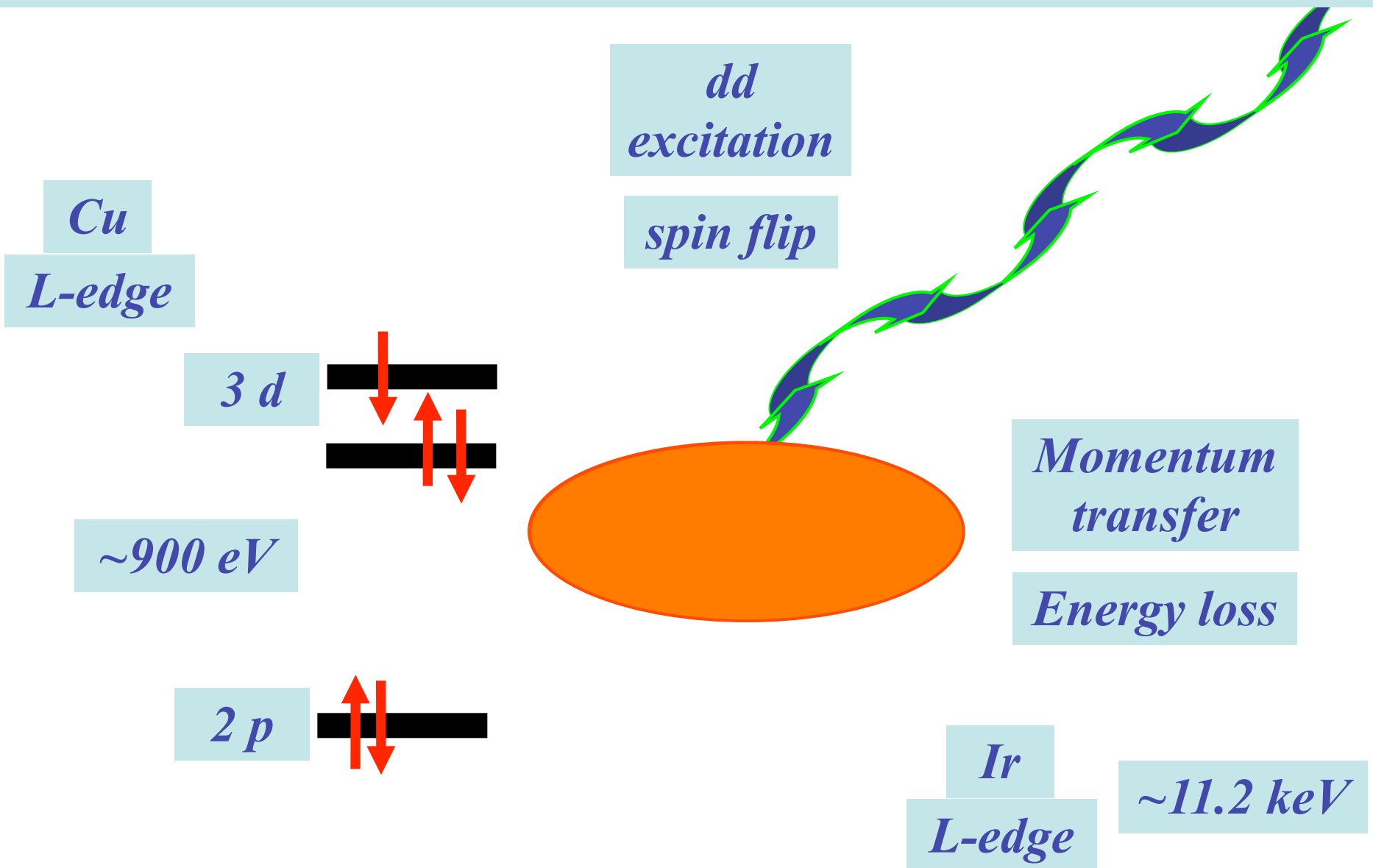
Direct RIXS @ TM L-edges



Direct RIXS @ TM L-edges



Direct RIXS @ TM L-edges



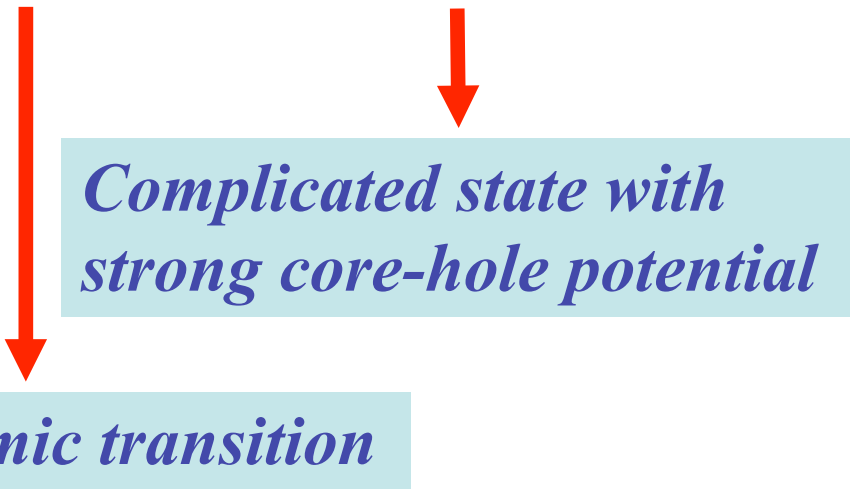
RIXS = $|GS\rangle \rightarrow XAS \rightarrow |INTERMEDIATE\rangle \rightarrow XES \rightarrow |FS\rangle$

$RIXS = |GS\rangle \rightarrow XAS \rightarrow |INTERMEDIATE\rangle \rightarrow XES \rightarrow |FS\rangle$

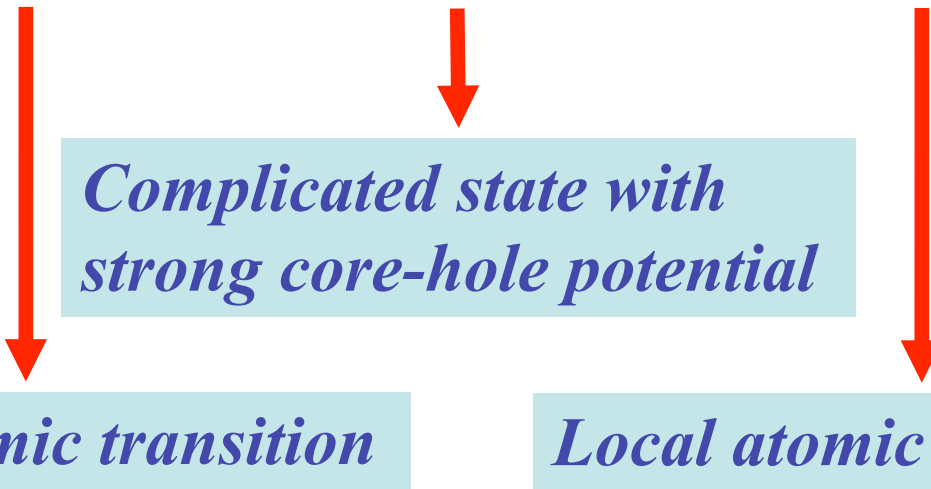


Local atomic transition

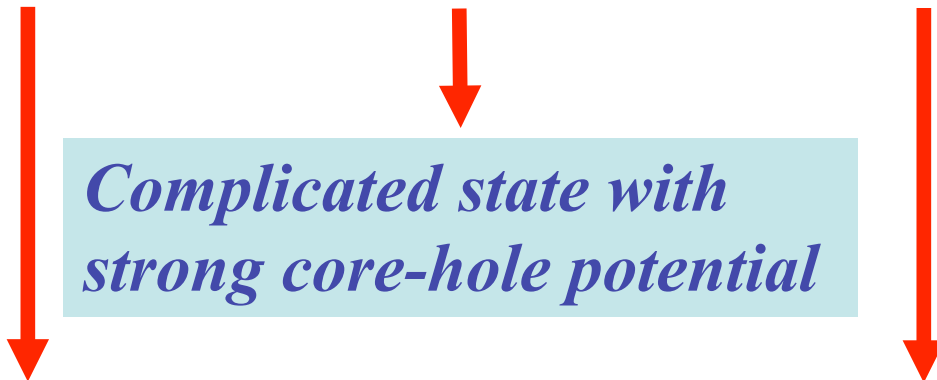
$RIXS = |GS\rangle \rightarrow XAS \rightarrow |INTERMEDIATE\rangle \rightarrow XES \rightarrow |FS\rangle$



$RIXS = |GS\rangle \rightarrow XAS \rightarrow |INTERMEDIATE\rangle \rightarrow XES \rightarrow |FS\rangle$



$RIXS = |GS\rangle \rightarrow XAS \rightarrow |INTERMEDIATE\rangle \rightarrow XES \rightarrow |FS\rangle$



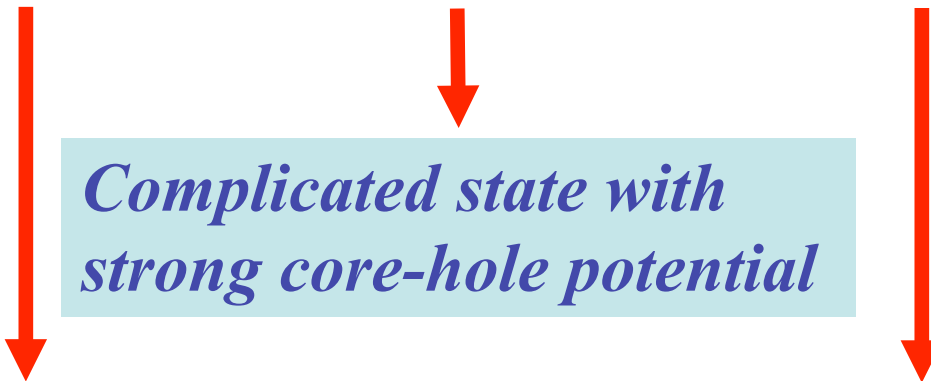
Local atomic transition

Local atomic transition

Contains chemical detail and atom specific physics

But:

$RIXS = |GS\rangle \rightarrow XAS \rightarrow |INTERMEDIATE\rangle \rightarrow XES \rightarrow |FS\rangle$



Local atomic transition

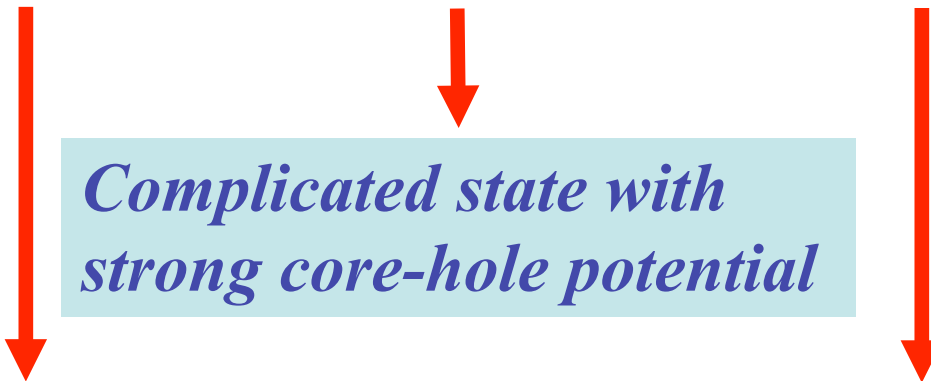
Local atomic transition

Contains chemical detail and atom specific physics

But:

$RIXS = |GS\rangle \rightarrow \dots \rightarrow |FS\rangle$

$RIXS = |GS\rangle \rightarrow XAS \rightarrow |INTERMEDIATE\rangle \rightarrow XES \rightarrow |FS\rangle$



Local atomic transition

Local atomic transition

Contains chemical detail and atom specific physics

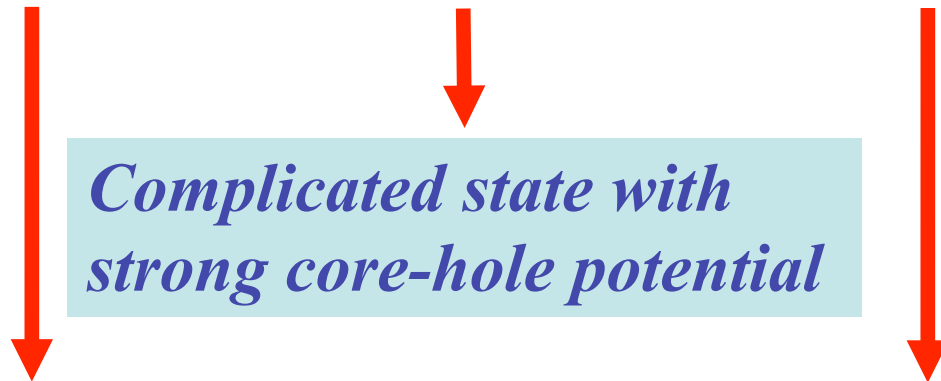
But:

$RIXS = |GS\rangle \rightarrow \dots \rightarrow |FS\rangle$



Carries low energy, long wavelength, elementary excitations

$RIXS = |GS\rangle \rightarrow XAS \rightarrow |INTERMEDIATE\rangle \rightarrow XES \rightarrow |FS\rangle$



Local atomic transition

Local atomic transition

Contains chemical detail and atom specific physics

But:

$RIXS = |GS\rangle \rightarrow \dots \rightarrow |FS\rangle$



Carries low energy, long wavelength, elementary excitations

Universal effective low energy behavior

5 distinguishing features of RIXS

Why

Inelastic Scattering

with X-rays

at a resonance

Why

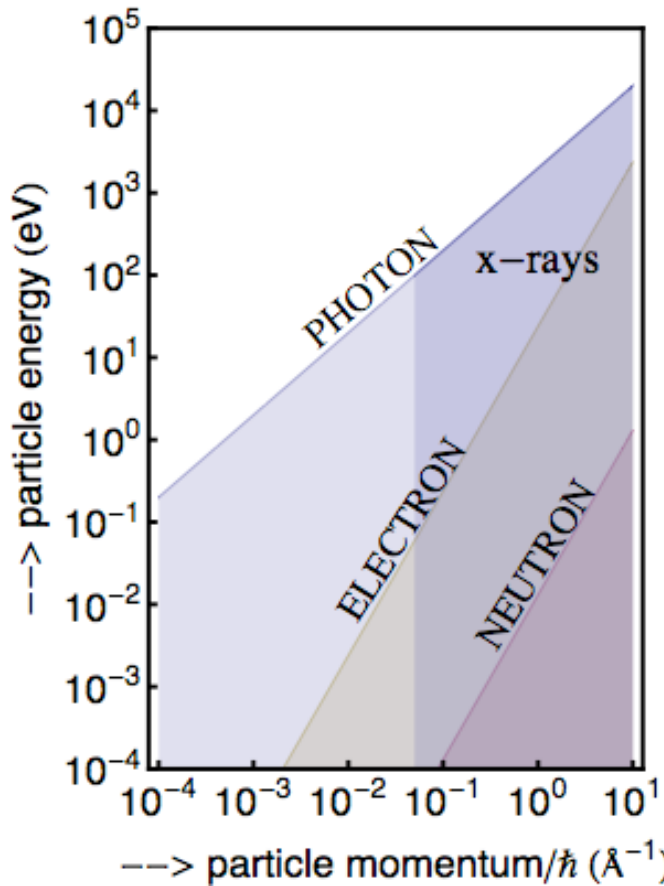
Inelastic Scattering

with X-rays

at a resonance

X-rays:

momentum $\sim \text{\AA}^{-1}$



Why

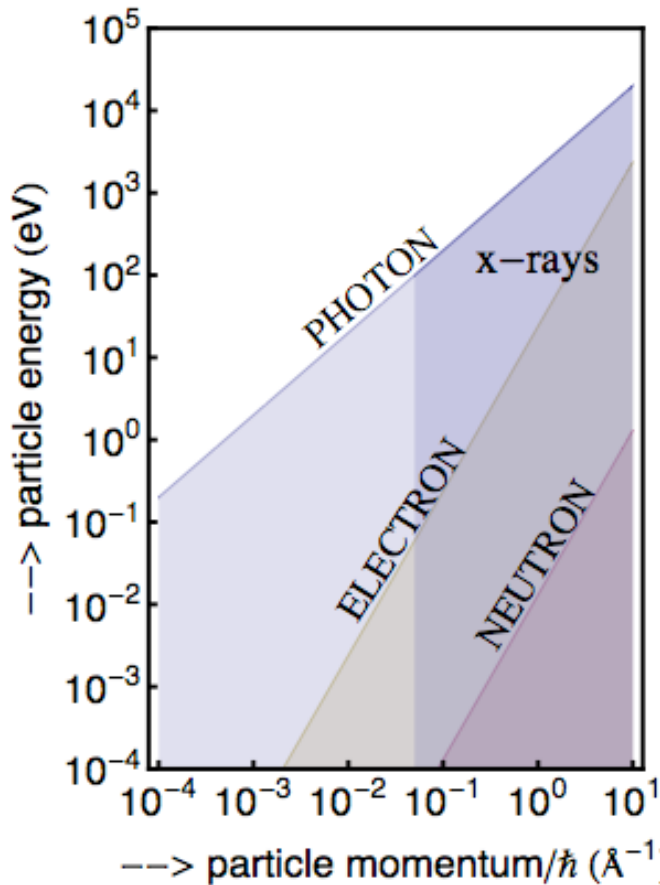
Inelastic Scattering

with X-rays

at a resonance

X-rays:

momentum $\sim \text{\AA}^{-1}$



Solid:

Lattice spacings $\sim \text{\AA}$

Brioullin zone $\sim \text{\AA}^{-1}$

Why

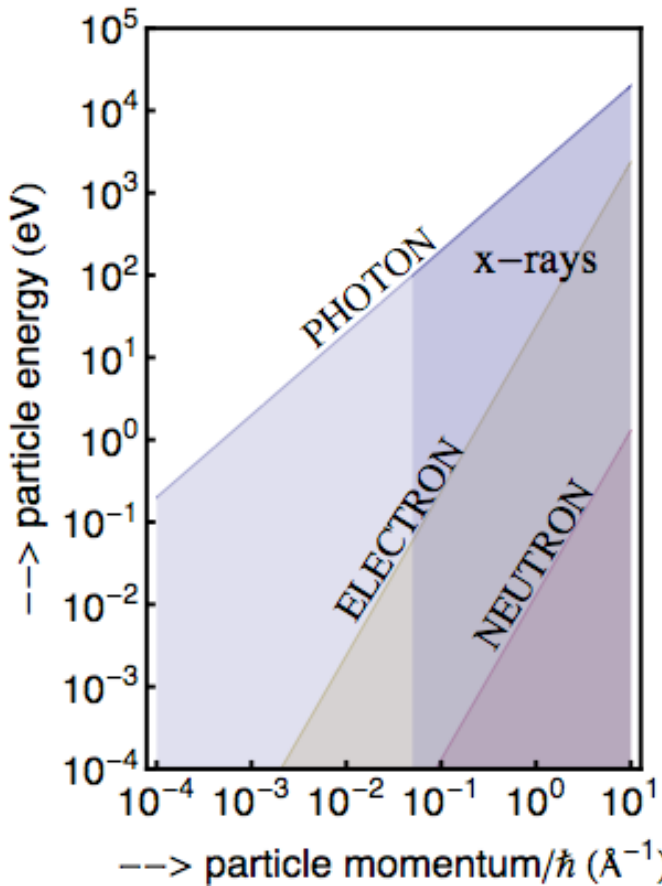
Inelastic Scattering

with X-rays

at a resonance

X-rays:

momentum $\sim \text{\AA}^{-1}$



Solid:

Lattice spacings $\sim \text{\AA}$

Brioullin zone $\sim \text{\AA}^{-1}$

*Visible
Photons:*

momentum $\sim 10^{-3} \text{\AA}^{-1}$

Why

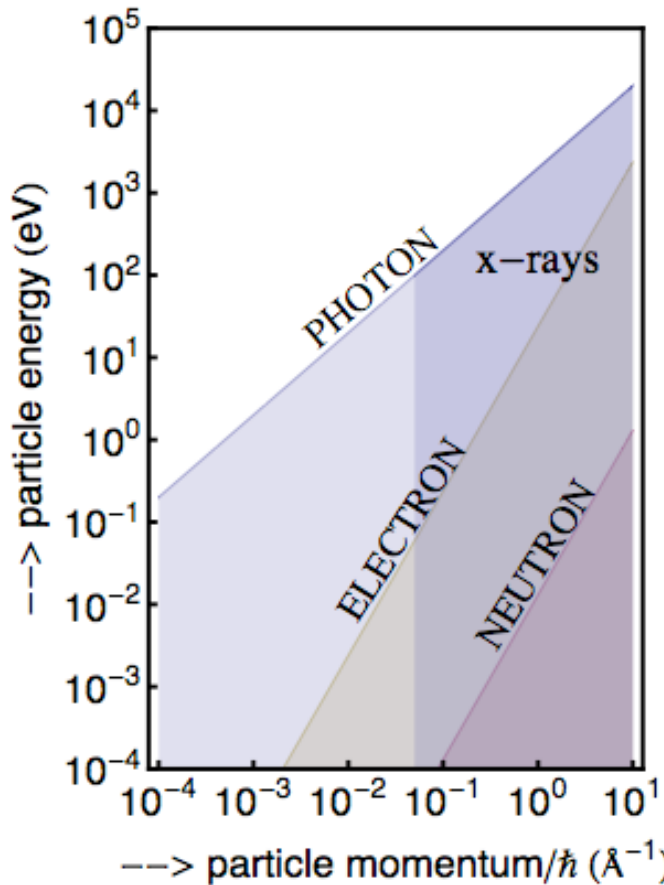
Inelastic Scattering

with X-rays

at a resonance

X-rays:

momentum $\sim \text{\AA}^{-1}$



Solid:

Lattice spacings $\sim \text{\AA}$

Brioullin zone $\sim \text{\AA}^{-1}$

*Visible
Photons:*

momentum $\sim 10^{-3} \text{\AA}^{-1}$

*X-rays at
10 keV*

momentum $\sim 5 \text{\AA}^{-1}$

several BZ's

Why

Inelastic Scattering

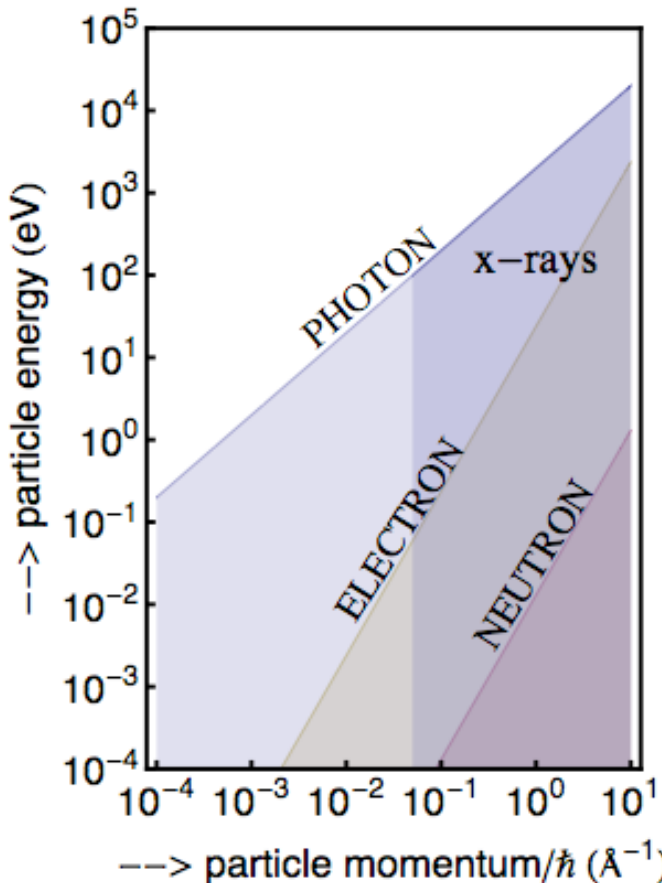
with X-rays

at a resonance

probe charged excitations

X-rays:

momentum $\sim \text{\AA}^{-1}$



Solid:

Lattice spacings $\sim \text{\AA}$

Brioullin zone $\sim \text{\AA}^{-1}$

*Visible
Photons:*

momentum $\sim 10^{-3} \text{\AA}^{-1}$

*X-rays at
10 keV*

momentum $\sim 5 \text{\AA}^{-1}$

several BZ's

Why

Inelastic Scattering

with X-rays

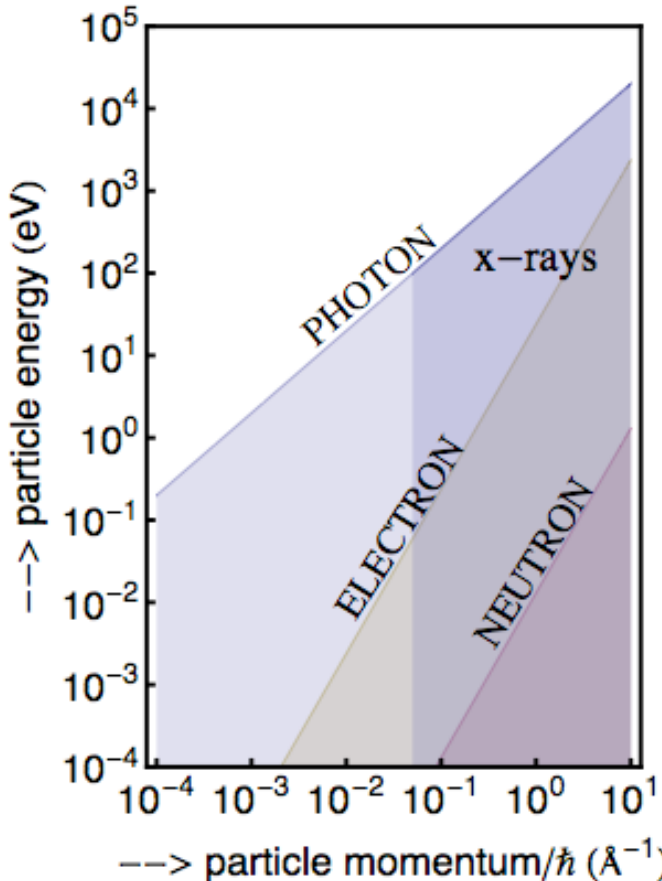
at a resonance

probe charged excitations

have angular momentum $l=1$

X-rays:

momentum $\sim \text{\AA}^{-1}$



Solid:

Lattice spacings $\sim \text{\AA}$

Brioullin zone $\sim \text{\AA}^{-1}$

*Visible
Photons:*

momentum $\sim 10^{-3} \text{\AA}^{-1}$

*X-rays at
10 keV*

momentum $\sim 5 \text{\AA}^{-1}$

several BZ's

Why

Inelastic Scattering

with X-rays

at a resonance

probe charged excitations

have angular momentum $l=1$

polarization dependence

Lattice spacings $\sim \text{\AA}$

Brioullin zone $\sim \text{\AA}^{-1}$

Solid:

*Visible
Photons:*

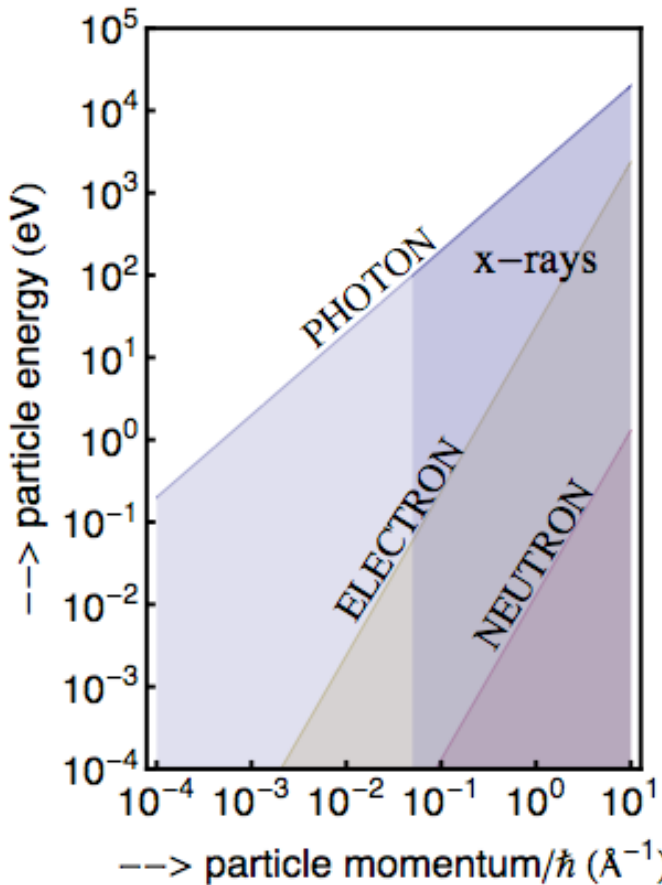
momentum $\sim 10^{-3} \text{\AA}^{-1}$

momentum $\sim 5 \text{\AA}^{-1}$

several BZ's

X-rays:

momentum $\sim \text{\AA}^{-1}$



*X-rays at
10 keV*

1. RIXS exploits both the *energy and momentum* dependence of the photon scattering cross-section. Comparing the energies of a neutron, electron, and photon, each with a wavelength on the order of the relevant length scale in a solid, *i.e.* the interatomic lattice spacing, which is on the order of a few Angstroms, it is obvious that an x-ray photon has much more energy than an equivalent neutron or electron.

1. RIXS exploits both the *energy and momentum* dependence of the photon scattering cross-section. Comparing the energies of a neutron, electron, and photon, each with a wavelength on the order of the relevant length scale in a solid, *i.e.* the interatomic lattice spacing, which is on the order of a few Angstroms, it is obvious that an x-ray photon has much more energy than an equivalent neutron or electron.

The scattering phase space (the range of energies and momenta that can be transferred in a scattering event) available to x-rays is therefore correspondingly larger and is in fact without equal. For instance, unlike photon scattering experiments with visible or infrared light, RIXS can probe the full dispersion of low energy excitations in solids.

2. RIXS can utilize the *polarization* of the photon: the nature of the excitations created in the material can be disentangled through polarization analysis of the incident and scattered photons, which allows one, through the use of various selection rules, to characterize the symmetry and nature of the excitations. To date, no experimental facility allows the polarization of the scattered photon to be measured, though the incident photon polarization is frequently varied.

2. RIXS can utilize the *polarization* of the photon: the nature of the excitations created in the material can be disentangled through polarization analysis of the incident and scattered photons, which allows one, through the use of various selection rules, to characterize the symmetry and nature of the excitations. To date, no experimental facility allows the polarization of the scattered photon to be measured, though the incident photon polarization is frequently varied. It is important to note that a polarization change of a photon is necessarily related to an angular momentum change. Conservation of angular momentum means that any angular momentum lost by the scattered photons has been transferred to elementary excitations in the solid.

Why

Inelastic Scattering

with X-rays

at a resonance

Why

Inelastic Scattering

At resonance:

enhanced loss features

with X-rays

at a resonance

Why

Inelastic Scattering

with X-rays

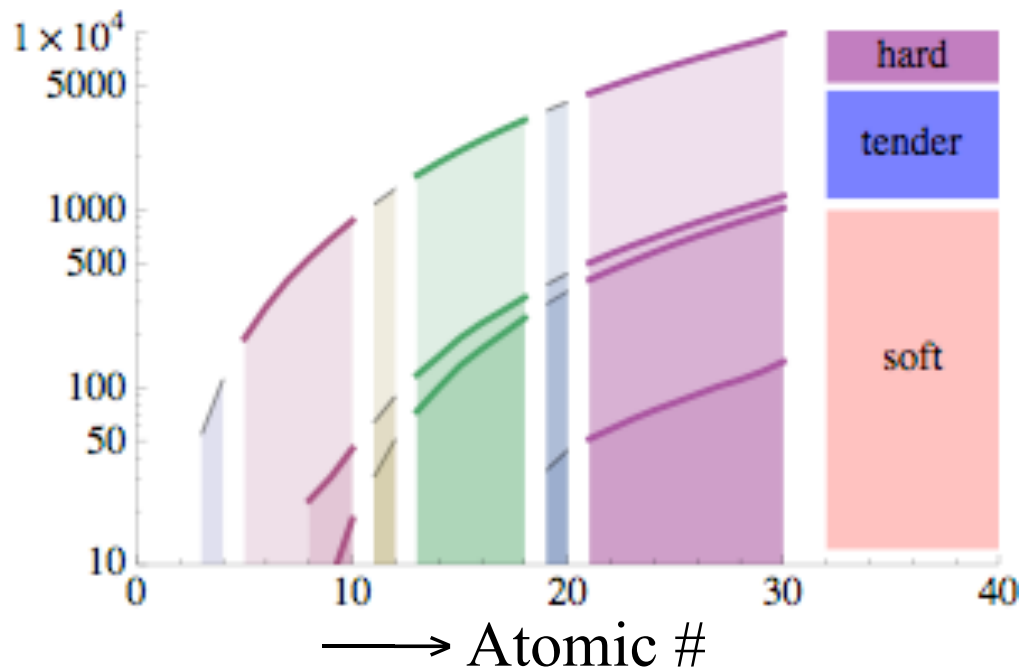
at a resonance

At resonance:

enhanced loss features

choose element & electronic shell

X-ray Absorption Edges



Why

Inelastic Scattering

with X-rays

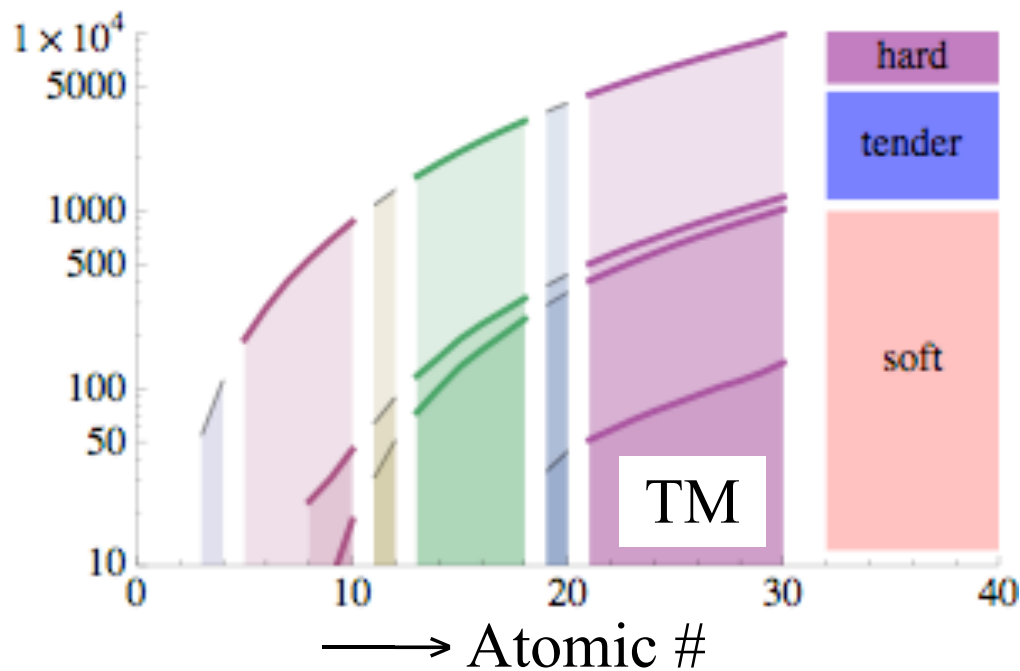
at a resonance

At resonance:

enhanced loss features

choose element & electronic shell

X-ray Absorption Edges



Why

Inelastic Scattering

with X-rays

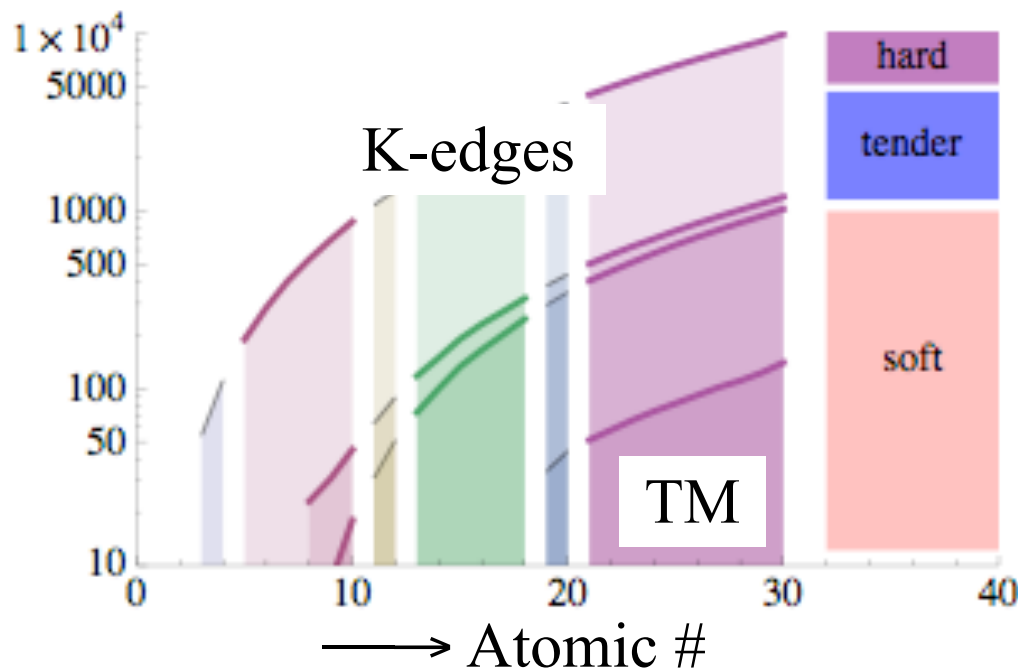
at a resonance

At resonance:

enhanced loss features

choose element & electronic shell

X-ray Absorption Edges



Why

Inelastic Scattering

with X-rays

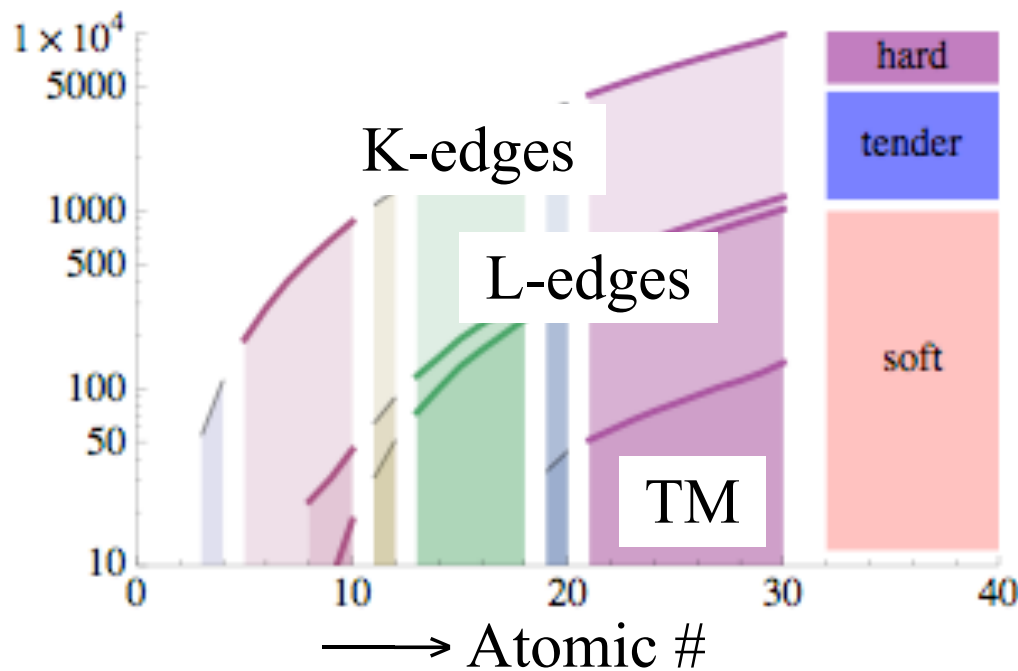
at a resonance

At resonance:

enhanced loss features

choose element & electronic shell

X-ray Absorption Edges



Why

Inelastic Scattering

with X-rays

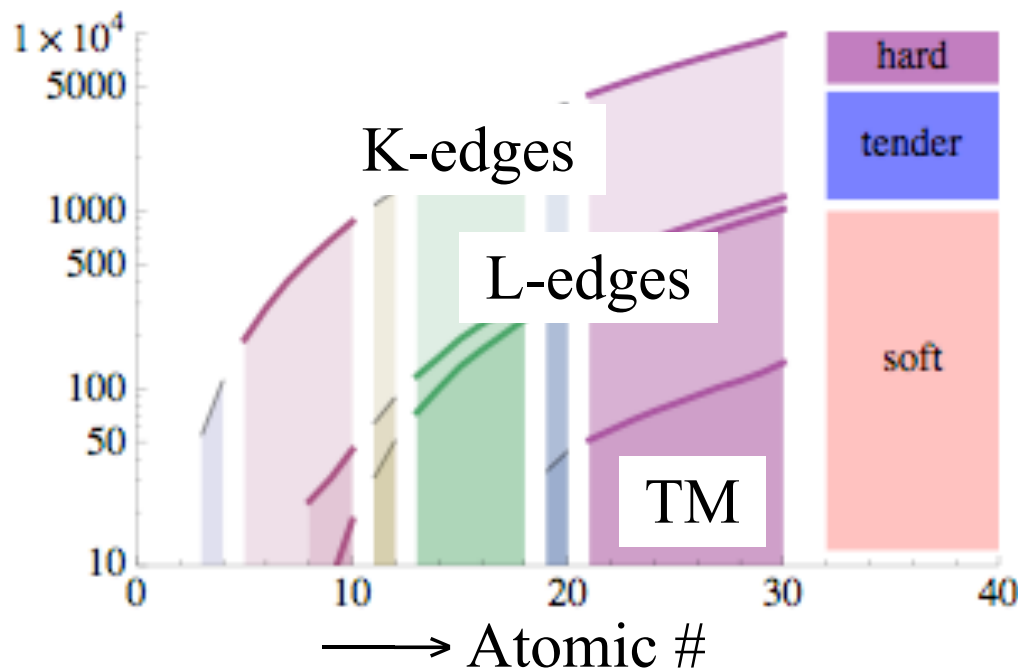
at a resonance

At resonance:

enhanced loss features

choose element & electronic shell

X-ray Absorption Edges



X-ray penetration depth: \sim microns

Why

Inelastic Scattering

with X-rays

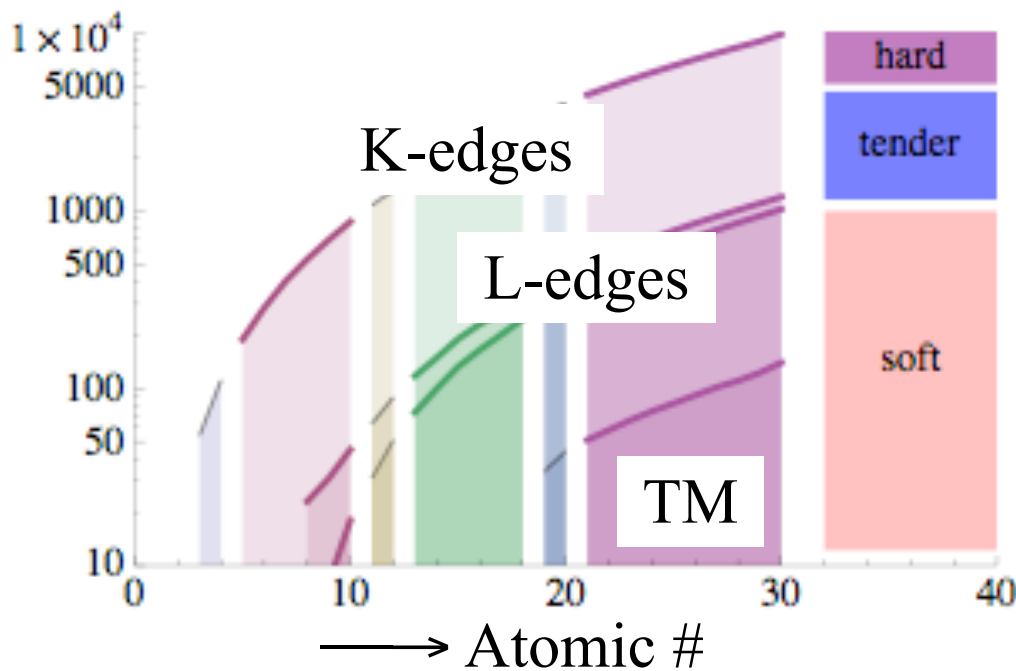
at a resonance

At resonance:

enhanced loss features

choose element & electronic shell

X-ray Absorption Edges

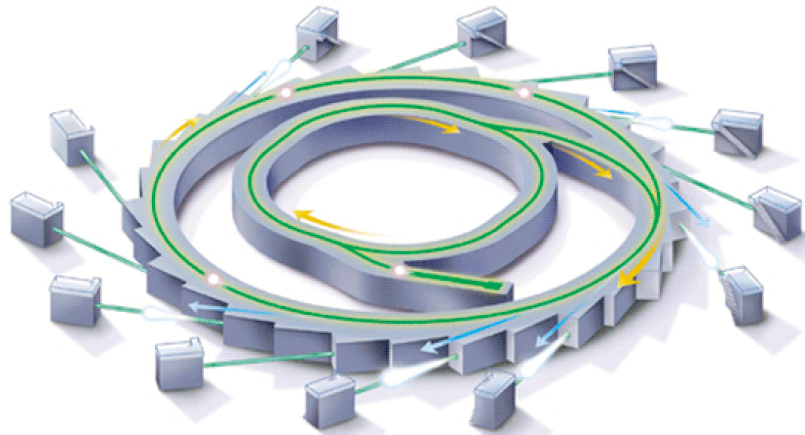


X-ray penetration depth: \sim microns

RIXS is bulk sensitive

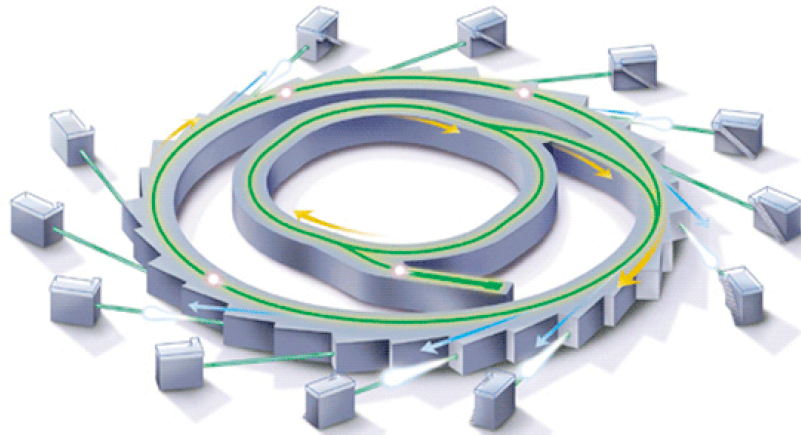
Tunable X-ray sources

synchrotron



Tunable X-ray sources

synchrotron



Tunable X-ray sources

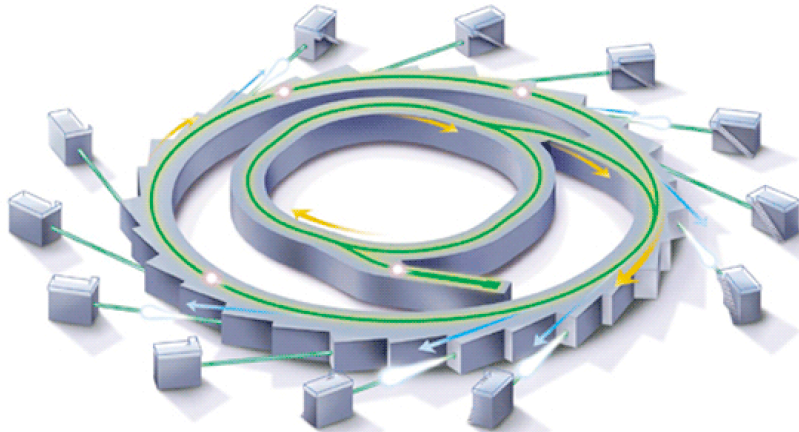
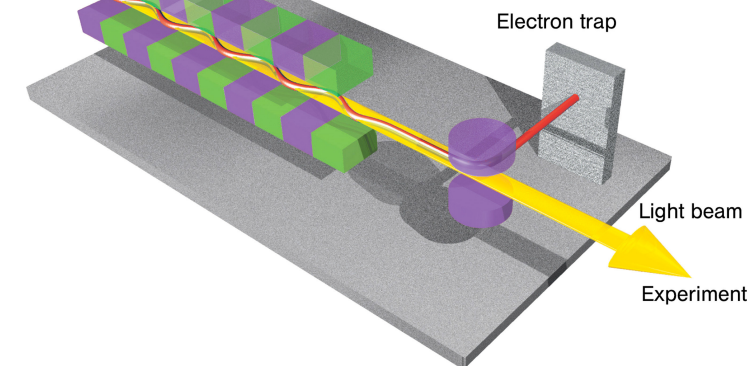
synchrotron



Electron source
and accelerator

Magnetic structure

X-ray laser



LCLS, Stanford

3. RIXS is *element and orbital specific*: Chemical sensitivity arises by tuning the incident photon energy to specific atomic transitions of the different types of atoms in a material. Such transitions are called absorption edges. RIXS can even differentiate between the same chemical element at sites with inequivalent chemical bondings, with different valencies or at inequivalent crystallographic positions if the absorption edges in these cases are distinguishable.

3. RIXS is *element and orbital specific*: Chemical sensitivity arises by tuning the incident photon energy to specific atomic transitions of the different types of atoms in a material. Such transitions are called absorption edges. RIXS can even differentiate between the same chemical element at sites with inequivalent chemical bondings, with different valencies or at inequivalent crystallographic positions if the absorption edges in these cases are distinguishable. In addition, the type of information that may be gleaned about the electronic excitations can be varied by tuning to different x-ray edges of the same chemical element (e.g., *K* edge for exciting $1s$ core electrons, *L* edge for electrons in the $n = 2$ shell or *M* edge for $n = 3$ electrons), since the photon excites different core-electrons into different valence orbitals at each edge.

4. RIXS is *bulk sensitive*: the penetration depth of resonant x-ray photons is material and scattering geometry-specific, but typically is on the order of a few μm in the hard x-ray regime (for example at transition metal *K*-edges) and on the order of 0.1 μm in the soft x-ray regime (e.g transition metal *L*-edges).

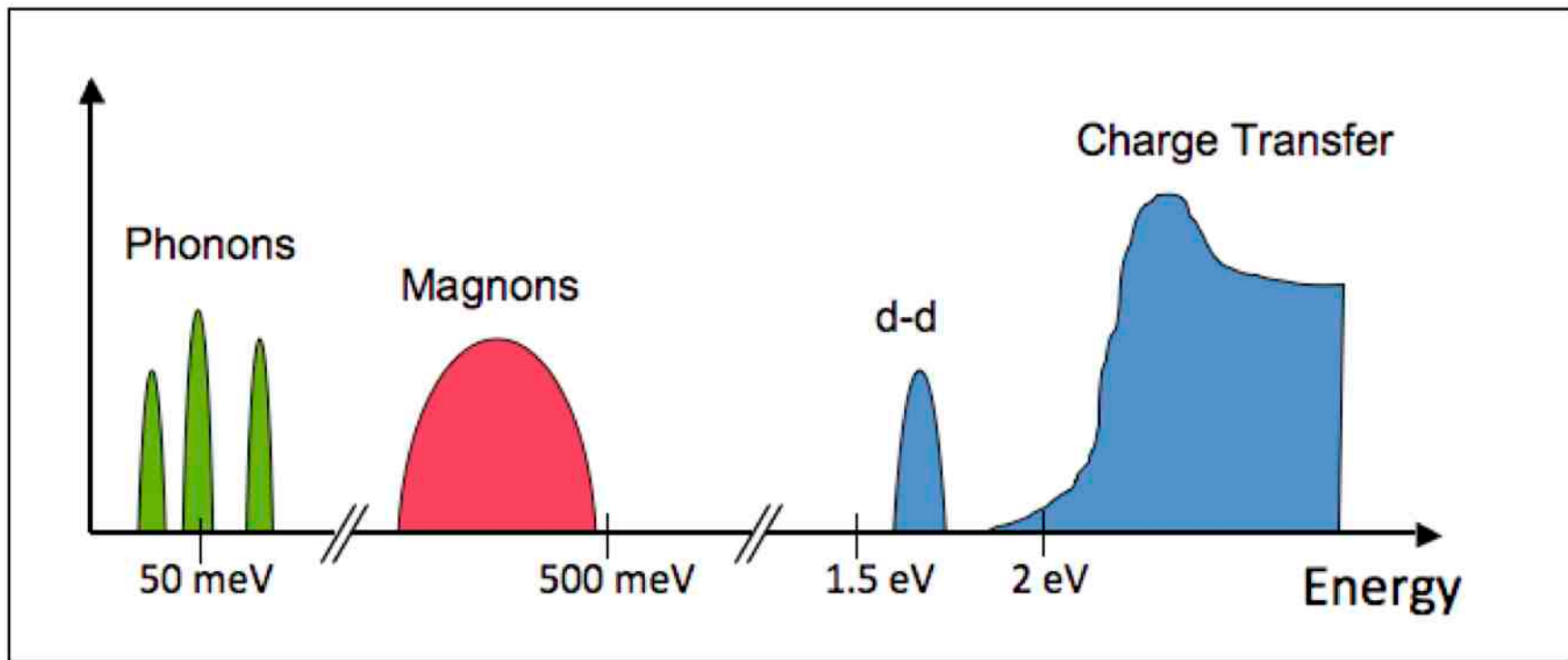
4. RIXS is *bulk sensitive*: the penetration depth of resonant x-ray photons is material and scattering geometry-specific, but typically is on the order of a few μm in the hard x-ray regime (for example at transition metal *K*-edges) and on the order of 0.1 μm in the soft x-ray regime (e.g transition metal *L*-edges).

5. RIXS needs only *small sample volumes*: the photon-matter interaction is relatively strong, compared to for instance the neutron-matter interaction strength. In addition, photon sources deliver many orders of magnitude more particles per second, in a much smaller spot, than do neutron sources. These facts make RIXS possible on very small volume samples, thin films, surfaces and nano-objects, in addition to bulk single crystal or powder samples.

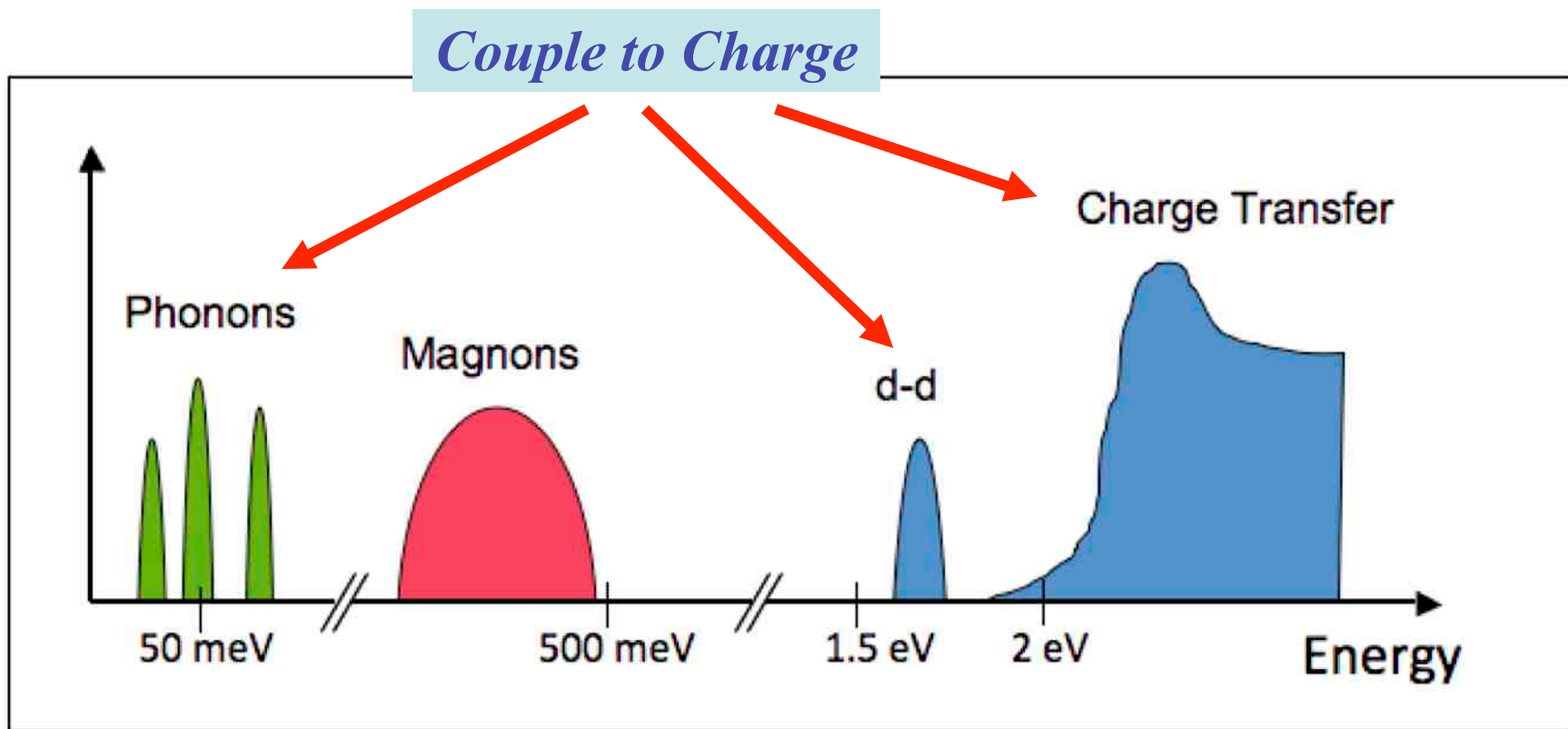
Elementary Excitations

accessible to RIXS

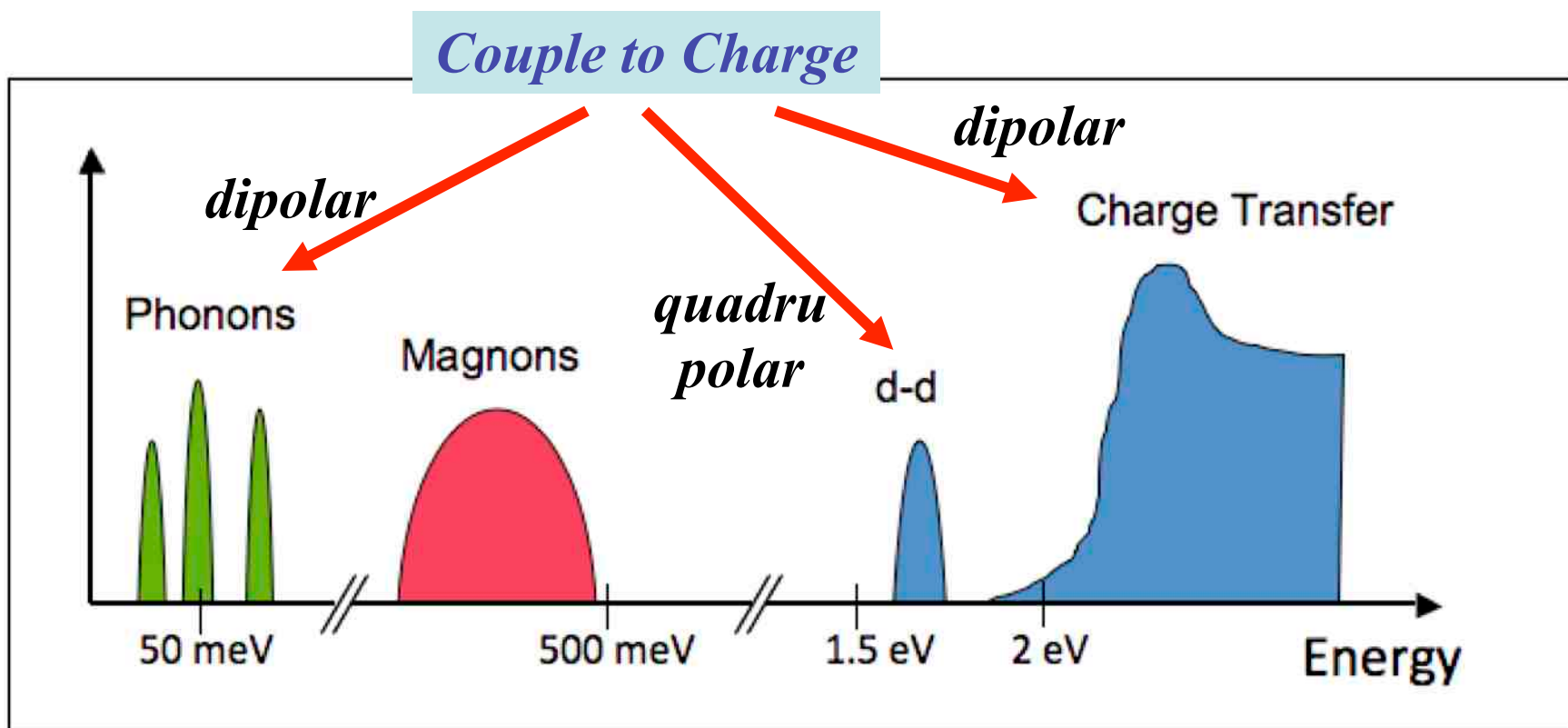
Elementary Excitations in TMO: Schematic



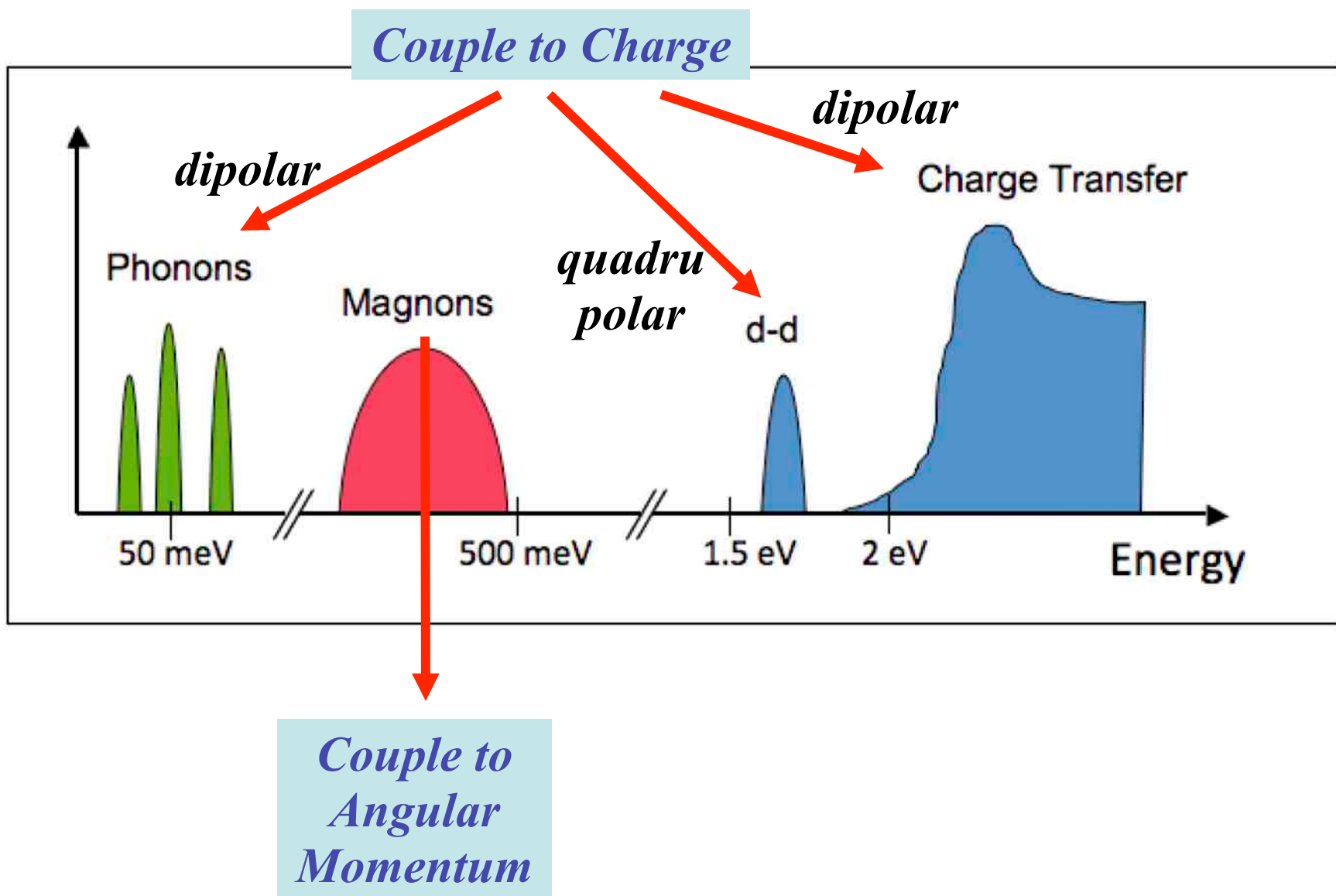
Elementary Excitations in TMO: Schematic



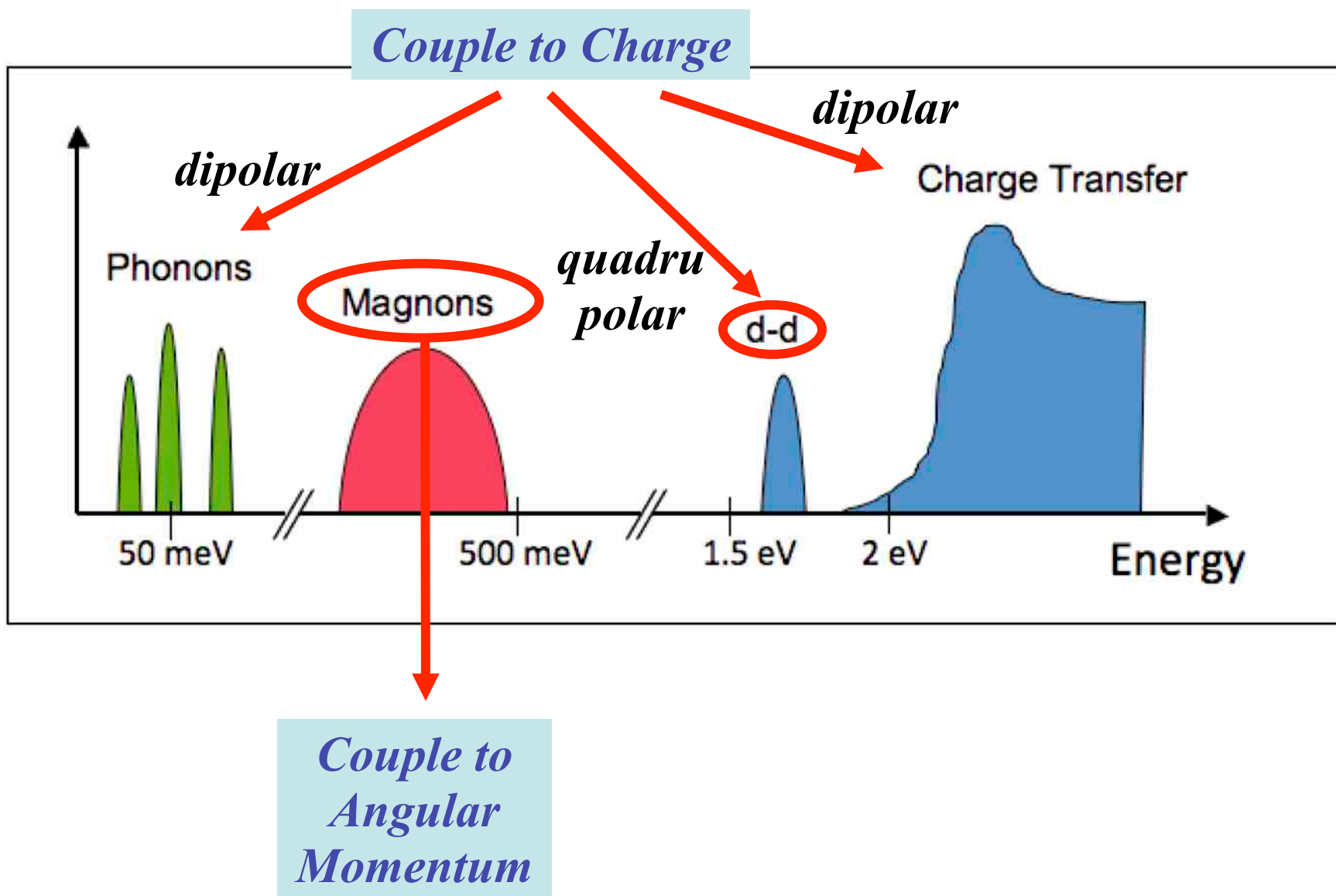
Elementary Excitations in TMO: Schematic



Elementary Excitations in TMO: Schematic



Elementary Excitations in TMO: Schematic



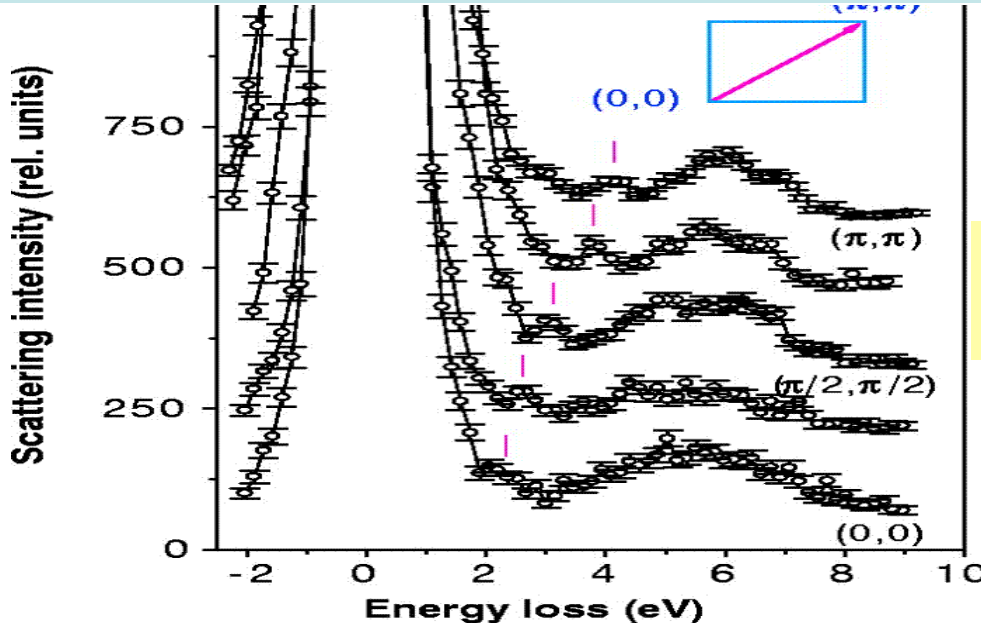
In principle RIXS can probe a very broad class of intrinsic excitations of the system under study – as long as these excitations are overall charge neutral. This constraint arises from the fact that in RIXS the scattered photons do not add or remove charge from the system under study.

In principle RIXS can probe a very broad class of intrinsic excitations of the system under study – as long as these excitations are overall charge neutral. This constraint arises from the fact that in RIXS the scattered photons do not add or remove charge from the system under study. In principle then, RIXS has a finite cross section for probing the energy, momentum and polarization dependence of, for instance, the electron-hole continuum and excitons in band metals and semiconductors, charge transfer and dd -excitations excitations in strongly correlated materials, lattice excitations and so on

In principle RIXS can probe a very broad class of intrinsic excitations of the system under study – as long as these excitations are overall charge neutral. This constraint arises from the fact that in RIXS the scattered photons do not add or remove charge from the system under study. In principle then, RIXS has a finite cross section for probing the energy, momentum and polarization dependence of, for instance, the electron-hole continuum and excitons in band metals and semiconductors, charge transfer and *dd*-excitations excitations in strongly correlated materials, lattice excitations and so on. In addition magnetic excitations are also symmetry-allowed in RIXS, because the orbital angular momentum that the photons carry can in principle be transferred to the electron's spin angular moment.

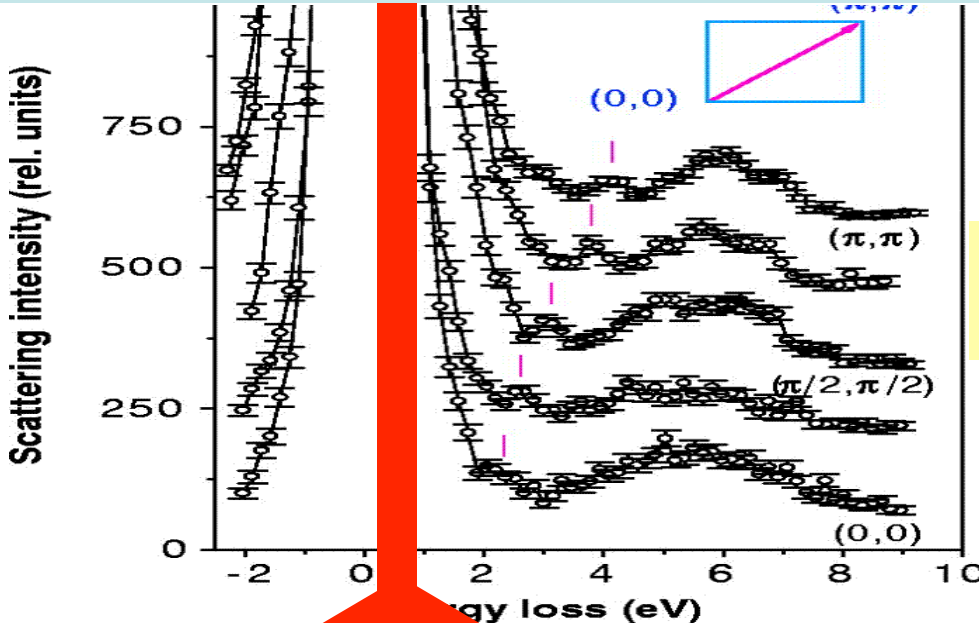
Progress in the Past Decades

Progress @ Cu K-edge resolution

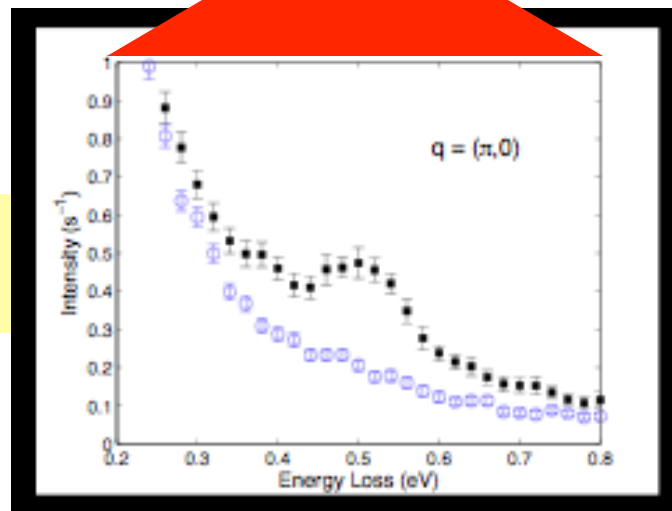


Zahid Hasan
et al., (2000)

Progress @ Cu K-edge resolution



Zahid Hasan
et al., (2000)

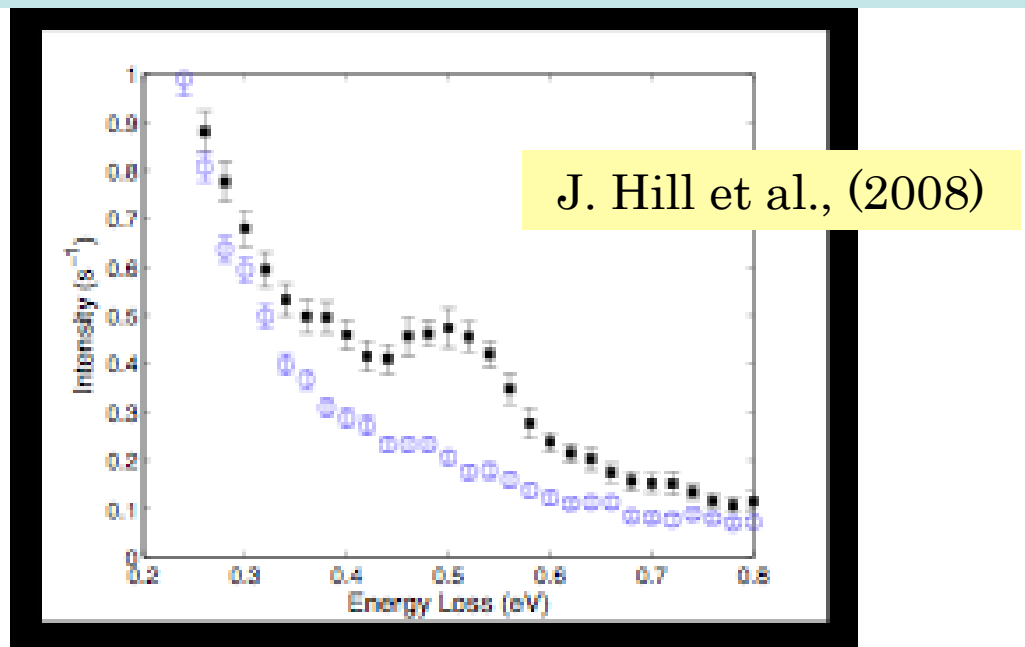


J. Hill et al., PRL
100, 097001 (2008)

*Cu K-edge on
 La_2CuO_4*

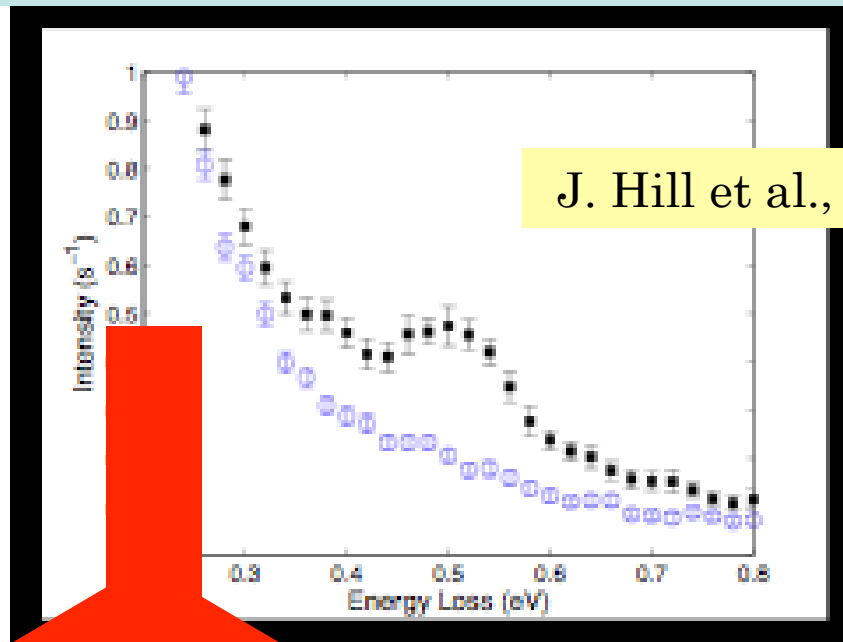
Progress @ Cu K-edge resolution II

Cu K-edge

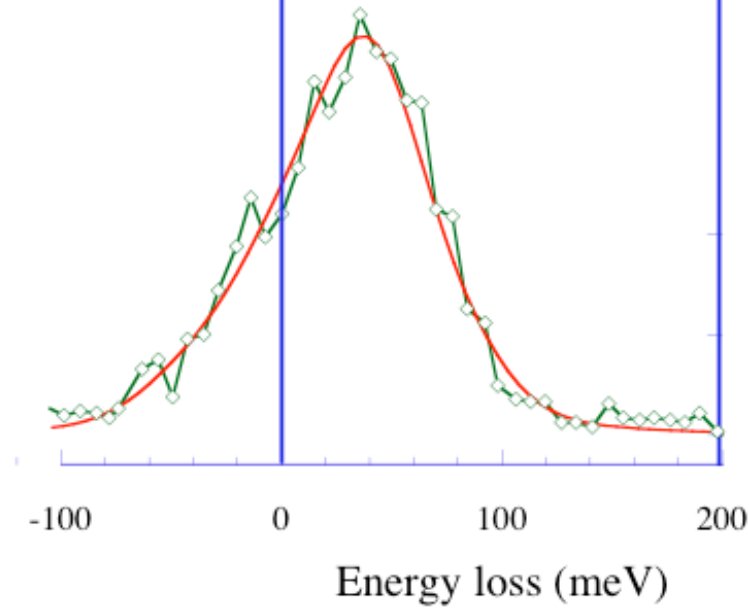


Progress @ Cu K-edge resolution II

Cu K-edge



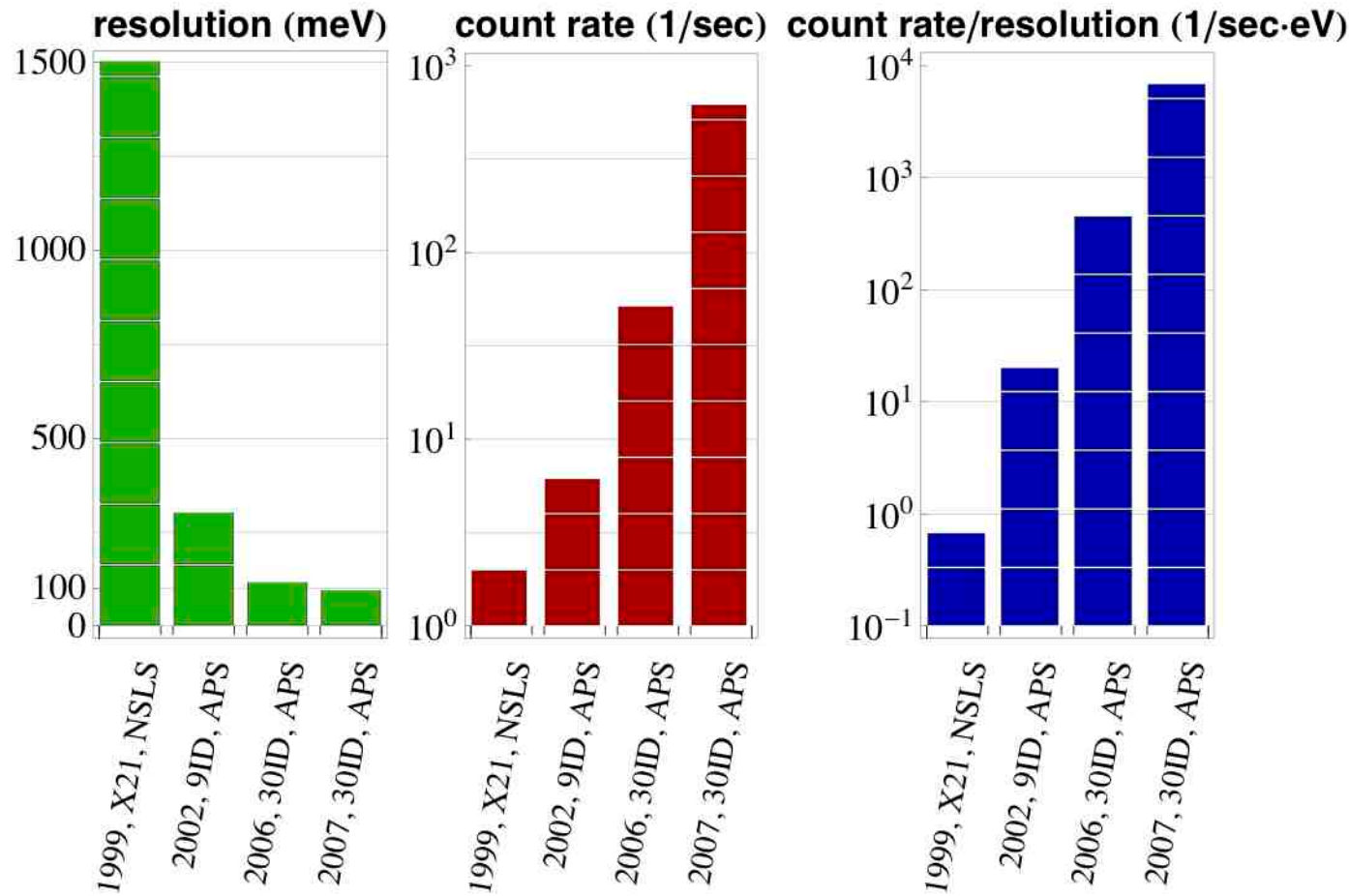
J. Hill et al., (2008)



Yavas, et al., JPCM
22, 485601 (2010)

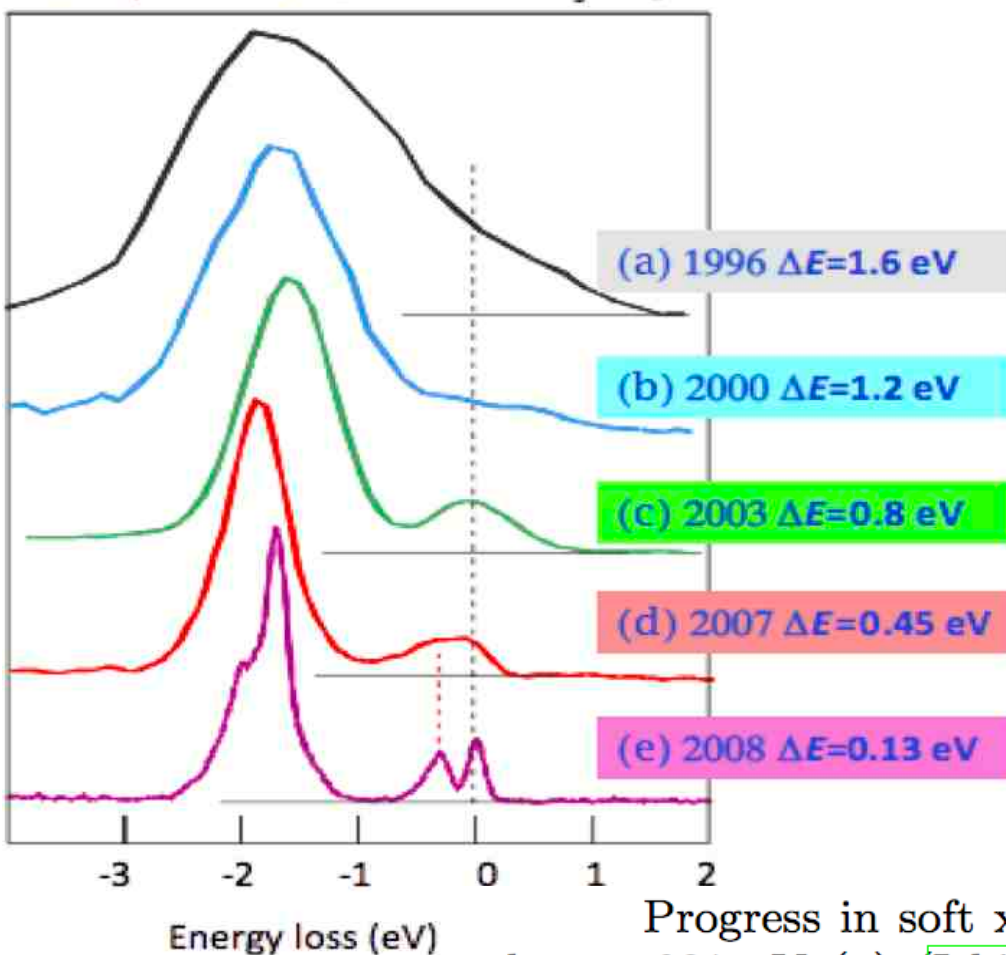
Progress @ Cu K-edge resolution III

Hard x-ray regime: Cu K-edge



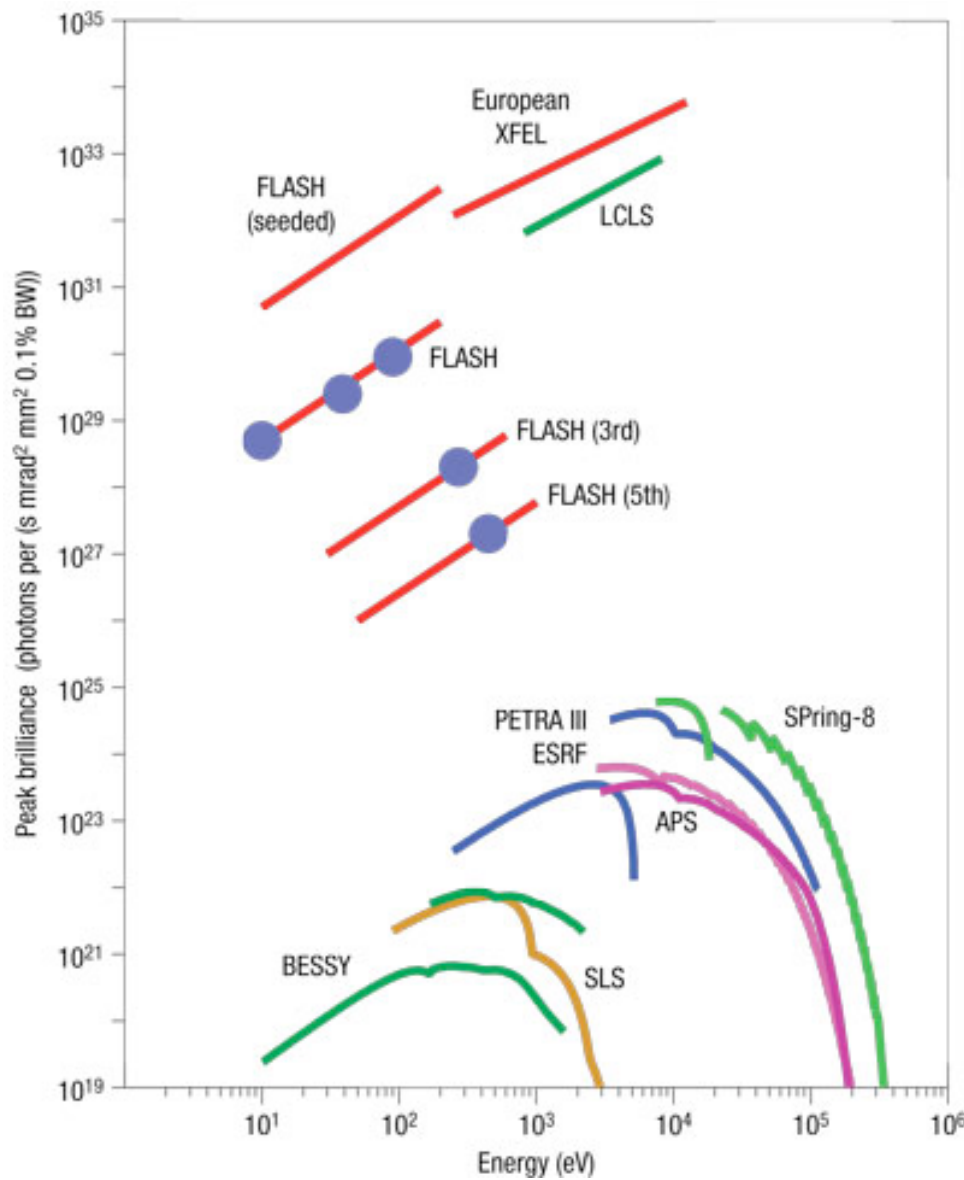
Progress @ Cu L-edge resolution

RIXS spectra of La_2CuO_4 at Cu L_3 -edge

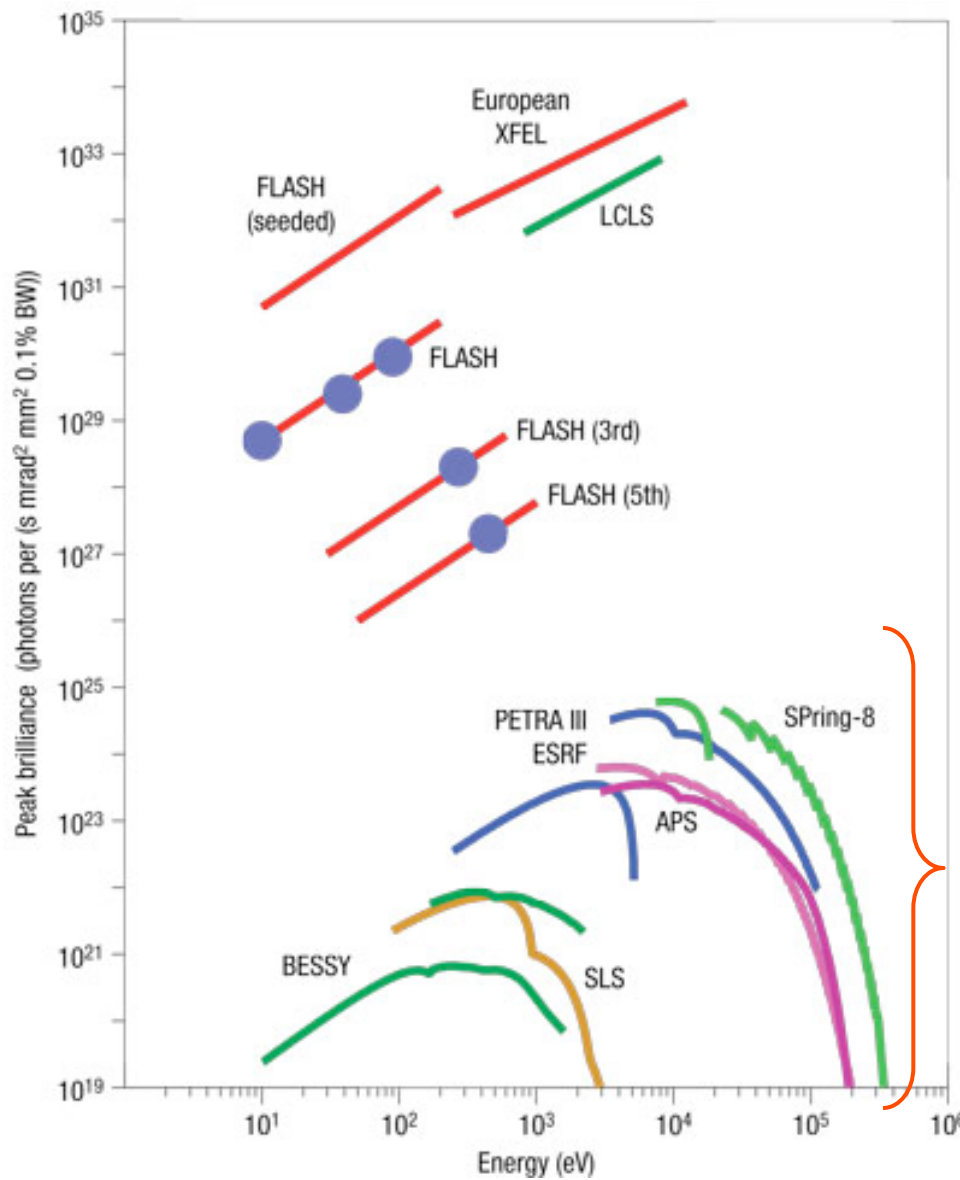


Progress in soft x-ray RIXS resolution at the Cu L-edge at 931 eV (a) (Ichikawa *et al.*, 1996), BLBB @ Photon Factory (b) I511-3 @ MAX II (Duda *et al.*, 2000b), (c) AXES @ ID08, ESRF (Ghiringhelli *et al.*, 2004) (d) AXES @ ID08, ESRF (Braicovich *et al.*, 2009), (e) SAXES @ SLS (Ghiringhelli *et al.*, 2010). Courtesy of G. Ghiringhelli and L. Braicovich.

Progress in X-ray sources...

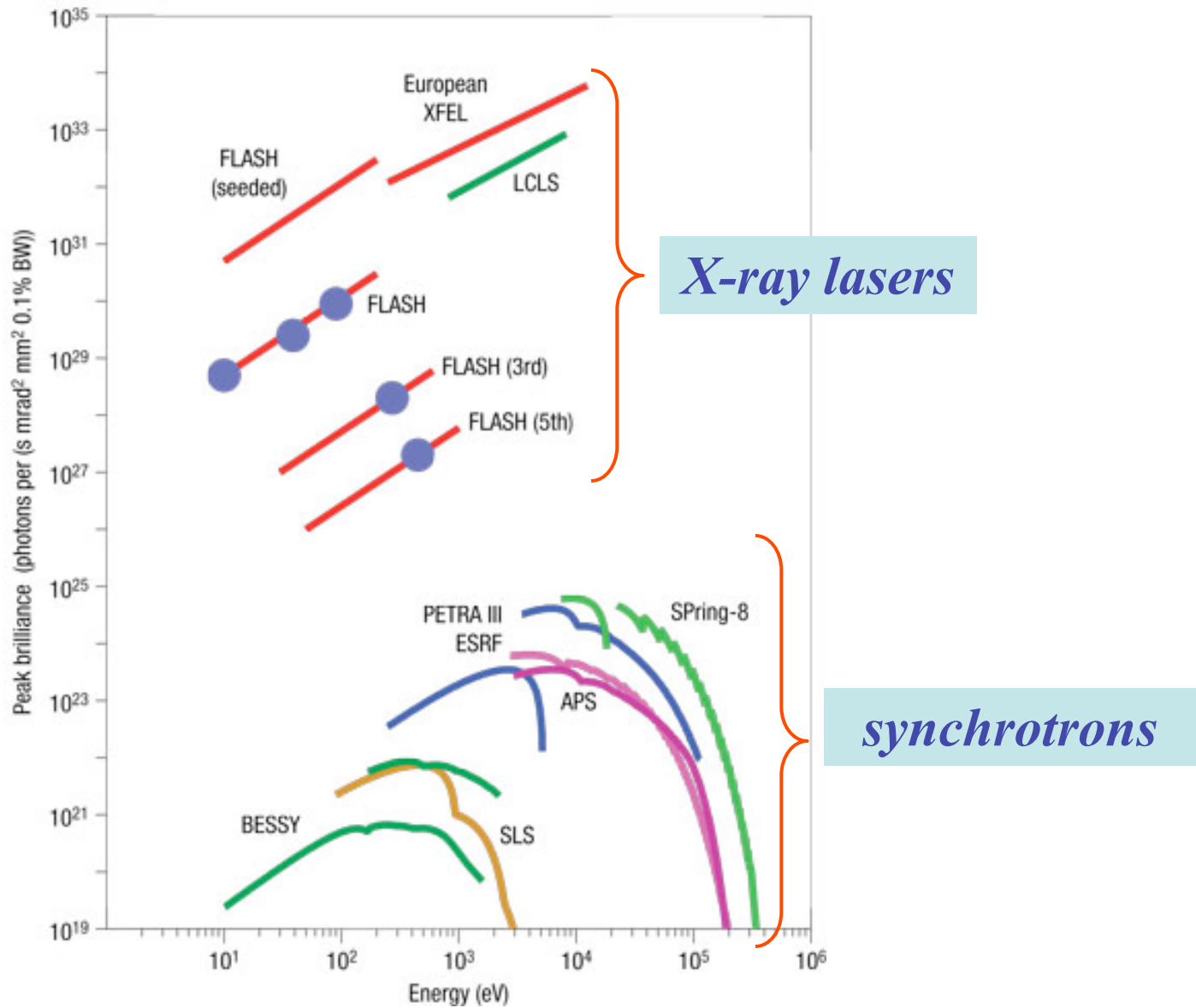


Progress in X-ray sources...



synchrotrons

Progress in X-ray sources...



Summary part I

Summary part I

- Direct and Indirect RIXS

Summary part I

- Direct and Indirect RIXS
- RIXS measures excitation energy & momentum

Summary part I

- Direct and Indirect RIXS
- RIXS measures excitation energy & momentum
- Polarization in/out dependence can be studied

Summary part I

- Direct and Indirect RIXS
- RIXS measures excitation energy & momentum
- Polarization in/out dependence can be studied
- Element and orbital sensitive

Summary part I

- Direct and Indirect RIXS
- RIXS measures excitation energy & momentum
- Polarization in/out dependence can be studied
- Element and orbital sensitive
- Bulk sensitive & needs small sample volumes

Summary part I

- Direct and Indirect RIXS
- RIXS measures excitation energy & momentum
- Polarization in/out dependence can be studied
- Element and orbital sensitive
- Bulk sensitive & needs small sample volumes
- Measures charge neutral elementary excitations
spin, orbital, lattice, charge excitons

Summary part I

- Direct and Indirect RIXS
- RIXS measures excitation energy & momentum
- Polarization in/out dependence can be studied
- Element and orbital sensitive
- Bulk sensitive & needs small sample volumes
- Measures charge neutral elementary excitations
 - spin, orbital, lattice, charge excitons
- Great progress in resolution in the past decade

2. Magnetic RIXS on low dimensional magnets

Quasi 2D cuprates

Quasi 1D cuprates

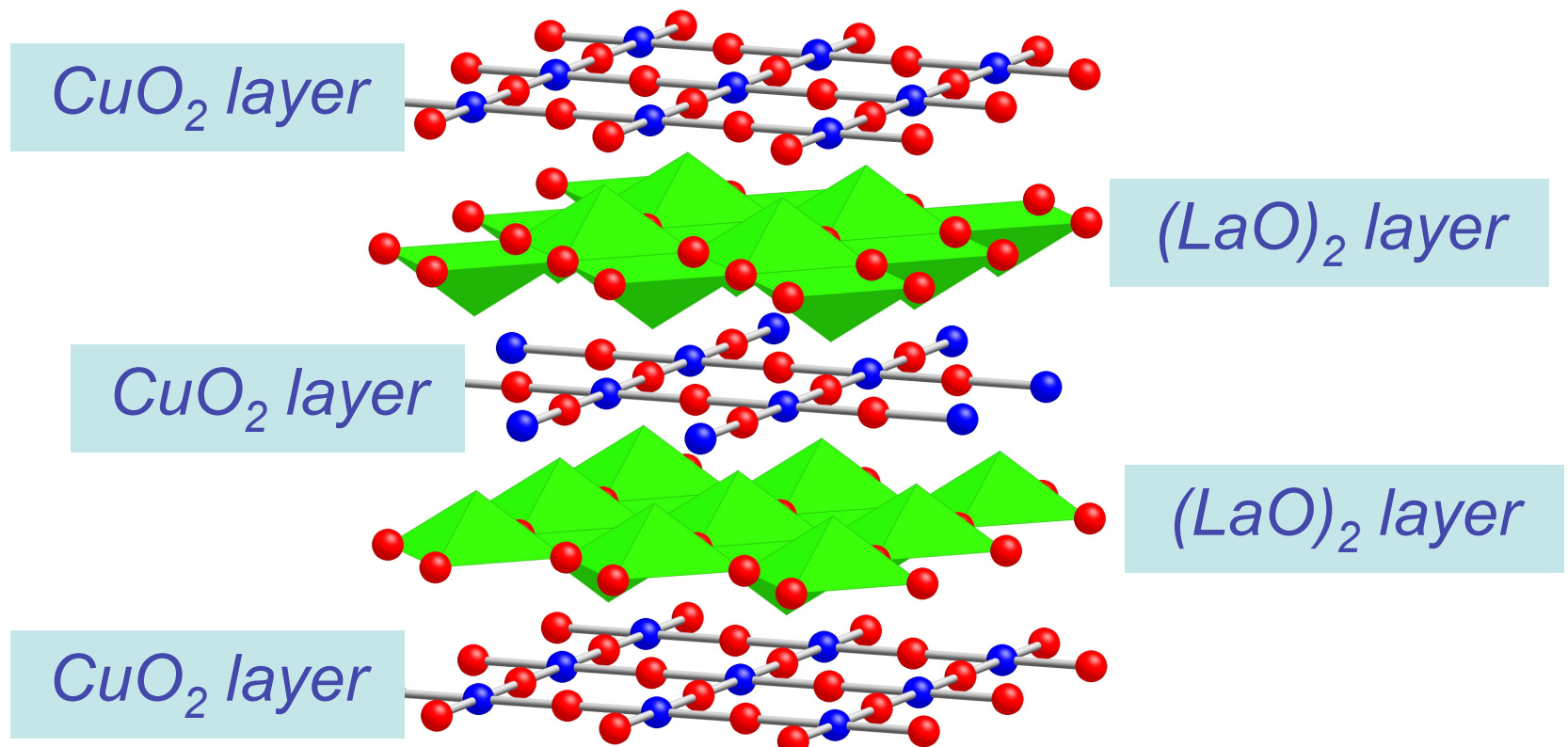
Quasi 2D iron pnictide

Quasi 2D iridate

Doped Cu & Fe systems

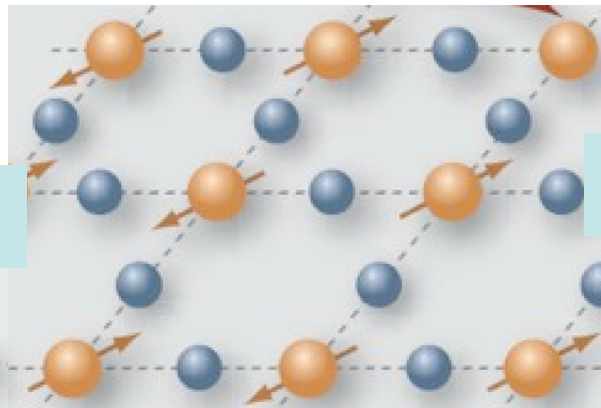
Quasi 2D cuprates

La_2CuO_4 crystal structure

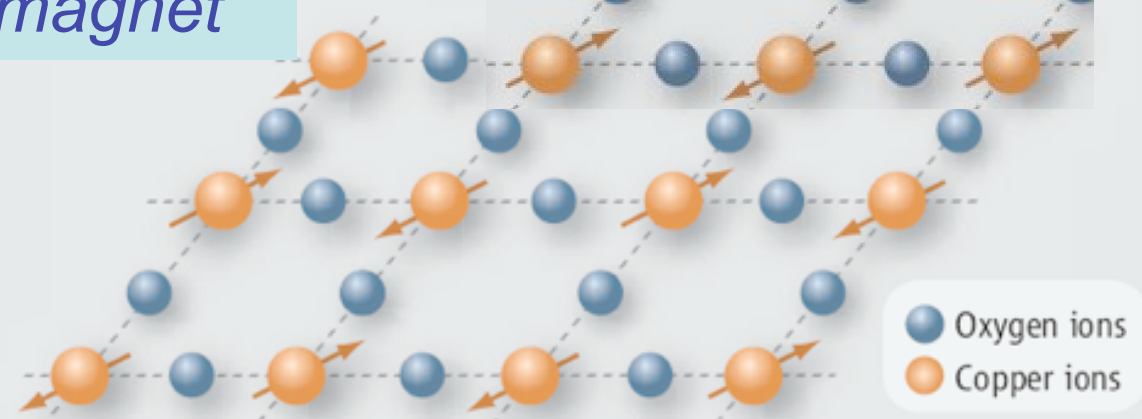


La_2CuO_4 magnetic structure

*strongly correlated
antiferromagnet*



spin 1/2

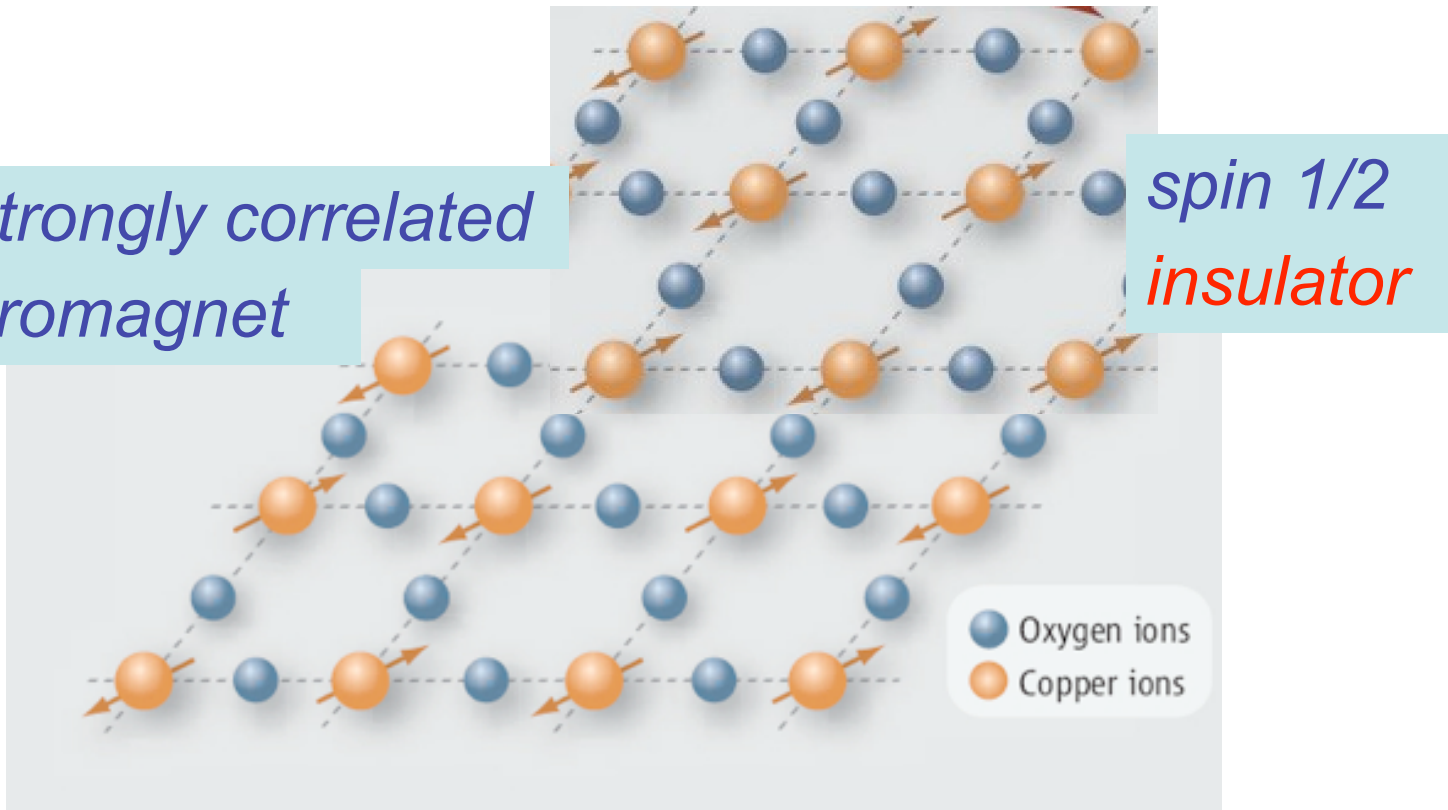


Oxygen ions
Copper ions

La_2CuO_4 magnetic structure

*strongly correlated
antiferromagnet*

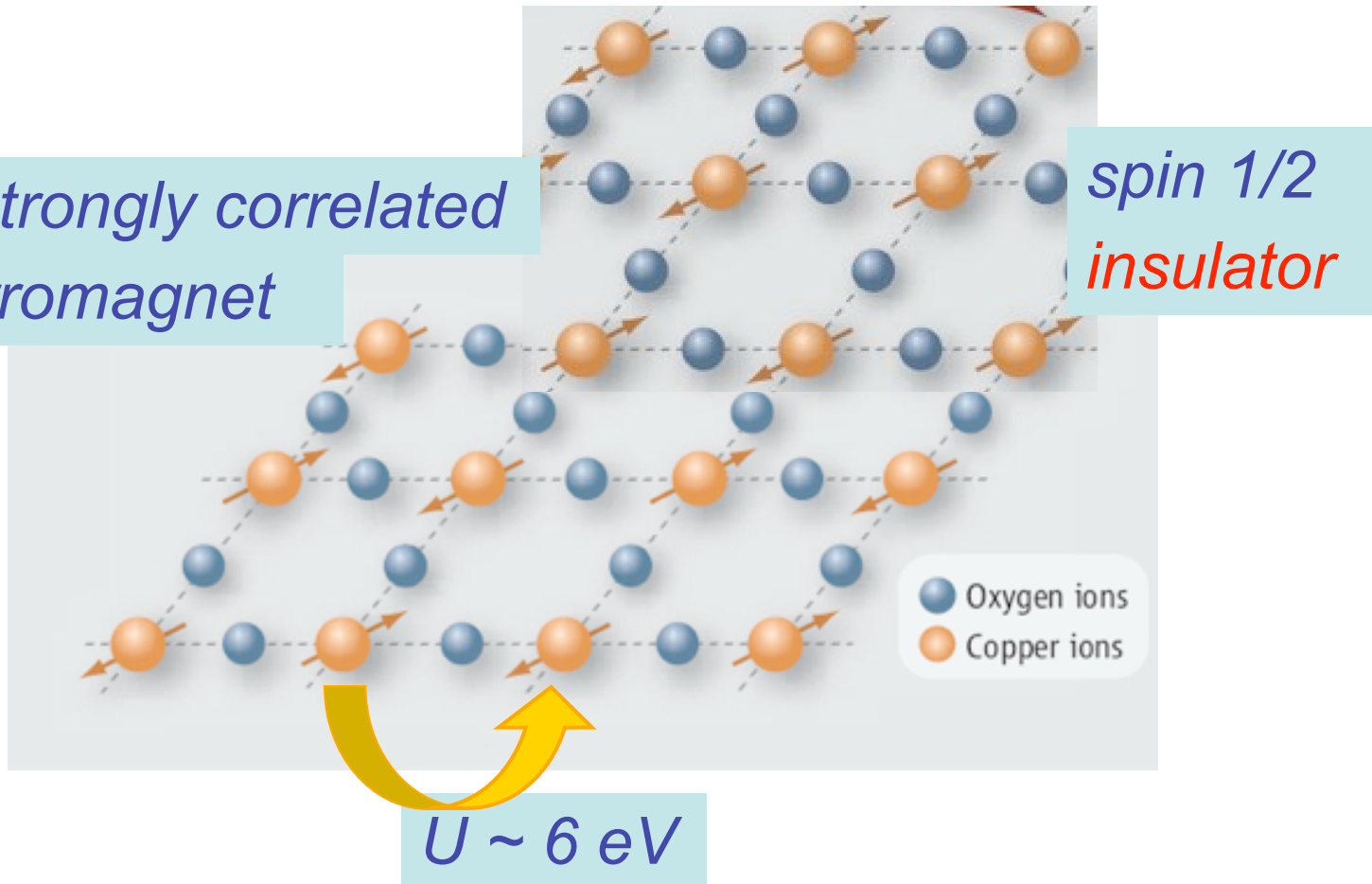
*spin 1/2
insulator*



La_2CuO_4 magnetic structure

*strongly correlated
antiferromagnet*

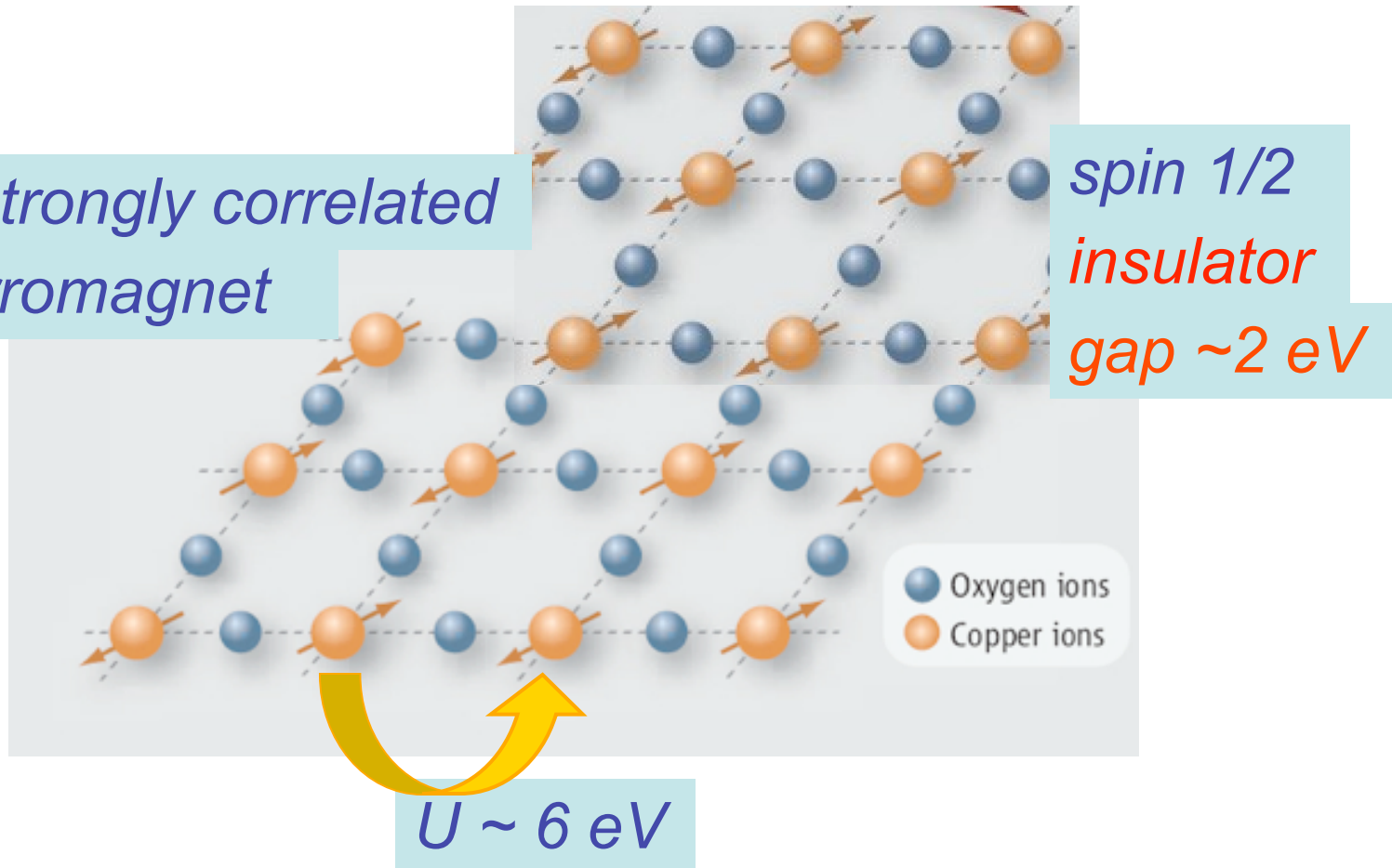
*spin 1/2
insulator*



La_2CuO_4 magnetic structure

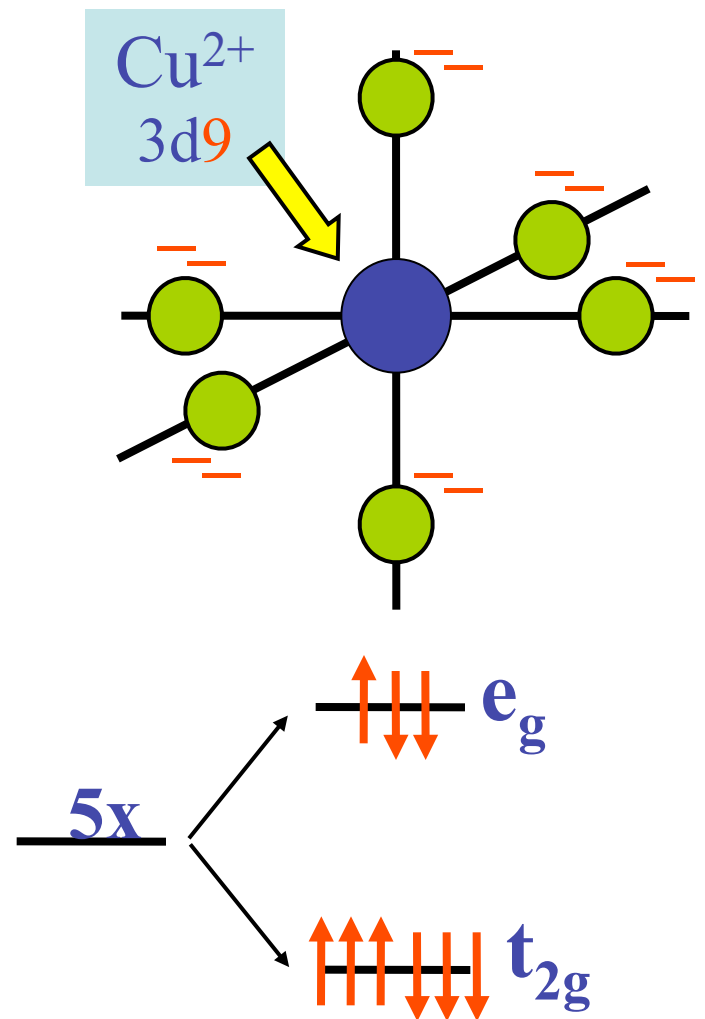
*strongly correlated
antiferromagnet*

*spin 1/2
insulator
gap ~ 2 eV*



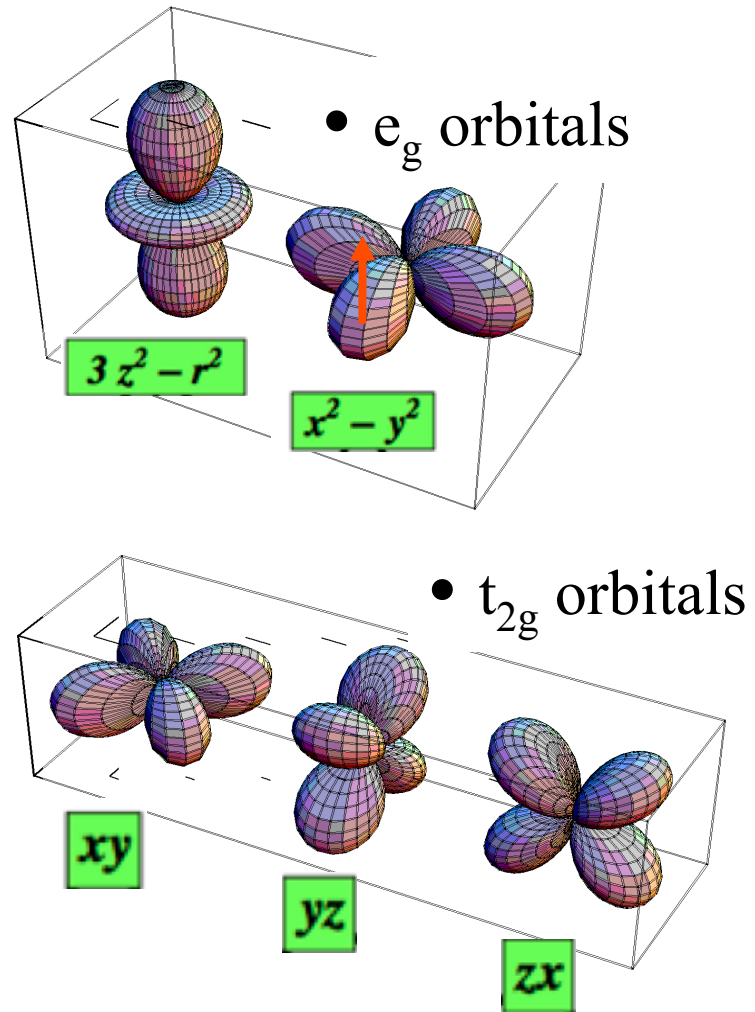
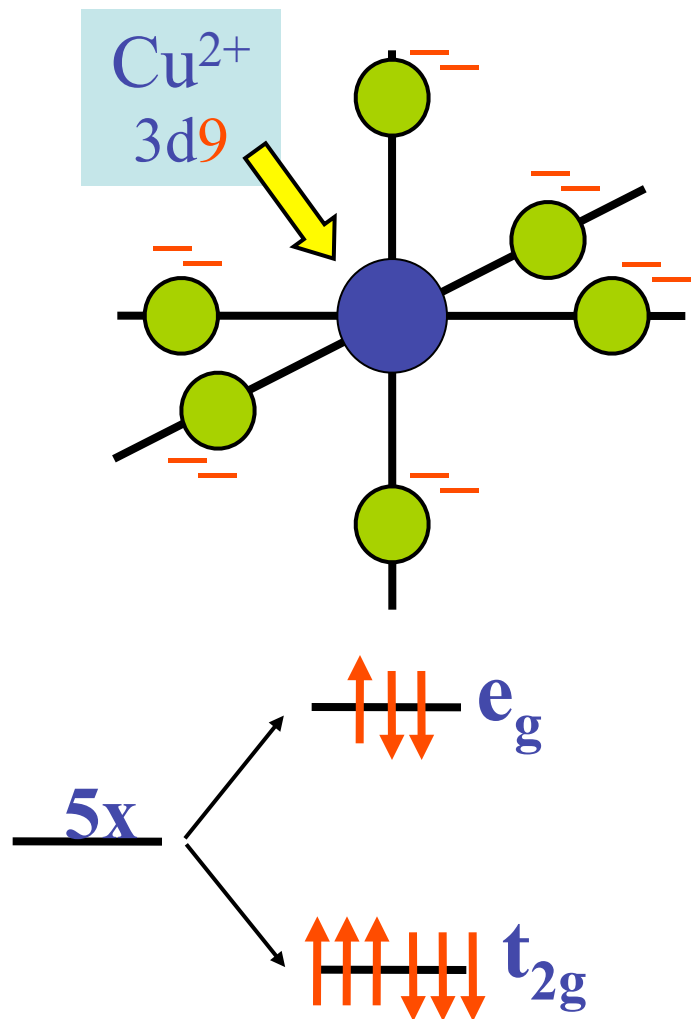
Atomic Model: Local d-d orbital splitting: Cu²⁺

Cubic Crystal field splitting



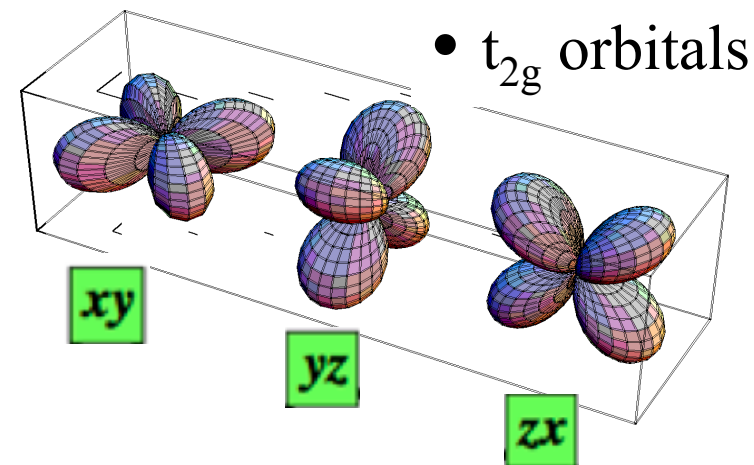
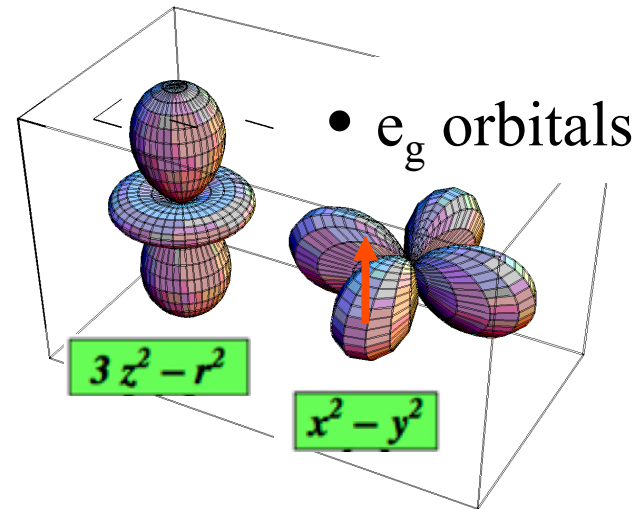
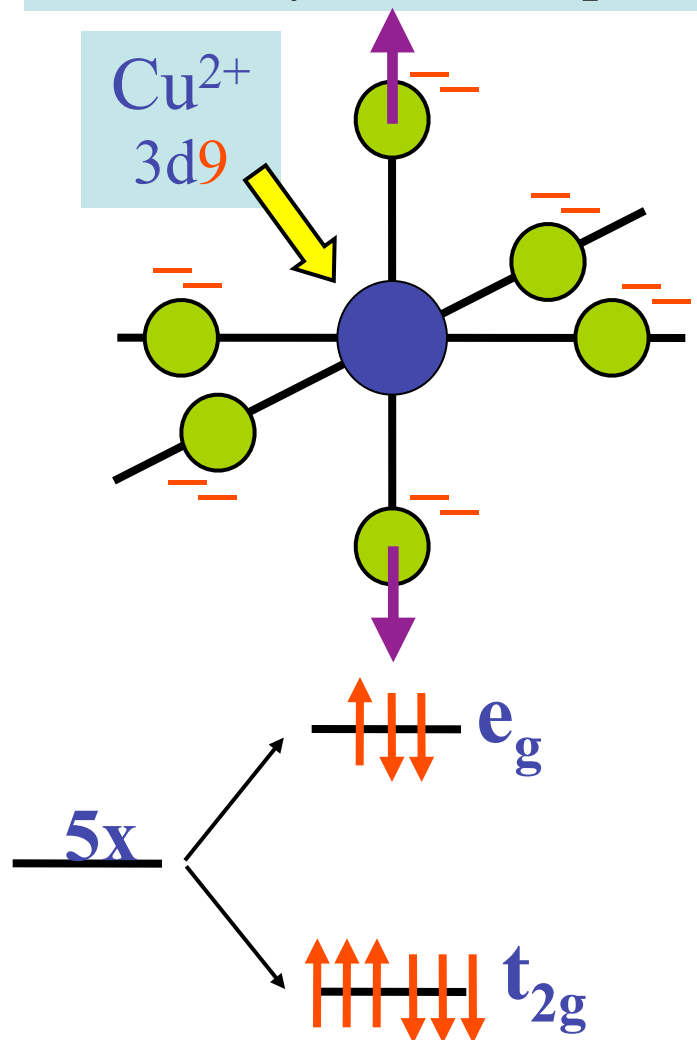
Atomic Model: Local d-d orbital splitting: Cu²⁺

Cubic Crystal field splitting



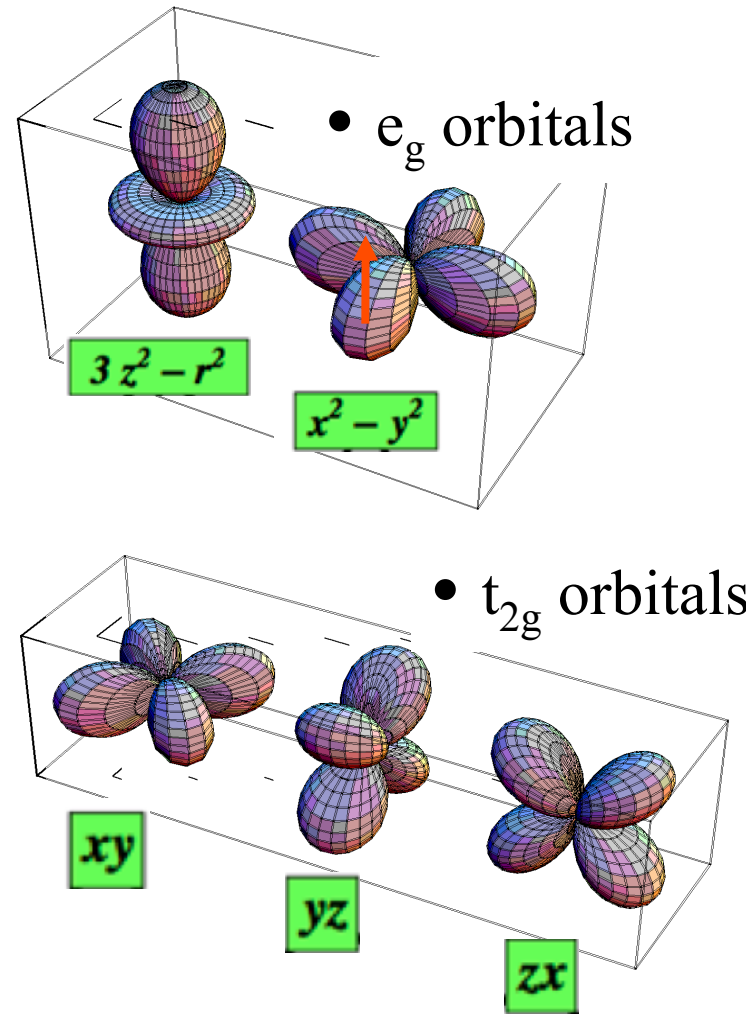
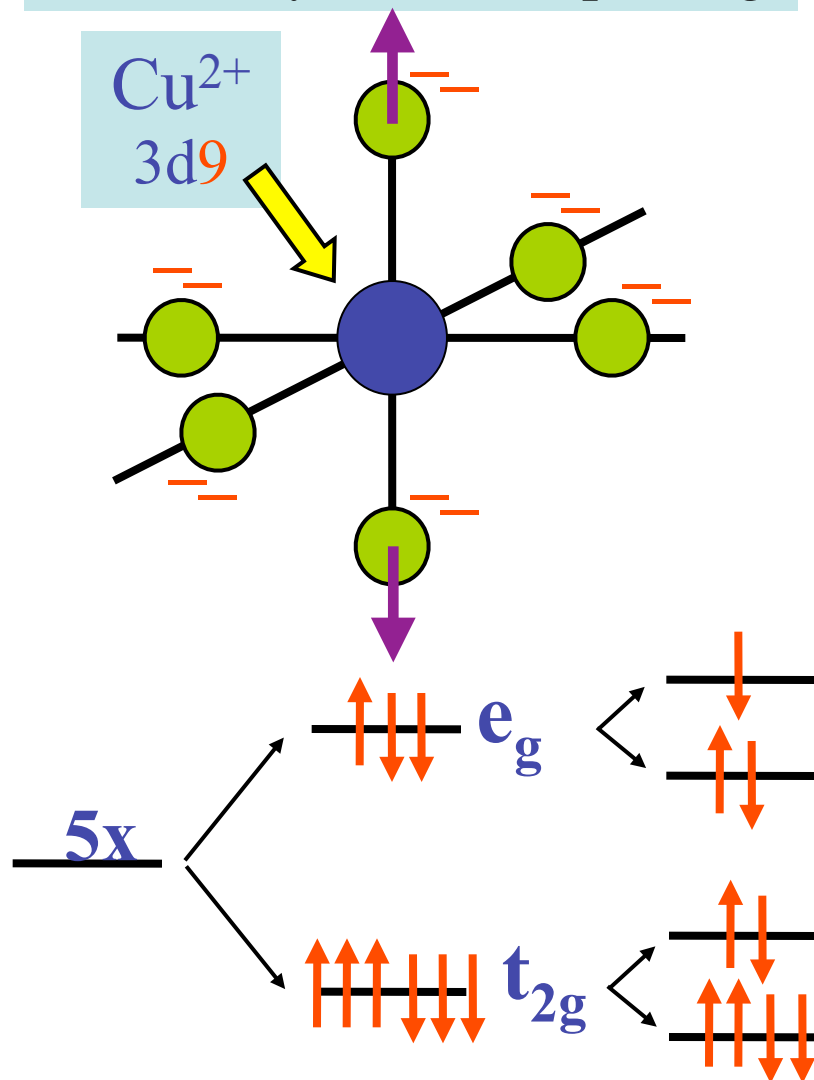
Atomic Model: Local d-d orbital splitting: Cu²⁺

Cubic Crystal field splitting

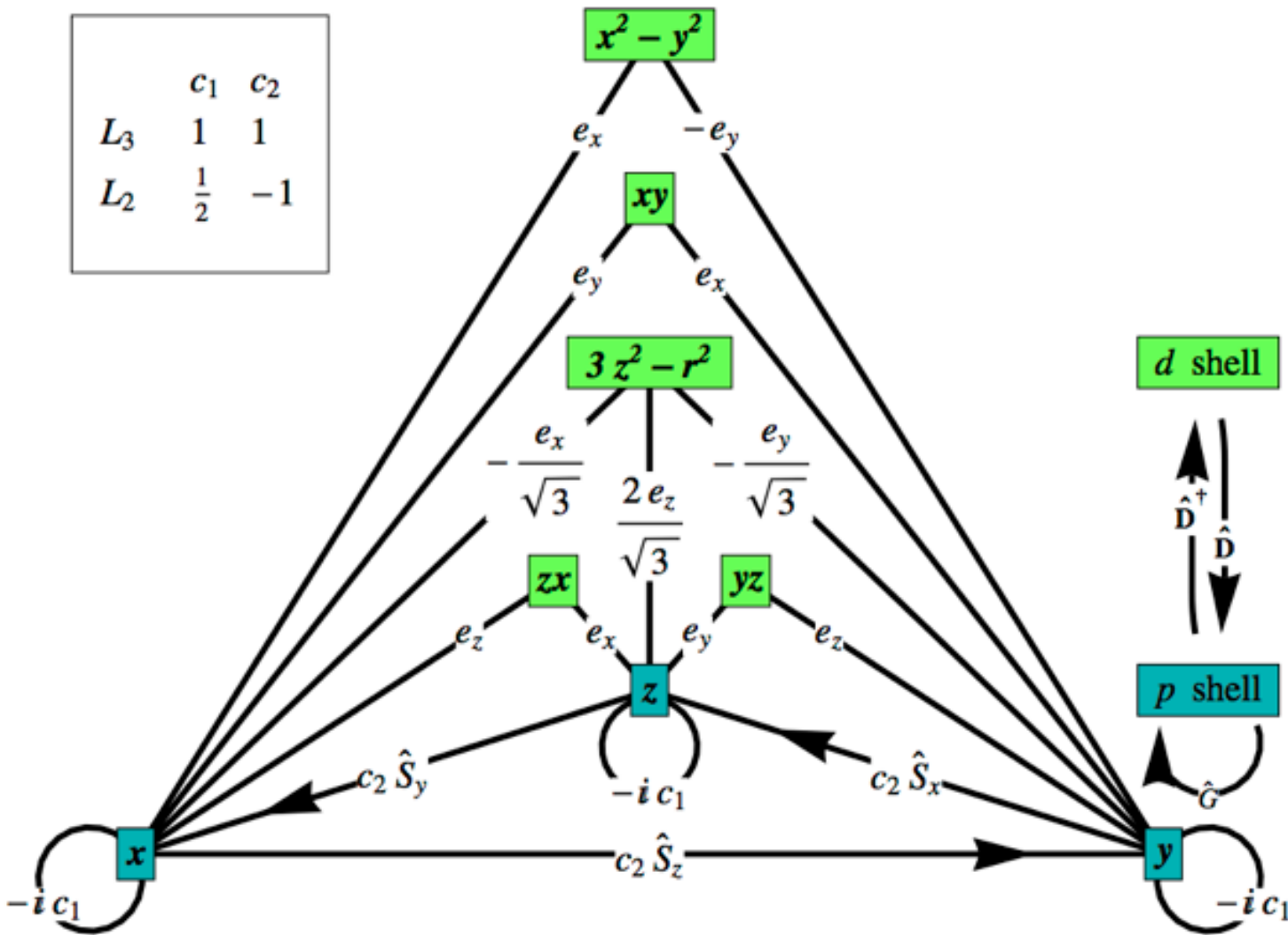


Atomic Model: Local d-d orbital splitting: Cu²⁺

Cubic Crystal field splitting



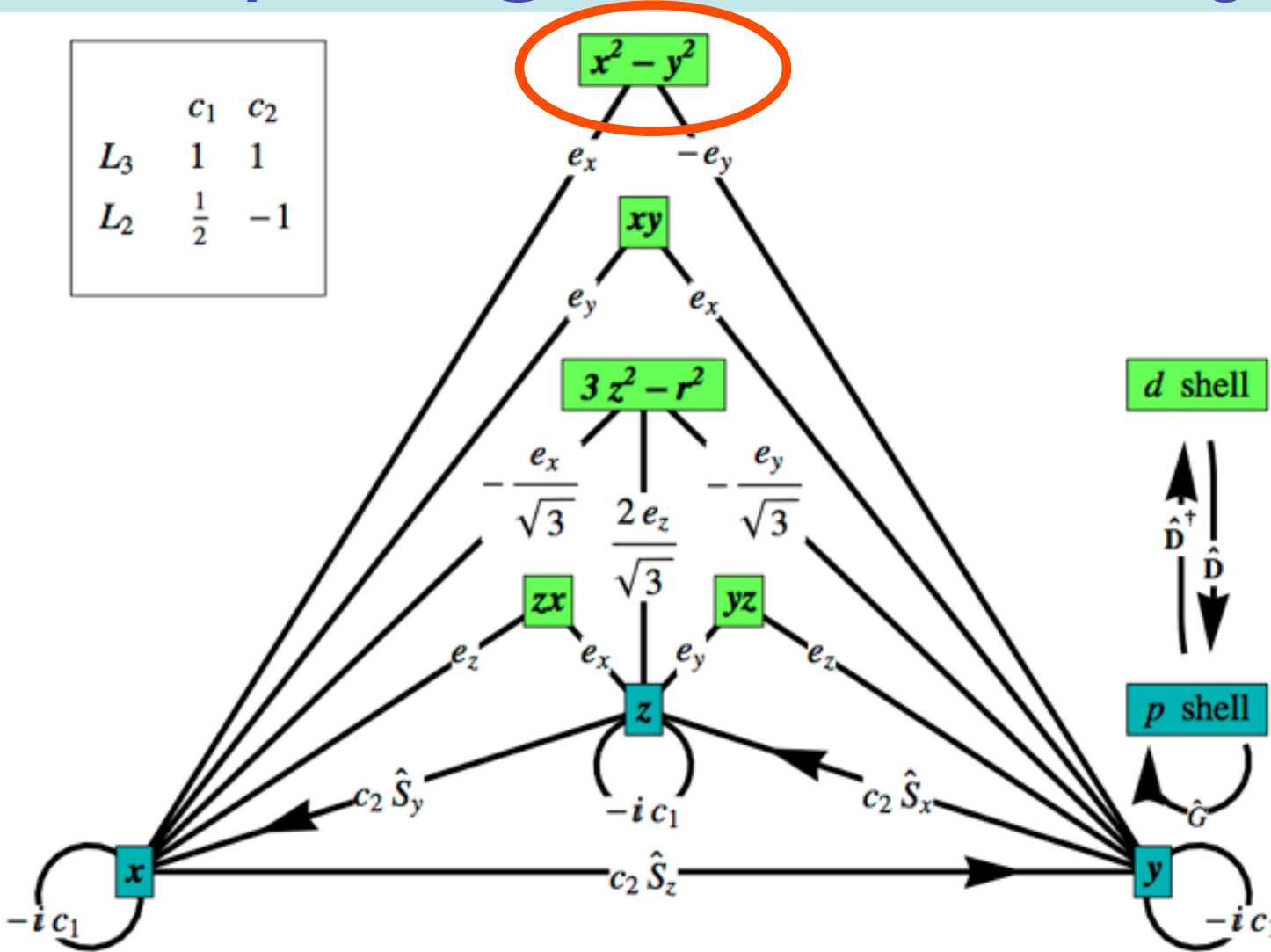
RIXS amplitude @ transition metal L-edge



Ament, Ghiringhelli, Moretti,
Braicovich & JvdB,
PRL 103, 117003 (2009)

Marra, Wohlfeld & JvdB,
PRL 109, 117401 (2012)

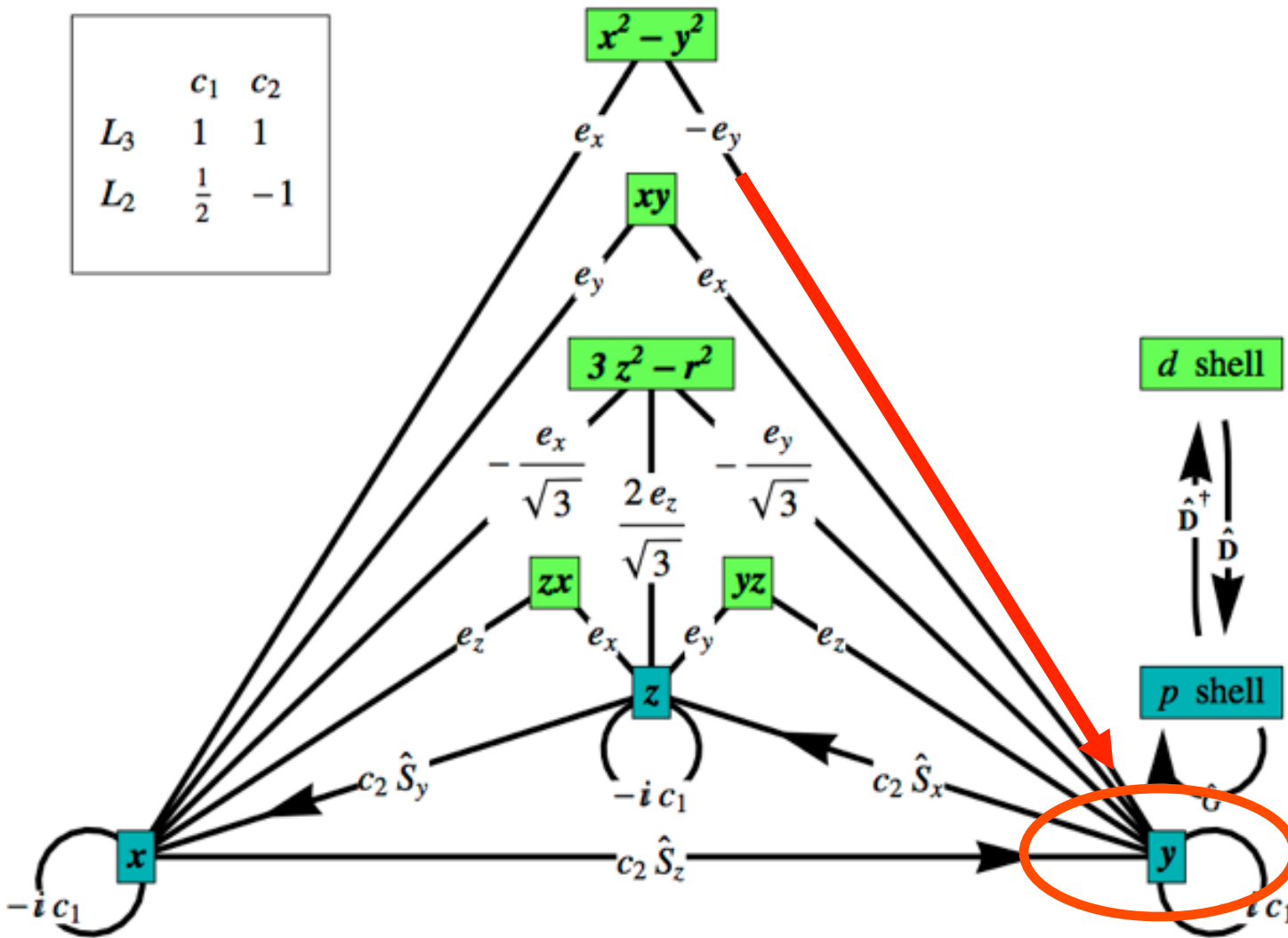
RIXS amplitude @ transition metal L-edge



Ament, Ghiringhelli, Moretti,
Braicovich & JvdB,
PRL 103, 117003 (2009)

Marra, Wohlfeld & JvdB,
PRL 109, 117401 (2012)

RIXS amplitude @ transition metal L-edge

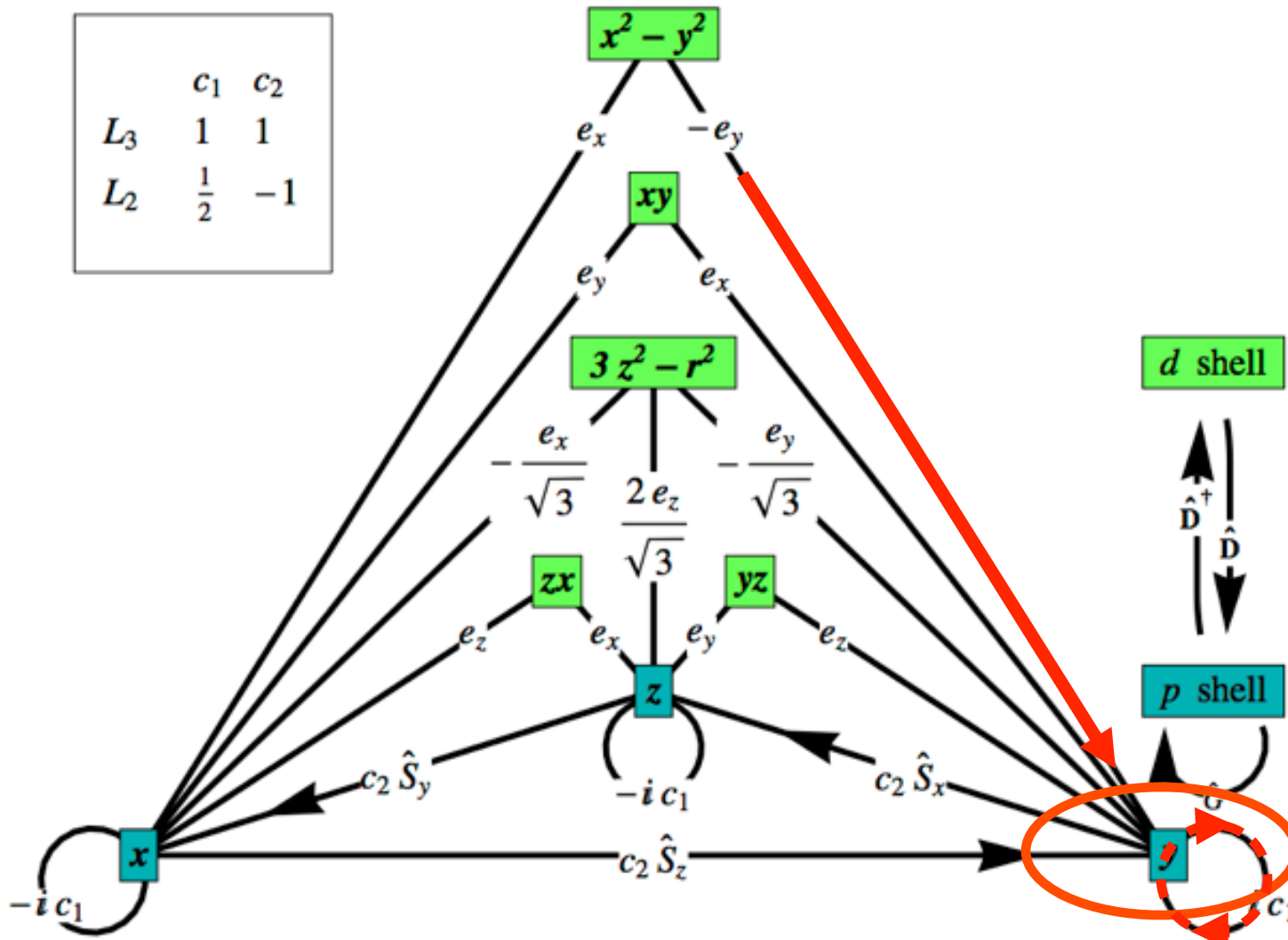


Ament, Ghiringhelli, Moretti,
Braicovich & JvdB,
PRL 103, 117003 (2009)

Marra, Wohlfeld & JvdB,
PRL 109, 117401 (2012)

RIXS amplitude @ transition metal L-edge

	c_1	c_2
L_3	1	1
L_2	$\frac{1}{2}$	-1

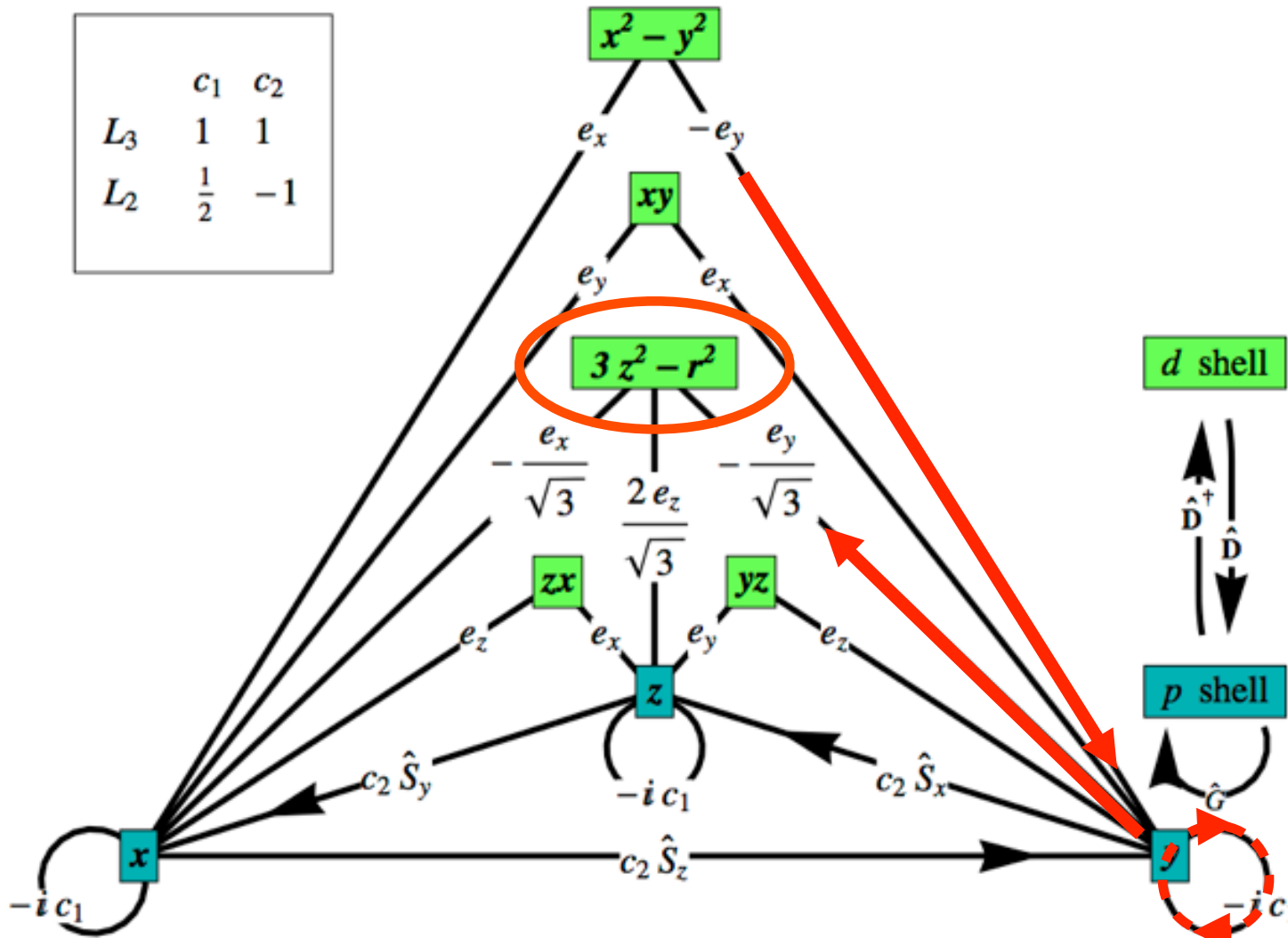


Ament, Ghiringhelli, Moretti,
Braicovich & JvdB,
PRL 103, 117003 (2009)

Marra, Wohlfeld & JvdB,
PRL 109, 117401 (2012)

RIXS amplitude @ transition metal L-edge

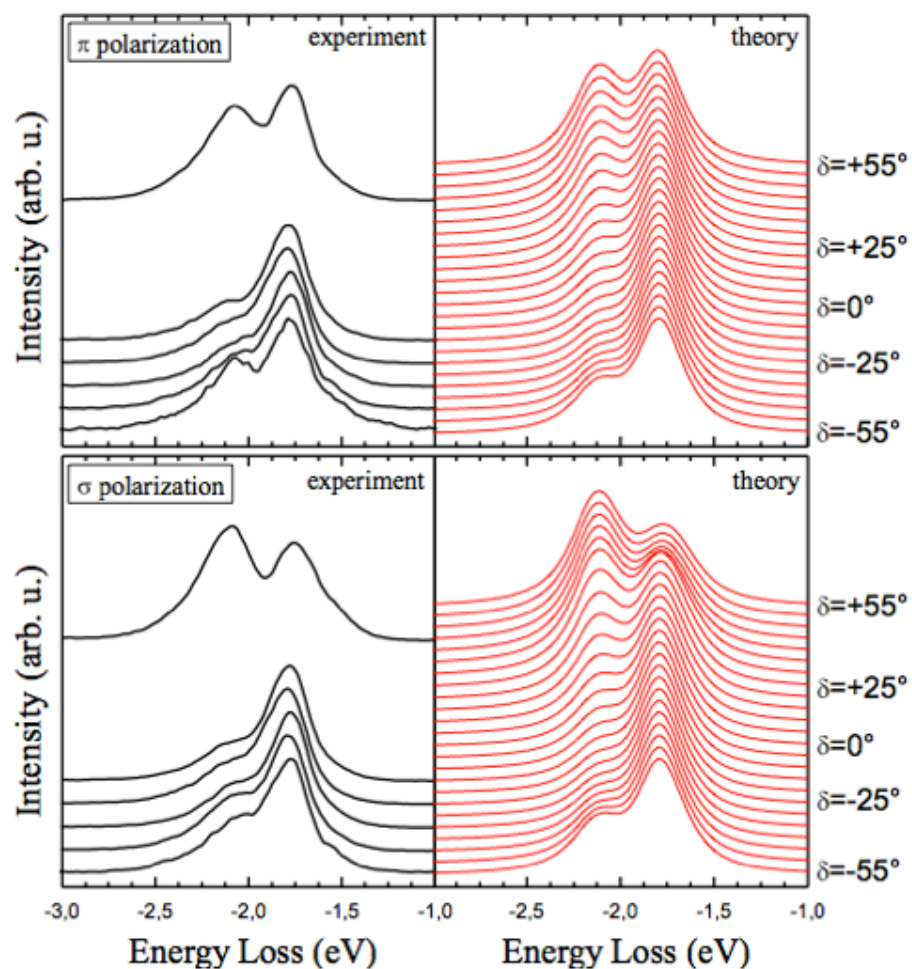
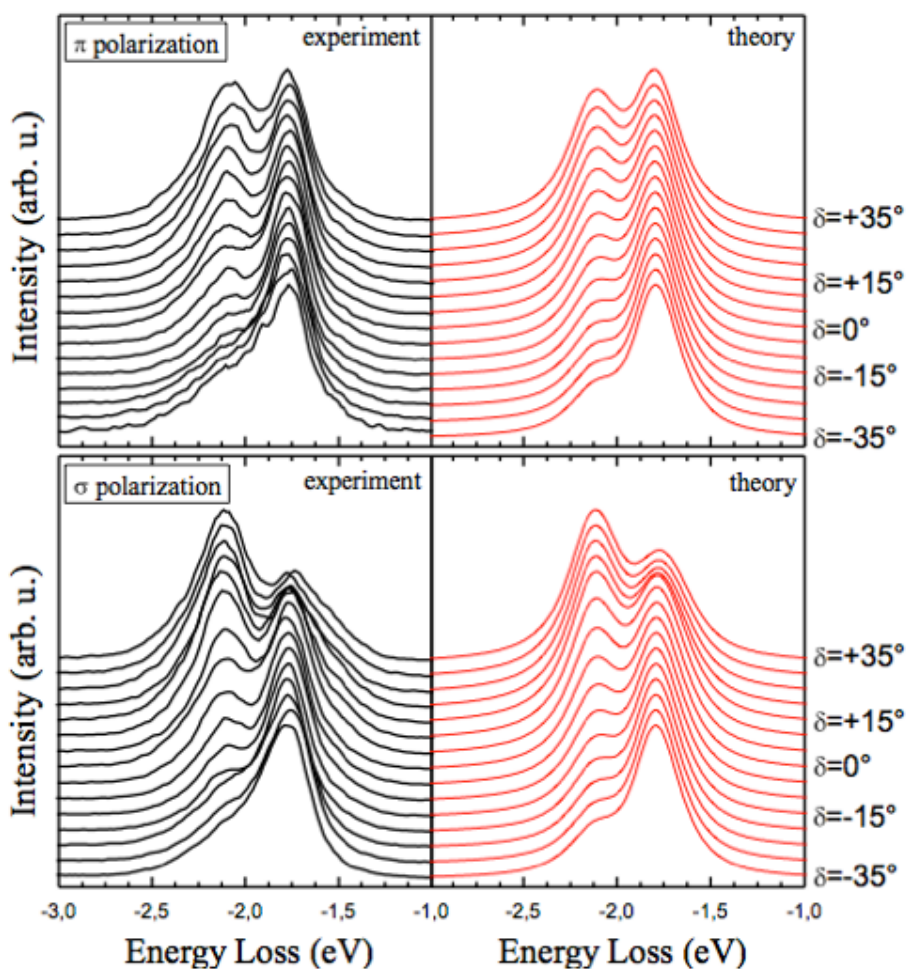
	c_1	c_2
L_3	1	1
L_2	$\frac{1}{2}$	-1



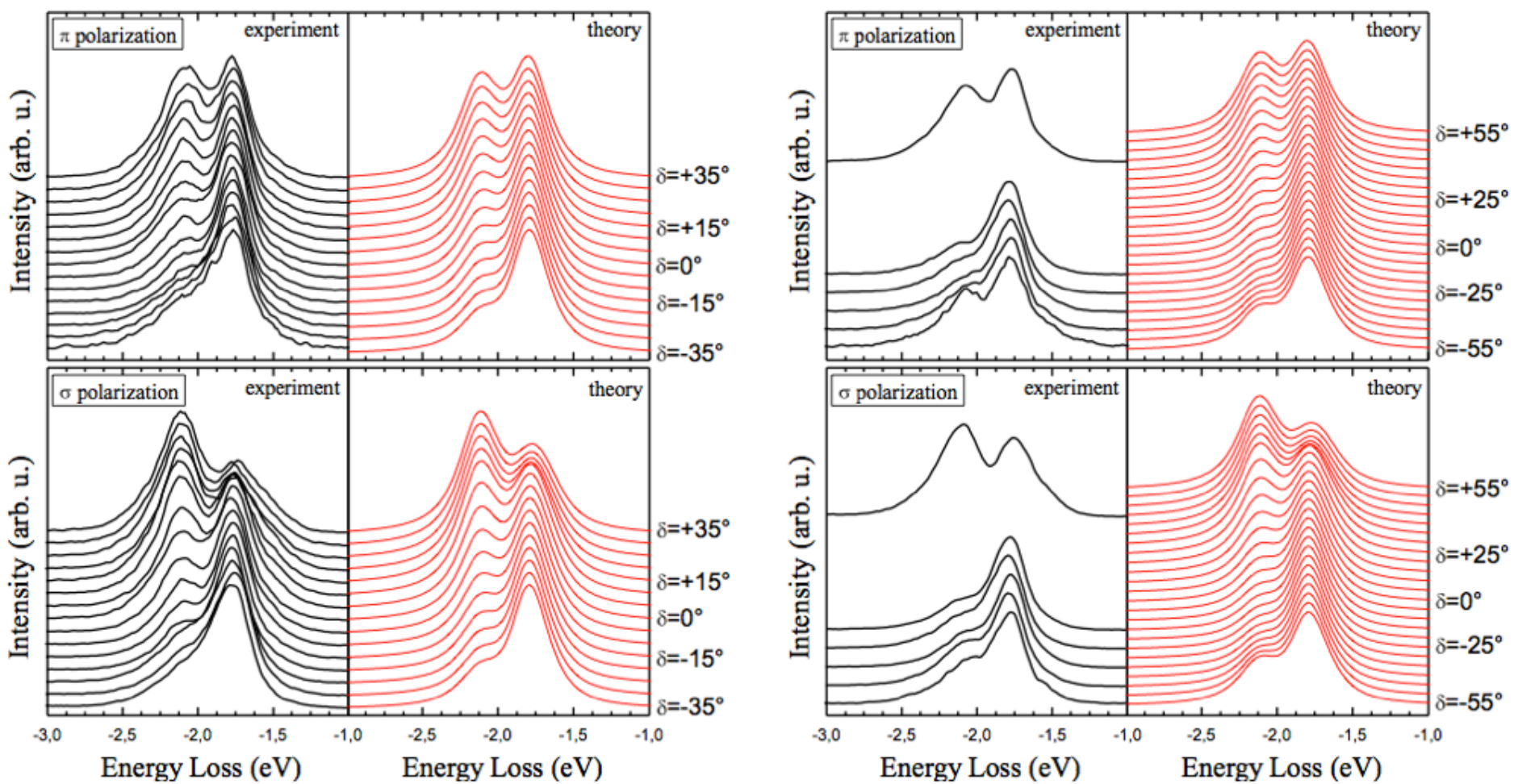
Ament, Ghiringhelli, Moretti,
Braicovich & JvdB,
PRL 103, 117003 (2009)

Marra, Wohlfeld & JvdB,
PRL 109, 117401 (2012)

Orbital excitations by direct RIXS on La_2CuO_4

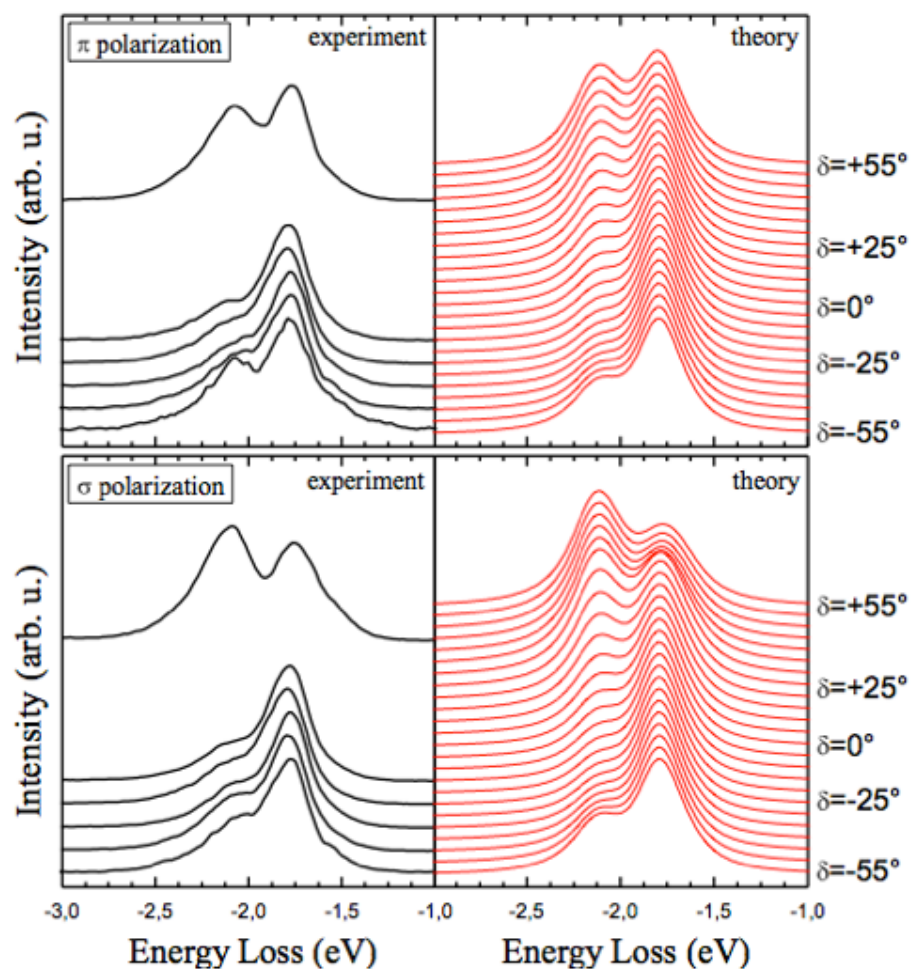
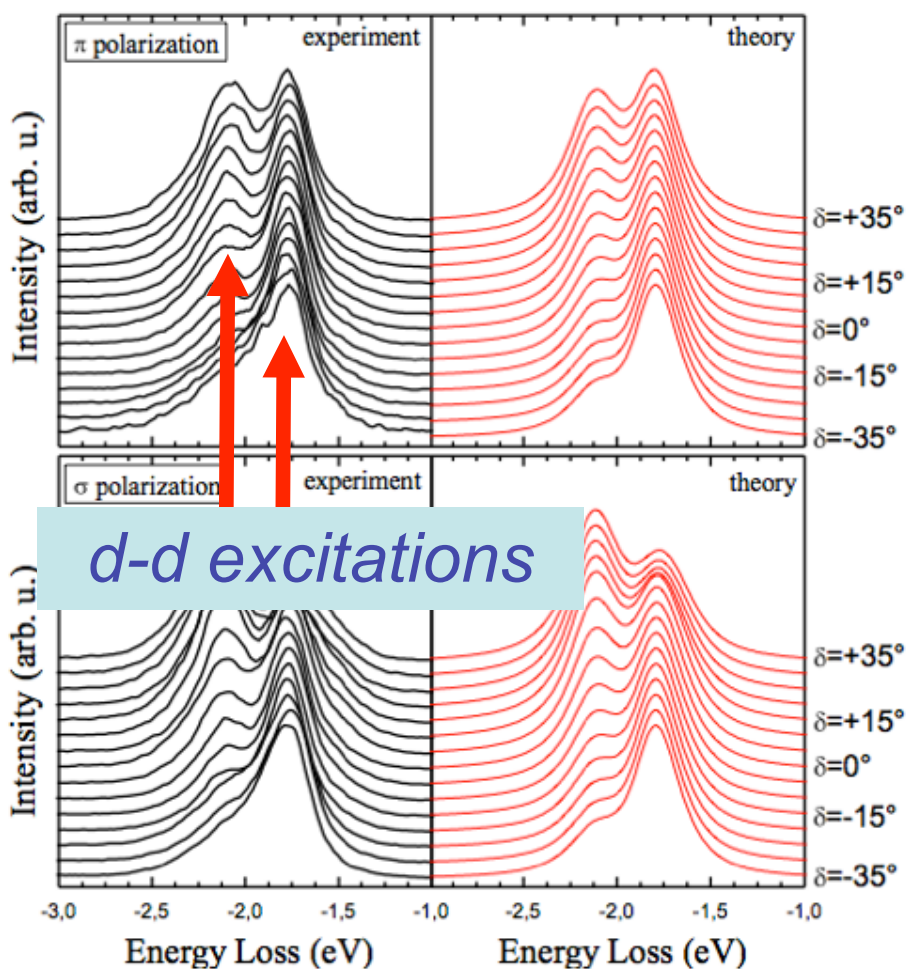


Orbital excitations by direct RIXS on La_2CuO_4



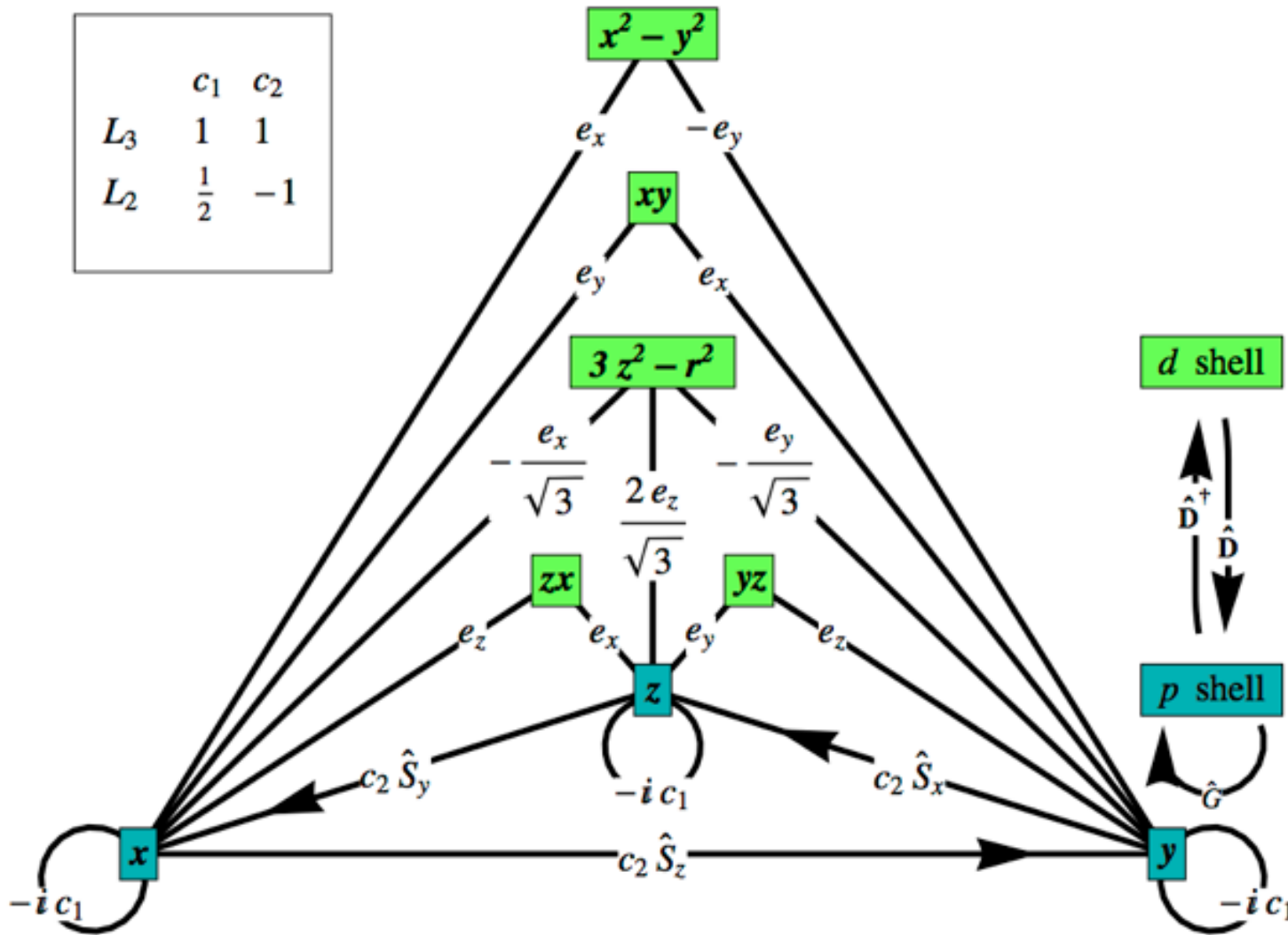
Moretti, Bisogni, Aruta, Balestrino, Berger, Brookes, Luca, Castro, Grioni, Guarise, Medaglia, Miletto, Minola, Perna, Radovic, Salluzzo, Schmitt, Zhou, Braicovich & Ghiringhelli, NJP 13, 043026 (2011)

Orbital excitations by direct RIXS on La_2CuO_4



Moretti, Bisogni, Aruta, Balestrino, Berger, Brookes, Luca, Castro, Grioni, Guarise, Medaglia, Miletto, Minola, Perna, Radovic, Salluzzo, Schmitt, Zhou, Braicovich & Ghiringhelli, NJP 13, 043026 (2011)

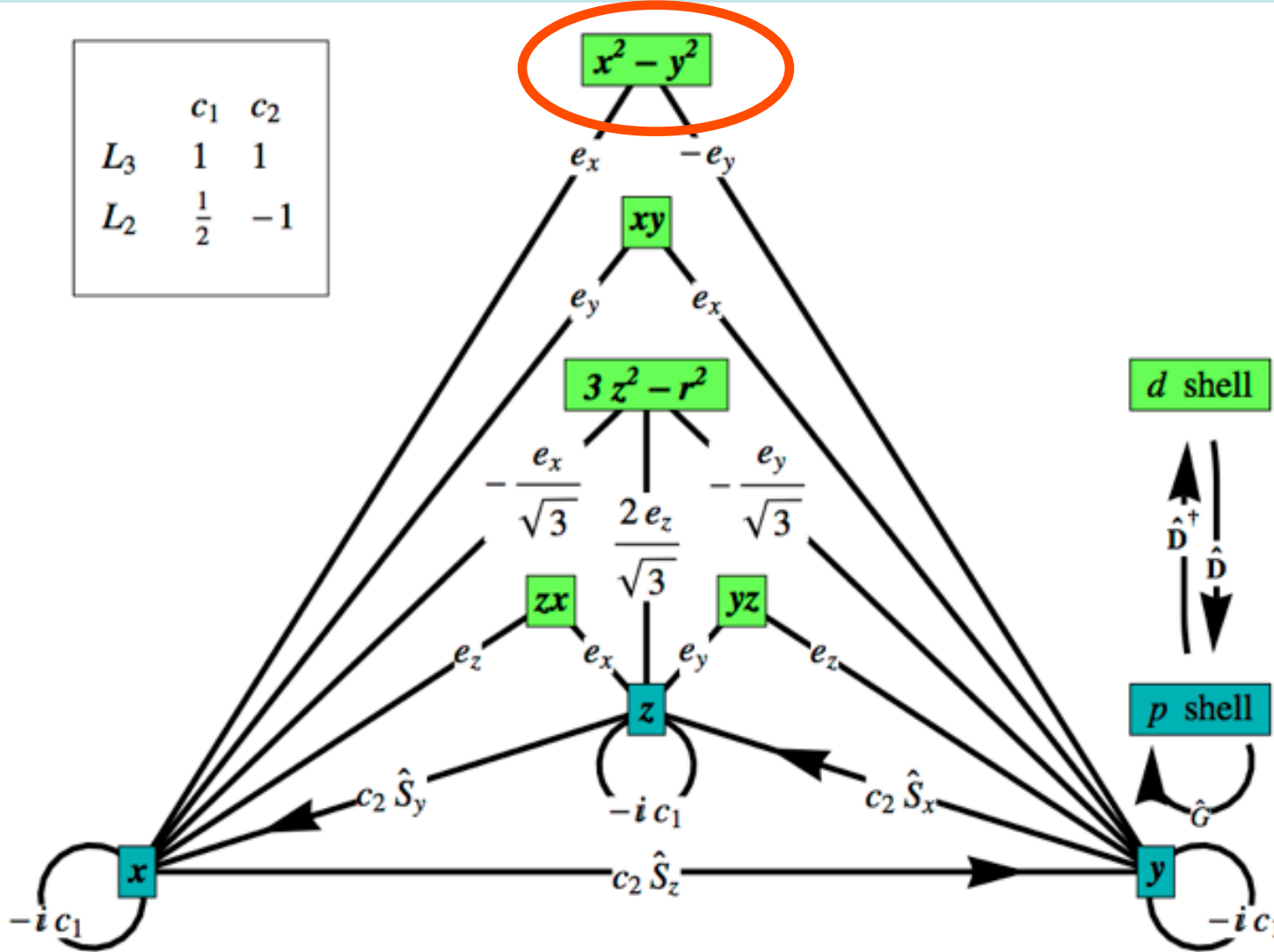
RIXS spin-flip amplitude @ transition metal L-edge



Ament, Ghiringhelli, Moretti,
Braicovich & JvdB,
PRL 103, 117003 (2009)

Marra, Wohlfeld & JvdB,
PRL 109, 117401 (2012)

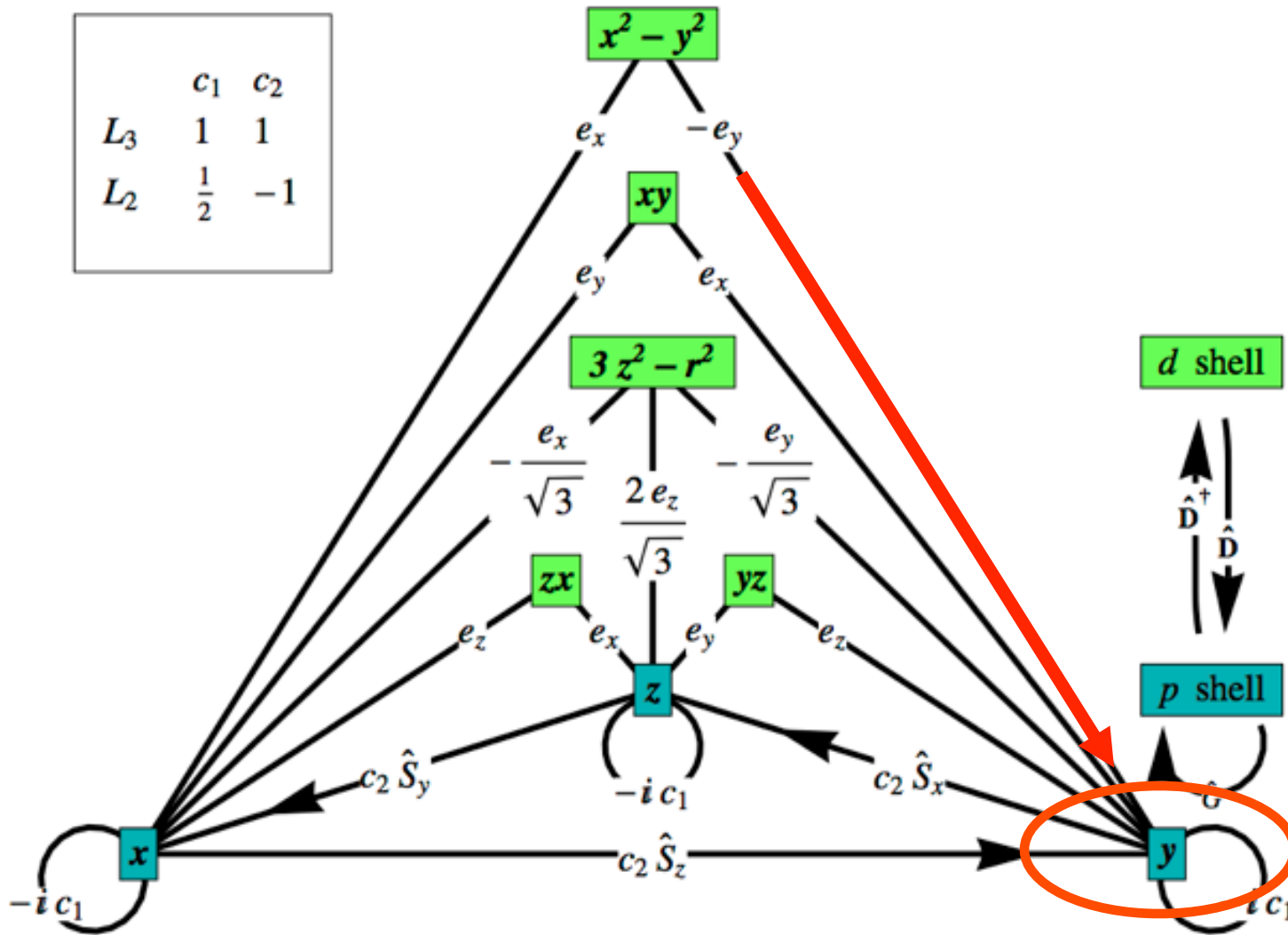
RIXS spin-flip amplitude @ transition metal L-edge



Ament, Ghiringhelli, Moretti,
Braicovich & JvdB,
PRL 103, 117003 (2009)

Marra, Wohlfeld & JvdB,
PRL 109, 117401 (2012)

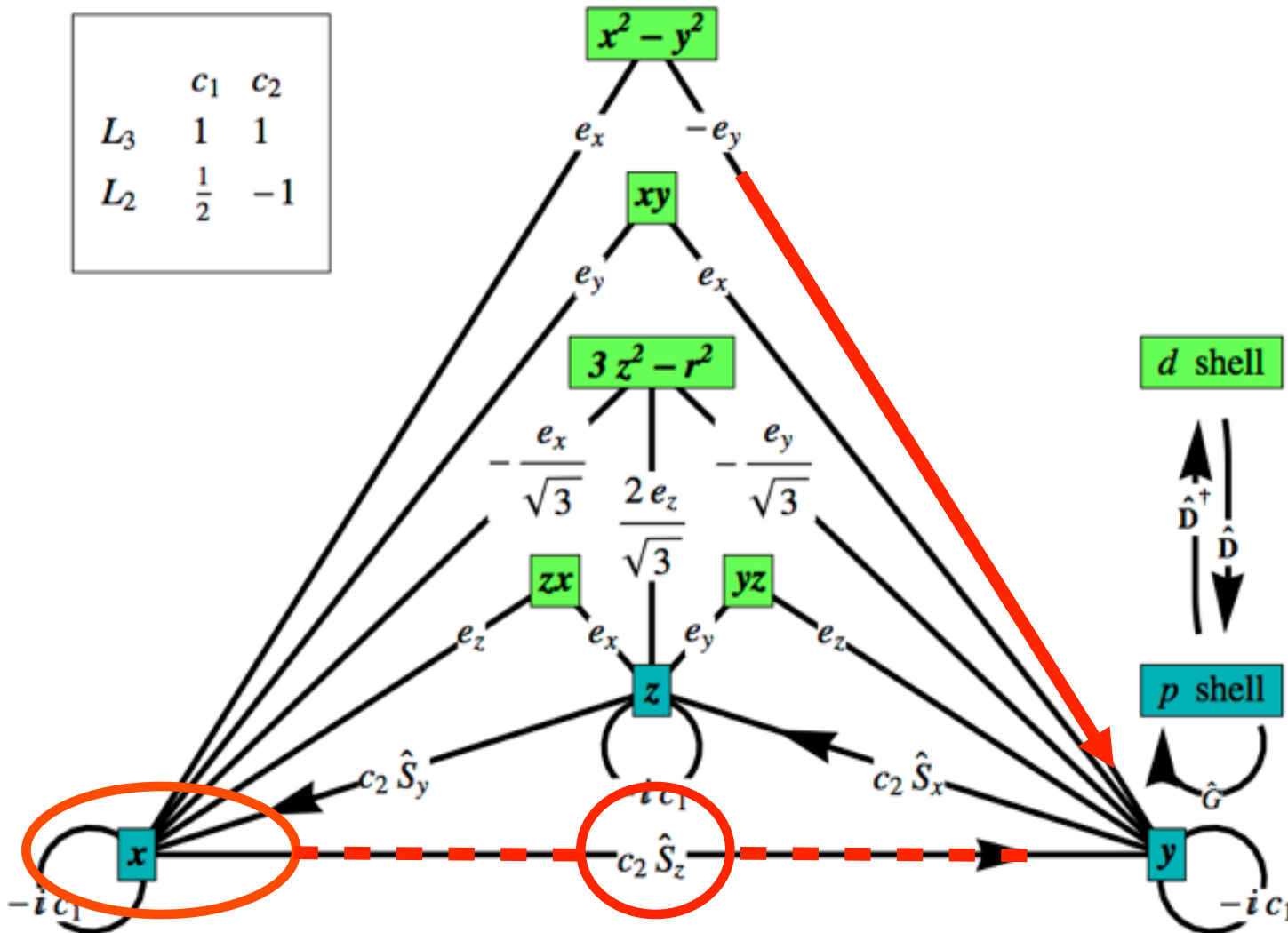
RIXS spin-flip amplitude @ transition metal L-edge



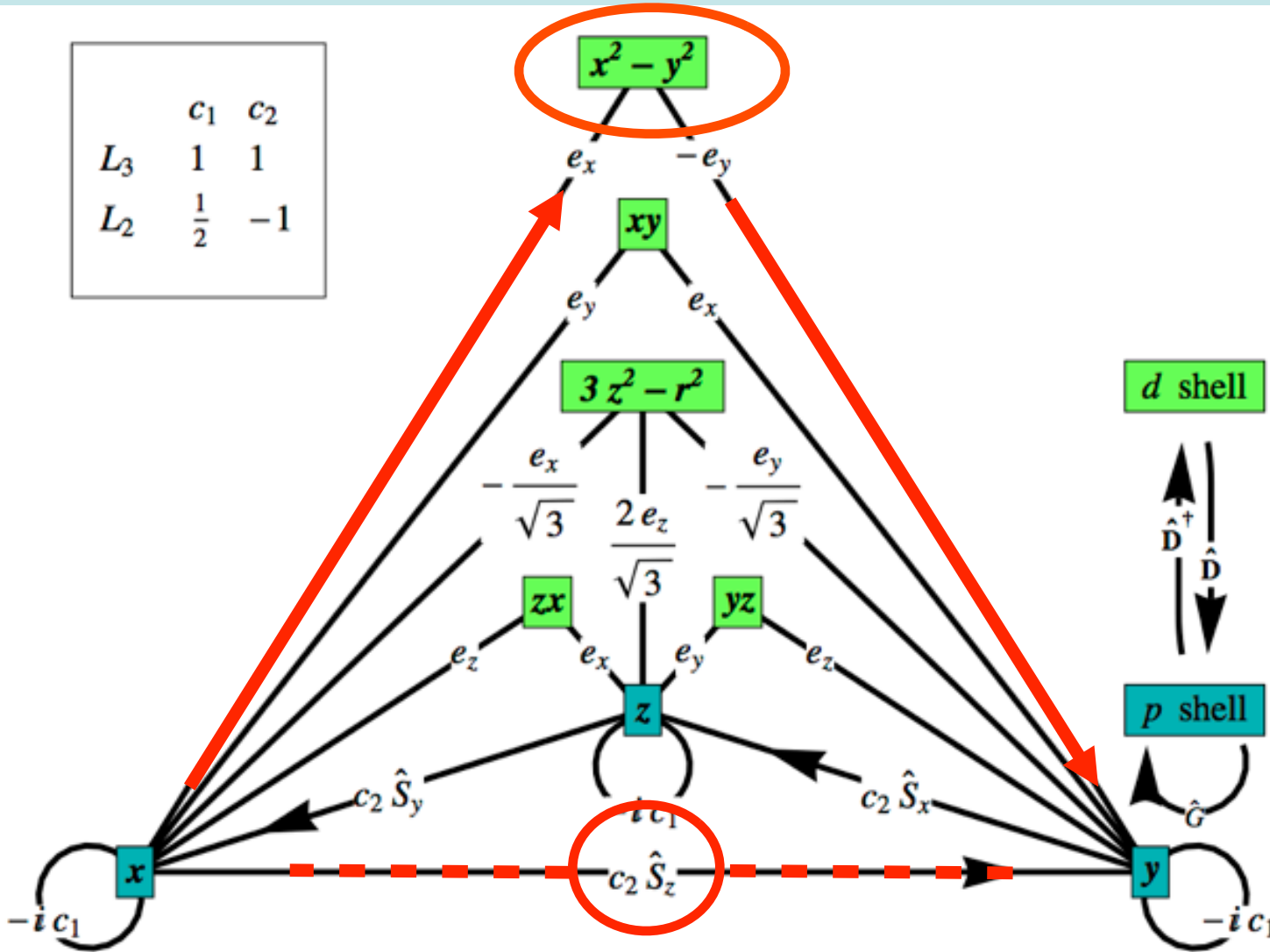
Ament, Ghiringhelli, Moretti,
Braicovich & JvdB,
PRL 103, 117003 (2009)

Marra, Wohlfeld & JvdB,
PRL 109, 117401 (2012)

RIXS spin-flip amplitude @ transition metal L-edge



RIXS spin-flip amplitude @ transition metal L-edge



Ament, Ghiringhelli, Moretti,
Braicovich & JvdB,
PRL 103, 117003 (2009)

**x^2-y^2 spin NOT // z:
pure spin flip**

Marra, Wohlfeld & JvdB,
PRL 109, 117401 (2012)

RIXS amplitude/intensity

Interaction light & matter

RIXS amplitude F and intensity I

$$I(\omega, \mathbf{k}, \mathbf{k}', \epsilon, \epsilon') = \sum_f |\mathcal{F}_{fg}(\mathbf{k}, \mathbf{k}', \epsilon, \epsilon', \omega_{\mathbf{k}})|^2 \\ \times \delta(E_f + \hbar\omega_{\mathbf{k}'} - E_g - \hbar\omega_{\mathbf{k}})$$

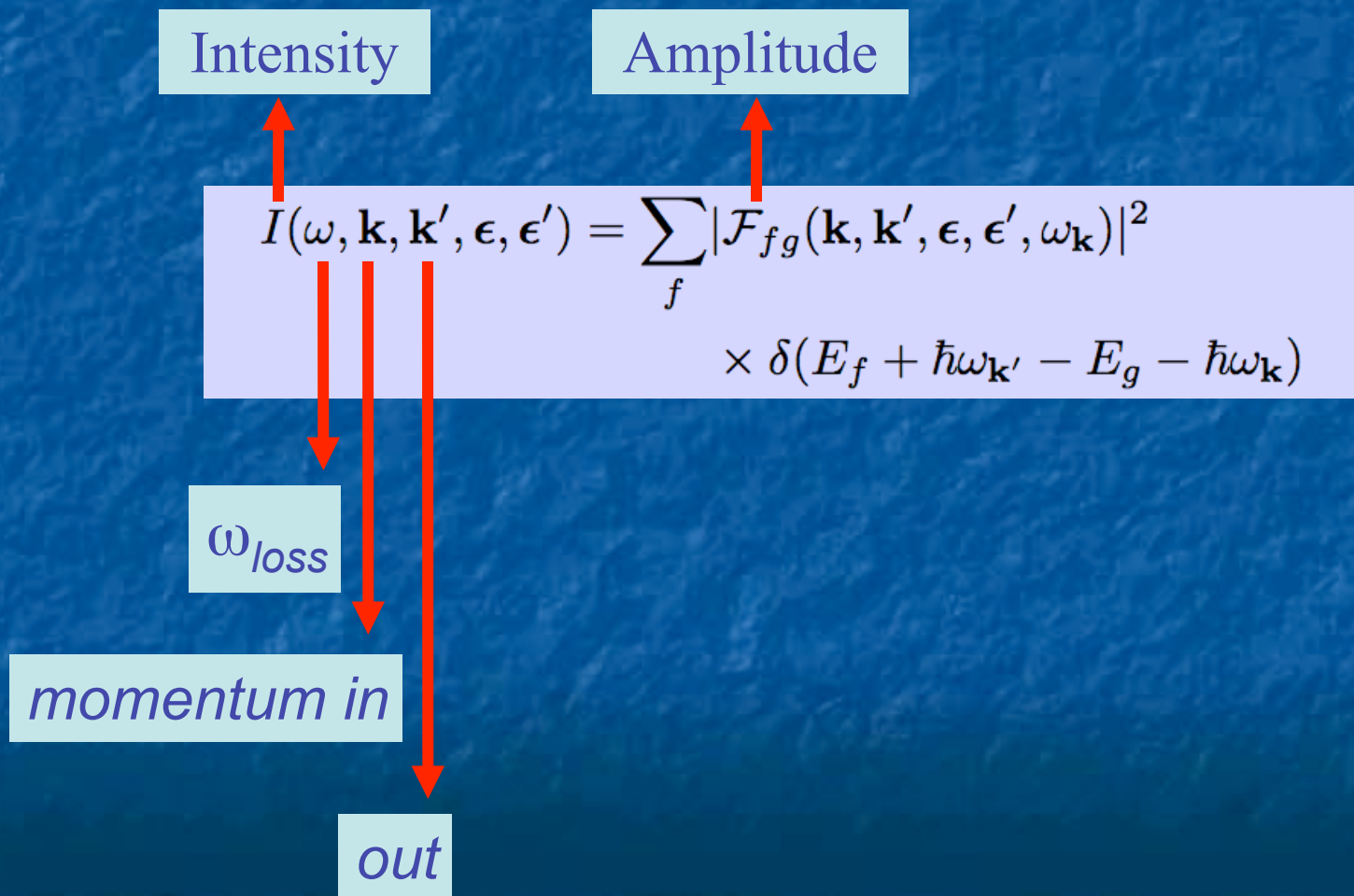
RIXS amplitude F and intensity I

Intensity

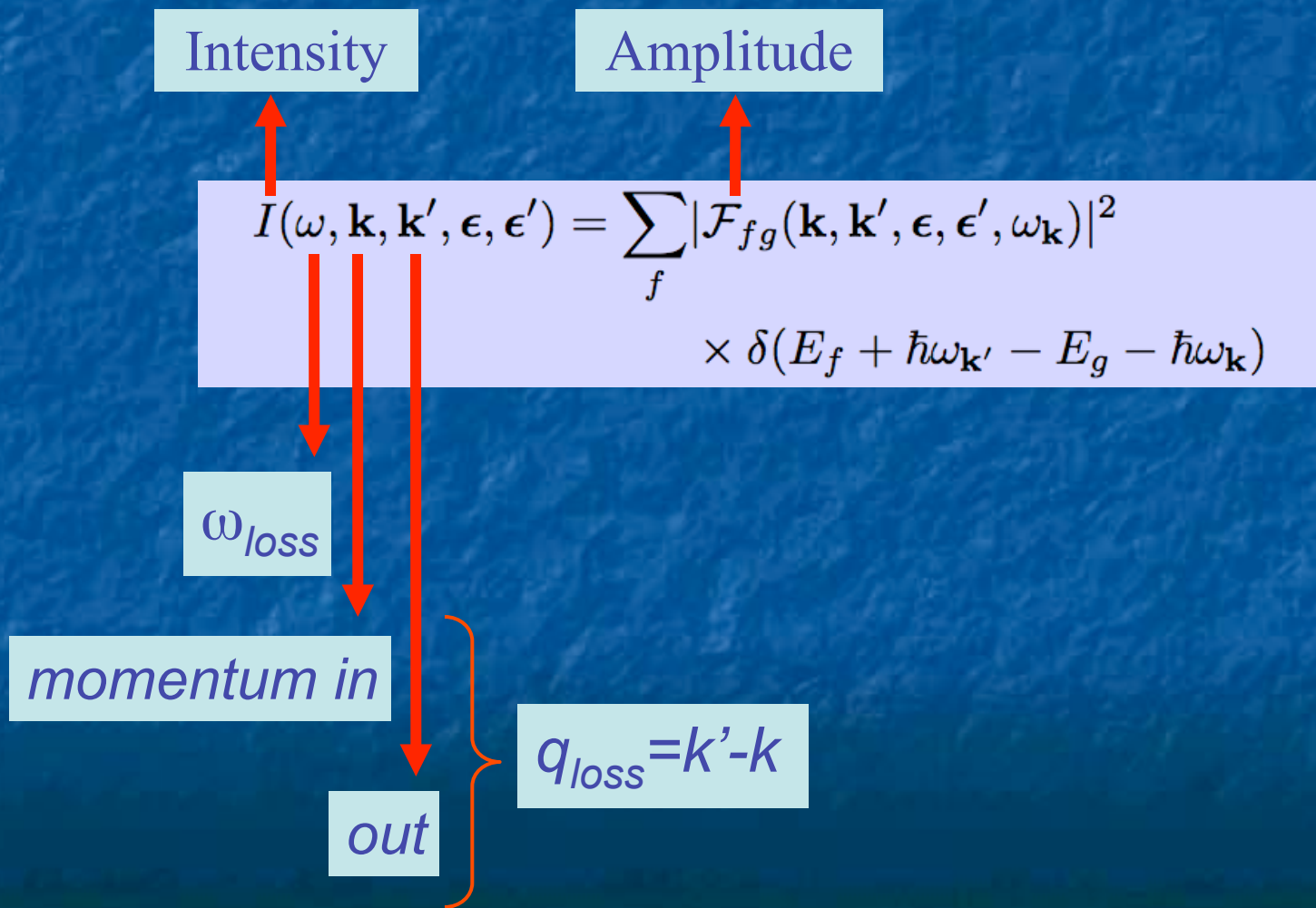
Amplitude

$$I(\omega, \mathbf{k}, \mathbf{k}', \epsilon, \epsilon') = \sum_f |\mathcal{F}_{fg}(\mathbf{k}, \mathbf{k}', \epsilon, \epsilon', \omega_{\mathbf{k}})|^2 \\ \times \delta(E_f + \hbar\omega_{\mathbf{k}'} - E_g - \hbar\omega_{\mathbf{k}})$$

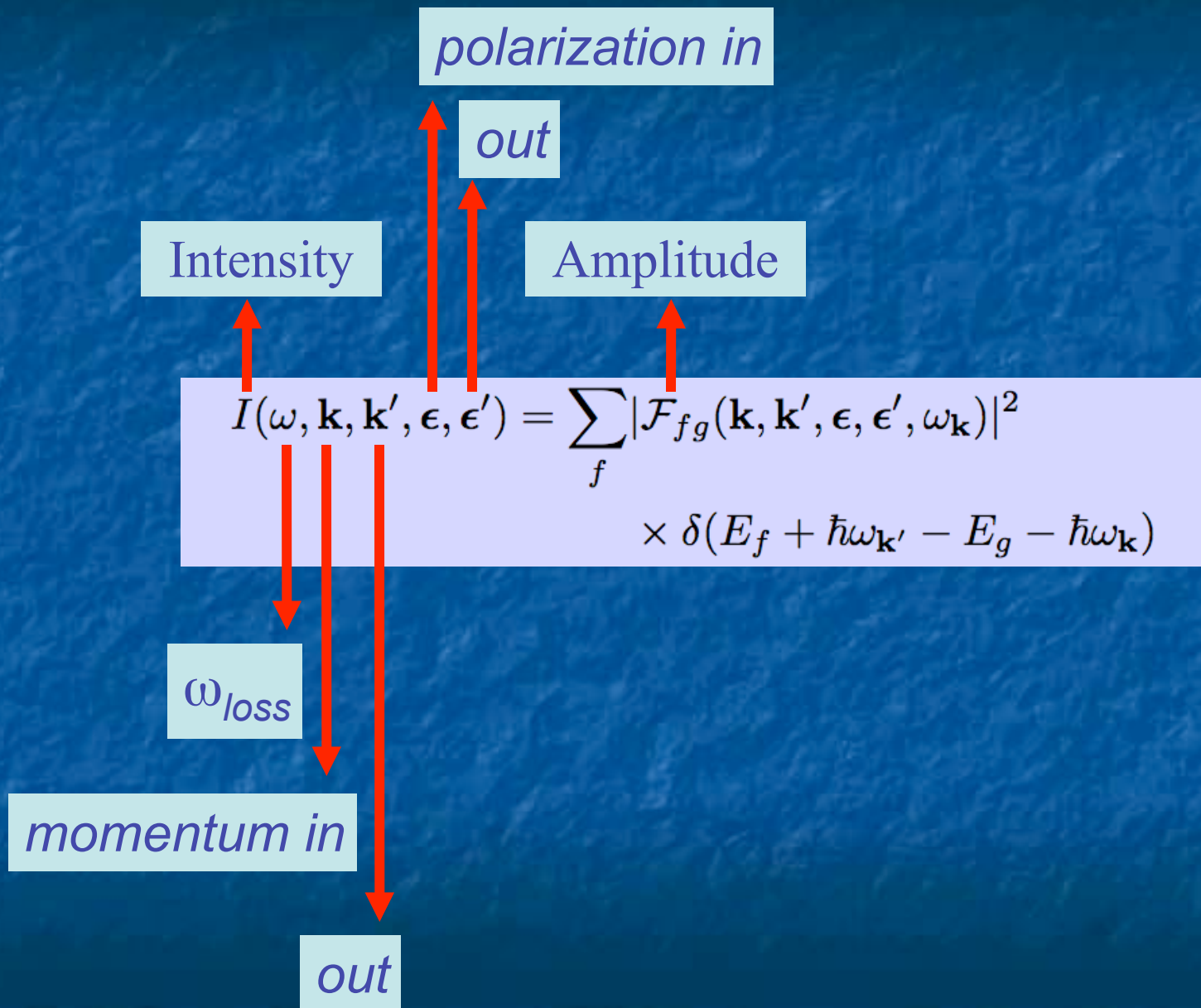
RIXS amplitude F and intensity I



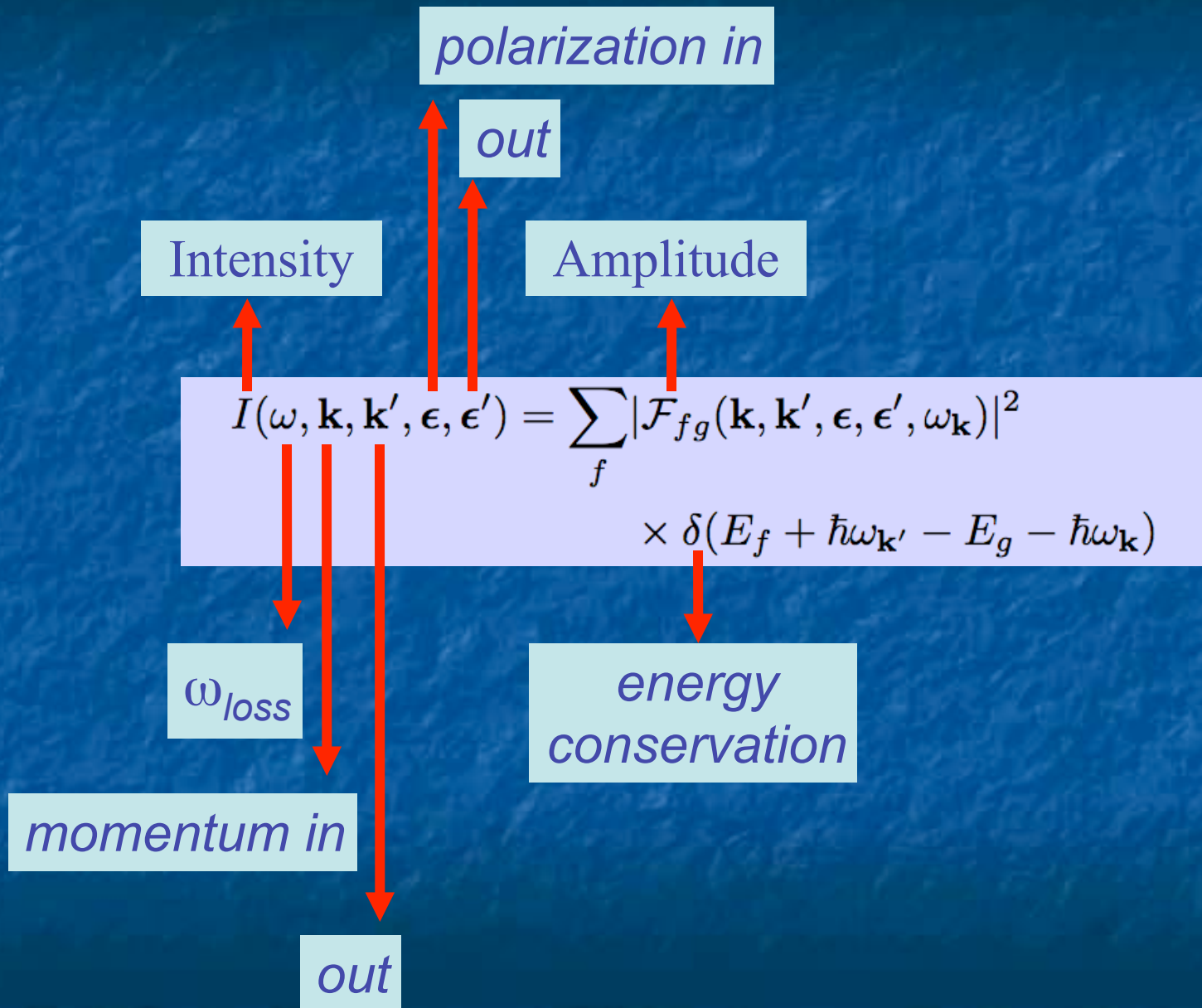
RIXS amplitude F and intensity I



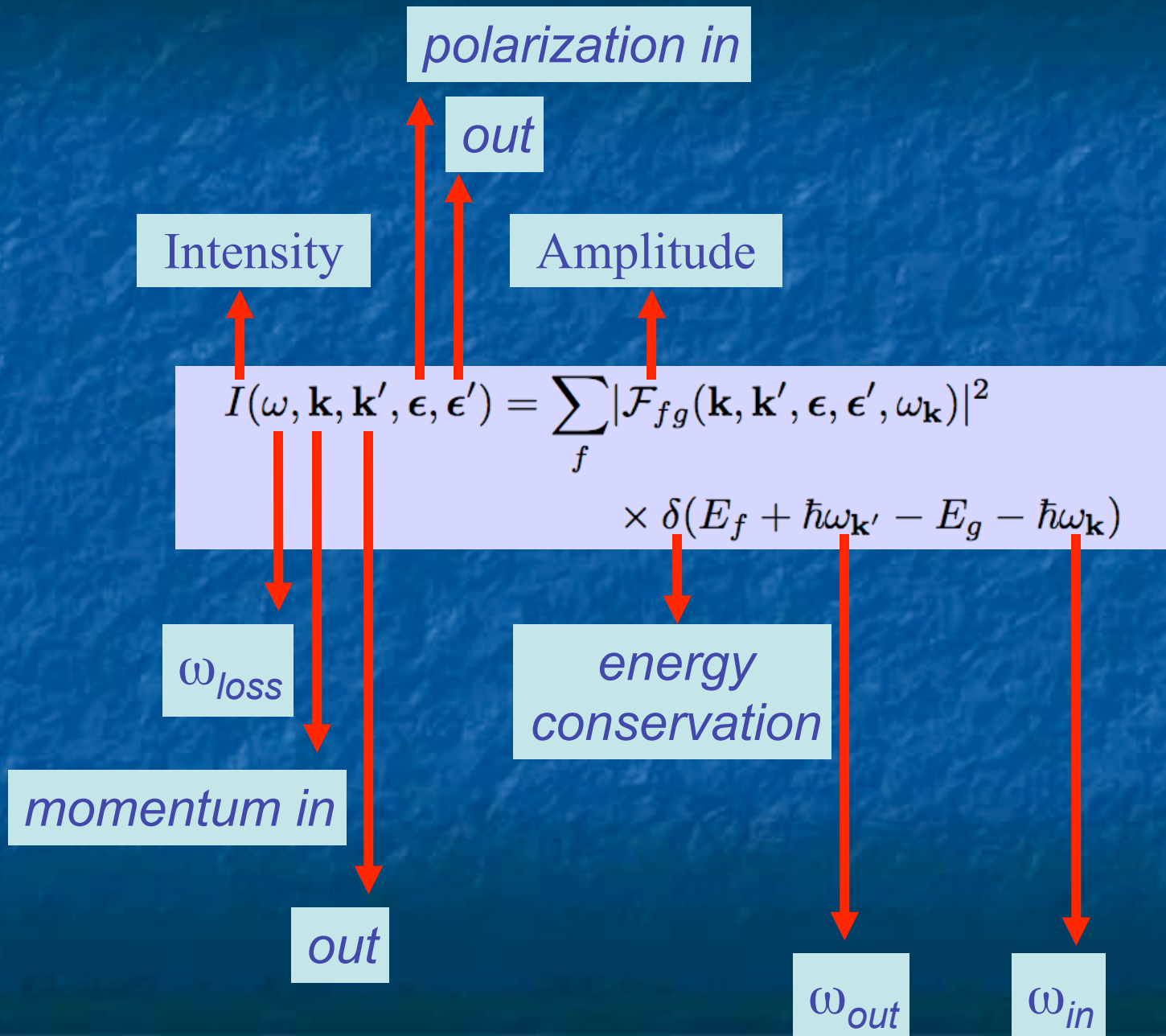
RIXS amplitude F and intensity I



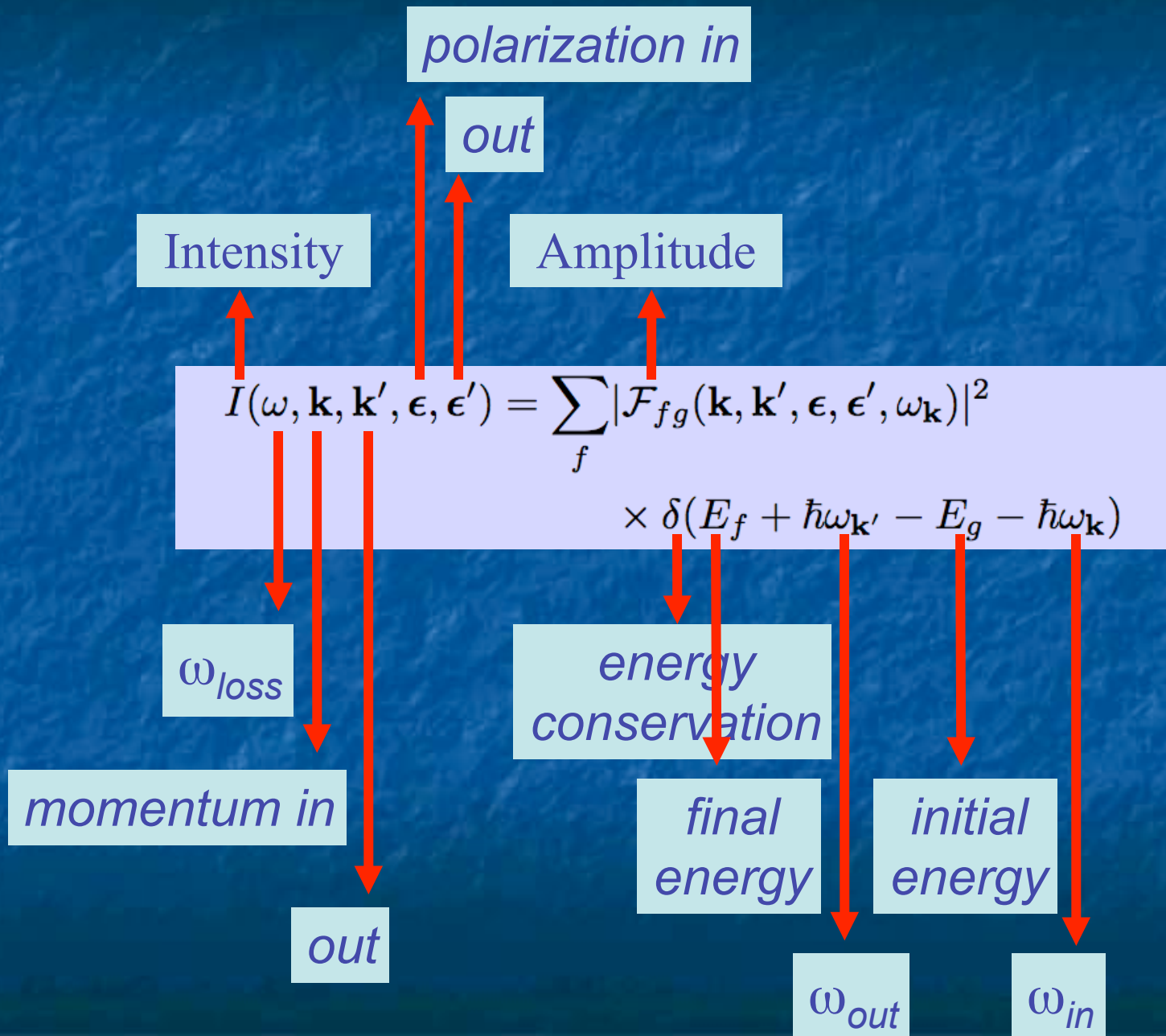
RIXS amplitude F and intensity I



RIXS amplitude F and intensity I



RIXS amplitude F and intensity I



Interaction of light and matter: Hamiltonian

$$H = \sum_{i=1}^N \left[\frac{(\mathbf{p}_i + e\mathbf{A}(\mathbf{r}_i))^2}{2m} + \frac{e\hbar}{2m} \boldsymbol{\sigma}_i \cdot \mathbf{B}(\mathbf{r}_i) + \frac{e\hbar}{2(2mc)^2} \times \right.$$
$$\left. \boldsymbol{\sigma}_i \cdot \left(\mathbf{E}(\mathbf{r}_i) \times (\mathbf{p}_i + e\mathbf{A}(\mathbf{r}_i)) - (\mathbf{p}_i + e\mathbf{A}(\mathbf{r}_i)) \times \mathbf{E}(\mathbf{r}_i) \right) \right] \\ + \frac{e\hbar^2 \rho(\mathbf{r}_i)}{8(mc)^2 \epsilon_0} + H_{\text{Coulomb}} + \sum_{\kappa, \varepsilon} \hbar \omega_\kappa \left(a_{\kappa\varepsilon}^\dagger a_{\kappa\varepsilon} + \frac{1}{2} \right)$$

Interaction of light and matter: Hamiltonian

kinetic

Zeeman

$$H = \sum_{i=1}^N \left[\frac{(\mathbf{p}_i + e\mathbf{A}(\mathbf{r}_i))^2}{2m} + \frac{e\hbar}{2m} \boldsymbol{\sigma}_i \cdot \mathbf{B}(\mathbf{r}_i) + \frac{e\hbar}{2(2mc)^2} \times \right.$$
$$\left. \boldsymbol{\sigma}_i \cdot \left(\mathbf{E}(\mathbf{r}_i) \times (\mathbf{p}_i + e\mathbf{A}(\mathbf{r}_i)) - (\mathbf{p}_i + e\mathbf{A}(\mathbf{r}_i)) \times \mathbf{E}(\mathbf{r}_i) \right) \right] + \frac{e\hbar^2 \rho(\mathbf{r}_i)}{8(mc)^2 \epsilon_0} + H_{\text{Coulomb}} + \sum_{\kappa, \varepsilon} \hbar \omega_\kappa \left(a_{\kappa\varepsilon}^\dagger a_{\kappa\varepsilon} + \frac{1}{2} \right)$$

Interaction of light and matter: Hamiltonian

kinetic

Zeeman

$$H = \sum_{i=1}^N \left[\frac{(\mathbf{p}_i + e\mathbf{A}(\mathbf{r}_i))^2}{2m} + \frac{e\hbar}{2m} \boldsymbol{\sigma}_i \cdot \mathbf{B}(\mathbf{r}_i) + \frac{e\hbar}{2(2mc)^2} \times \right.$$
$$\left. \boldsymbol{\sigma}_i \cdot \left(\mathbf{E}(\mathbf{r}_i) \times (\mathbf{p}_i + e\mathbf{A}(\mathbf{r}_i)) - (\mathbf{p}_i + e\mathbf{A}(\mathbf{r}_i)) \times \mathbf{E}(\mathbf{r}_i) \right) \right] + \frac{e\hbar^2 \rho(\mathbf{r}_i)}{8(mc)^2 \epsilon_0} + H_{\text{Coulomb}} + \sum_{\kappa, \varepsilon} \hbar \omega_\kappa \left(a_{\kappa\varepsilon}^\dagger a_{\kappa\varepsilon} + \frac{1}{2} \right)$$

*spin-orbit
coupling*

Interaction of light and matter: Hamiltonian

$$H = \sum_{i=1}^N \left[\frac{(\mathbf{p}_i + e\mathbf{A}(\mathbf{r}_i))^2}{2m} + \frac{e\hbar}{2m} \boldsymbol{\sigma}_i \cdot \mathbf{B}(\mathbf{r}_i) + \frac{e\hbar}{2(2mc)^2} \times \right.$$
$$\left. \boldsymbol{\sigma}_i \cdot \left(\mathbf{E}(\mathbf{r}_i) \times (\mathbf{p}_i + e\mathbf{A}(\mathbf{r}_i)) - (\mathbf{p}_i + e\mathbf{A}(\mathbf{r}_i)) \times \mathbf{E}(\mathbf{r}_i) \right) \right] + \frac{e\hbar^2 \rho(\mathbf{r}_i)}{8(mc)^2 \epsilon_0} + H_{\text{Coulomb}} + \sum_{\kappa, \varepsilon} \hbar \omega_\kappa \left(a_{\kappa\varepsilon}^\dagger a_{\kappa\varepsilon} + \frac{1}{2} \right)$$

Diagram illustrating the components of the Hamiltonian:

- kinetic**: Points to the first term $\frac{(\mathbf{p}_i + e\mathbf{A}(\mathbf{r}_i))^2}{2m}$.
- Zeeman**: Points to the second term $\frac{e\hbar}{2m} \boldsymbol{\sigma}_i \cdot \mathbf{B}(\mathbf{r}_i)$.
- Darwin**: Points to the third term $\frac{e\hbar}{2(2mc)^2} \times \boldsymbol{\sigma}_i \cdot (\mathbf{E}(\mathbf{r}_i) \times (\mathbf{p}_i + e\mathbf{A}(\mathbf{r}_i)) - (\mathbf{p}_i + e\mathbf{A}(\mathbf{r}_i)) \times \mathbf{E}(\mathbf{r}_i))$.
- free photons**: Points to the fourth term $\sum_{\kappa, \varepsilon} \hbar \omega_\kappa (a_{\kappa\varepsilon}^\dagger a_{\kappa\varepsilon} + \frac{1}{2})$.
- spin-orbit coupling**: Points to the fifth term $\frac{e\hbar^2 \rho(\mathbf{r}_i)}{8(mc)^2 \epsilon_0}$.

Interaction of light and matter: Hamiltonian

$$H = \sum_{i=1}^N \left[\frac{(\mathbf{p}_i + e\mathbf{A}(\mathbf{r}_i))^2}{2m} + \frac{e\hbar}{2m} \boldsymbol{\sigma}_i \cdot \mathbf{B}(\mathbf{r}_i) + \frac{e\hbar}{2(2mc)^2} \times \right.$$
$$\left. \boldsymbol{\sigma}_i \cdot \left(\mathbf{E}(\mathbf{r}_i) \times (\mathbf{p}_i + e\mathbf{A}(\mathbf{r}_i)) - (\mathbf{p}_i + e\mathbf{A}(\mathbf{r}_i)) \times \mathbf{E}(\mathbf{r}_i) \right) \right] + \frac{e\hbar^2 \rho(\mathbf{r}_i)}{8(mc)^2 \epsilon_0} + H_{\text{Coulomb}} + \sum_{\kappa, \varepsilon} \hbar \omega_\kappa \left(a_{\kappa\varepsilon}^\dagger a_{\kappa\varepsilon} + \frac{1}{2} \right)$$

Diagram illustrating the components of the Hamiltonian:

- kinetic**: $\frac{(\mathbf{p}_i + e\mathbf{A}(\mathbf{r}_i))^2}{2m}$ (indicated by a red arrow pointing up)
- Zeeman**: $\frac{e\hbar}{2m} \boldsymbol{\sigma}_i \cdot \mathbf{B}(\mathbf{r}_i)$ (indicated by a red arrow pointing up)
- Darwin**: $\frac{e\hbar^2 \rho(\mathbf{r}_i)}{8(mc)^2 \epsilon_0}$ (indicated by a red arrow pointing down)
- free photons**: $\sum_{\kappa, \varepsilon} \hbar \omega_\kappa (a_{\kappa\varepsilon}^\dagger a_{\kappa\varepsilon} + \frac{1}{2})$ (indicated by a red arrow pointing down)
- spin-orbit coupling**: $\frac{e\hbar}{2(2mc)^2} \times \boldsymbol{\sigma}_i \cdot (\mathbf{E}(\mathbf{r}_i) \times (\mathbf{p}_i + e\mathbf{A}(\mathbf{r}_i)) - (\mathbf{p}_i + e\mathbf{A}(\mathbf{r}_i)) \times \mathbf{E}(\mathbf{r}_i))$ (indicated by a red arrow pointing right)

Below the Hamiltonian, the vector potential $\mathbf{A}(\mathbf{r})$ is expressed as a sum of plane waves:

$$\mathbf{A}(\mathbf{r}) = \sum_{\kappa, \varepsilon} \sqrt{\frac{\hbar}{2\mathcal{V}\epsilon_0\omega_\kappa}} (\varepsilon a_{\kappa\varepsilon} e^{i\kappa \cdot \mathbf{r}} + \varepsilon^* a_{\kappa\varepsilon}^\dagger e^{-i\kappa \cdot \mathbf{r}})$$

Lowest order perturbing Hamiltonian: small A

$$H' = \sum_{i=1}^N \left[\frac{e}{m} \mathbf{A}(\mathbf{r}_i) \cdot \mathbf{p}_i + \frac{e^2}{2m} \mathbf{A}^2(\mathbf{r}_i) + \frac{e\hbar}{2m} \boldsymbol{\sigma}_i \cdot \nabla \times \mathbf{A}(\mathbf{r}_i) - \frac{e^2\hbar}{(2mc)^2} \boldsymbol{\sigma}_i \cdot \frac{\partial \mathbf{A}(\mathbf{r}_i)}{\partial t} \times \mathbf{A}(\mathbf{r}_i) \right],$$

Lowest order perturbing Hamiltonian: small A

$$H' = \sum_{i=1}^N \left[\frac{e}{m} \mathbf{A}(\mathbf{r}_i) \cdot \mathbf{p}_i + \frac{e^2}{2m} \mathbf{A}^2(\mathbf{r}_i) + \frac{e\hbar}{2m} \boldsymbol{\sigma}_i \cdot \nabla \times \mathbf{A}(\mathbf{r}_i) \right. \\ \left. - \frac{e^2\hbar}{(2mc)^2} \boldsymbol{\sigma}_i \cdot \frac{\partial \mathbf{A}(\mathbf{r}_i)}{\partial t} \times \mathbf{A}(\mathbf{r}_i) \right],$$

small

Lowest order perturbing Hamiltonian: small A

$$H' = \sum_{i=1}^N \left[\frac{e}{m} \mathbf{A}(\mathbf{r}_i) \cdot \mathbf{p}_i + \frac{e^2}{2m} \mathbf{A}^2(\mathbf{r}_i) + \frac{e\hbar}{2m} \boldsymbol{\sigma}_i \cdot \nabla \times \mathbf{A}(\mathbf{r}_i) \right. \\ \left. - \frac{e^2\hbar}{(2mc)^2} \boldsymbol{\sigma}_i \cdot \frac{\partial \mathbf{A}(\mathbf{r}_i)}{\partial t} \times \mathbf{A}(\mathbf{r}_i) \right], \quad \xrightarrow{\text{small}} \text{small}$$

Fermi Golden Rule, to second order:

transition rate

$$w = \frac{2\pi}{\hbar} \sum_{\mathbf{f}} \left| \langle \mathbf{f} | H' | \mathbf{g} \rangle \right. \\ \left. + \sum_n \frac{\langle \mathbf{f} | H' | n \rangle \langle n | H' | \mathbf{g} \rangle}{E_{\mathbf{g}} - E_n} \right|^2 \delta(E_{\mathbf{f}} - E_{\mathbf{g}})$$

1st Order: Thompson Scattering

$$\frac{e^2}{2m} \langle \mathbf{f} | \sum_i \mathbf{A}^2(\mathbf{r}_i) | \mathbf{g} \rangle = \frac{\hbar e^2}{2m\mathcal{V}\epsilon_0} \frac{\boldsymbol{\epsilon}'^* \cdot \boldsymbol{\epsilon}}{\sqrt{\omega_{\mathbf{k}}\omega_{\mathbf{k}'}}} \langle f | \sum_i e^{i\mathbf{q} \cdot \mathbf{r}_i} | g \rangle$$

1st Order: Thompson Scattering

$$\frac{e^2}{2m} \langle f | \sum_i \mathbf{A}^2(\mathbf{r}_i) | g \rangle = \frac{\hbar e^2}{2m\mathcal{V}\epsilon_0} \frac{\epsilon'^* \cdot \epsilon}{\sqrt{\omega_{\mathbf{k}}\omega_{\mathbf{k}'}}} \langle f | \sum_i e^{i\mathbf{q} \cdot \mathbf{r}_i} | g \rangle$$



Fourier transform of charge density

Elastic part: causes Bragg scattering & diffraction

1st Order: Thompson Scattering

$$\frac{e^2}{2m} \langle f | \sum_i \mathbf{A}^2(\mathbf{r}_i) | g \rangle = \frac{\hbar e^2}{2m\mathcal{V}\epsilon_0} \frac{\epsilon'^* \cdot \epsilon}{\sqrt{\omega_{\mathbf{k}}\omega_{\mathbf{k}'}}} \langle f | \sum_i e^{i\mathbf{q} \cdot \mathbf{r}_i} | g \rangle$$



Fourier transform of charge density

Elastic part: causes Bragg scattering & diffraction

Inelastic part: causes Inelastic X-ray Scattering (IXS)

= Non-Resonant Inelastic X-ray Scattering (NIXS)

1st Order: Thompson Scattering

$$\frac{e^2}{2m} \langle f | \sum_i \mathbf{A}^2(\mathbf{r}_i) | g \rangle = \frac{\hbar e^2}{2m\mathcal{V}\epsilon_0} \frac{\epsilon'^* \cdot \epsilon}{\sqrt{\omega_{\mathbf{k}}\omega_{\mathbf{k}'}}} \langle f | \sum_i e^{i\mathbf{q} \cdot \mathbf{r}_i} | g \rangle$$



Fourier transform of charge density

Elastic part: causes Bragg scattering & diffraction

Inelastic part: causes Inelastic X-ray Scattering (IXS)

= Non-Resonant Inelastic X-ray Scattering (NIXS)

transition operator

$$e^{iqr} \approx 1 + iqr - \frac{1}{2}(qr)^2 + \dots$$

1st Order: Thompson Scattering

$$\frac{e^2}{2m} \langle \mathbf{f} | \sum_i \mathbf{A}^2(\mathbf{r}_i) | \mathbf{g} \rangle = \frac{\hbar e^2}{2m\mathcal{V}\epsilon_0} \frac{\boldsymbol{\epsilon}'^* \cdot \boldsymbol{\epsilon}}{\sqrt{\omega_{\mathbf{k}}\omega_{\mathbf{k}'}}} \langle f | \sum_i e^{i\mathbf{q} \cdot \mathbf{r}_i} | g \rangle$$



Fourier transform of charge density

Elastic part: causes Bragg scattering & diffraction

Inelastic part: causes Inelastic X-ray Scattering (IXS)

= Non-Resonant Inelastic X-ray Scattering (NIXS)

quadrupole

transition operator

$$e^{iqr} \approx 1 + iqr - \frac{1}{2}(qr)^2 + \dots$$



dipole



1st order: X-ray Absorption

$$\langle f | A \cdot p | g \rangle$$

1st order: X-ray Absorption

$$\langle f | A \cdot p | g \rangle \propto \langle f | e^{ikr} \varepsilon \cdot p | g \rangle$$

1st order: X-ray Absorption

$$\langle f | A \cdot p | g \rangle \propto \langle f | e^{ikr} \varepsilon \cdot p | g \rangle \approx \langle f | \varepsilon \cdot p | g \rangle$$

when expanding

$$e^{iqr} \approx 1 + iqr - \frac{1}{2}(qr)^2 + \dots$$

1st order: X-ray Absorption

$$\langle f | A \cdot p | g \rangle \propto \langle f | e^{ikr} \varepsilon \cdot p | g \rangle \approx \langle f | \varepsilon \cdot p | g \rangle$$

when expanding

$$e^{iqr} \approx 1 + iqr - \frac{1}{2}(qr)^2 + \dots$$

dipole:

transitions caused by momentum operator p

2nd Order...

$$H' = \sum_{i=1}^N \frac{e}{m} \mathbf{A}(\mathbf{r}_i) \cdot \mathbf{p}_i + \frac{e^2}{2m} \mathbf{A}^2(\mathbf{r}_i) + \frac{e\hbar}{2m} \boldsymbol{\sigma}_i \cdot \nabla \times \mathbf{A}(\mathbf{r}_i)$$

Fermi Golden Rule, to second order:

transition rate

$$w = \frac{2\pi}{\hbar} \sum_{\mathbf{f}} \left| \langle \mathbf{f} | H' | \mathbf{g} \rangle \right. \\ \left. + \sum_n \frac{\langle \mathbf{f} | H' | n \rangle \langle n | H' | \mathbf{g} \rangle}{E_{\mathbf{g}} - E_n} \right|^2 \delta(E_{\mathbf{f}} - E_{\mathbf{g}})$$

2nd Order...

$$H' = \sum_{i=1}^N \frac{e}{m} \mathbf{A}(\mathbf{r}_i) \cdot \mathbf{p}_i + \frac{e\hbar}{2m} \boldsymbol{\sigma}_i \cdot \nabla \times \mathbf{A}(\mathbf{r}_i)$$

Fermi Golden Rule, to second order:

transition rate

$$w = \frac{2\pi}{\hbar} \sum_{\mathbf{f}} \left| \langle \mathbf{f} | H' | \mathbf{g} \rangle \right. \\ \left. + \sum_n \frac{\langle \mathbf{f} | H' | n \rangle \langle n | H' | \mathbf{g} \rangle}{E_{\mathbf{g}} - E_n} \right|^2 \delta(E_{\mathbf{f}} - E_{\mathbf{g}})$$

2nd Order: Resonant Scattering I

RIXS
amplitude

$$\begin{aligned} & \frac{e^2 \hbar}{2m^2 \mathcal{V} \epsilon_0 \sqrt{\omega_{\mathbf{k}} \omega_{\mathbf{k}'}}} \sum_n \sum_{i,j=1}^N \\ & \times \frac{\langle f | e^{-i\mathbf{k}' \cdot \mathbf{r}_i} (\boldsymbol{\epsilon}'^* \cdot \mathbf{p}_i - \frac{i\hbar}{2} \boldsymbol{\sigma}_i \cdot \mathbf{k}' \times \boldsymbol{\epsilon}'^*) | n \rangle}{E_g + \hbar\omega_{\mathbf{k}} - E_n + i\Gamma_n} \\ & \times \langle n | e^{i\mathbf{k} \cdot \mathbf{r}_j} \left(\boldsymbol{\epsilon} \cdot \mathbf{p}_j + \frac{i\hbar}{2} \boldsymbol{\sigma}_j \cdot \mathbf{k} \times \boldsymbol{\epsilon} \right) | g \rangle \end{aligned}$$

2nd Order: Resonant Scattering I

RIXS
amplitude

$$\begin{aligned} & \frac{e^2 \hbar}{2m^2 \mathcal{V} \epsilon_0 \sqrt{\omega_{\mathbf{k}} \omega_{\mathbf{k}'}}} \sum_n \sum_{i,j=1}^N \\ & \times \frac{\langle f | e^{-i\mathbf{k}' \cdot \mathbf{r}_i} (\boldsymbol{\epsilon}'^* \cdot \mathbf{p}_i - \frac{i\hbar}{2} \boldsymbol{\sigma}_i \cdot \mathbf{k}' \times \boldsymbol{\epsilon}'^*) | n \rangle}{E_g + \hbar\omega_{\mathbf{k}} - E_n + i\Gamma_n} \\ & \times \langle n | e^{i\mathbf{k} \cdot \mathbf{r}_j} \left(\boldsymbol{\epsilon} \cdot \mathbf{p}_j + \frac{i\hbar}{2} \boldsymbol{\sigma}_j \cdot \mathbf{k} \times \boldsymbol{\epsilon} \right) | g \rangle \end{aligned}$$

small

2nd Order: Resonant Scattering I

RIXS
amplitude

$$\begin{aligned} & \frac{e^2 \hbar}{2m^2 \mathcal{V} \epsilon_0 \sqrt{\omega_{\mathbf{k}} \omega_{\mathbf{k}'}}} \sum_n \sum_{i,j=1}^N \\ & \times \frac{\langle f | e^{-i\mathbf{k}' \cdot \mathbf{r}_i} (\boldsymbol{\epsilon}'^* \cdot \mathbf{p}_i - \frac{i\hbar}{2} \boldsymbol{\sigma}_i \cdot \mathbf{k}' \times \boldsymbol{\epsilon}'^*) | n \rangle}{E_g + \hbar\omega_{\mathbf{k}} - E_n + i\Gamma_n} \\ & \times \langle n | e^{i\mathbf{k} \cdot \mathbf{r}_j} \left(\boldsymbol{\epsilon} \cdot \mathbf{p}_j + \frac{i\hbar}{2} \boldsymbol{\sigma}_j \cdot \mathbf{k} \times \boldsymbol{\epsilon} \right) | g \rangle \end{aligned}$$

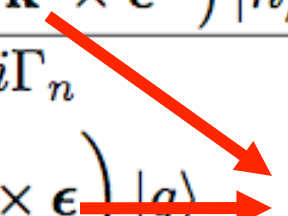
small

RIXS
transition
operator

$$\mathcal{D} = \frac{1}{im\omega_{\mathbf{k}}} \sum_{i=1}^N e^{i\mathbf{k} \cdot \mathbf{r}_i} \boldsymbol{\epsilon} \cdot \mathbf{p}_i,$$

2nd Order: Resonant Scattering I

RIXS
amplitude

$$\begin{aligned}
 & \frac{e^2 \hbar}{2m^2 \mathcal{V} \epsilon_0 \sqrt{\omega_{\mathbf{k}} \omega_{\mathbf{k}'}}} \sum_n \sum_{i,j=1}^N \\
 & \times \frac{\langle f | e^{-i\mathbf{k}' \cdot \mathbf{r}_i} (\epsilon'^* \cdot \mathbf{p}_i - \frac{i\hbar}{2} \boldsymbol{\sigma}_i \cdot \mathbf{k}' \times \epsilon'^*) | n \rangle}{E_g + \hbar\omega_{\mathbf{k}} - E_n + i\Gamma_n} \\
 & \times \langle n | e^{i\mathbf{k} \cdot \mathbf{r}_j} \left(\epsilon \cdot \mathbf{p}_j + \frac{i\hbar}{2} \boldsymbol{\sigma}_j \cdot \mathbf{k} \times \epsilon \right) | g \rangle
 \end{aligned}$$


small

RIXS
transition
operator

$$\mathcal{D} = \frac{1}{im\omega_{\mathbf{k}}} \sum_{i=1}^N e^{i\mathbf{k} \cdot \mathbf{r}_i} \epsilon \cdot \mathbf{p}_i,$$

RIXS
amplitude

$$\mathcal{F}_{fg}(\mathbf{k}, \mathbf{k}', \epsilon, \epsilon', \omega_{\mathbf{k}}, \omega_{\mathbf{k}'}) = \sum_n \frac{\langle f | \mathcal{D}'^\dagger | n \rangle \langle n | \mathcal{D} | g \rangle}{E_g + \hbar\omega_{\mathbf{k}} - E_n + i\Gamma_n}$$

2nd Order: Resonant Scattering I

RIXS
amplitude

$$\begin{aligned}
 & \frac{e^2 \hbar}{2m^2 \mathcal{V} \epsilon_0 \sqrt{\omega_{\mathbf{k}} \omega_{\mathbf{k}'}}} \sum_n \sum_{i,j=1}^N \\
 & \times \frac{\langle f | e^{-i\mathbf{k}' \cdot \mathbf{r}_i} (\epsilon'^* \cdot \mathbf{p}_i - \frac{i\hbar}{2} \boldsymbol{\sigma}_i \cdot \mathbf{k}' \times \epsilon'^*) | n \rangle}{E_g + \hbar\omega_{\mathbf{k}} - E_n + i\Gamma_n} \\
 & \times \langle n | e^{i\mathbf{k} \cdot \mathbf{r}_j} \left(\epsilon \cdot \mathbf{p}_j + \frac{i\hbar}{2} \boldsymbol{\sigma}_j \cdot \mathbf{k} \times \epsilon \right) | g \rangle
 \end{aligned}$$

small

RIXS
transition
operator

$$\mathcal{D} = \frac{1}{im\omega_{\mathbf{k}}} \sum_{i=1}^N e^{i\mathbf{k} \cdot \mathbf{r}_i} \epsilon \cdot \mathbf{p}_i,$$

RIXS
amplitude

$$\mathcal{F}_{fg}(\mathbf{k}, \mathbf{k}', \epsilon, \epsilon', \omega_{\mathbf{k}}, \omega_{\mathbf{k}'}) = \sum_n \frac{\langle f | \mathcal{D}'^\dagger | n \rangle \langle n | \mathcal{D} | g \rangle}{E_g + \hbar\omega_{\mathbf{k}} - E_n + i\Gamma_n}$$

Kramers-Heisenberg expression

H.A. Kramers and W. Heisenberg, Z. Phys. 31, 681 (1925)

2nd Order: Resonant Scattering II

RIXS
amplitude

$$\mathcal{F}_{fg}(\mathbf{k}, \mathbf{k}', \epsilon, \epsilon', \omega_{\mathbf{k}}, \omega_{\mathbf{k}'}) = \sum_n \frac{\langle f | \mathcal{D}'^\dagger | n \rangle \langle n | \mathcal{D} | g \rangle}{E_g + \hbar\omega_{\mathbf{k}} - E_n + i\Gamma_n}$$

2nd Order: Resonant Scattering II

RIXS
amplitude

$$\mathcal{F}_{fg}(\mathbf{k}, \mathbf{k}', \epsilon, \epsilon', \omega_{\mathbf{k}}, \omega_{\mathbf{k}'}) = \sum_n \frac{\langle f | \mathcal{D}'^\dagger | n \rangle \langle n | \mathcal{D} | g \rangle}{E_g + \hbar\omega_{\mathbf{k}} - E_n + i\Gamma_n}$$

RIXS intensity:

$$I(\omega, \mathbf{k}, \mathbf{k}', \epsilon, \epsilon') = r_e^2 m^2 \omega_{\mathbf{k}'}^3 \omega_{\mathbf{k}} \sum_{\mathbf{f}} |\mathcal{F}_{fg}(\mathbf{k}, \mathbf{k}', \epsilon, \epsilon', \omega_{\mathbf{k}}, \omega_{\mathbf{k}'})|^2 \\ \times \delta(E_g - E_f + \hbar\omega),$$

2nd Order: Resonant Scattering II

RIXS
amplitude

$$\mathcal{F}_{fg}(\mathbf{k}, \mathbf{k}', \epsilon, \epsilon', \omega_{\mathbf{k}}, \omega_{\mathbf{k}'}) = \sum_n \frac{\langle f | \mathcal{D}'^\dagger | n \rangle \langle n | \mathcal{D} | g \rangle}{E_g + \hbar\omega_{\mathbf{k}} - E_n + i\Gamma_n}$$

RIXS intensity:

$$I(\omega, \mathbf{k}, \mathbf{k}', \epsilon, \epsilon') = r_e^2 m^2 \omega_{\mathbf{k}'}^3 \omega_{\mathbf{k}} \sum_{\mathbf{f}} |\mathcal{F}_{fg}(\mathbf{k}, \mathbf{k}', \epsilon, \epsilon', \omega_{\mathbf{k}}, \omega_{\mathbf{k}'})|^2 \\ \times \delta(E_g - E_f + \hbar\omega),$$

*This expression is essentially exact
(non-relativistic limit)*

Resonant ELASTIC Scattering (REXS or RXS)

RIXS
amplitude

$$\mathcal{F}_{fg}(\mathbf{k}, \mathbf{k}', \epsilon, \epsilon', \omega_{\mathbf{k}}, \omega_{\mathbf{k}'}) = \sum_n \frac{\langle f | \mathcal{D}'^\dagger | n \rangle \langle n | \mathcal{D} | g \rangle}{E_g + \hbar\omega_{\mathbf{k}} - E_n + i\Gamma_n}$$

Resonant ELASTIC Scattering (REXS or RXS)

REXS
amplitude

$$\mathcal{F}_{g\bar{g}}(\mathbf{k}, \mathbf{k}', \epsilon, \epsilon', \omega_{\mathbf{k}}, \omega_{\mathbf{k}'}) = \sum_n \frac{\langle \bar{g} | \mathcal{D}'^\dagger | n \rangle \langle n | \mathcal{D} | g \rangle}{E_g + \hbar\omega_{\mathbf{k}} - E_n + i\Gamma_n}$$

Resonant ELASTIC Scattering (REXS or RXS)

REXS
amplitude

$$\mathcal{F}_{g\bar{g}}(\mathbf{k}, \mathbf{k}', \epsilon, \epsilon', \omega_{\mathbf{k}}, \omega_{\mathbf{k}'}) = \sum_n \frac{\langle \bar{g} | \mathcal{D}'^\dagger | n \rangle \langle n | \mathcal{D} | g \rangle}{E_g + \hbar\omega_{\mathbf{k}} - E_n + i\Gamma_n}$$

REXS intensity:

$$I(\omega, \mathbf{k}, \mathbf{k}', \epsilon, \epsilon') = r_e^2 m^2 \omega_{\mathbf{k}'}^3 \omega_{\mathbf{k}} \sum_{\mathbf{f}} |\mathcal{F}_{fg}(\mathbf{k}, \mathbf{k}', \epsilon, \epsilon', \omega_{\mathbf{k}}, \omega_{\mathbf{k}'})|^2 \\ \times \delta(E_g - E_f + \hbar\omega),$$

Resonant ELASTIC Scattering (REXS or RXS)

REXS
amplitude

$$\mathcal{F}_{g\bar{g}}(\mathbf{k}, \mathbf{k}', \epsilon, \epsilon', \omega_{\mathbf{k}}, \omega_{\mathbf{k}'}) = \sum_n \frac{\langle \bar{g} | \mathcal{D}'^\dagger | n \rangle \langle n | \mathcal{D} | g \rangle}{E_g + \hbar\omega_{\mathbf{k}} - E_n + i\Gamma_n}$$

REXS intensity:

$$I(-\mathbf{k}, \mathbf{k}', \epsilon, \epsilon') = r_e^2 m^2 \omega_{\mathbf{k}'}^3 \omega_{\mathbf{k}} \sum_{\mathbf{f}} |\mathcal{F}_{g\bar{g}}(\mathbf{k}, \mathbf{k}', \epsilon, \epsilon', \omega_{\mathbf{k}}, \omega_{\mathbf{k}'})|^2$$

Greens function expression for F

*RIXS
amplitude*

$$\mathcal{F}_{fg}(\mathbf{k}, \mathbf{k}', \epsilon, \epsilon', \omega_{\mathbf{k}}, \omega_{\mathbf{k}'}) = \sum_n \frac{\langle f | \mathcal{D}'^\dagger | n \rangle \langle n | \mathcal{D} | g \rangle}{E_g + \hbar\omega_{\mathbf{k}} - E_n + i\Gamma_n}$$

Greens function expression for F

*RIXS
amplitude*

$$\mathcal{F}_{fg}(\mathbf{k}, \mathbf{k}', \epsilon, \epsilon', \omega_{\mathbf{k}}, \omega_{\mathbf{k}'}) = \sum_n \frac{\langle f | \mathcal{D}'^\dagger | n \rangle \langle n | \mathcal{D} | g \rangle}{E_g + \hbar\omega_{\mathbf{k}} - E_n + i\Gamma_n}$$

Greens function

$$G(z_{\mathbf{k}}) = \frac{1}{z_{\mathbf{k}} - H} = \sum_n \frac{|n\rangle\langle n|}{z_{\mathbf{k}} - E_n}$$

Greens function expression for F

*RIXS
amplitude*

$$\mathcal{F}_{fg}(\mathbf{k}, \mathbf{k}', \epsilon, \epsilon', \omega_{\mathbf{k}}, \omega_{\mathbf{k}'}) = \sum_n \frac{\langle f | \mathcal{D}'^\dagger | n \rangle \langle n | \mathcal{D} | g \rangle}{E_g + \hbar\omega_{\mathbf{k}} - E_n + i\Gamma_n}$$

Greens function

$$G(z_{\mathbf{k}}) = \frac{1}{z_{\mathbf{k}} - H} = \sum_n \frac{|n\rangle\langle n|}{z_{\mathbf{k}} - E_n}$$

with

$$z_{\mathbf{k}} = E_g + \hbar\omega_{\mathbf{k}} + i\Gamma$$

Greens function expression for F

*RIXS
amplitude*

$$\mathcal{F}_{fg}(\mathbf{k}, \mathbf{k}', \epsilon, \epsilon', \omega_{\mathbf{k}}, \omega_{\mathbf{k}'}) = \sum_n \frac{\langle f | \mathcal{D}'^\dagger | n \rangle \langle n | \mathcal{D} | g \rangle}{E_g + \hbar\omega_{\mathbf{k}} - E_n + i\Gamma_n}$$

Greens function

$$G(z_{\mathbf{k}}) = \frac{1}{z_{\mathbf{k}} - H} = \sum_n \frac{|n\rangle\langle n|}{z_{\mathbf{k}} - E_n}$$

=intermediate state propagator

with

$$z_{\mathbf{k}} = E_g + \hbar\omega_{\mathbf{k}} + i\Gamma$$

Greens function expression for F

*RIXS
amplitude*

$$\mathcal{F}_{fg}(\mathbf{k}, \mathbf{k}', \epsilon, \epsilon', \omega_{\mathbf{k}}, \omega_{\mathbf{k}'}) = \sum_n \frac{\langle f | \mathcal{D}'^\dagger | n \rangle \langle n | \mathcal{D} | g \rangle}{E_g + \hbar\omega_{\mathbf{k}} - E_n + i\Gamma_n}$$

Greens function

$$G(z_{\mathbf{k}}) = \frac{1}{z_{\mathbf{k}} - H} = \sum_n \frac{|n\rangle\langle n|}{z_{\mathbf{k}} - E_n}$$

=*intermediate state propagator*

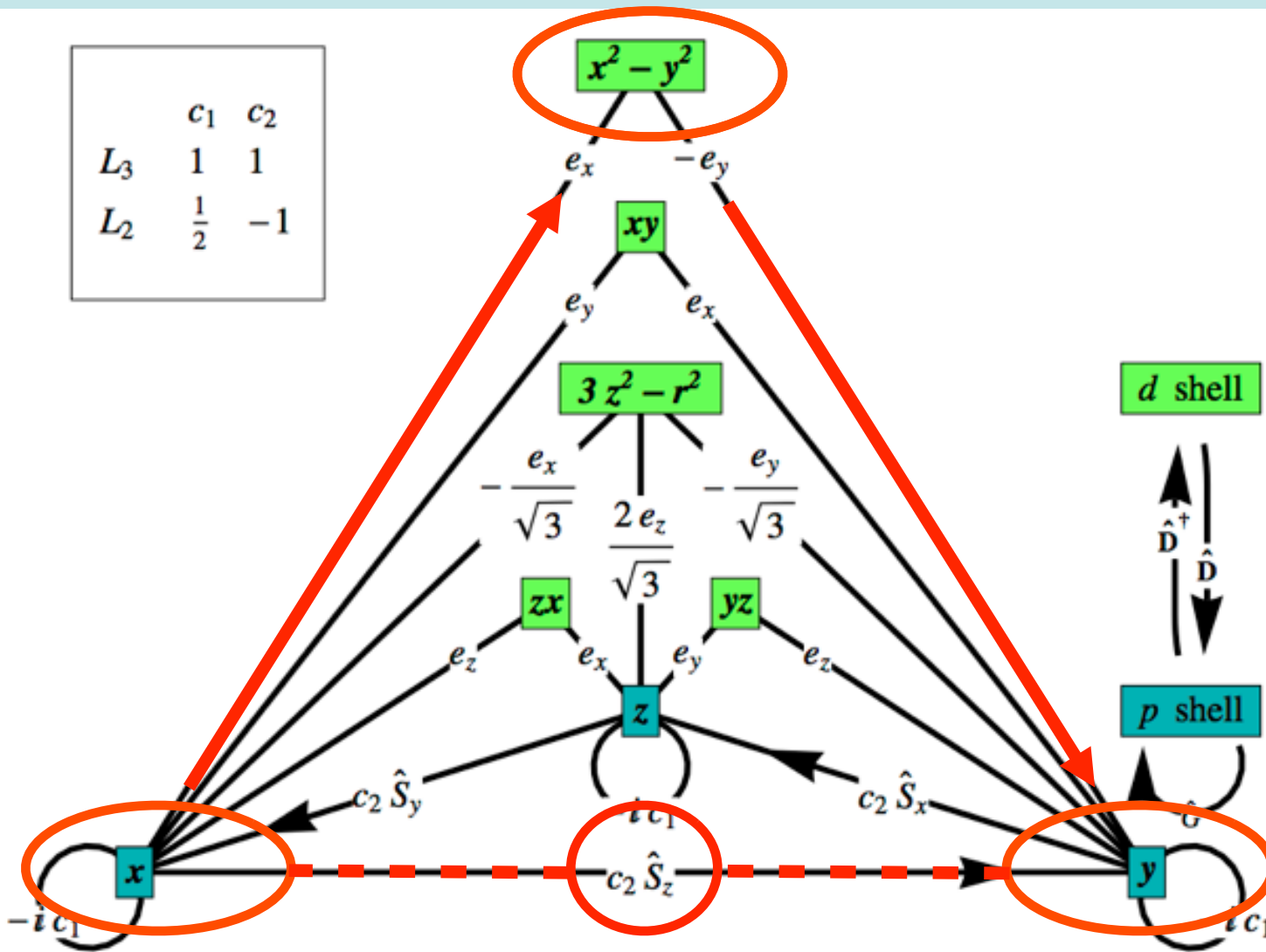
with

$$z_{\mathbf{k}} = E_g + \hbar\omega_{\mathbf{k}} + i\Gamma$$

so that:

$$\mathcal{F}_{fg} = \langle f | \mathcal{D}'^\dagger G(z_{\mathbf{k}}) \mathcal{D} | g \rangle$$

RIXS spin-flip amplitude @ transition metal L-edge



Ament, Ghiringhelli, Moretti,
Braicovich & JvdB,
PRL 103, 117003 (2009)

**x²-y² spin NOT // z:
pure spin flip**

Marra, Wohlfeld & JvdB,
PRL 109, 117401 (2012)

Quasi 2D Cuprates

Magnetic RIXS on La_2CuO_4 @ Cu L-edge

Magnetic RIXS on La_2CuO_4 @ Cu L-edge

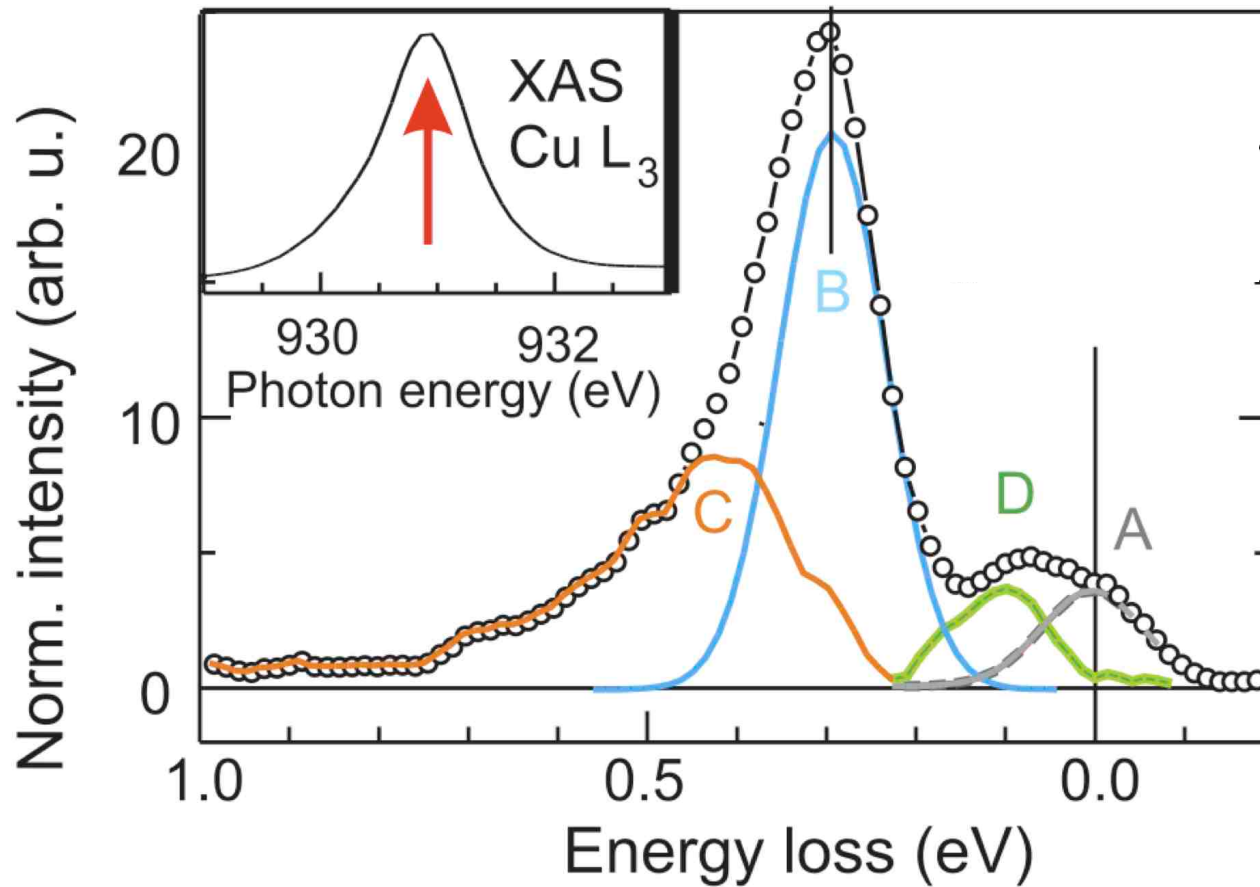
In special cases direct spin-flip scattering is allowed at Cu L-edge

CuO's are such special cases...

Magnetic RIXS on La_2CuO_4 @ Cu L-edge

In special cases direct spin-flip scattering is allowed at Cu L-edge

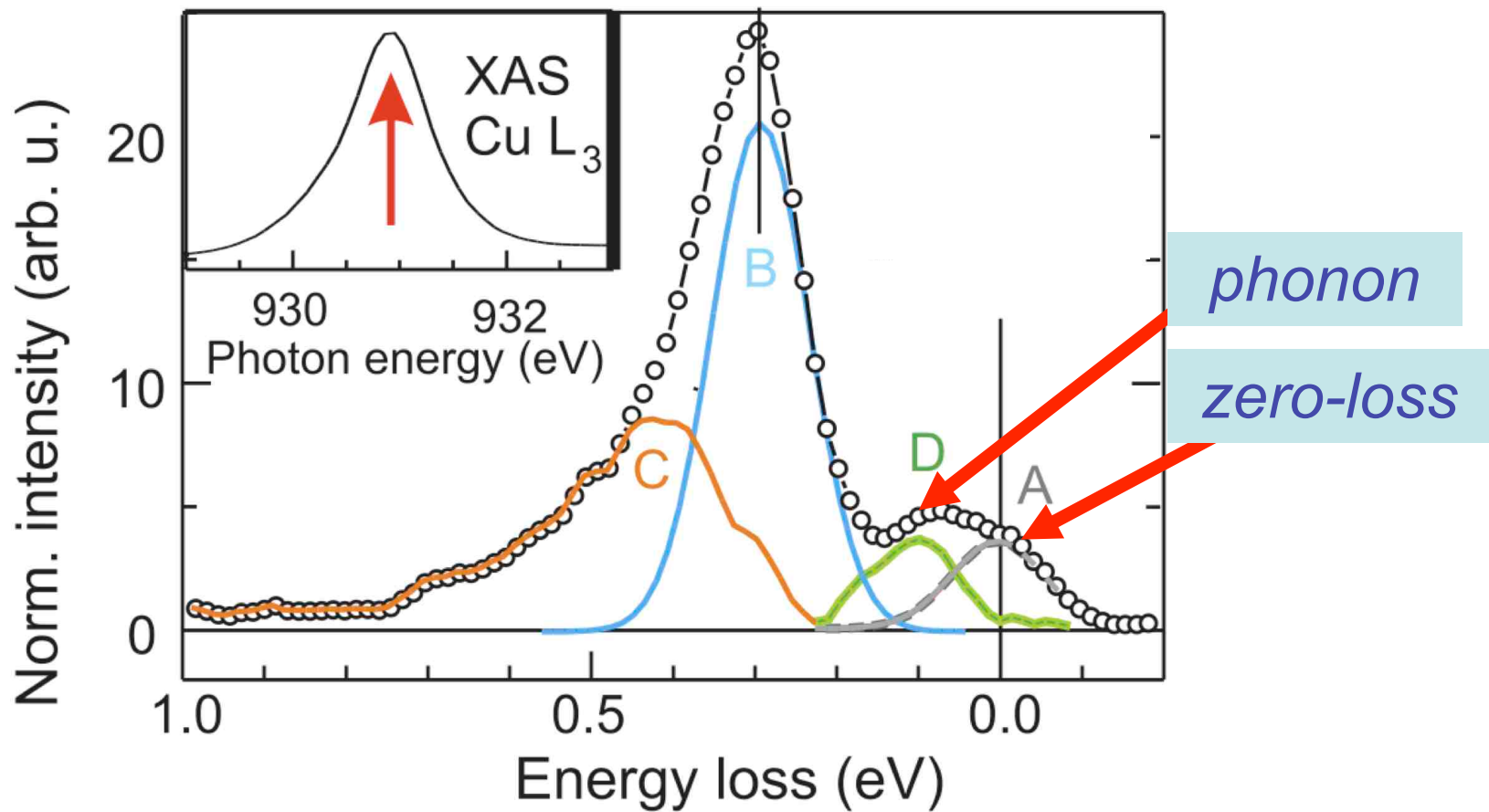
CuO's are such special cases...



Magnetic RIXS on La_2CuO_4 @ Cu L-edge

In special cases direct spin-flip scattering is allowed at Cu L-edge

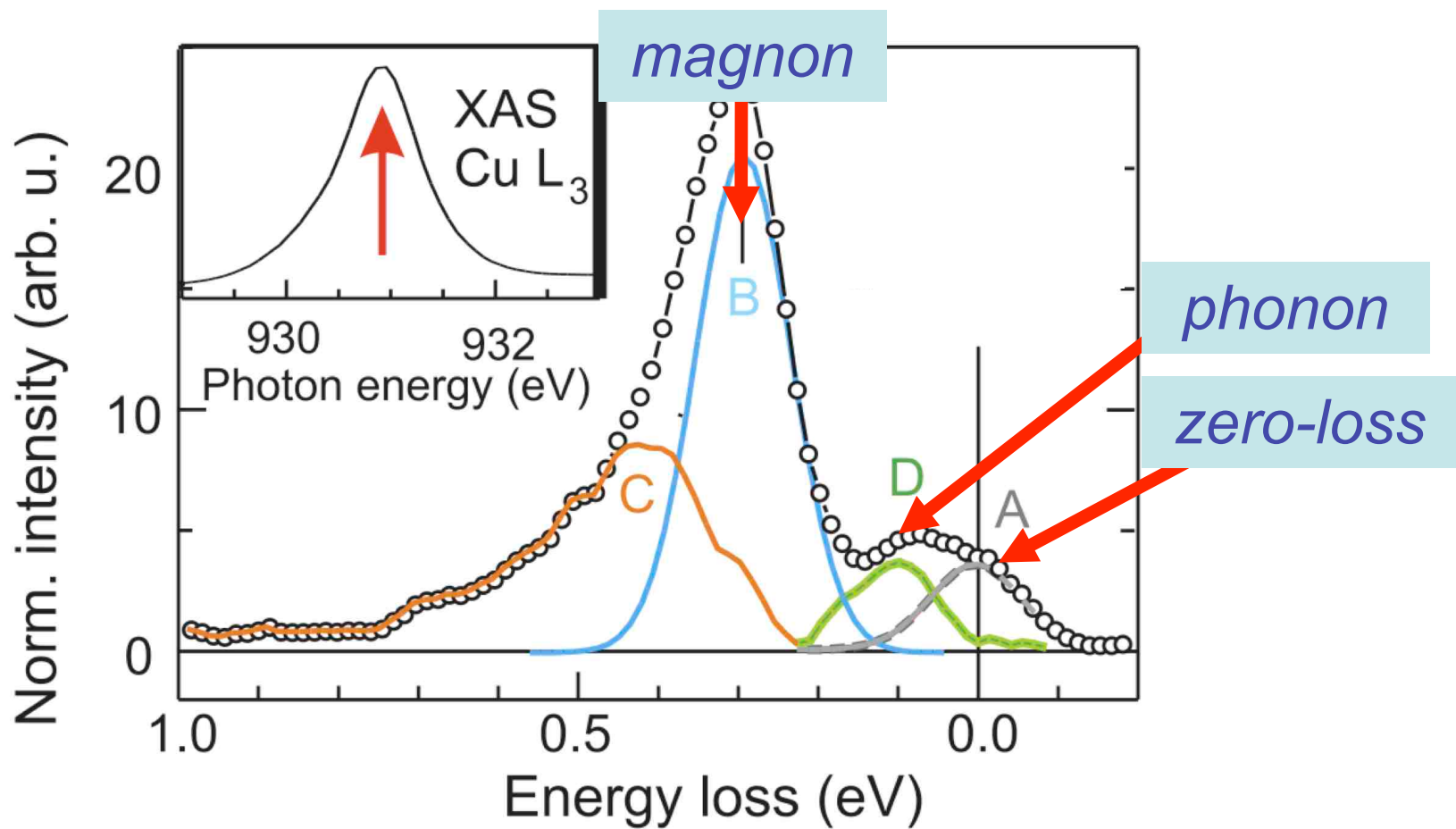
CuO's are such special cases...



Magnetic RIXS on La_2CuO_4 @ Cu L-edge

In special cases direct spin-flip scattering is allowed at Cu L-edge

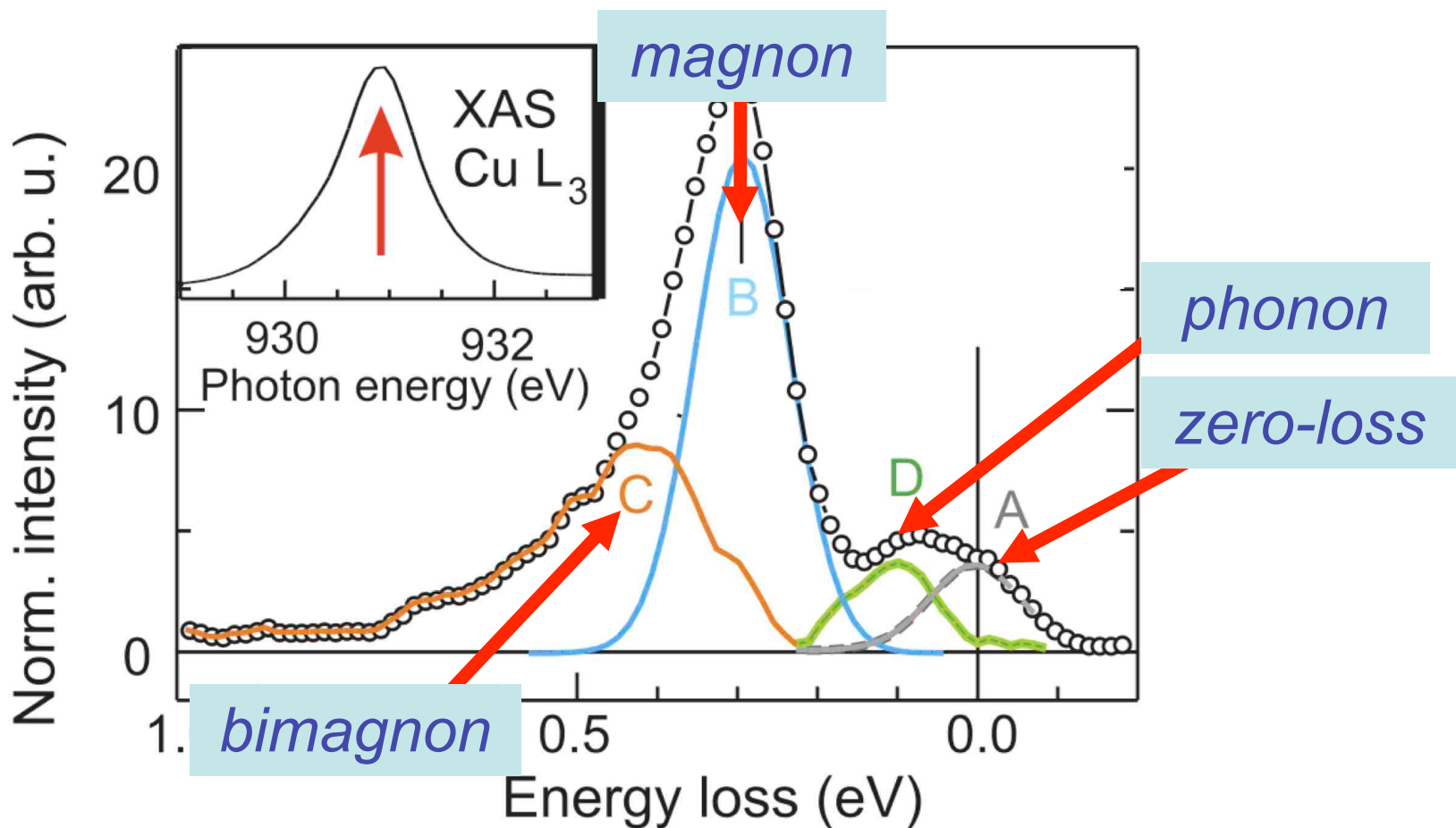
CuO's are such special cases...



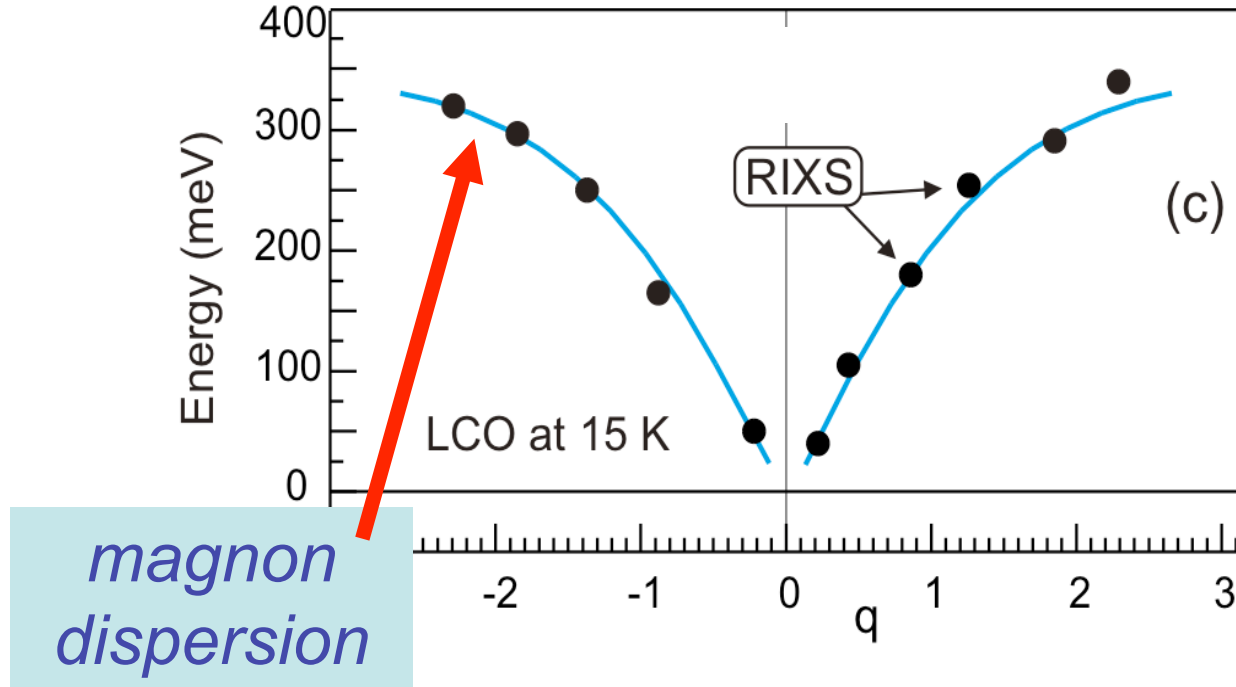
Magnetic RIXS on La_2CuO_4 @ Cu L-edge

In special cases direct spin-flip scattering is allowed at Cu L-edge

CuO's are such special cases...

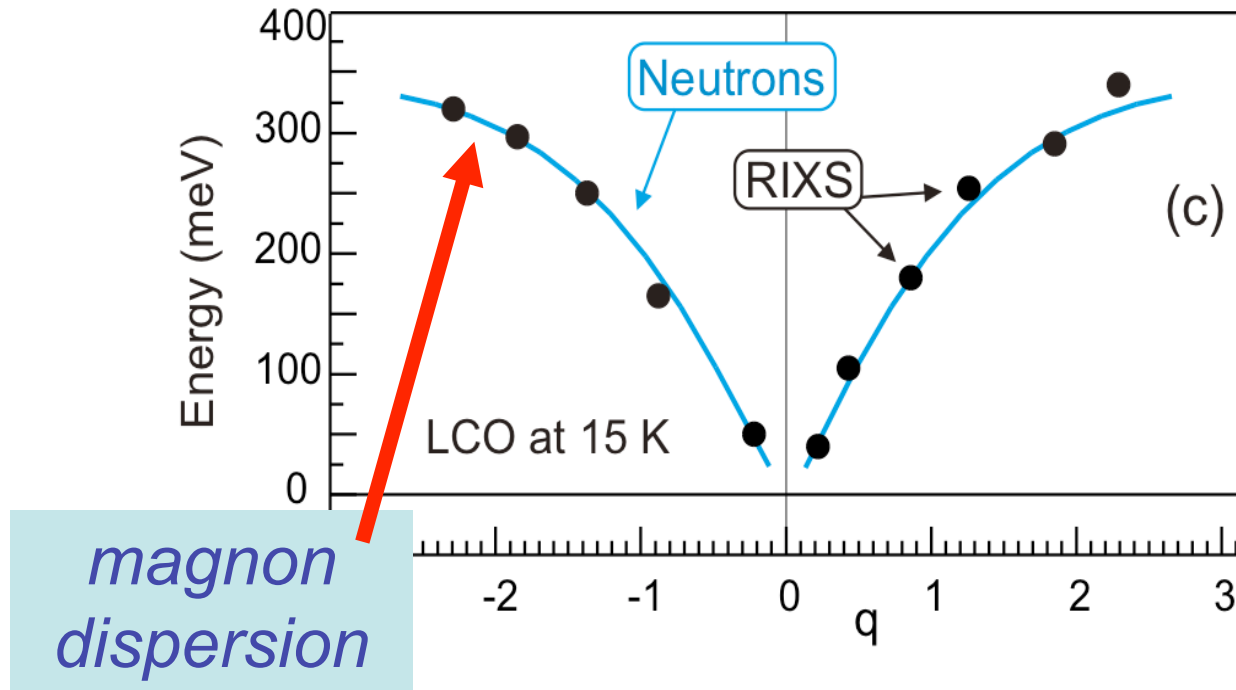


Magnetic direct RIXS on La_2CuO_4 @ Cu L-edge



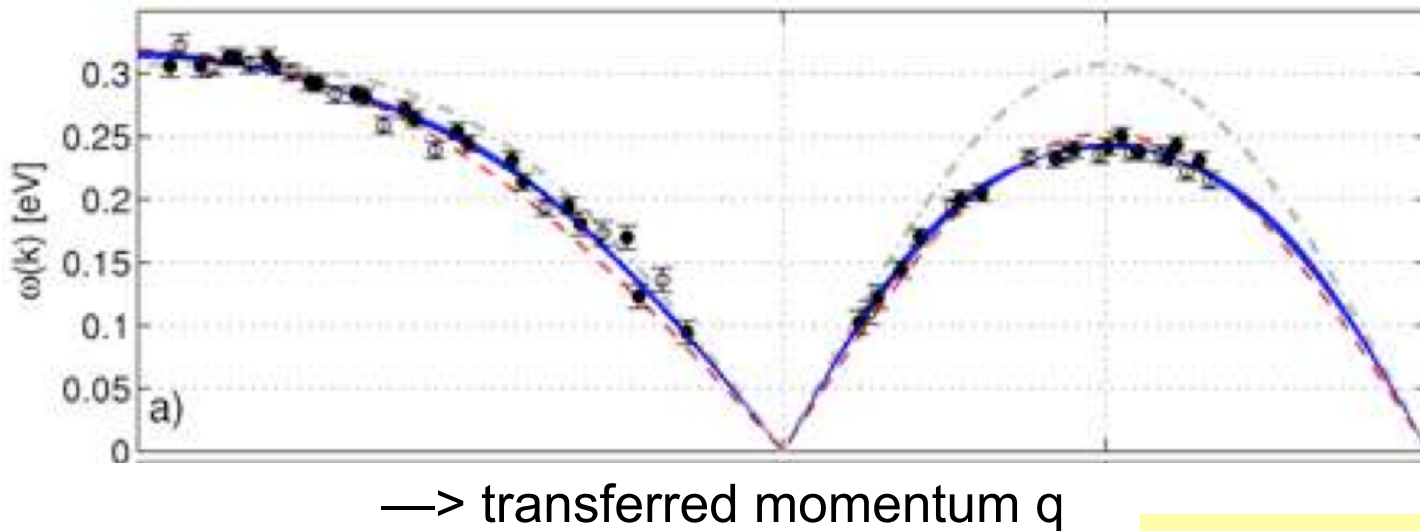
Braicovich, JvdB *et al.*,
PRL 104, 077002 (2010)

Magnetic direct RIXS on La_2CuO_4 @ Cu L-edge



Braicovich, JvdB *et al.*,
PRL 104, 077002 (2010)

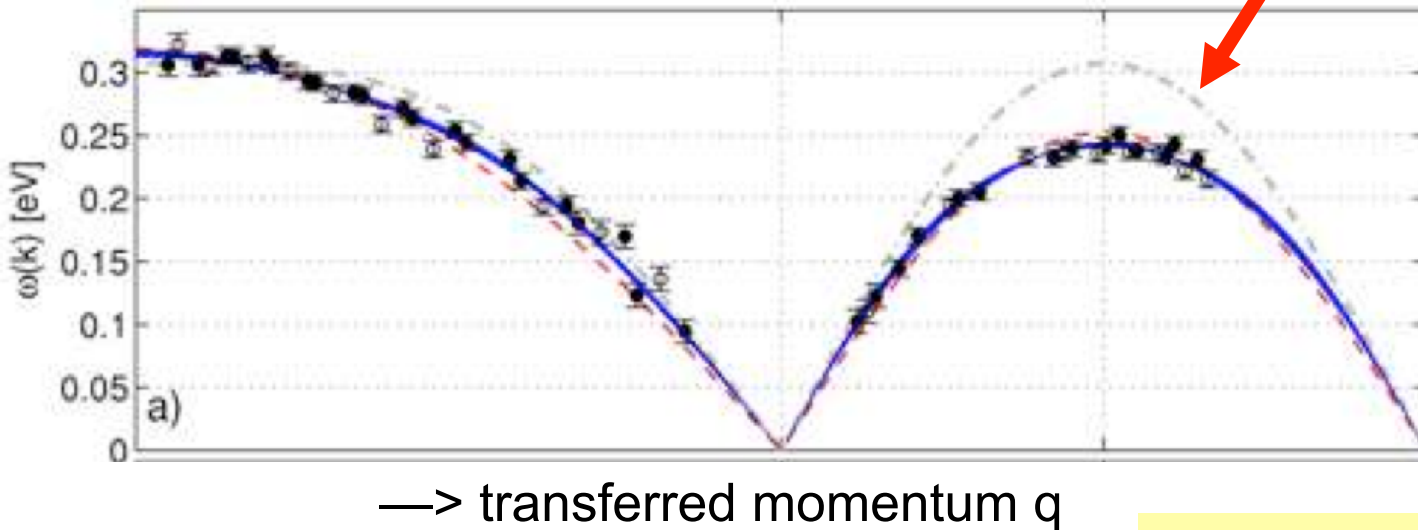
RIXS magnon dispersion of $Sr_2CuO_2Cl_2$



Guarise *et al.*,
PRL 105, 157006 (2010)

RIXS magnon dispersion of $Sr_2CuO_2Cl_2$

*deviation from
simple Heisenberg*

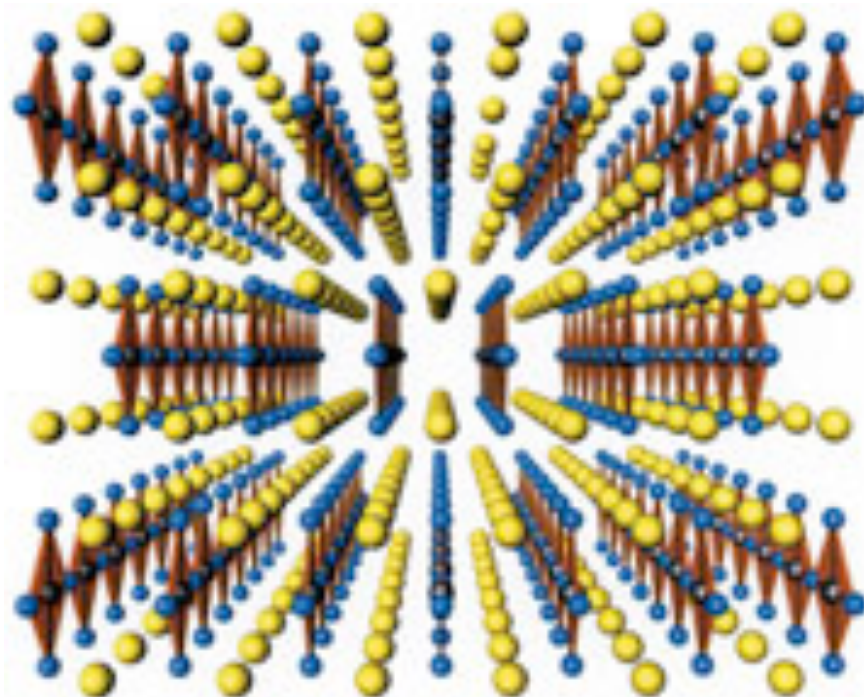


Guarise *et al.*,
PRL 105, 157006 (2010)

Quasi 1D Cuprate

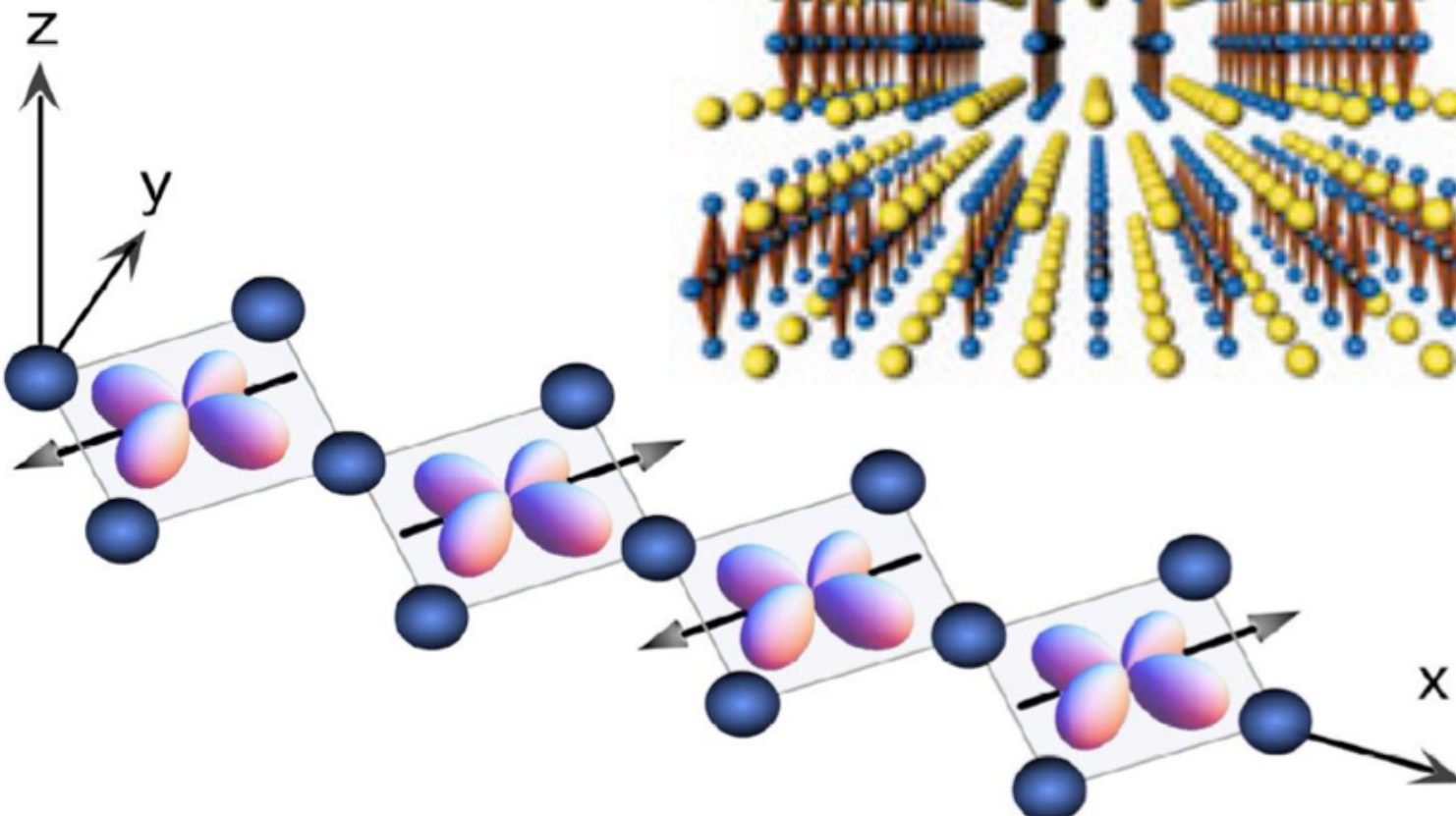
Cuprate spin chain system Sr_2CuO_3

*weakly coupled
spin chains*



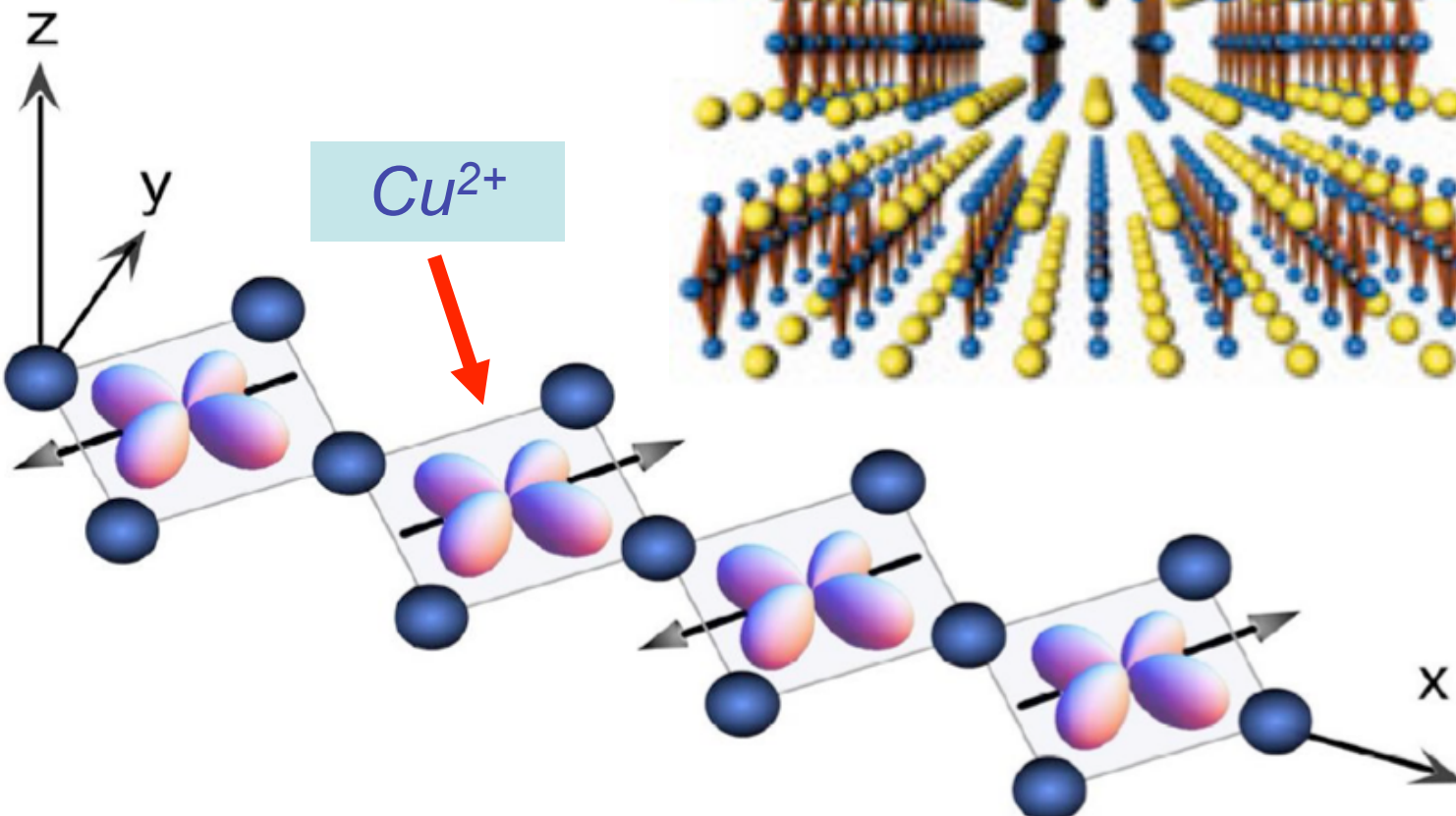
Cuprate spin chain system Sr_2CuO_3

*weakly coupled
spin chains*



Cuprate spin chain system Sr_2CuO_3

weakly coupled
spin chains



Heisenberg antiferromagnet

$S^z = +\hbar/2$

$S^z = -\hbar/2$



$$H = J S^z_i S^z_{i+1}$$

Allow for spin-exchange



Heisenberg antiferromagnet

$S^z = +\hbar/2$

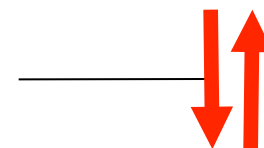


$S^z = -\hbar/2$



$$H = J S^z_i S^z_{i+1}$$

Allow for spin-exchange



Heisenberg antiferromagnet

$S^z = +\hbar/2$

$S^z = -\hbar/2$



$$H = J S^z_i S^z_{i+1}$$

Allow for spin-exchange



Heisenberg antiferromagnet

$S^z = +\hbar/2$

$S^z = -\hbar/2$



$$H = J S^z_i S^z_{i+1}$$

Allow for spin-exchange



Heisenberg antiferromagnet

$S^z = +\hbar/2$

$S^z = -\hbar/2$



$$H = J S^z_i S^z_{i+1} + J S^y_i S^y_{i+1} + J S^x_i S^x_{i+1}$$

Allow for spin-exchange



Heisenberg antiferromagnet

$S^z = +\hbar/2$

$S^z = -\hbar/2$



$$H = J S^z_i S^z_{i+1} + J S^y_i S^y_{i+1} + J S^x_i S^x_{i+1} = J \mathbf{S}_i \cdot \mathbf{S}_{i+1}$$

Allow for spin-exchange



Heisenberg antiferromagnet

$$S^z = +\hbar/2$$

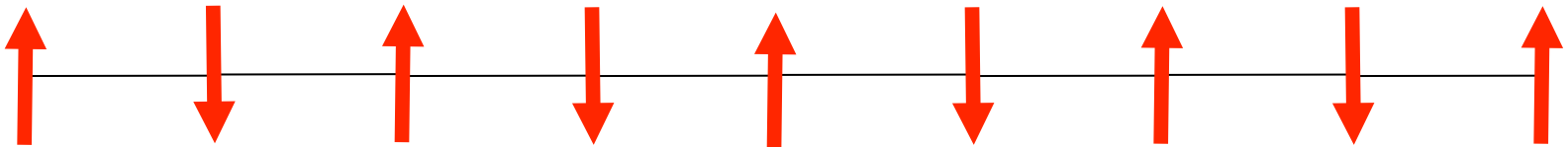
$$S^z = -\hbar/2$$

$$H = J S^z_i S^z_{i+1} + J S^y_i S^y_{i+1} + J S^x_i S^x_{i+1} = J \mathbf{S}_i \cdot \mathbf{S}_{i+1}$$

Allow for spin-exchange



ground state



Heisenberg antiferromagnet

$$S^z = +\hbar/2$$

$$S^z = -\hbar/2$$

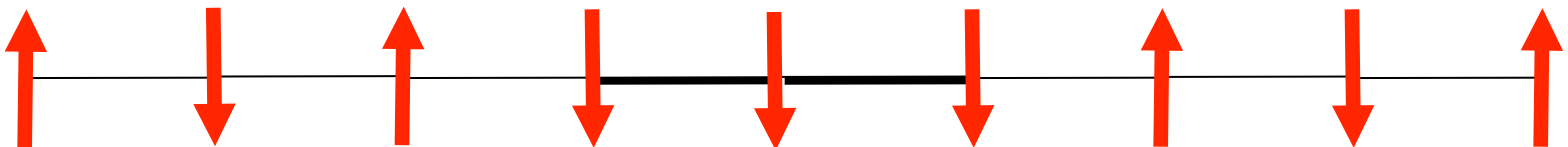
$$H = J S^z_i S^z_{i+1} + J S^y_i S^y_{i+1} + J S^x_i S^x_{i+1} = J \mathbf{S}_i \cdot \mathbf{S}_{i+1}$$

Allow for spin-exchange



spin flip $\Delta S^z = \hbar$

in $d=3$: magnon



Heisenberg antiferromagnet

$$S^z = +\hbar/2$$

$$S^z = -\hbar/2$$

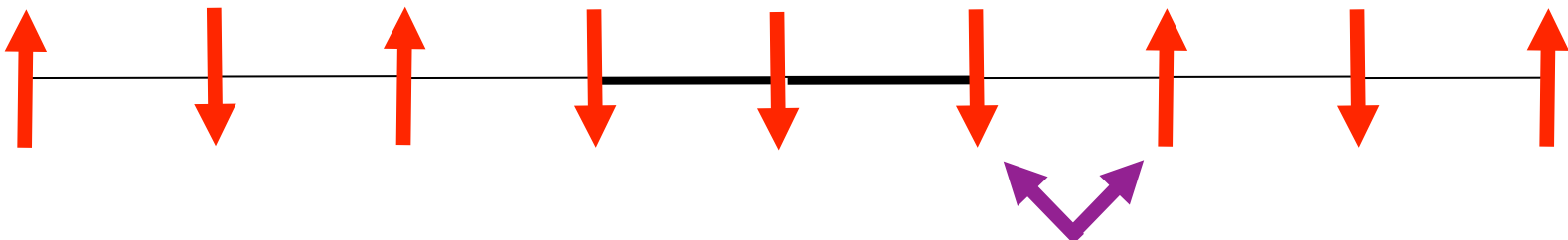
$$H = J S^z_i S^z_{i+1} + J S^y_i S^y_{i+1} + J S^x_i S^x_{i+1} = J \mathbf{S}_i \cdot \mathbf{S}_{i+1}$$

Allow for spin-exchange



spin flip $\Delta S^z = \hbar$

in $d=3$: magnon



Heisenberg antiferromagnet

$$S^z = +\hbar/2$$

$$S^z = -\hbar/2$$

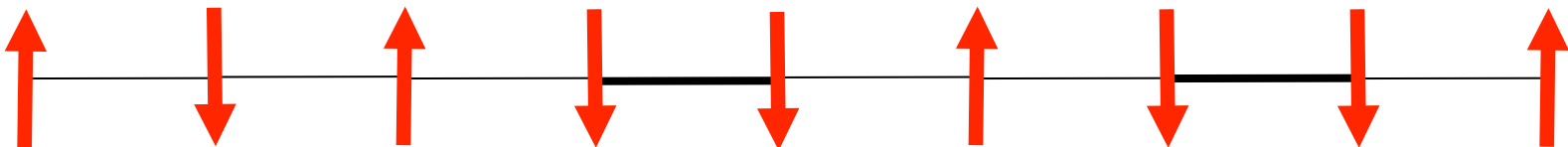
$$H = J S^z_i S^z_{i+1} + J S^y_i S^y_{i+1} + J S^x_i S^x_{i+1} = J \mathbf{S}_i \cdot \mathbf{S}_{i+1}$$

Allow for spin-exchange



spin flip $\Delta S^z = \hbar$

in $d=3$: magnon



Heisenberg antiferromagnet

$$S^z = +\hbar/2$$

$$S^z = -\hbar/2$$

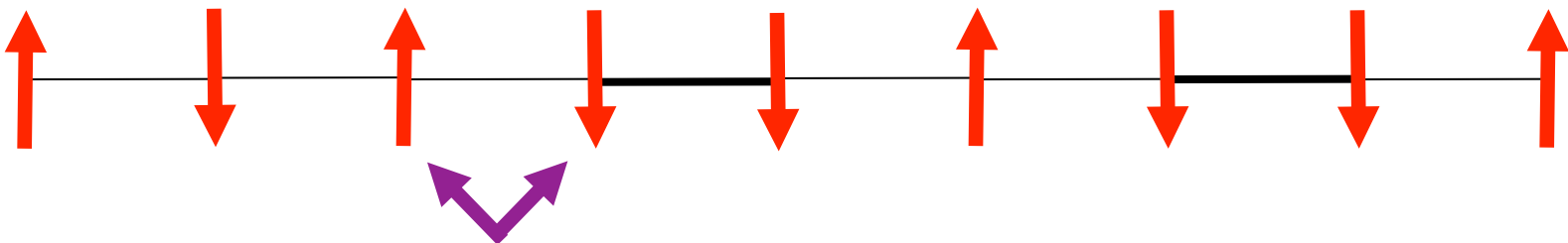
$$H = J S^z_i S^z_{i+1} + J S^y_i S^y_{i+1} + J S^x_i S^x_{i+1} = J \mathbf{S}_i \cdot \mathbf{S}_{i+1}$$

Allow for spin-exchange



spin flip $\Delta S^z = \hbar$

in $d=3$: magnon



Heisenberg antiferromagnet

$$S^z = +\hbar/2$$

$$S^z = -\hbar/2$$

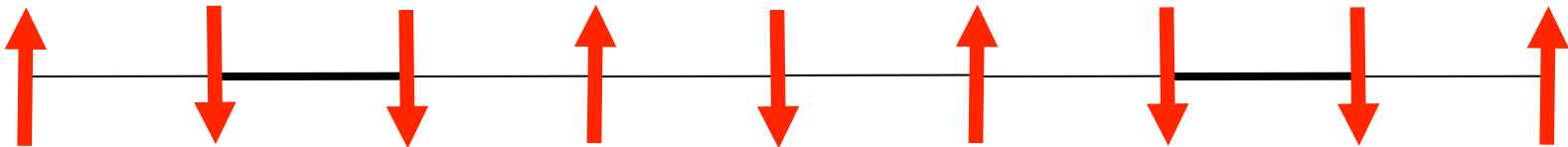
$$H = J S^z_i S^z_{i+1} + J S^y_i S^y_{i+1} + J S^x_i S^x_{i+1} = J \mathbf{S}_i \cdot \mathbf{S}_{i+1}$$

Allow for spin-exchange



spin flip $\Delta S^z = \hbar$

in $d=3$: magnon



Heisenberg antiferromagnet

$$S^z = +\hbar/2$$

$$S^z = -\hbar/2$$

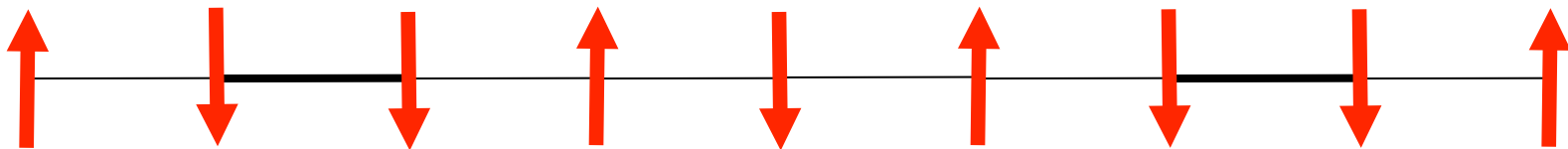
$$H = J S^z_i S^z_{i+1} + J S^y_i S^y_{i+1} + J S^x_i S^x_{i+1} = J \mathbf{S}_i \cdot \mathbf{S}_{i+1}$$

Allow for spin-exchange



spin flip $\Delta S^z = \hbar$

in $d=3$: magnon



two domain walls, each with $\Delta S^z = \hbar/2$



spinon

Heisenberg antiferromagnet

$$S^z = +\hbar/2$$

$$S^z = -\hbar/2$$

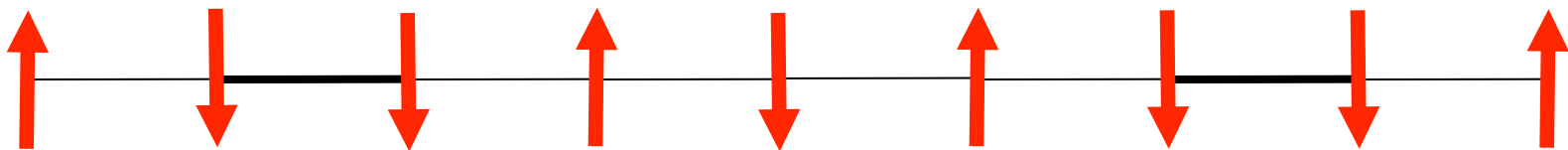
$$H = J S^z_i S^z_{i+1} + J S^y_i S^y_{i+1} + J S^x_i S^x_{i+1} = J \mathbf{S}_i \cdot \mathbf{S}_{i+1}$$

Allow for spin-exchange



spin flip $\Delta S^z = \hbar$

in $d=3$: magnon



two domain walls, each with $\Delta S^z = \hbar/2$



spinon

$d=1$: magnon fractionalizes into spinons

Heisenberg antiferromagnet

$$S^z = +\hbar/2$$

$$S^z = -\hbar/2$$

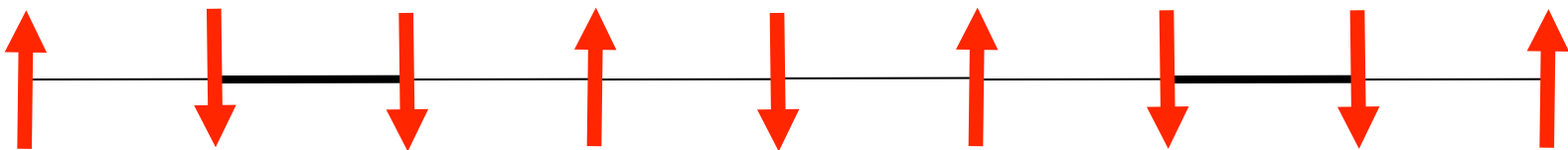
$$H = J S^z_i S^z_{i+1} + J S^y_i S^y_{i+1} + J S^x_i S^x_{i+1} = J \mathbf{S}_i \cdot \mathbf{S}_{i+1}$$

Allow for spin-exchange



spin flip $\Delta S^z = \hbar$

in $d=3$: magnon



two domain walls, each with $\Delta S^z = \hbar/2$



spinon

$d=1$: magnon fractionalizes into spinons

magnon q, ω



spinon k_1, ω_1
spinon k_2, ω_2

Heisenberg antiferromagnet

$$S^z = +\hbar/2$$

$$S^z = -\hbar/2$$

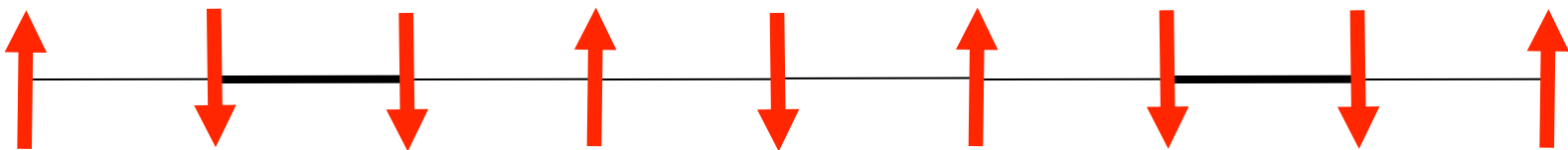
$$H = J S^z_i S^z_{i+1} + J S^y_i S^y_{i+1} + J S^x_i S^x_{i+1} = J \mathbf{S}_i \cdot \mathbf{S}_{i+1}$$

Allow for spin-exchange



spin flip $\Delta S^z = \hbar$

in $d=3$: magnon



two domain walls, each with $\Delta S^z = \hbar/2$



spinon

$d=1$: magnon fractionalizes into spinons

magnon q, ω



spinon k_1, ω_1
spinon k_2, ω_2

$q = k_1 + k_2, \omega = \omega_1 + \omega_2$

Spinons in 1d Heisenberg antiferromagnet

magnon q, ω



spinon k_1, ω_1
spinon k_2, ω_2

$q = k_1 + k_2, \omega = \omega_1 + \omega_2$

Spinons in 1d Heisenberg antiferromagnet

magnon q, ω



spinon k_1, ω_1
spinon k_2, ω_2

$q = k_1 + k_2, \omega = \omega_1 + \omega_2$

relative momentum of spinons
 $p = k_2 - k_1$ *not yet determined*

Spinons in 1d Heisenberg antiferromagnet

magnon q, ω



spinon k_1, ω_1
spinon k_2, ω_2

$q = k_1 + k_2, \omega = \omega_1 + \omega_2$

*excitation
continuum* q, ω



relative momentum of spinons
 $p = k_2 - k_1$ *not yet determined*

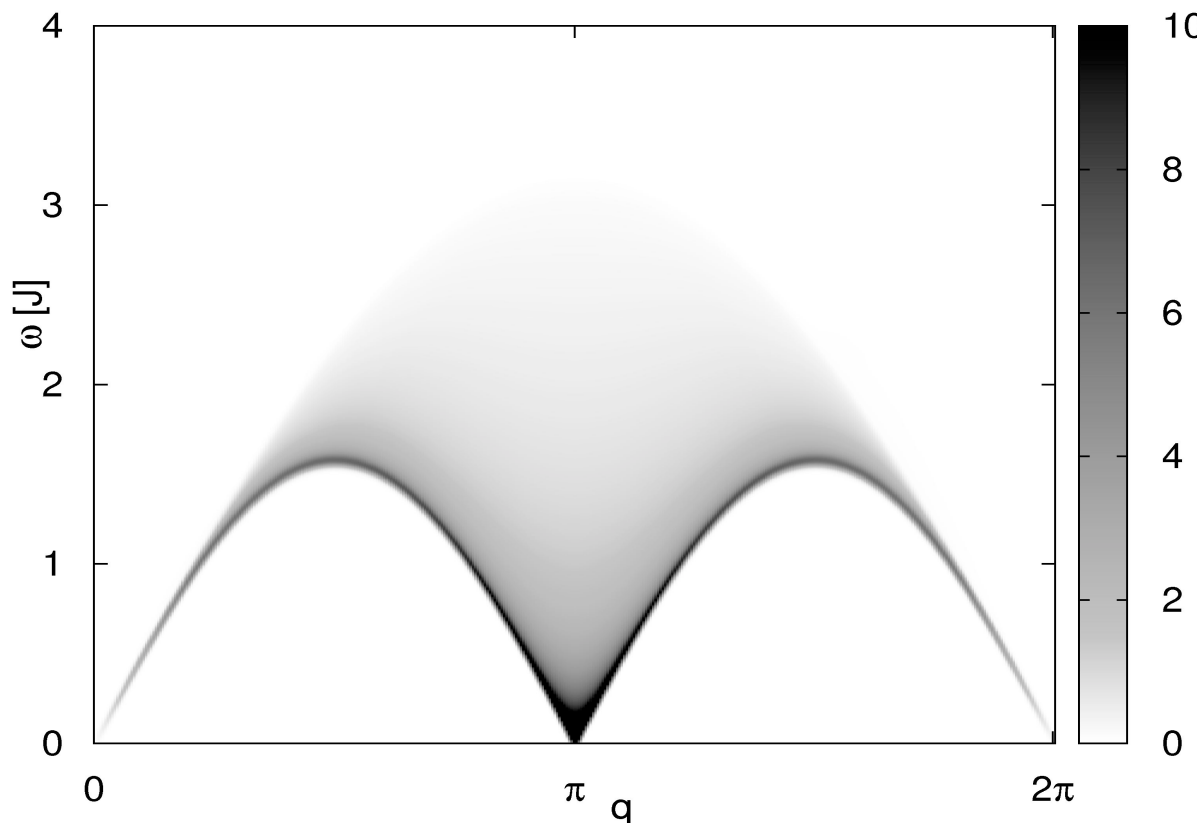
Spinon excitations in 1d Heisenberg antiferromagnet

*excitation
continuum q, ω*



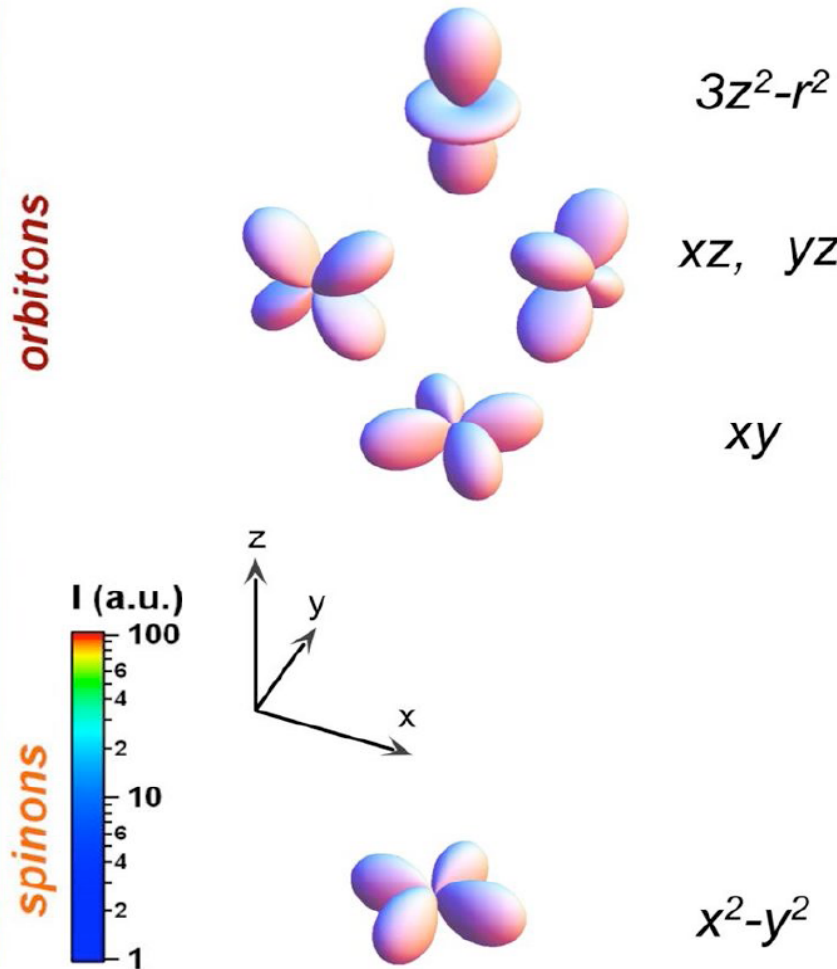
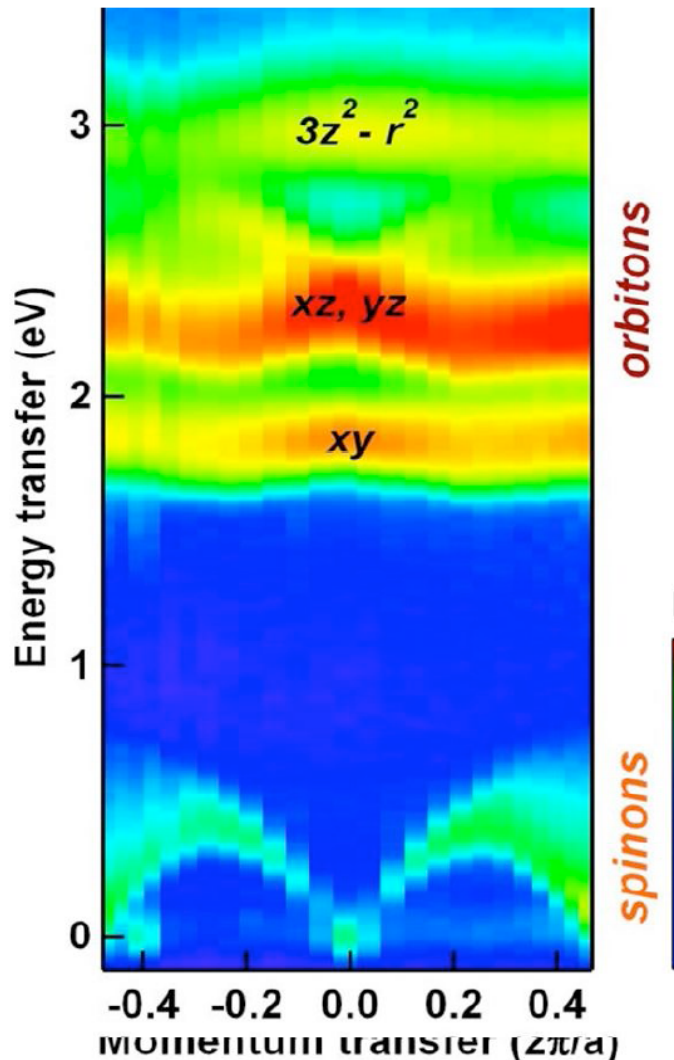
*relative momentum of spinons
 $q = k_2 - k_1$ not yet determined*

neutron scattering magnetic excitations



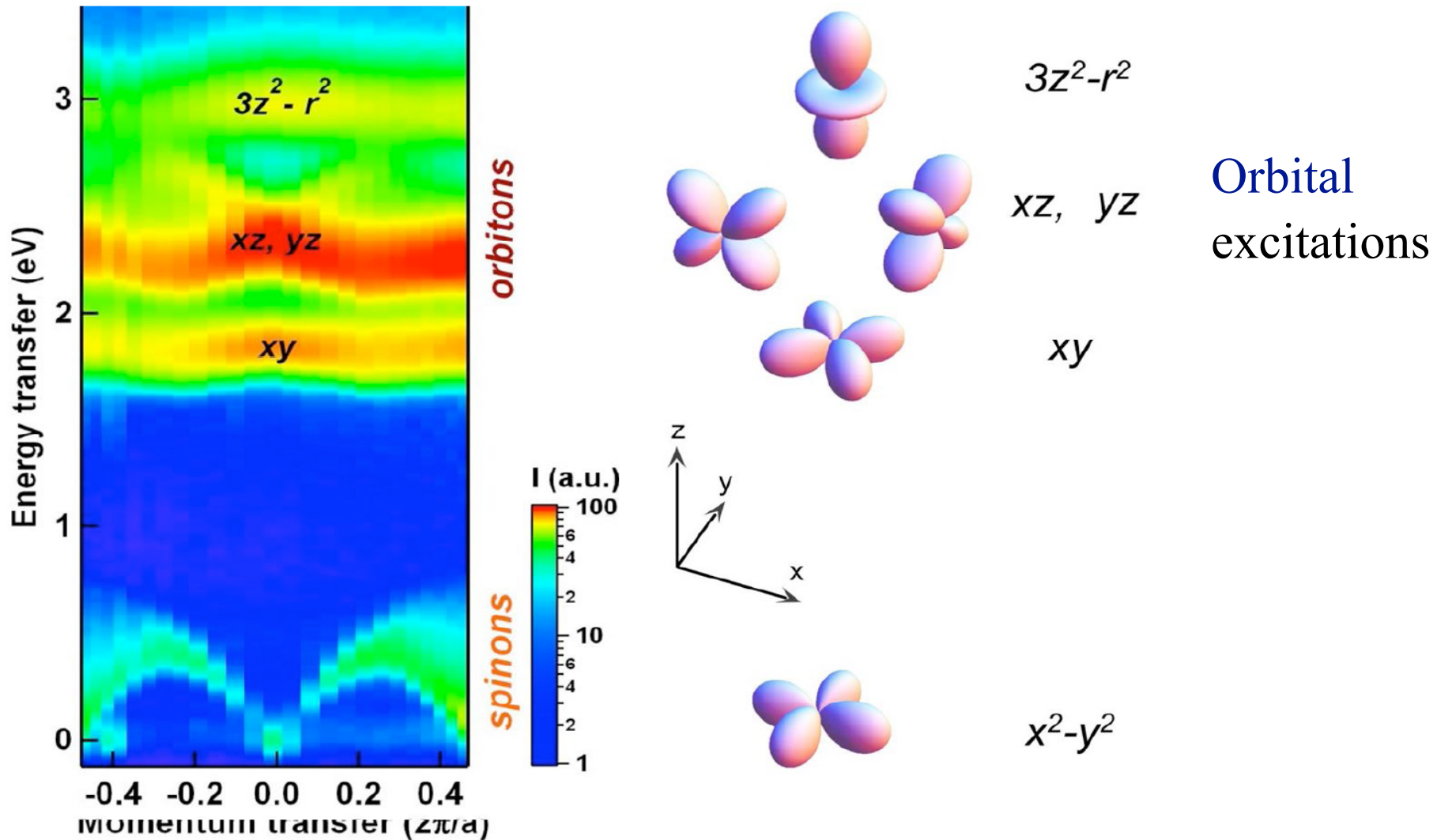
*Bethe-Ansatz
exact solution*

RIXS spectrum of Sr_2CuO_3 spin chain



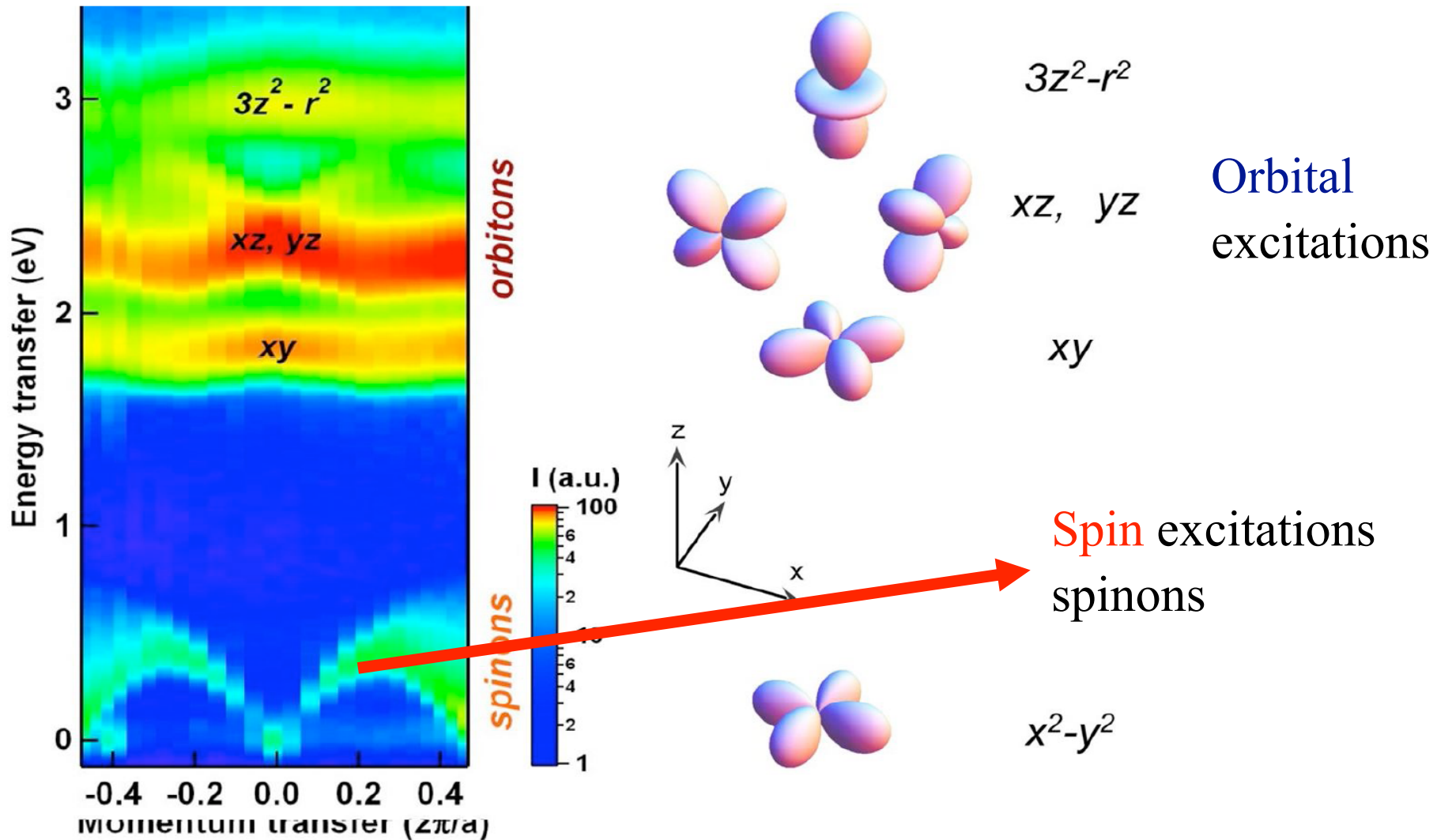
Schlappa, Wohlfeld, Zhou, Mourigal, Haverkort, Strocov, Hozoi, Monney, Nishimoto, Singh, Revcolevschi, Caux, Patthey, Ronnow, JvdB, Schmitt, Nature 485, 82 (2012)

RIXS spectrum of Sr_2CuO_3 spin chain



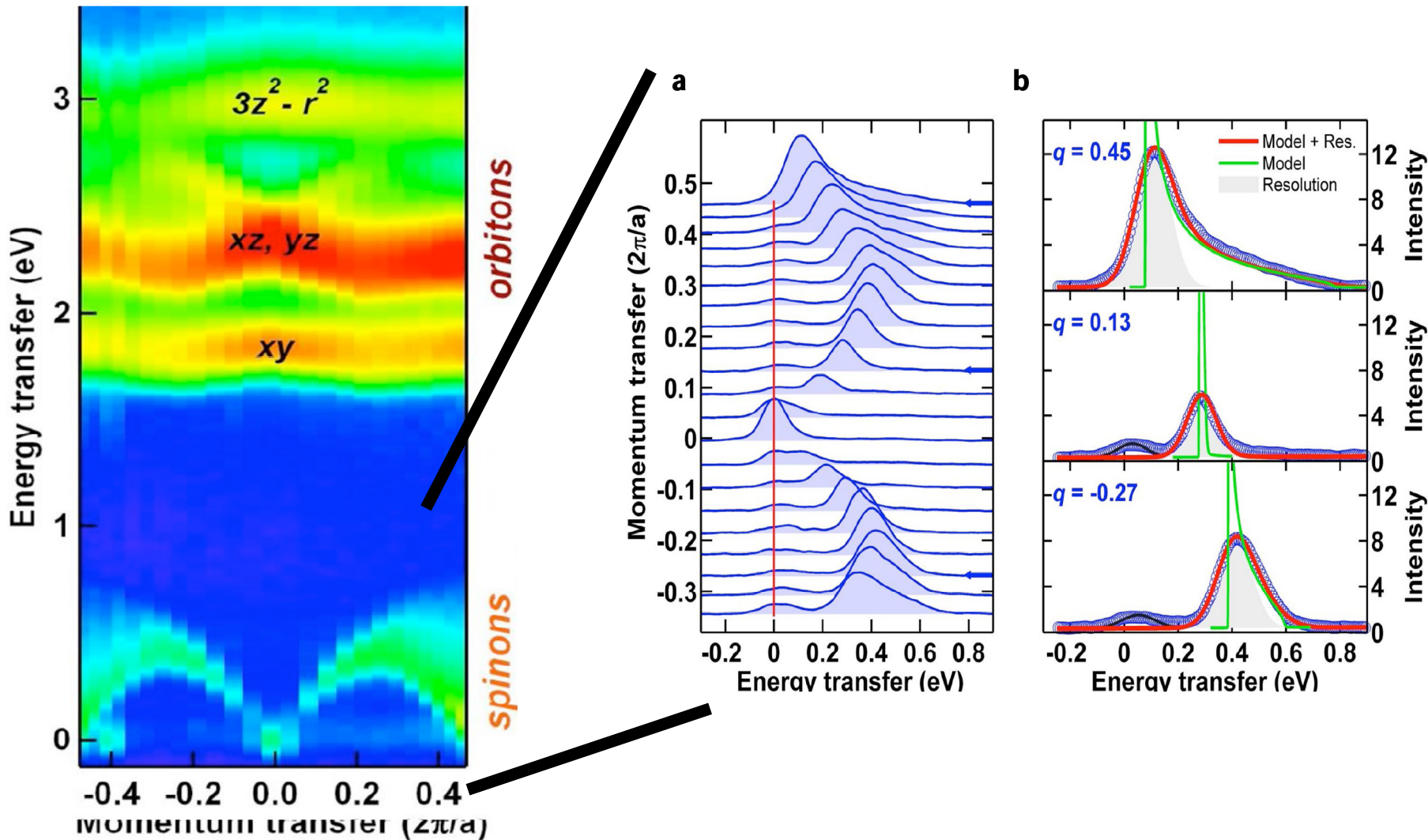
Schlappa, Wohlfeld, Zhou, Mourigal, Haverkort, Strocov, Hozoi, Monney, Nishimoto, Singh, Revcolevschi, Caux, Patthey, Ronnow, JvdB, Schmitt, Nature 485, 82 (2012)

RIXS spectrum of Sr_2CuO_3 spin chain



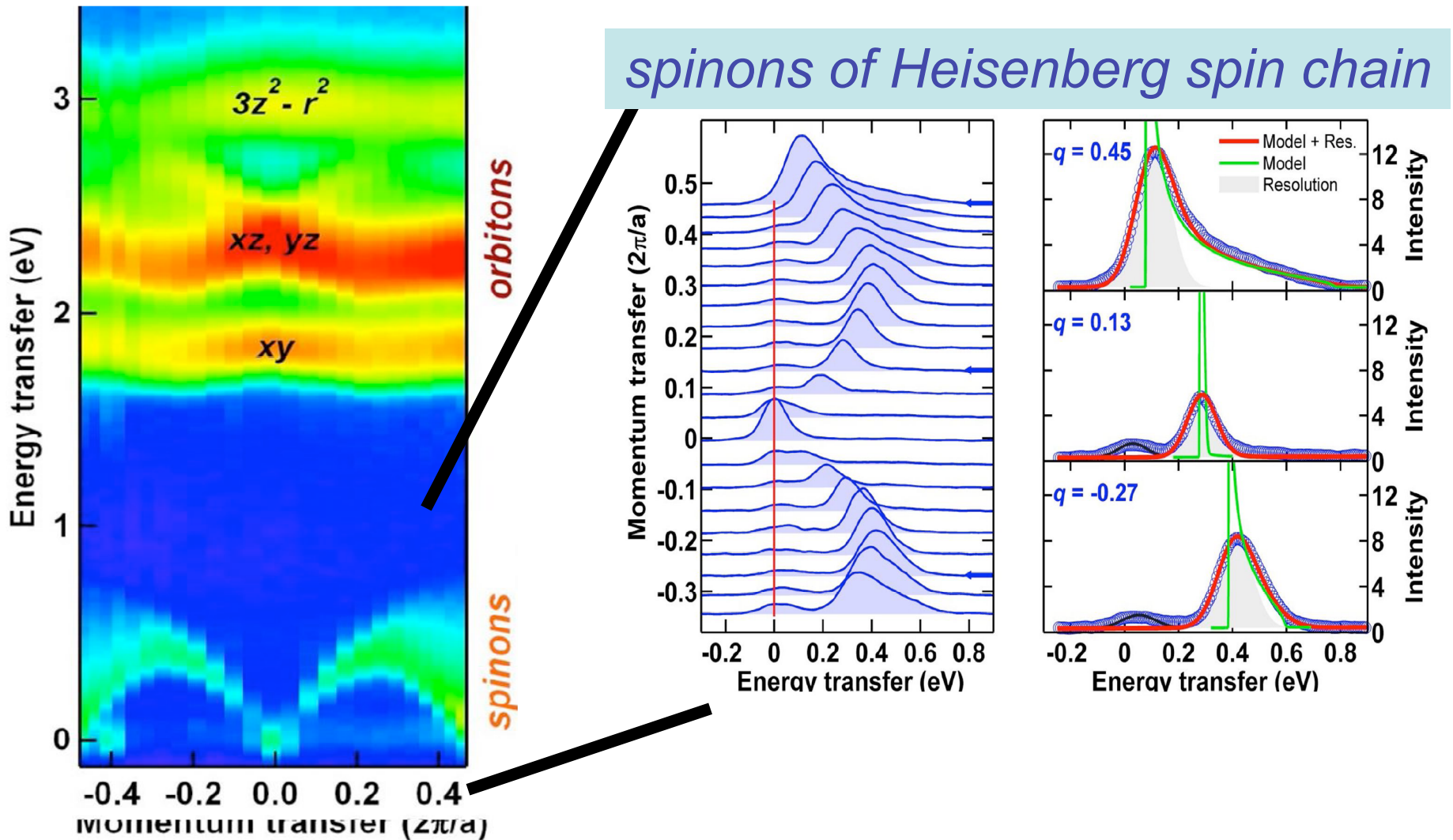
Schlappa, Wohlfeld, Zhou, Mourigal, Haverkort, Strocov, Hozoi, Monney, Nishimoto, Singh, Revcolevschi, Caux, Patthey, Ronnow, JvdB, Schmitt, Nature 485, 82 (2012)

Spinons in Sr_2CuO_3



Schlappa, Wohlfeld, Zhou, Mourigal, Haverkort, Strocov, Hozoi, Monney, Nishimoto, Singh, Revcolevschi, Caux, Patthey, Ronnow, JvdB, Schmitt, Nature 485, 82 (2012)

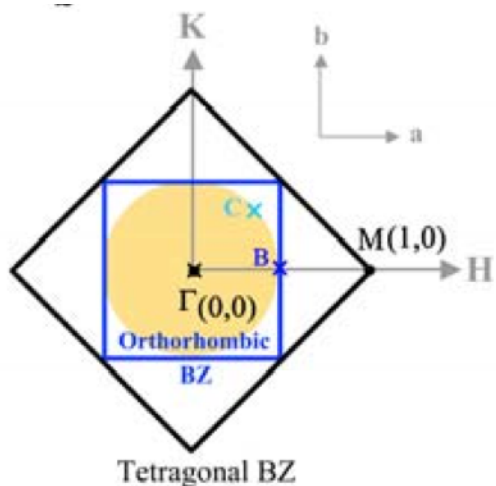
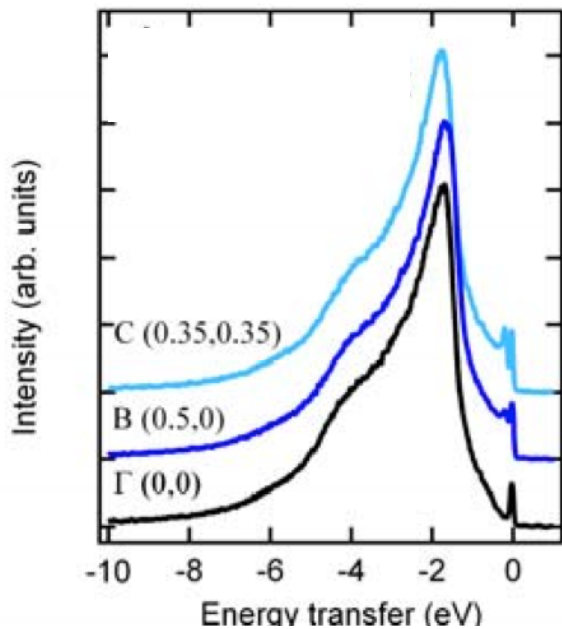
Spinons in Sr_2CuO_3



Schlappa, Wohlfeld, Zhou, Mourigal, Haverkort, Strocov, Hozoi, Monney, Nishimoto, Singh, Revcolevschi, Caux, Patthey, Ronnow, JvdB, Schmitt, Nature 485, 82 (2012)

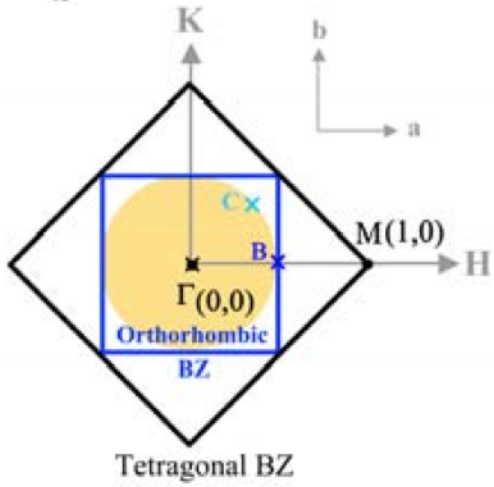
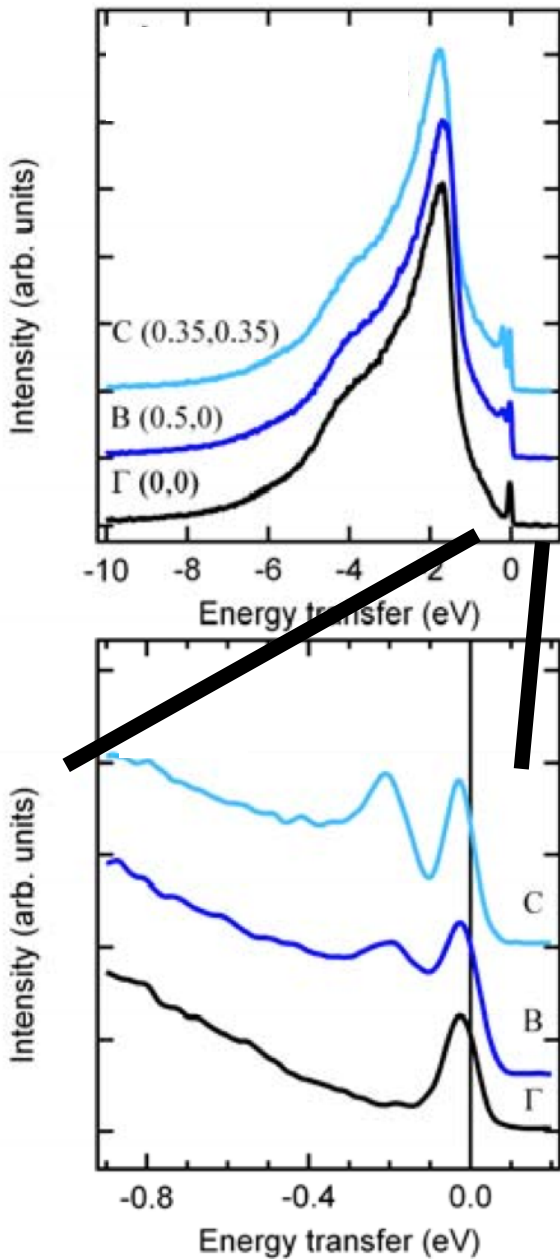
Quasi 2D Iron Pnictide

Magnetic RIXS on BaFe_2As_2 @ Fe L-edge



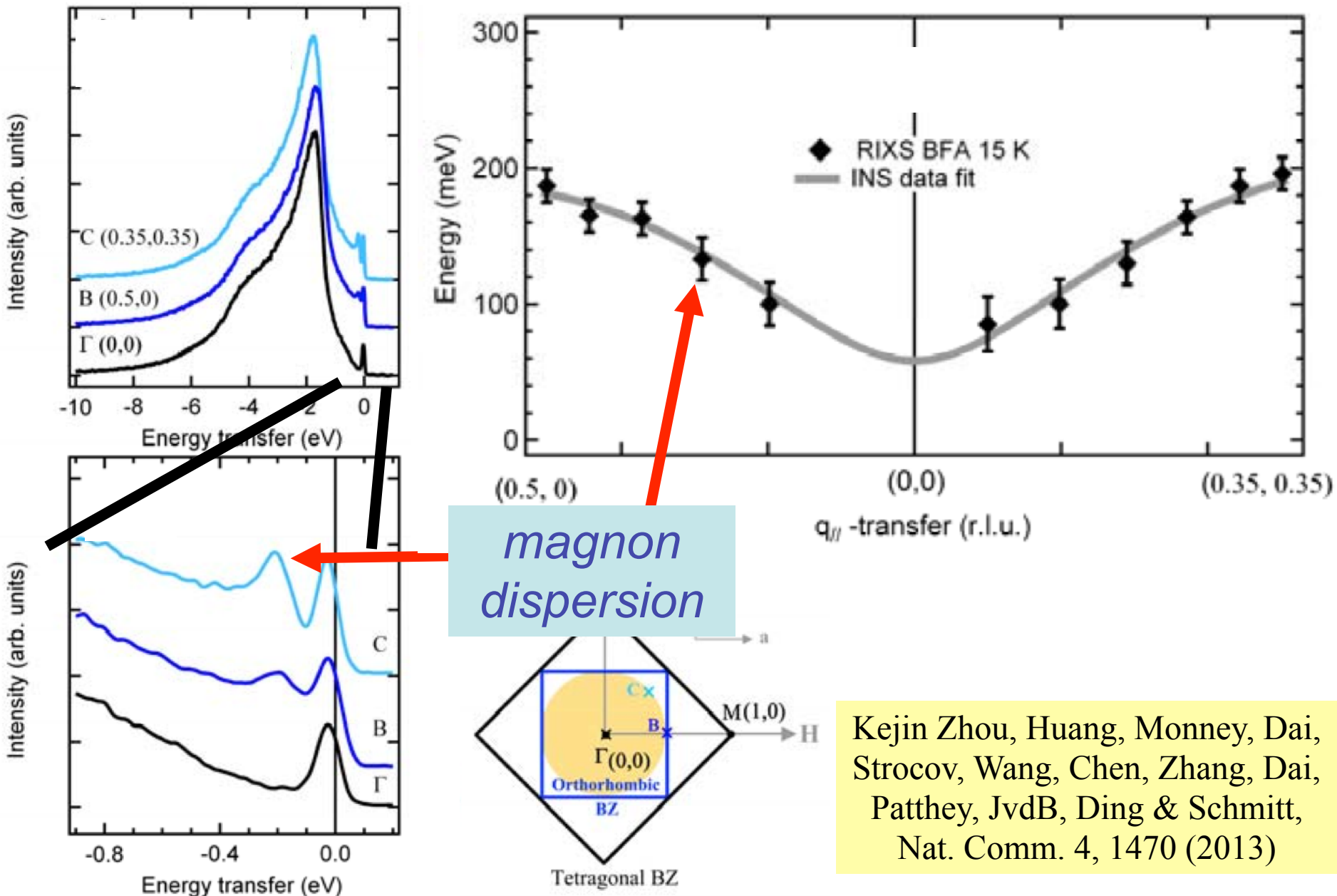
Kejin Zhou, Huang, Monney, Dai,
Strocov, Wang, Chen, Zhang, Dai,
Patthey, JvdB, Ding & Schmitt,
Nat. Comm. 4, 1470 (2013)

Magnetic RIXS on BaFe_2As_2 @ Fe L-edge



Kejin Zhou, Huang, Monney, Dai,
Strocov, Wang, Chen, Zhang, Dai,
Patthey, JvdB, Ding & Schmitt,
Nat. Comm. 4, 1470 (2013)

Magnetic RIXS on BaFe_2As_2 @ Fe L-edge



Magnetic RIXS vs. Inelastic Neutron Scattering

RIXS

Neutrons

*amount of
material needed*

*magnon energy
accessible*

materials

Magnetic RIXS vs. Inelastic Neutron Scattering

RIXS

*amount of
material needed*

Neutrons

small

large

*magnon energy
accessible*

materials

Magnetic RIXS vs. Inelastic Neutron Scattering

RIXS

*amount of
material needed*

Neutrons

small

large

*magnon energy
accessible*

high ($>10^2 \text{ meV}$)

low ($<10^2 \text{ meV}$)

materials

Magnetic RIXS vs. Inelastic Neutron Scattering

RIXS

Neutrons

*amount of
material needed*

small

large

*magnon energy
accessible*

high ($>10^2 \text{ meV}$)

low ($<10^2 \text{ meV}$)

materials

Cu, Fe ...

non-absorbers

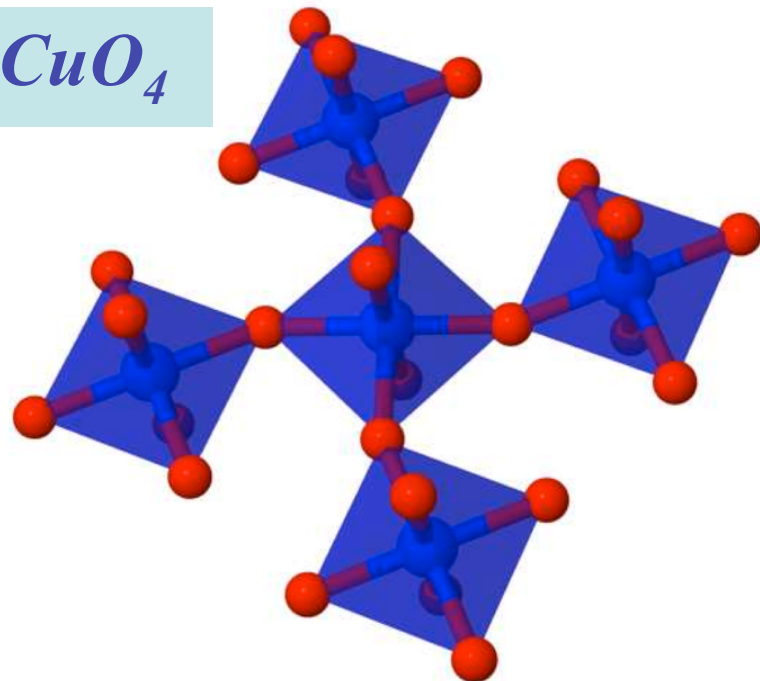
Quasi 2D Iridate

Magnetic Iridium Oxides

Sr_2IrO_4 : equivalent of cuprate La_2CuO_4

Jackeli & Khaliullin, PRL 102,017205 (2009)

B.J. Kim, Ohsumi, Komesu, Sakai, Morita, Takagi, Arima, Science 323, 1329 (2009)

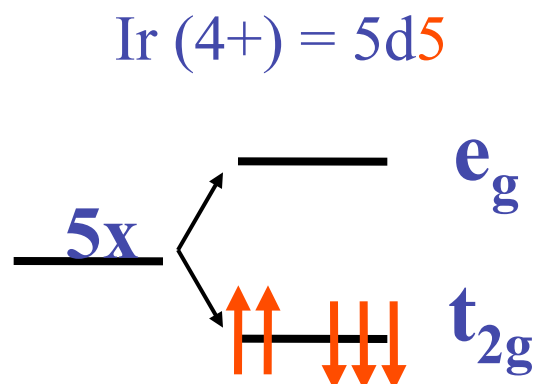
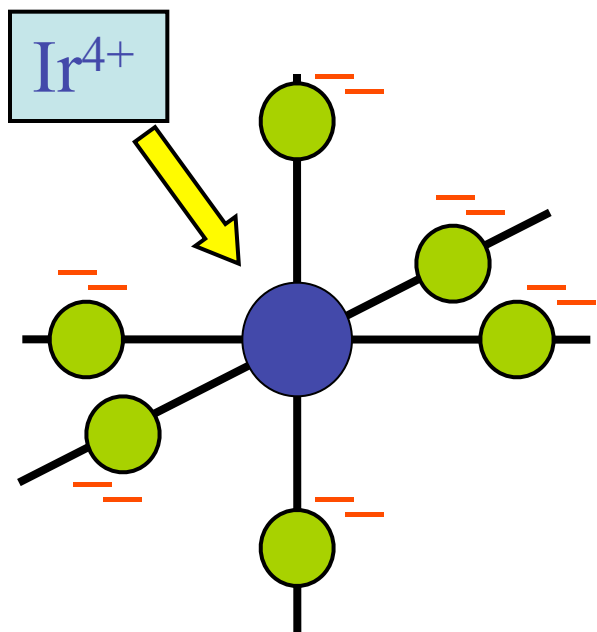
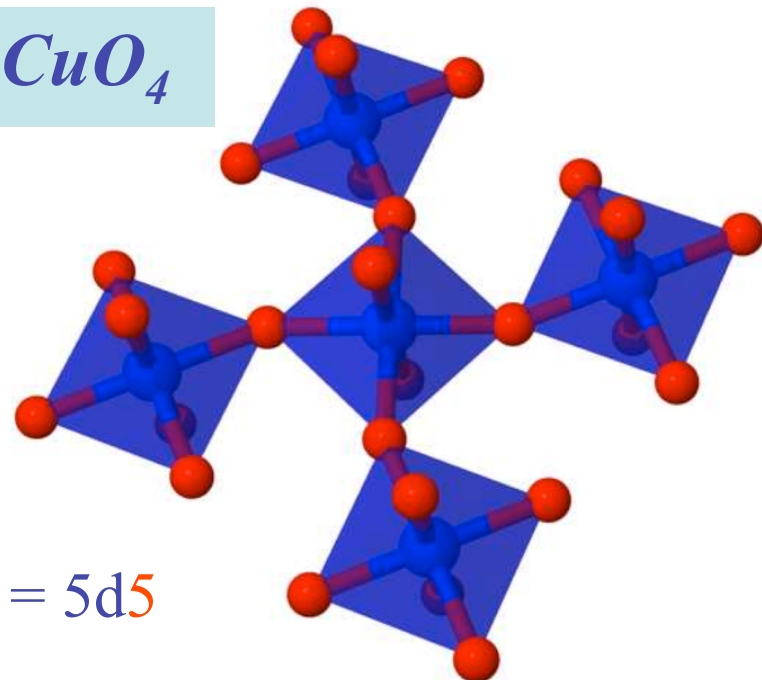


Magnetic Iridium Oxides

Sr_2IrO_4 : equivalent of cuprate La_2CuO_4

Jackeli & Khaliullin, PRL 102,017205 (2009)

B.J. Kim, Ohsumi, Komesu, Sakai, Morita, Takagi, Arima, Science 323, 1329 (2009)



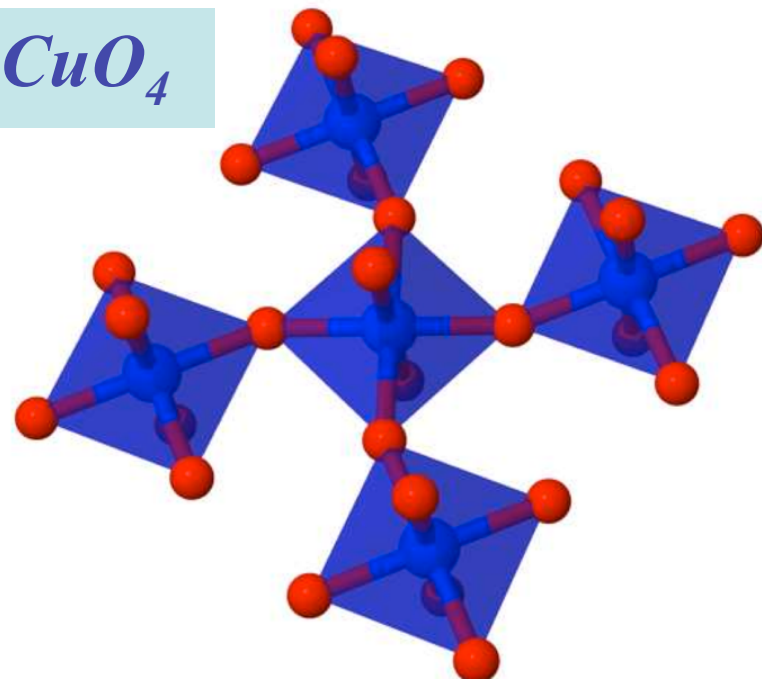
Magnetic Iridium Oxides

Sr_2IrO_4 : equivalent of cuprate La_2CuO_4

Jackeli & Khaliullin, PRL 102,017205 (2009)

B.J. Kim, Ohsumi, Komesu, Sakai, Morita, Takagi, Arima, Science 323, 1329 (2009)

t_{2g}^5 : single hole $s=1/2$ in 3-fold
degenerate $l=1$ state



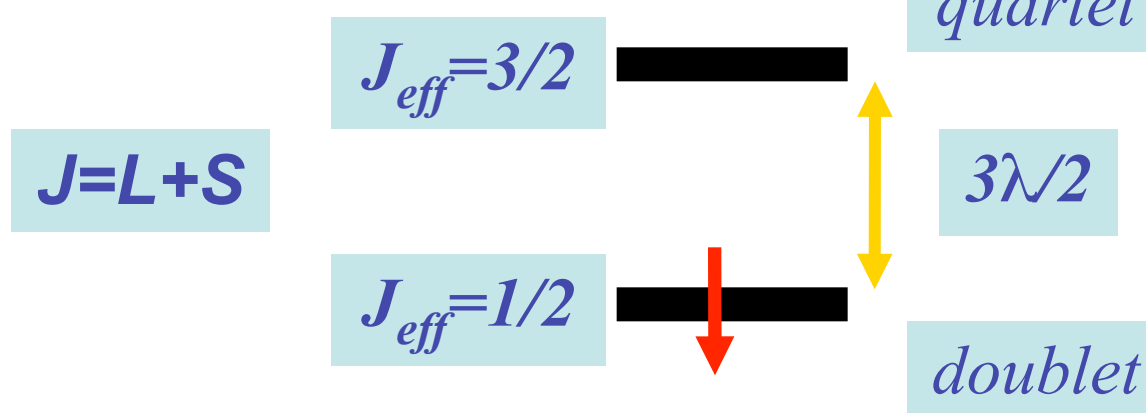
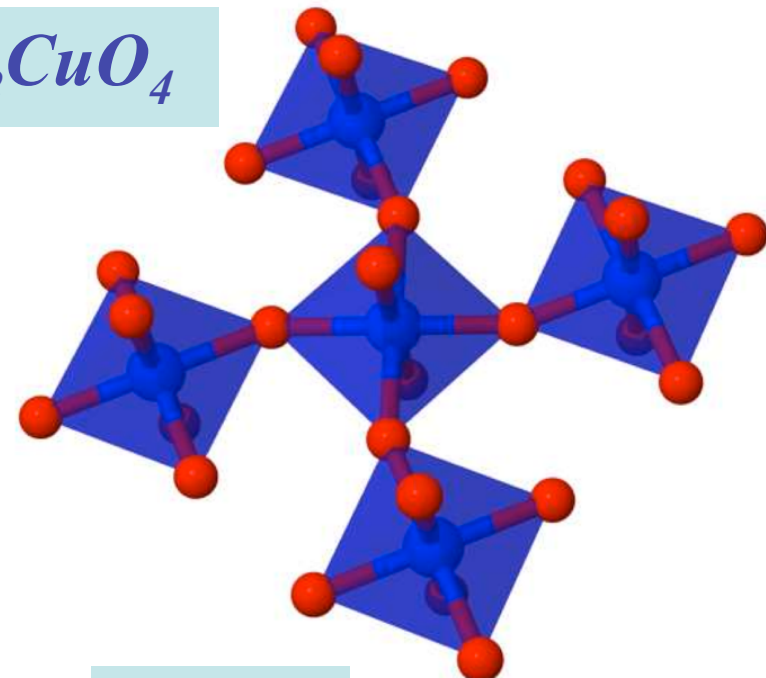
Magnetic Iridium Oxides

Sr_2IrO_4 : equivalent of cuprate La_2CuO_4

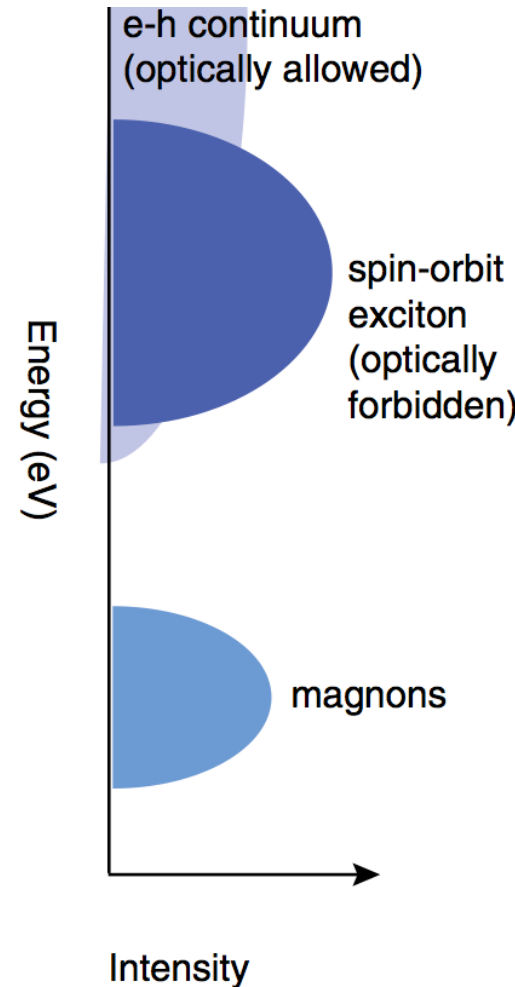
Jackeli & Khaliullin, PRL 102,017205 (2009)

B.J. Kim, Ohsumi, Komesu, Sakai, Morita, Takagi, Arima, Science 323, 1329 (2009)

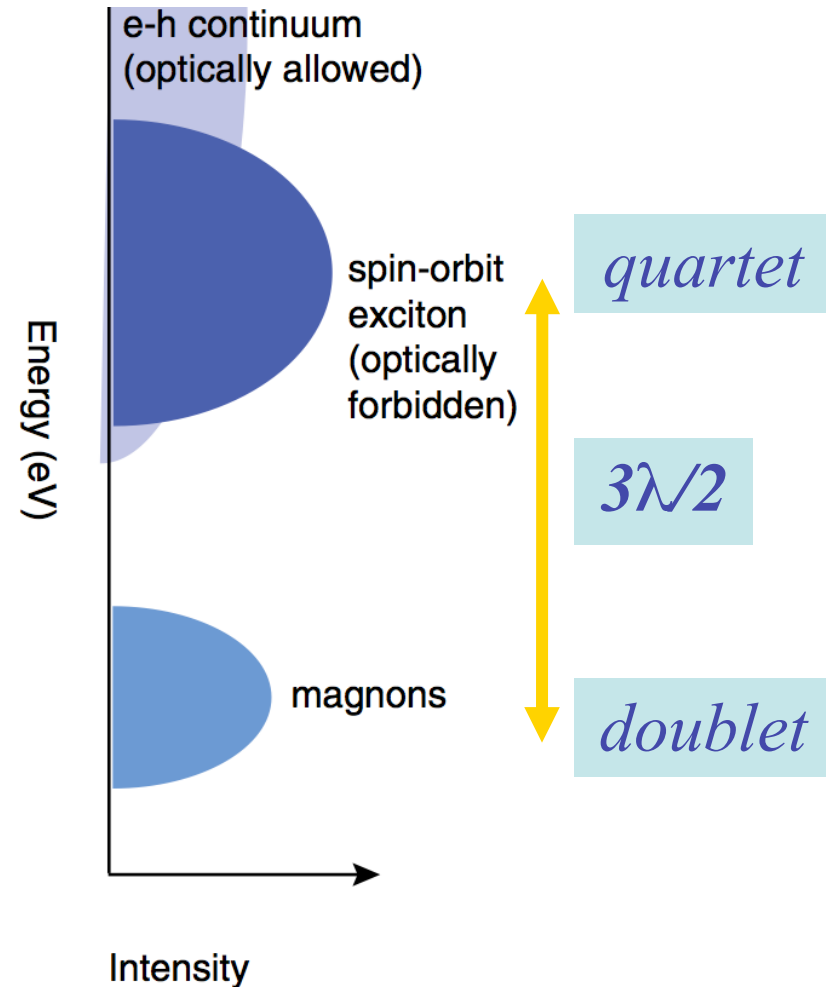
t_{2g}^5 : single hole $s=1/2$ in 3-fold degenerate $l=1$ state



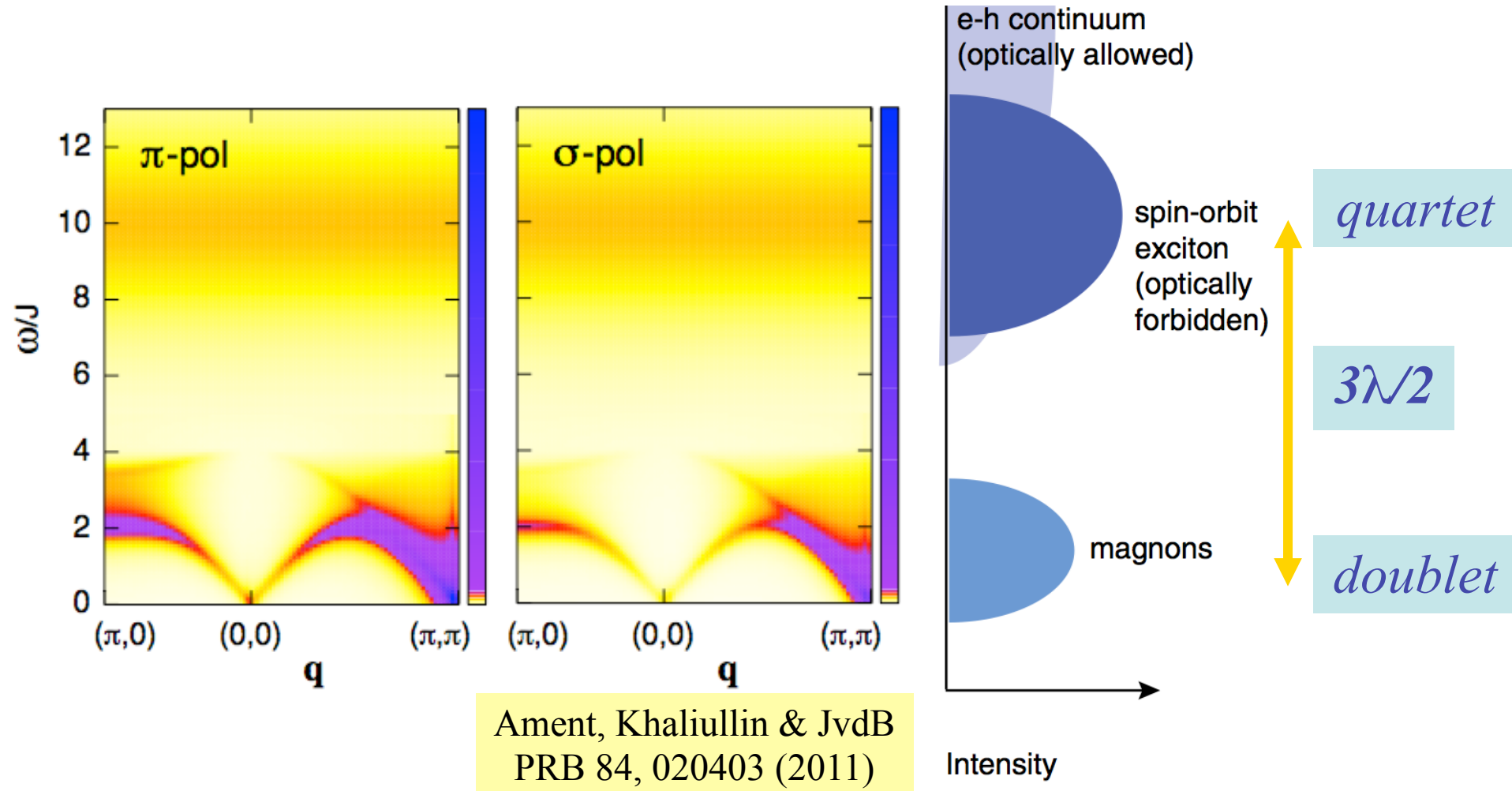
Direct RIXS on Sr_2IrO_4



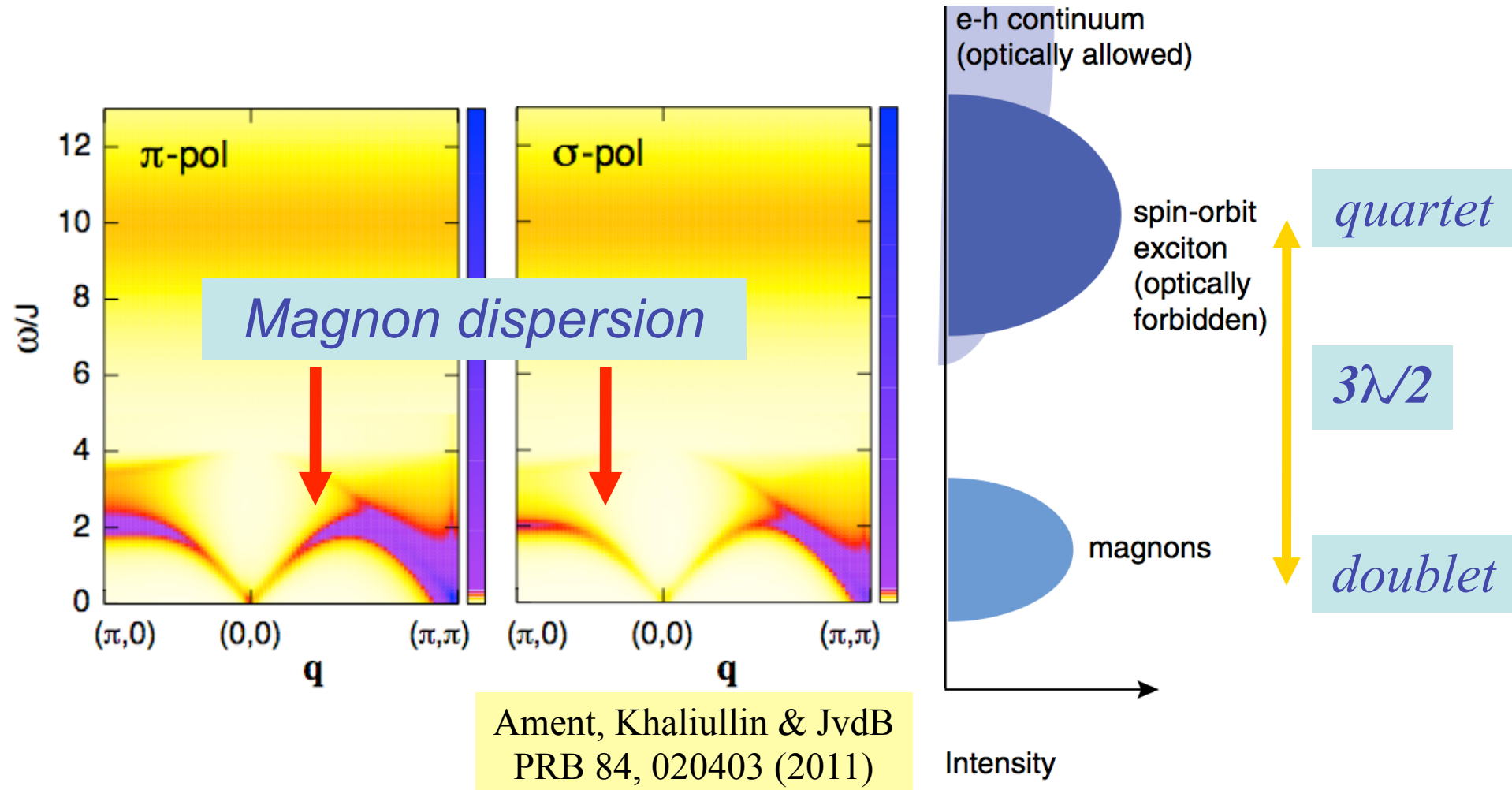
Direct RIXS on Sr_2IrO_4



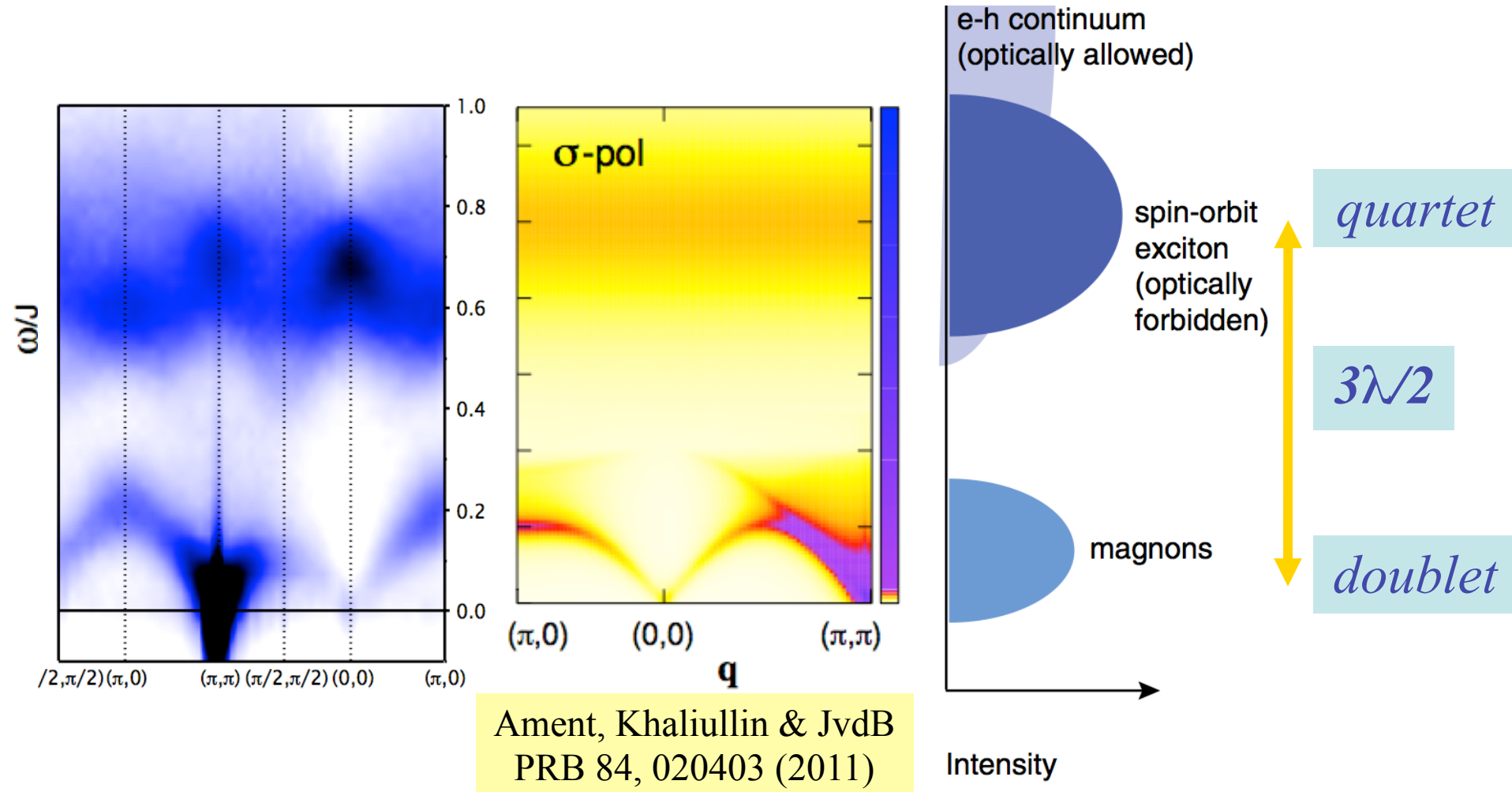
Direct RIXS on Sr_2IrO_4



Direct RIXS on Sr_2IrO_4



Direct RIXS on Sr_2IrO_4



Jungho Kim,¹ D. Casa,¹ M. H. Upton,¹ T. Gog,¹ Young-June Kim,²
J. F. Mitchell,³ M. van Veenendaal,^{1,4} M. Daghofer,⁵ J. van den Brink,⁵
G. Khaliullin,⁶ B. J. Kim^{3,*} PRL 108, 177003 (2012)

Magnetic RIXS on

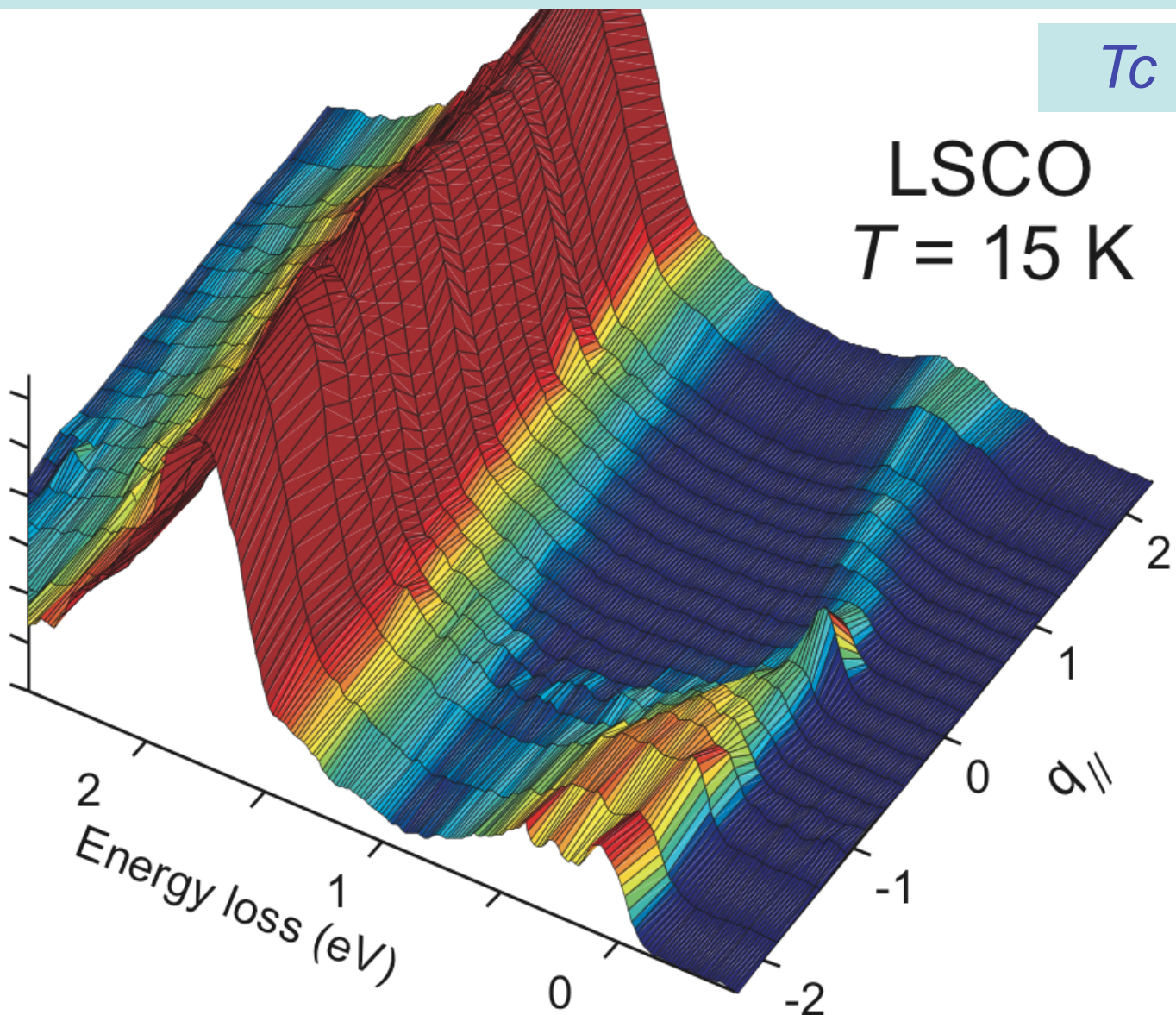
doped quasi-2D

Cu-oxides and Fe-pnictides

Magnetic L-edge RIXS on 8% doped $\text{La}_{2-x}\text{Sr}_x\text{CuO}_4$

$T_c = 21\text{K}$

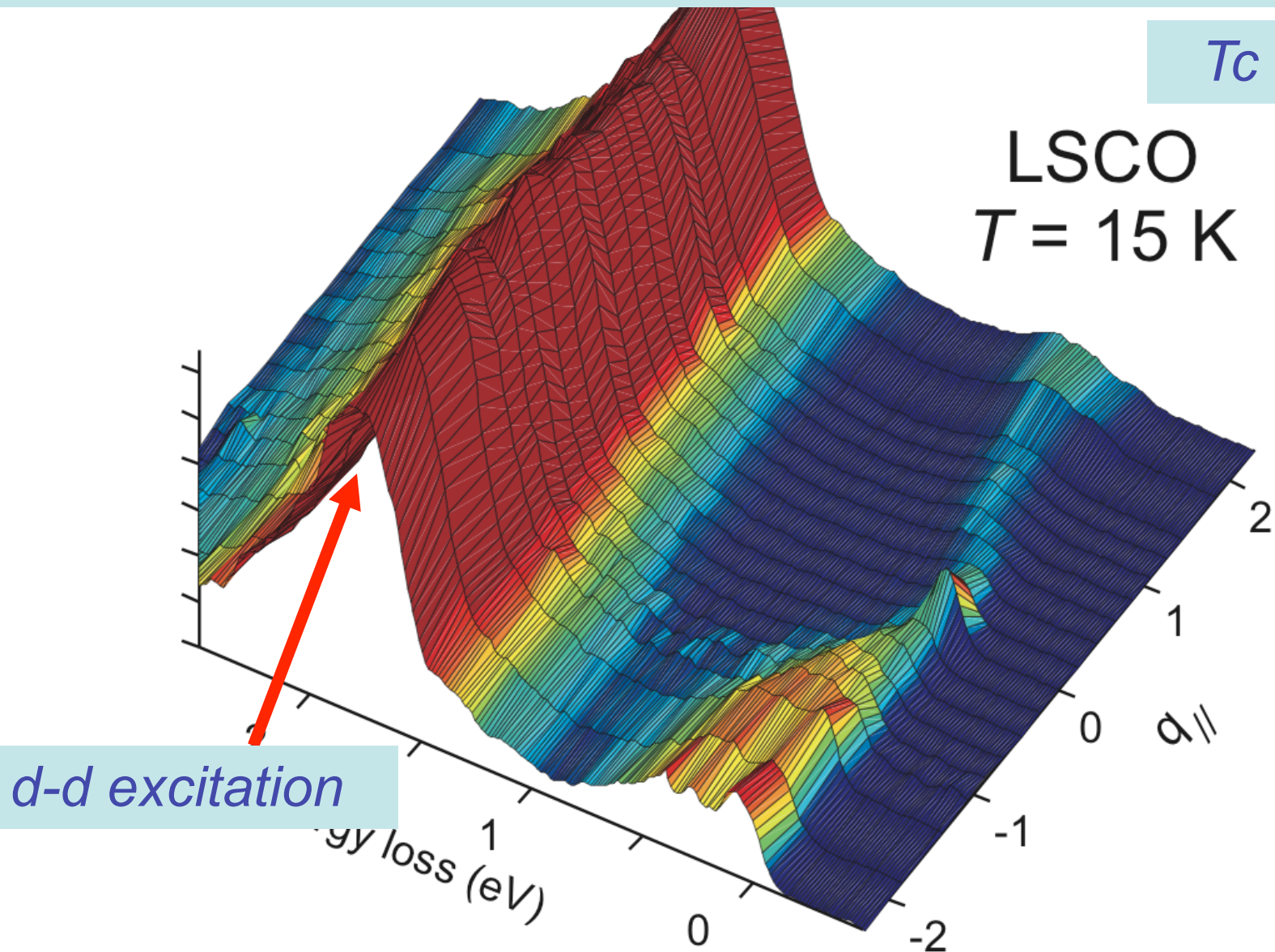
LSCO
 $T = 15\text{ K}$



Magnetic L-edge RIXS on 8% doped $\text{La}_{2-x}\text{Sr}_x\text{CuO}_4$

$T_c = 21\text{K}$

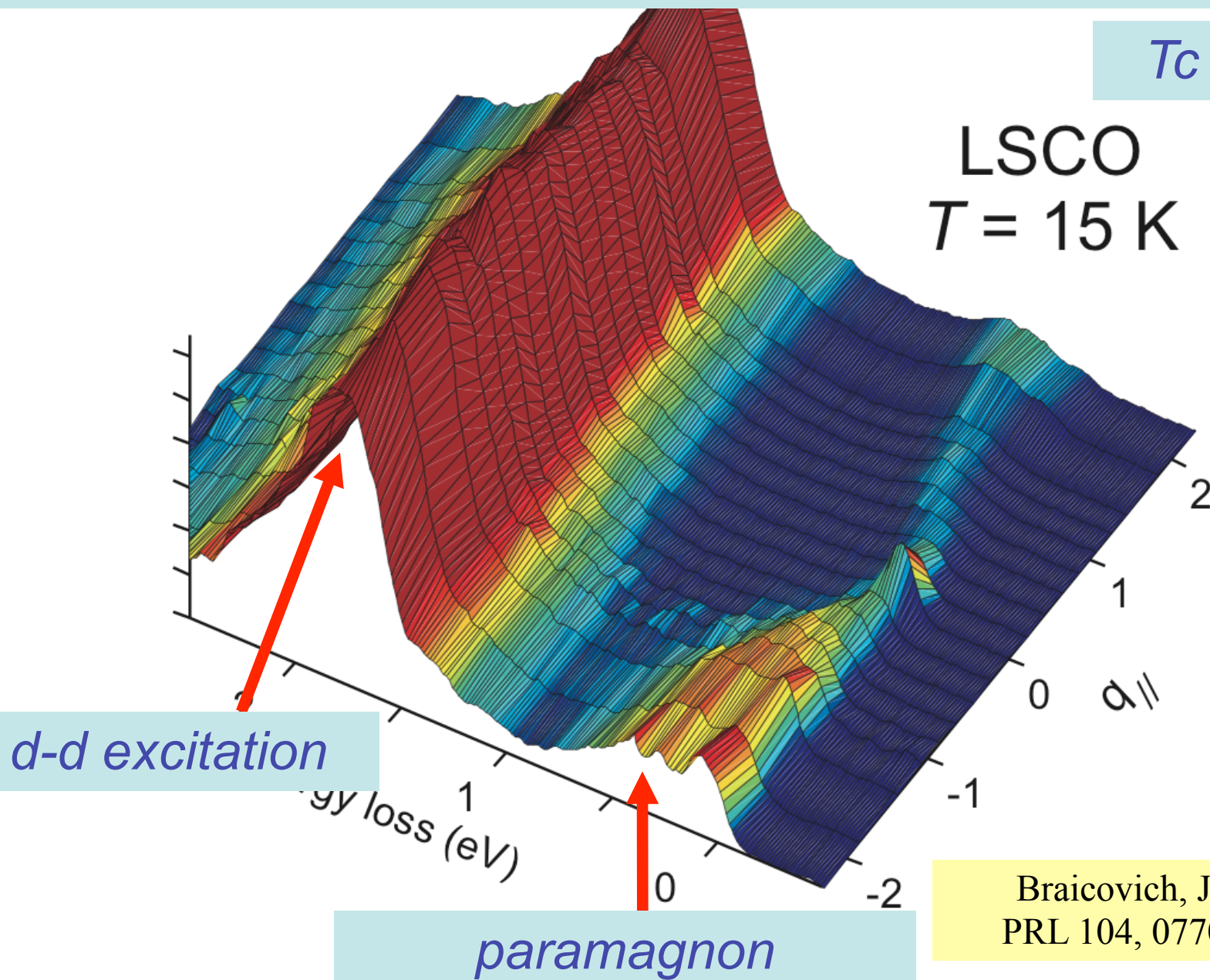
LSCO
 $T = 15\text{ K}$



Magnetic L-edge RIXS on 8% doped $\text{La}_{2-x}\text{Sr}_x\text{CuO}_4$

$T_c = 21\text{K}$

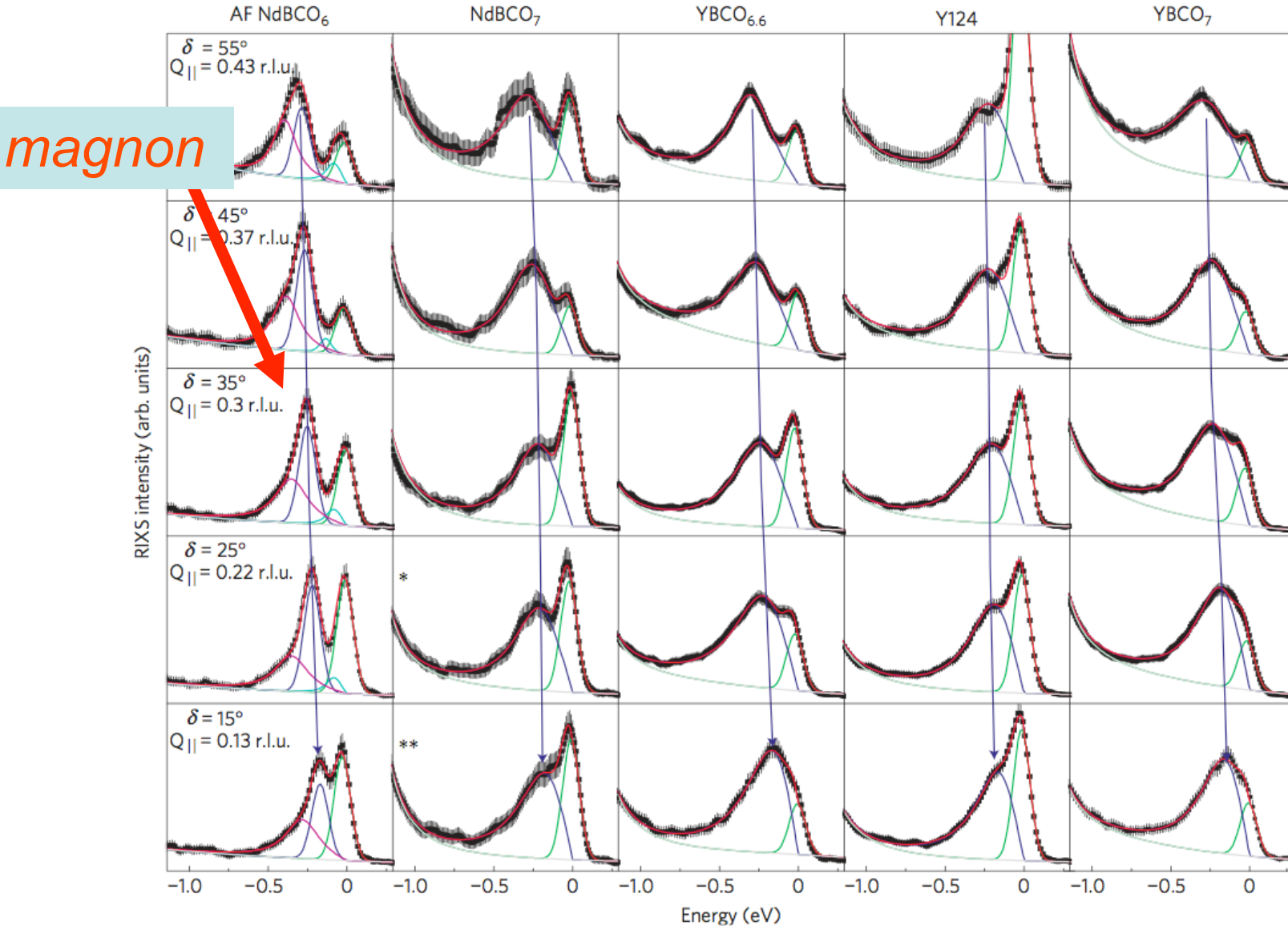
LSCO
 $T = 15\text{ K}$



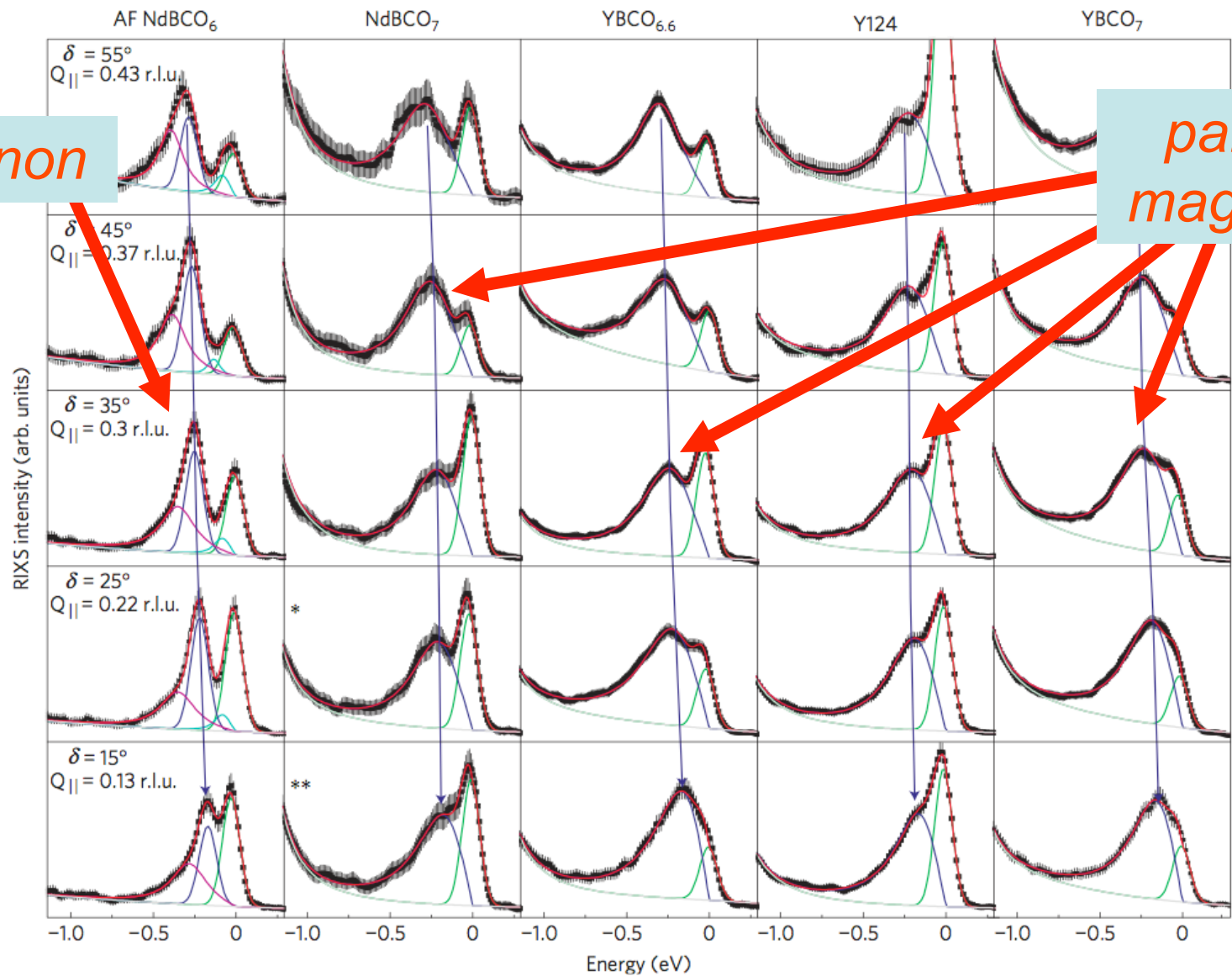
Braicovich, JvdB *et al.*
PRL 104, 077002 (2010)

Intense paramagnon excitations in a large family of high-temperature superconductors

M. Le Tacon^{1*}, G. Ghiringhelli², J. Chaloupka¹, M. Moretti Sala², V. Hinkov^{1,3}, M. W. Haverkort¹, M. Minola², M. Bakr¹, K. J. Zhou⁴, S. Blanco-Canosa¹, C. Monney⁴, Y. T. Song¹, G. L. Sun¹, C. T. Lin¹, G. M. De Luca⁵, M. Salluzzo⁵, G. Khaliullin¹, T. Schmitt⁴, L. Braicovich² and B. Keimer^{1*}



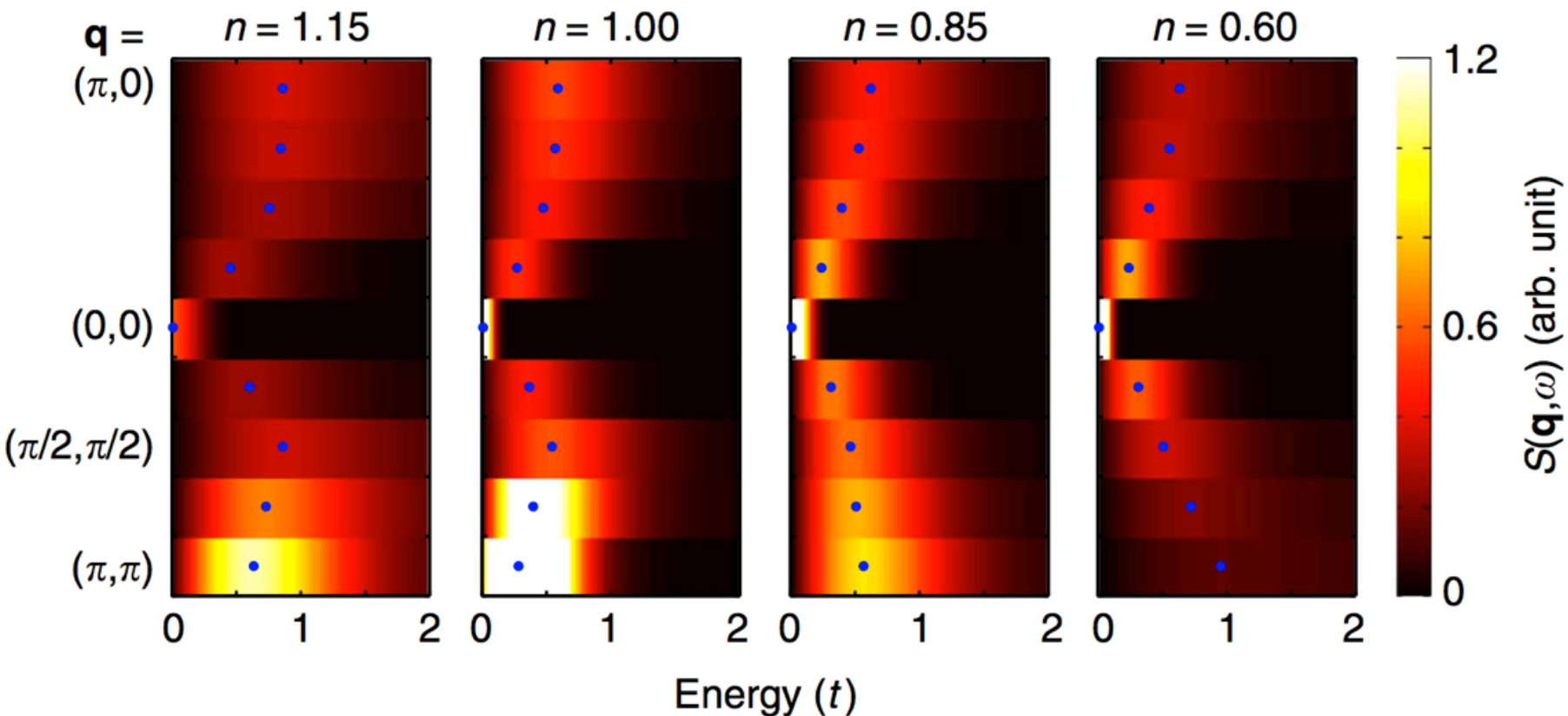
M. Le Tacon^{1*}, G. Ghiringhelli², J. Chaloupka¹, M. Moretti Sala², V. Hinkov^{1,3}, M. W. Haverkort¹,
M. Minola², M. Bakr¹, K. J. Zhou⁴, S. Blanco-Canosa¹, C. Monney⁴, Y. T. Song¹, G. L. Sun¹, C. T. Lin¹,
G. M. De Luca⁵, M. Salluzzo⁵, G. Khaliullin¹, T. Schmitt⁴, L. Braicovich² and B. Keimer^{1*}



M. Le Tacon^{1*}, G. Ghiringhelli², J. Chaloupka¹, M. Moretti Sala², V. Hinkov^{1,3}, M. W. Haverkort¹,
M. Minola², M. Bakr¹, K. J. Zhou⁴, S. Blanco-Canosa¹, C. Monney⁴, Y. T. Song¹, G. L. Sun¹, C. T. Lin¹,
G. M. De Luca⁵, M. Salluzzo⁵, G. Khaliullin¹, T. Schmitt⁴, L. Braicovich² and B. Keimer^{1*}

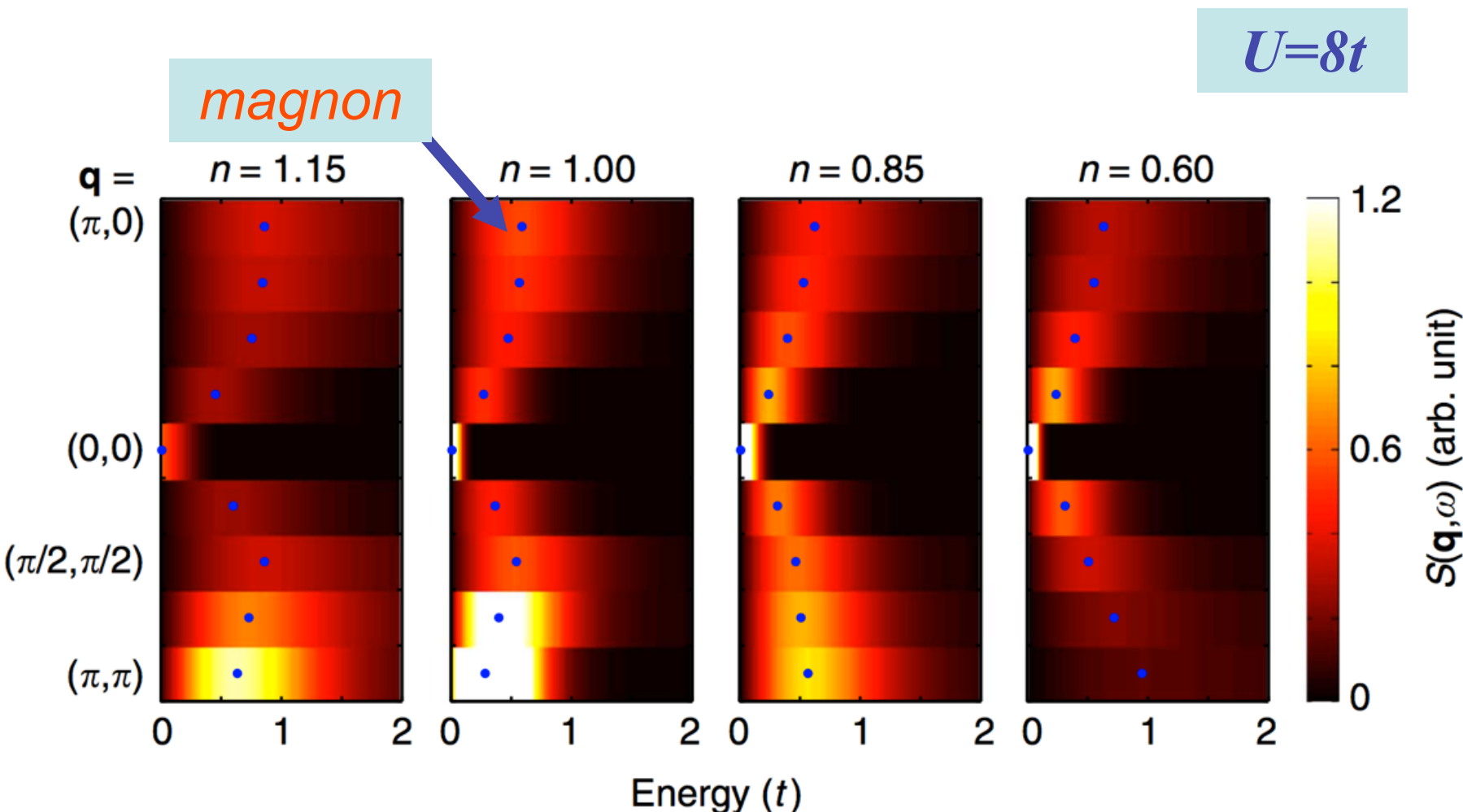
Dynamical structure factor Hubbard model, QMC

$U=8t$



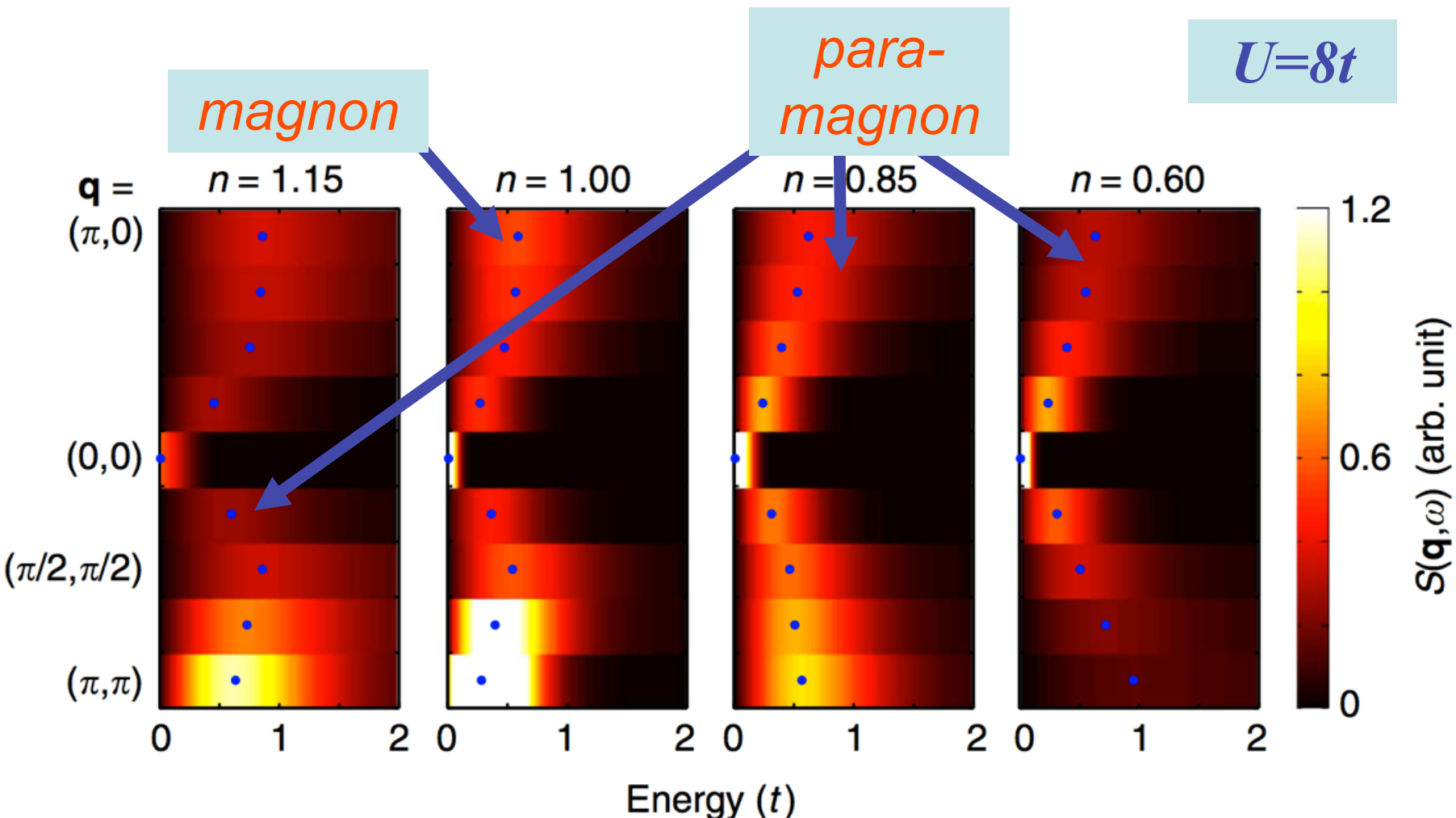
Jia, Nowadnick, Wohlfeld, Kung, Chen,
Johnston, Tohyama, Moritz & Devereaux
Nat. Comm. 5, 3314 (2014)

Dynamical structure factor Hubbard model, QMC



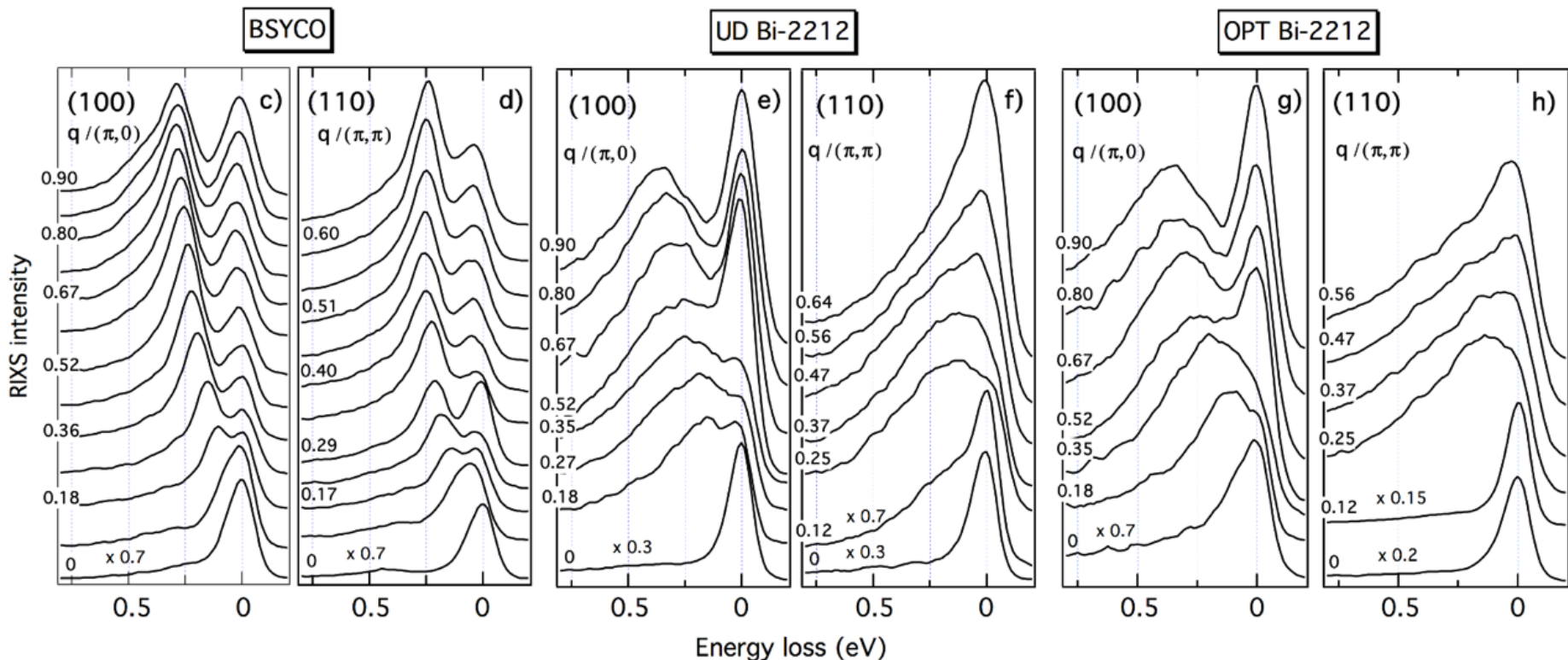
Jia, Nowadnick, Wohlfeld, Kung, Chen,
Johnston, Tohyama, Moritz & Devereaux
Nat. Comm. 5, 3314 (2014)

Dynamical structure factor Hubbard model, QMC



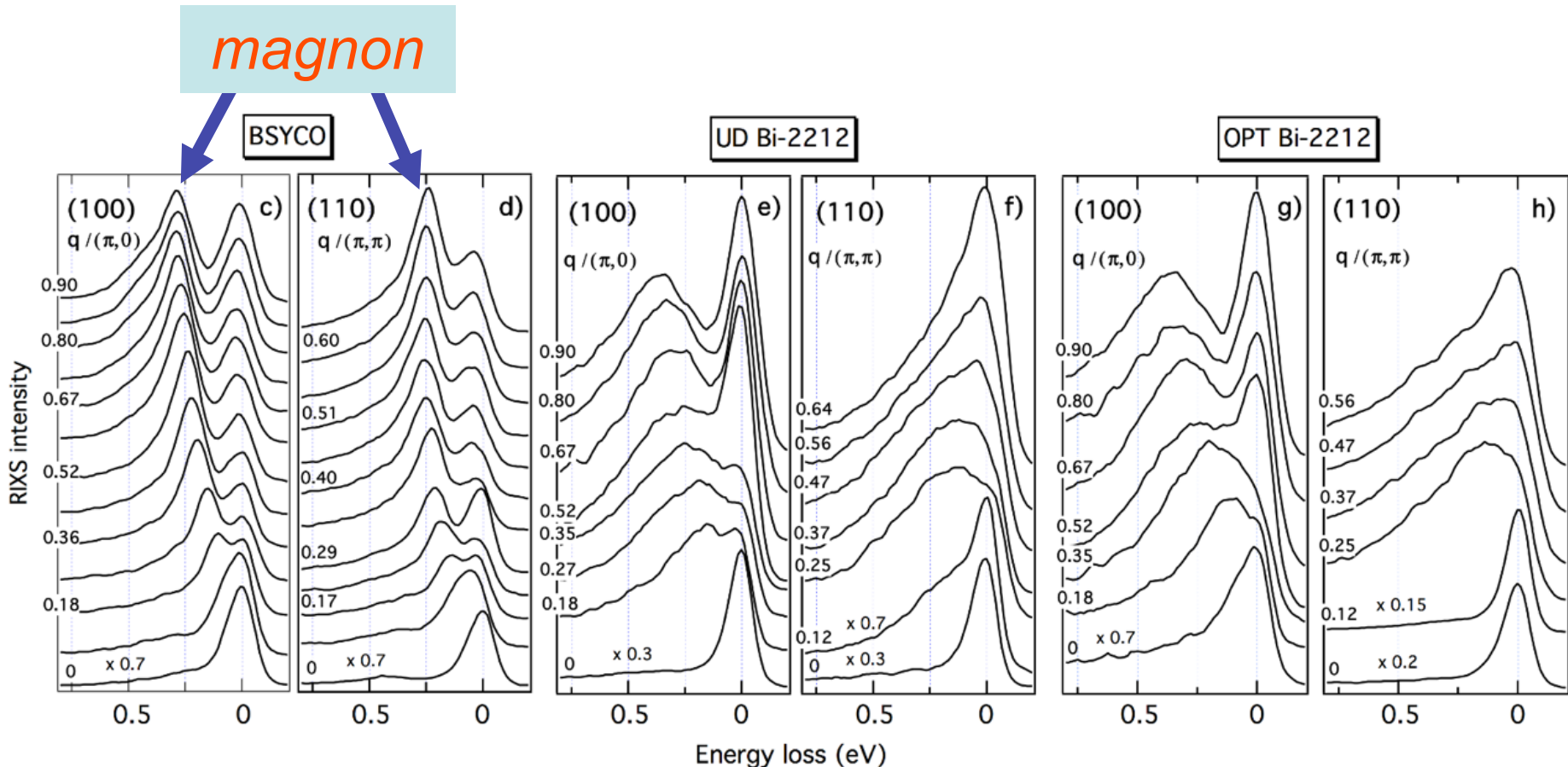
Jia, Nowadnick, Wohlfeld, Kung, Chen,
Johnston, Tohyama, Moritz & Devereaux
Nat. Comm. 5, 3314 (2014)

RIXS on Bi-2212 cuprate



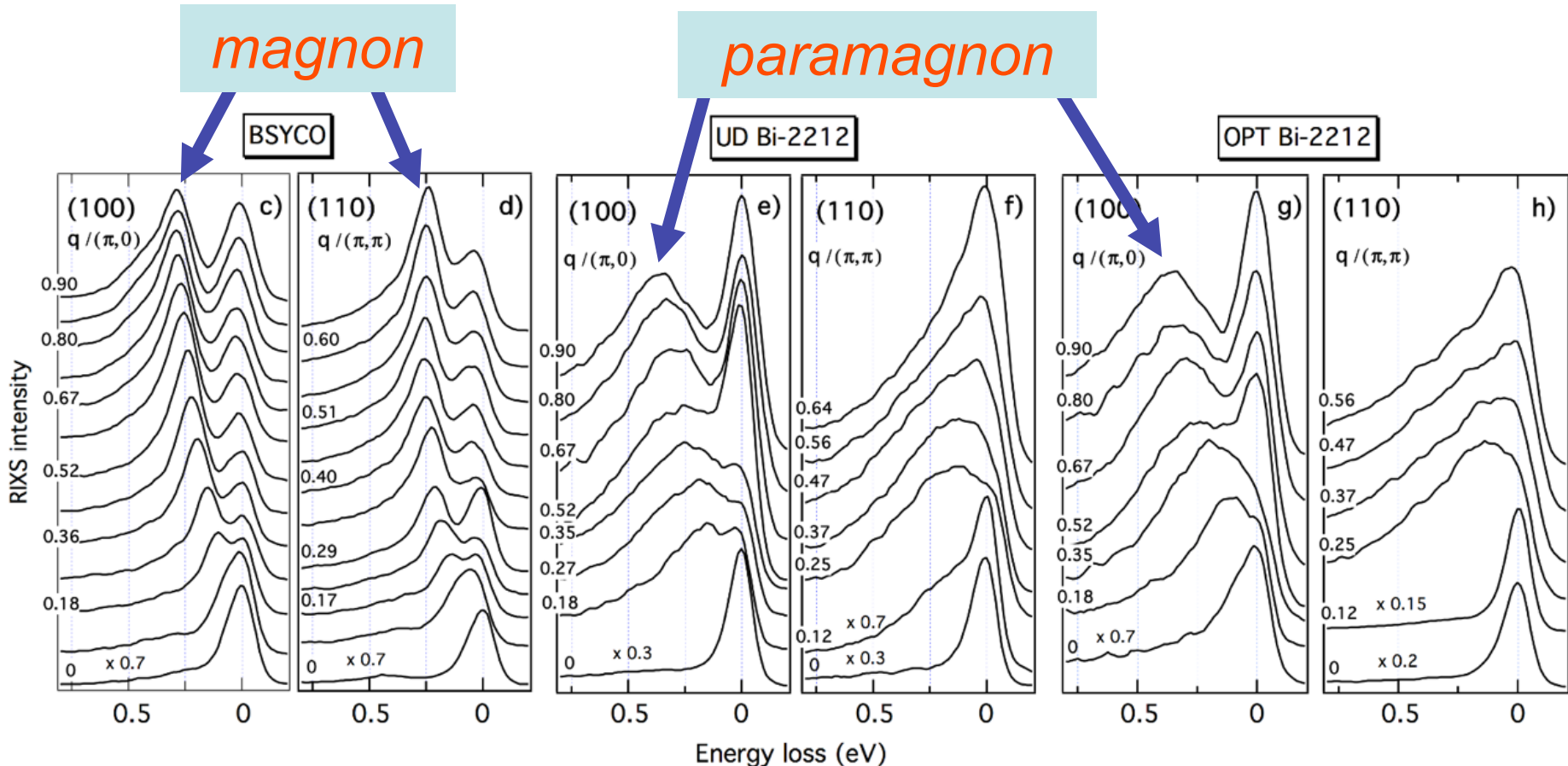
Guarise, Piazza, Berger, Giannini, Schmitt, Rønnow,
Sawatzky, JvdB, Altenfeld, Eremin & Grioni (2014)

RIXS on Bi-2212 cuprate



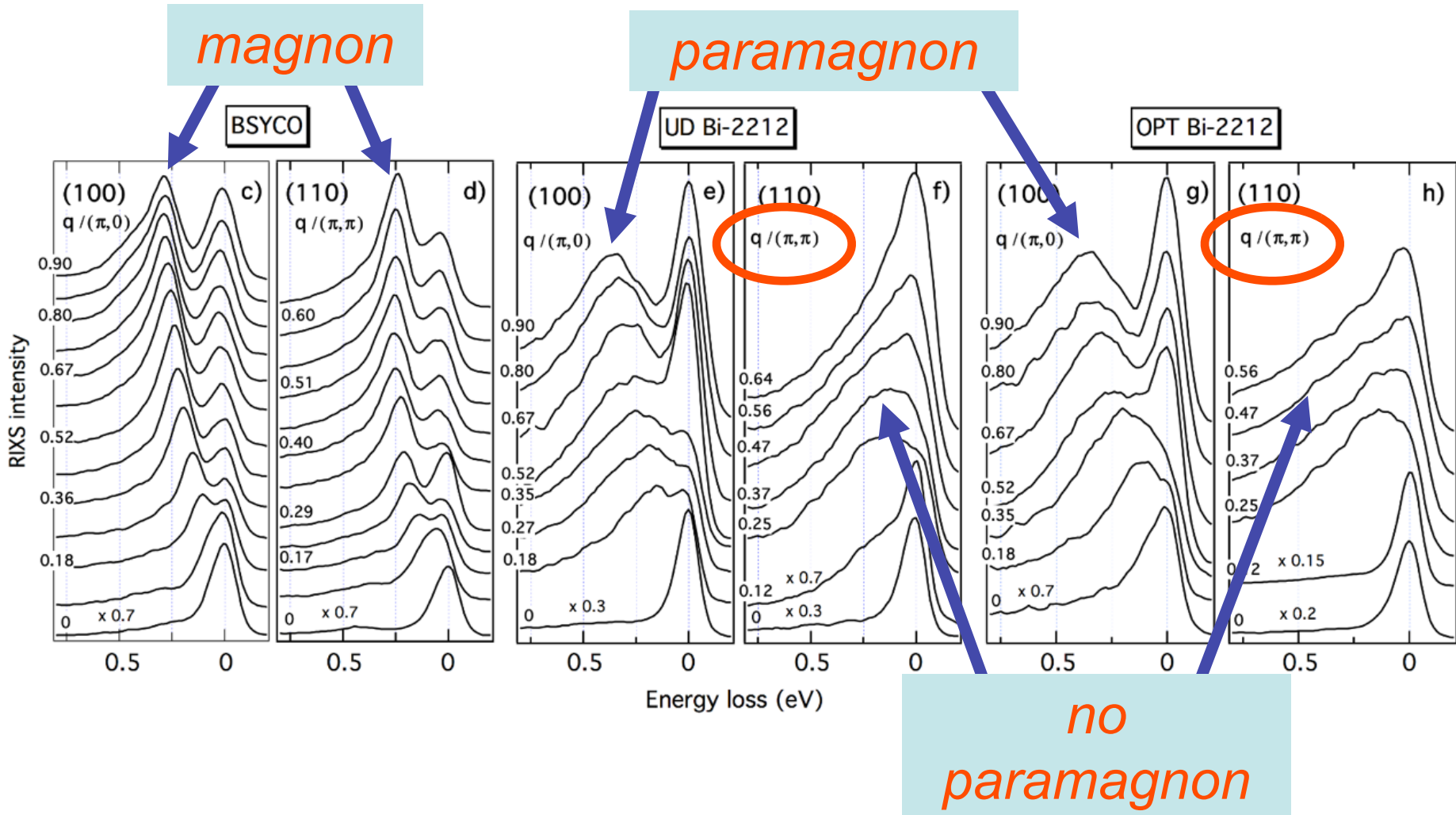
Guarise, Piazza, Berger, Giannini, Schmitt, Rønnow, Sawatzky, JvdB, Altenfeld, Eremin & Grioni (2014)

RIXS on Bi-2212 cuprate



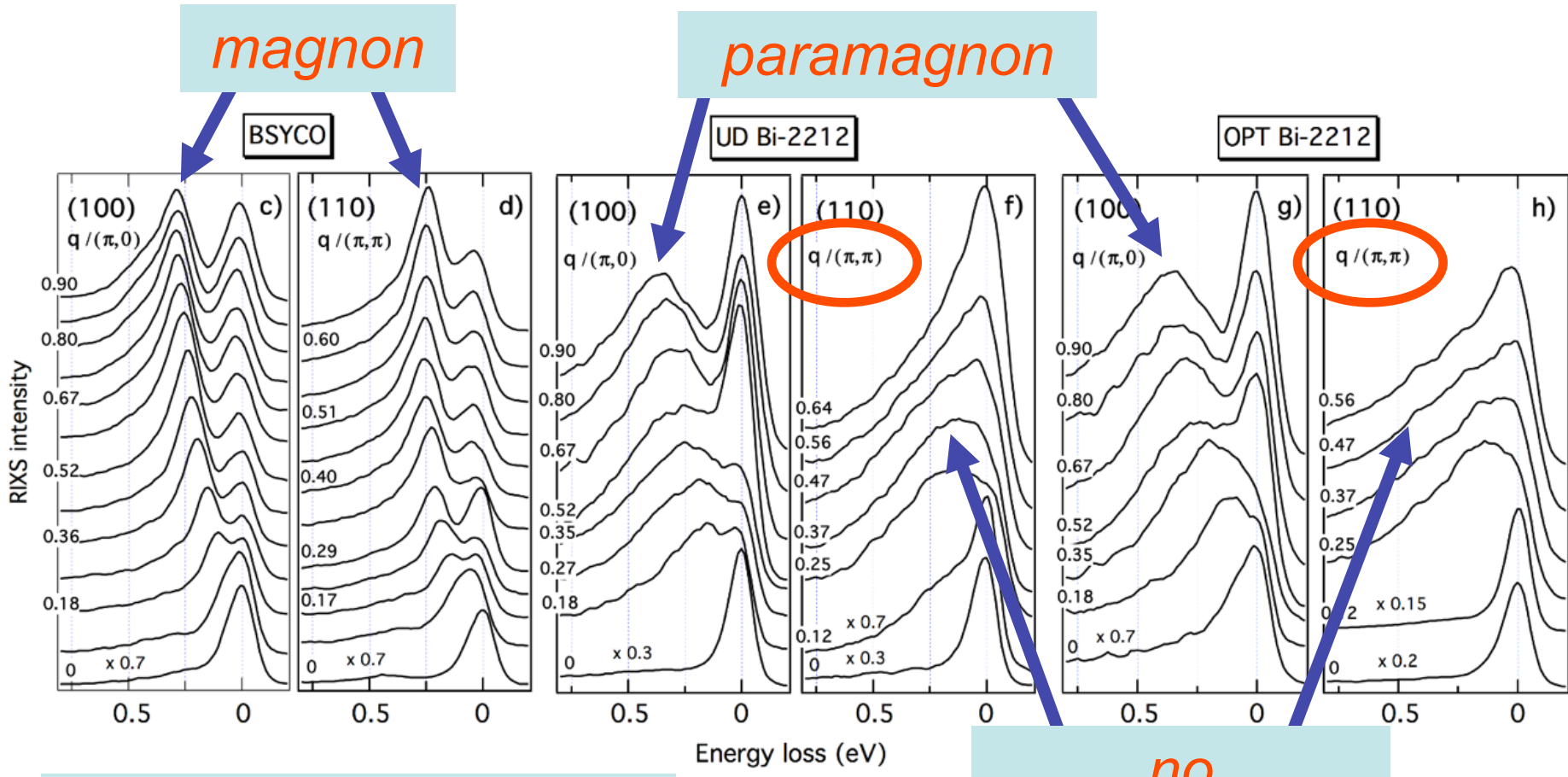
Guarise, Piazza, Berger, Giannini, Schmitt, Rønnow,
Sawatzky, JvdB, Altenfeld, Eremin & Grioni (2014)

RIXS on Bi-2212 cuprate



Guarise, Piazza, Berger, Giannini, Schmitt, Rønnow, Sawatzky, JvdB, Altenfeld, Eremin & Grioni (2014)

RIXS on Bi-2212 cuprate

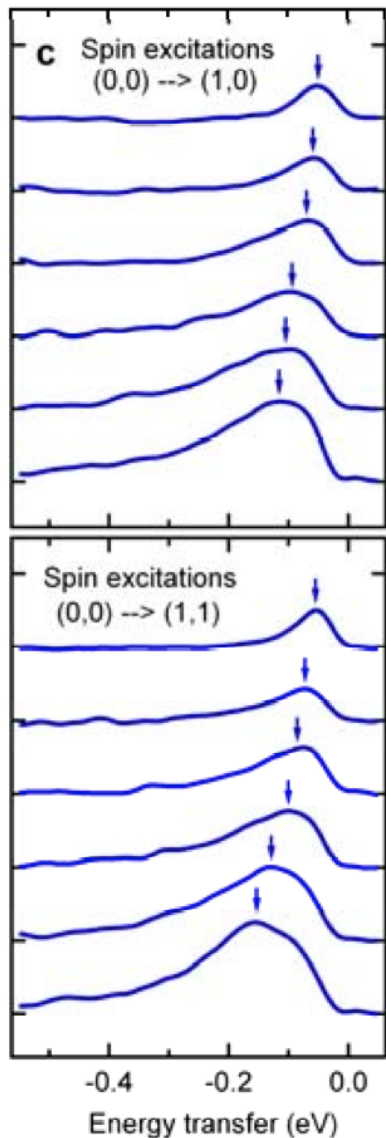


Related to presence of
e-h continuum?

Benjamin, Klich & Demler
PRL 112, 247002 (2014)

Guarise, Piazza, Berger, Giannini, Schmitt, Rønnow,
Sawatzky, JvdB, Altenfeld, Eremin & Grioni (2014)

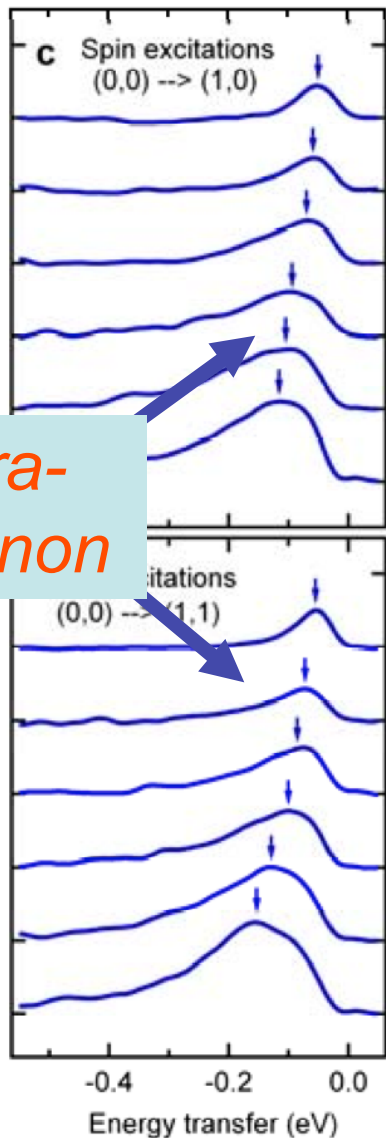
Magnetic RIXS on $\text{Ba}_{0.6}\text{K}_{0.4}\text{Fe}_2\text{As}_2$



Zhou, Huang, Monney, Dai, Strocov, Wang,
Chen, Zhang, Dai, Patthey, JvdB, Ding &
Schmitt, Nat. Comm. 4, 1470 (2013)

Magnetic RIXS on $\text{Ba}_{0.6}\text{K}_{0.4}\text{Fe}_2\text{As}_2$

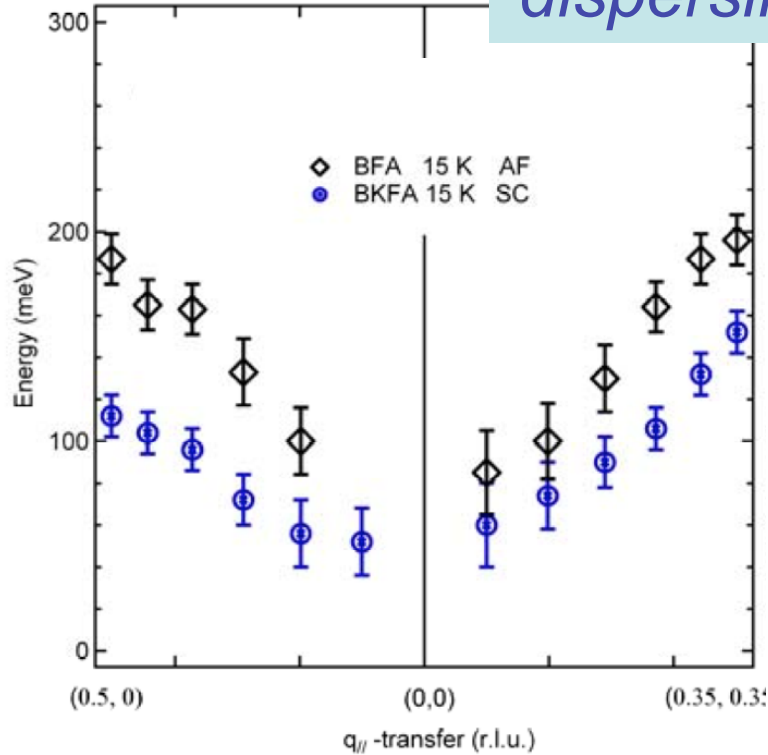
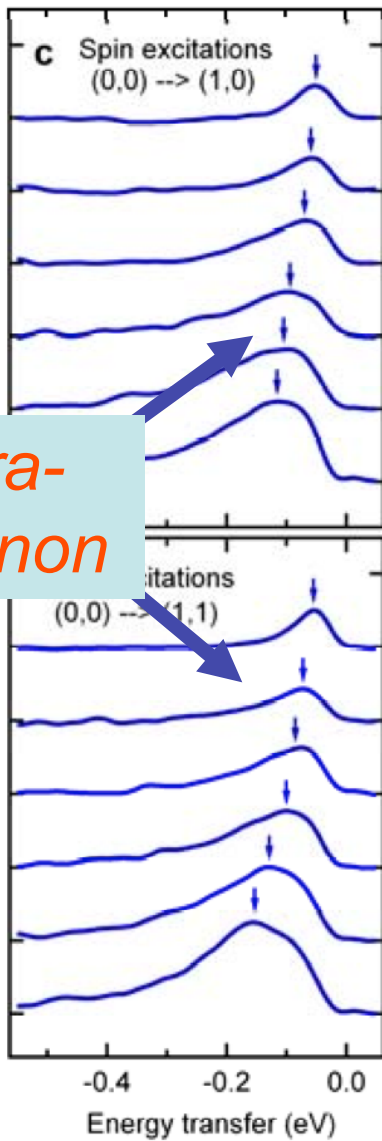
para-magnon



Zhou, Huang, Monney, Dai, Strocov, Wang,
Chen, Zhang, Dai, Patthey, JvdB, Ding &
Schmitt, Nat. Comm. 4, 1470 (2013)

Magnetic RIXS on $\text{Ba}_{0.6}\text{K}_{0.4}\text{Fe}_2\text{As}_2$

para-magnon



dispersing paramagnon

Significant softening

Zhou, Huang, Monney, Dai, Strocov, Wang, Chen, Zhang, Dai, Patthey, JvdB, Ding & Schmitt, Nat. Comm. 4, 1470 (2013)

Summary part 2

Summary part 2

- RIXS sensitive to magnetic excitations of e.g.
low D cuprates, iron pnictides and iridates

Summary part 2

- RIXS sensitive to magnetic excitations of e.g.
low D cuprates, iron pnictides and iridates
- Magnons, spinons and paramagnons are observed

Summary part 2

- RIXS sensitive to magnetic excitations of e.g.
low D cuprates, iron pnictides and iridates
- Magnons, spinons and paramagnons are observed
- Dispersion of these modes can be determined

Summary part 2

- RIXS sensitive to magnetic excitations of e.g.
low D cuprates, iron pnictides and iridates
- Magnons, spinons and paramagnons are observed
- Dispersion of these modes can be determined
- Observed paramagnons are challenge for theory

Summary part 2

- RIXS sensitive to magnetic excitations of e.g.
low D cuprates, iron pnictides and iridates
- Magnons, spinons and paramagnons are observed
- Dispersion of these modes can be determined
- Observed paramagnons are challenge for theory
- It can reasonably be assumed that the future of
RIXS is even brighter than its past

Summary part 2

- RIXS sensitive to magnetic excitations of e.g.
low D cuprates, iron pnictides and iridates
- Magnons, spinons and paramagnons are observed
- Dispersion of these modes can be determined
- Observed paramagnons are challenge for theory
- It can reasonably be assumed that the future of
RIXS is even brighter than its past
- More and better beam-lines, experiments, theory